frontiers | Research Topics

Lianas, ecosystems, and global change

Edited by
Geertje M. F. Van Der Heijden, Félicien Meunier and
Stefan A. Schnitzer

Published in
Frontiers in Forests and Global Change

ISSN 1664-8714
ISBN 978-2-83251-702-4
DOI 10.3389/978-2-83251-702-4

About Frontiers

Frontiers is more than just an open access publisher of scholarly articles: it is a pioneering approach to the world of academia, radically improving the way scholarly research is managed. The grand vision of Frontiers is a world where all people have an equal opportunity to seek, share and generate knowledge. Frontiers provides immediate and permanent online open access to all its publications, but this alone is not enough to realize our grand goals.

Frontiers journal series

The Frontiers journal series is a multi-tier and interdisciplinary set of open-access, online journals, promising a paradigm shift from the current review, selection and dissemination processes in academic publishing. All Frontiers journals are driven by researchers for researchers; therefore, they constitute a service to the scholarly community. At the same time, the *Frontiers journal series* operates on a revolutionary invention, the tiered publishing system, initially addressing specific communities of scholars, and gradually climbing up to broader public understanding, thus serving the interests of the lay society, too.

Dedication to quality

Each Frontiers article is a landmark of the highest quality, thanks to genuinely collaborative interactions between authors and review editors, who include some of the world's best academicians. Research must be certified by peers before entering a stream of knowledge that may eventually reach the public - and shape society; therefore, Frontiers only applies the most rigorous and unbiased reviews. Frontiers revolutionizes research publishing by freely delivering the most outstanding research, evaluated with no bias from both the academic and social point of view. By applying the most advanced information technologies, Frontiers is catapulting scholarly publishing into a new generation.

What are Frontiers Research Topics?

Frontiers Research Topics are very popular trademarks of the *Frontiers journals series*: they are collections of at least ten articles, all centered on a particular subject. With their unique mix of varied contributions from Original Research to Review Articles, Frontiers Research Topics unify the most influential researchers, the latest key findings and historical advances in a hot research area.

Find out more on how to host your own Frontiers Research Topic or contribute to one as an author by contacting the Frontiers editorial office: frontiersin.org/about/contact

Lianas, ecosystems, and global change

Topic editors
Geertje M. F. Van Der Heijden — University of Nottingham, United Kingdom
Félicien Meunier — Ghent University, Belgium
Stefan A. Schnitzer — Marquette University, United States

Citation
Van Der Heijden, G. M. F., Meunier, F., Schnitzer, S. A., eds. (2023). *Lianas, ecosystems, and global change*. Lausanne: Frontiers Media SA.
doi: 10.3389/978-2-83251-702-4

Table of contents

frontiers | Frontiers in Forest and Global Change

TYPE Editorial
PUBLISHED 02 February 2023
DOI 10.3389/ffgc.2023.1079620

OPEN ACCESS

EDITED BY
Nophea Sasaki,
Asian Institute of Technology, Thailand

REVIEWED BY
Francis Edward Putz,
University of Florida, United States

*CORRESPONDENCE
Geertje M. F. van der Heijden
✉ geertje.vanderheijden@nottingham.ac.uk

†These authors have contributed equally to this work

SPECIALTY SECTION
This article was submitted to
Tropical Forests,
a section of the journal
Frontiers in Forests and Global Change

RECEIVED 25 October 2022
ACCEPTED 23 January 2023
PUBLISHED 02 February 2023

CITATION
van der Heijden GMF, Schnitzer SA and Meunier F (2023) Editorial: Lianas, ecosystems, and global change.
Front. For. Glob. Change 6:1079620.
doi: 10.3389/ffgc.2023.1079620

Editorial: Lianas, ecosystems, and global change

Geertje M. F. van der Heijden[1]*†, Stefan A. Schnitzer[2,3]† and Félicien Meunier[4]†

[1]School of Geography, University of Nottingham, University Park, Nottingham, United Kingdom, [2]Smithsonian Tropical Research Institute, Balboa, Panama, [3]Department of Biological Sciences, Marquette University, Milwaukee, WI, United States, [4]Department of Environment, Ghent University, Ghent, Belgium

KEYWORDS

plant life-forms, functional traits, tropical forests, liana ecology, liana diversity

Editorial on the Research Topic
Lianas, ecosystems, and global change

Lianas (woody vines) are an abundant and diverse plant group in tropical ecosystems (Gentry, 1991; Dewalt et al., 2014). While they enhance forest canopy connectivity and provide food and shelter for tropical fauna (Yanoviak and Schnitzer, 2013; Schnitzer, 2018), lianas also intensely compete with trees for resources, and hence negatively influence a wide range of tropical ecosystem processes (van der Heijden et al., 2013), such as regeneration (Schnitzer et al., 2000; Pérez-Salicrup, 2001), tree reproduction (García León et al., 2018), and carbon storage and sequestration (van der Heijden et al., 2015).

Although the knowledge on lianas has developed significantly since Darwin's initial work on climbing plants (Darwin, 1865), studies in tropical forests still overwhelmingly focus on trees (da Cunha Vargas et al., 2020). This special issue brings together a collection of papers that provide new insights into the diversity of lianas, their impact on the ecosystem, and their relationships with climate.

Liana (functional) diversity

Lianas are plants that rely on the architecture of other plants to ascend to the forest canopy (Schnitzer and Bongers, 2002). They have therefore developed a wide diversity of techniques for finding and climbing hosts (Darwin, 1865; Putz, 1984; Dias et al., 2021). For example, many liana species use searcher shoots capable of movement. Hatterman et al. found that liana species vary considerably in their reach, i.e., the distance these searcher shoots can span. The liana species with the longest reach required sufficient rigidity at its basal part, an attribute that comes at the cost of their ability for active movements of the distal parts. There may therefore be a trade-off in lianas between reach and movement, possibly explaining differences in their ability to explore the environment.

Lianas are hypothesized to possess fast-acquisitive functional traits while trees are generally thought to be more conservative (Collins et al., 2016). In concurrence with this hypothesis, Harrison et al. showed that lianas had an increased cellular infrastructure with a high turnover of nutrients and leaf volume demands when compared to trees. Being able to find and use resources effectively may give lianas a growth advantage in dry conditions (Schnitzer, 2005; Schnitzer and van der Heijden, 2019). To test this hypothesis, Smith-Martin et al. compared xylem anatomical traits in lianas and trees both in a wet and seasonally dry forest. They found that lianas have greater vessel diameters than trees particularly in dry forests, but that there was no difference in levels of resistance to embolism, hydraulic failure nor in withstanding greater levels of water-deficit between life-forms. The larger vessels of lianas may support greater hydraulic conductive capacity (Tyree and Ewers, 1999), needed to support the proportionally greater leaf canopy of lianas (Wyka et al., 2013), without the risk of embolism formation.

Lianas, however, are not a functionally homogeneous entity. For example, Coppieters et al. found that two abundant, co-occurring liana species differed substantially in their hydraulic traits, as found in previous studies (Ewers et al., 1989, 1990). Liana diversity is highly variable across the landscape. Souza Gerolamo et al. showed that liana taxonomic diversity across the Brazilian Amazon increased along a hydro-edaphic gradient but decreased slightly along a forest disturbance gradient. Reduction in liana habitat specialization occurred on plateaus with deeper water tables while in valleys liana assemblages were phylogenetically overdispersed. Further research into the spectrum of liana traits and the relationships defining their economic spectrum (see Harrison et al.), ecological filtering, and phylogenetic history is needed to increase our understanding of liana ecology.

The effect of lianas on tropical forest ecosystems

Lianas have long been associated with decreased tree growth (Putz, 1984), but the evidence that supports this negative impact mostly came from primary and seasonally moist forests. However, Becknell et al. now reported significant decreases of the relative growth of trees heavily infested by lianas in a secondary seasonally dry tropical forest. Estrada-Villegas et al. further provided unequivocal evidence that a negative liana impact on trees is found across continents, climates, and forest types. Using a meta-analysis of 50 liana removal experiments across the tropics, they showed that lianas have a significant impact on tree growth, reproduction and recruitment, as well as on biomass accretion and physiological performance.

Meunier et al. further suggested that by accounting for belowground biomass the reduced carbon sequestration and storage in trees and ecosystems caused by lianas could be larger than previously anticipated.

Lianas and global change

Lianas have repeatedly been shown to be increasing in abundance and biomass in the Neotropics (e.g. Phillips et al., 2002 and illustrated in this issue by Becknell et al.). Yet, evidence from other parts of the tropics remains scarce or contradictory (see e.g., Bongers et al., 2020). The underlying drivers of such trends could be related to global change (Schnitzer and Bongers, 2011). Using 15-years of liana fruiting and flowering data, Vogado et al. showed that liana reproduction increased as a response to higher temperatures, reduced rainfall, and following El Niño events in a tropical Australian site. Liana reproduction and abundance are therefore likely to increase under future climate regimes.

Novel methods to study lianas

Liana ecology is benefiting from emerging methods to study lianas. Firstly, the incorporation of lianas in a vegetation model has previously enabled an exhaustive quantification of the impact of lianas on the carbon (di Porcia E Brugnera et al., 2019) and energy (Meunier et al., 2022) cycles. Here, it further provided a first assessment of the effects of lianas on below-ground carbon storage (Meunier et al.), which is inherently challenging to quantify using field techniques. Secondly, Kaçamak et al. demonstrated that combining RGB and multispectral images with Lidar data from drones could generate high resolution views of liana distribution at the top of the canopy that ground-based measurements alone cannot provide. Combining ground- and drone- based data therefore have the potential to provide a major step forward in liana ecology.

Liana research is on the rise, which offers an exciting opportunity to answer many important research questions in liana ecology. As such, we hope that this special issue will contribute to a better understanding of the current and future effects of lianas on tropical forests across continents in a changing climate.

Author contributions

All authors listed have made a substantial, direct, and intellectual contribution to the work and approved it for publication.

Funding

During the preparation of this manuscript, FM was funded by the FWO as a junior postdoc (grant no. 1214720N) and is thankful to this organization for its financial support.

Acknowledgments

The editors would like to thank all the authors that contributed to this Research Topic as well as specifically thank the reviewers for their support and expertise in evaluating the contributions to this Research Topic.

Conflict of interest

The authors declare that the research was conducted in the absence of any commercial or financial relationships that could be construed as a potential conflict of interest.

Publisher's note

References

Bongers, F., Ewango, C. E. N., van der Sande, M. T., and Poorter, L. (2020). Liana species decline in Congo basin contrasts with global patterns. *Ecology* 101, e03004. doi: 10.1002/ecy.3004

Collins, C. G., Wright, S. J., and Wurzburger, N. (2016). Root and leaf traits reflect distinct resource acquisition strategies in tropical lianas and trees. *Oecologia* 180, 1037–1047. doi: 10.1007/s00442-015-3410-7

da Cunha Vargas, B., Grombone-Guaratini, M. T., and Cerdeira Morellato, L. P. (2020). Lianas research in the neotropics: overview, interaction with trees, and future perspectives. *Trees.* 35, 333–345. doi: 10.1007/s00468-020-02056-w

Darwin, C. (1865). On the movement of climbing plants. *J. Linn. Soc.* 9, 1–118. doi: 10.1111/j.1095-8339.1865.tb00011.x

Dewalt, S. J., Schnitzer, S. A., Alves, L. F., Bongers, F., Burnham, R. J., Cai, Z., et al. (2014). "Biogeographical patterns of liana abundance and diversity," in *Ecology of Lianas*, eds S. A. Schnitzer, F. Bongers, R. J. Burnham, and F. E. Putz, 131—146. doi: 10.1002/9781118392409.ch11

di Porcia E Brugnera, M., Meunier, F., Longo, M., Krishna Moorthy, S. M., De Deurwaerder, H., Schnitzer, S. A., et al. (2019). Modeling the impact of liana infestation on the demography and carbon cycle of tropical forests. *Glob. Change Biol.* 25, 3767–3780. doi: 10.1111/gcb.14769

Dias, A., Oliveira, R., Martins, F., Bongers, F., Anten, N., Sterck, F., et al. (2021). *Climbing Mechanisms as a Central Trait to Understand the Ecology of Lianas – a Global Synthesis. Authorea.* doi: 10.22541/au.162004148.87250667/v1

Ewers, F. W., Fisher, J. B., Chiu, S., Ewers, W., and Chi, S. (1990). A survey of vessel dimensions in stems of tropical lianas and other growth forms. *Oecologia* 84, 544–552. doi: 10.1007/BF00328172

Ewers, F. W., Fisher, J. B., Ewers, F. W., and Fisher, J. B. (1989). Variation in vessel length and diameter in stems of six tropical and subtropical lianas. *Am. J. Botany* 76, 1452–1459. doi: 10.1002/j.1537-2197.1989.tb15126.x

García León, M. M., Izquierdo, L. M., Arantes Mello, F. N., Powers, J. S., and Schnitzer, S. A. (2018). Lianas reduce community-level canopy tree reproduction in a Panamanian forest. *J. Ecol.* 106, 737–745. doi: 10.1111/1365-2745.12807

Gentry, A. H. (1991). "The distribution and evolution of climbing plants," in *The Biology of Vines*, eds F. E. Putz, and H. A. Mooney (Cambridge: Cambridge University Press), 3–49 doi: 10.1017/CBO9780511897658.003

Meunier, F., Visser, M. D., Shiklomanov, A., Dietze, M. C., Guzmán, Q., Sanchez-Azofeifa, J. A., et al. (2022). Liana optical traits increase tropical forest albedo and reduce ecosystem productivity. *Global Change Biol.* 28, 227–244. doi: 10.1111/gcb.15928

Pérez-Salicrup, D. R. (2001). Effect of liana cutting on tree regeneration in a liana forest in Amazonian Bolivia. *Ecology* 82, 389–396. doi: 10.1890/0012-9658(2001)082(0389:EOLCOT)2.0.CO;2

Phillips, O. L., Vásquez Martínez, R., Arroyo, L., Baker, T. R., Killeen, T., Lewis, S. L., et al. (2002). Increasing dominance of large lianas in Mazonian forests. *Nature* 418, 770–774. doi: 10.1038/nature00926

Putz, F. E. (1984). The natural history of lianas on Barro Colorado Island, Panama. *Ecology* 65, 1713–1724. doi: 10.2307/1937767

Schnitzer, S. A. (2005). A mechanistic explanation for global patterns of liana abundance and distribution. *Am. Nat.* 166, 262–276. doi: 10.1086/431250

Schnitzer, S. A. (2018). Testing ecological theory with lianas. *New Phytol.* 220, 366–380. doi: 10.1111/nph.15431

Schnitzer, S. A., and Bongers, F. (2002). The ecology of lianas and their role in forests. *Trends Ecol. Evol.* 17, 223–230. doi: 10.1016/S0169-5347(02)02491-6

Schnitzer, S. A., and Bongers, F. (2011). Increasing liana abundance and biomass in tropical forests: emerging patterns and putative mechanisms. *Ecol. Lett.* 14, 397–406. doi: 10.1111/j.1461-0248.2011.01590.x

Schnitzer, S. A., Dalling, J. A., and Carson, W. (2000). The impact of lianas on tree regeneration in tropical forest canopy gaps: evidence for an alternative pathway of gap-phase regeneration. *J. Ecol.* 88, 656–666. doi: 10.1046/j.1365-2745.2000.00489.x

Schnitzer, S. A., and van der Heijden, G. M. F. (2019). Lianas have a seasonal growth advantage over co-occurring trees. *Ecology* 100, e02655. doi: 10.1002/ecy.2655

Tyree, M. T., and Ewers, F. W. (1999). "Hydraulic architecture of woody tropical plants," in *Tropical Plant Ecophysiology*, eds S. S. Mulkey, R. L. Chazdon, and A. P. Smith (New York, NY: Chapman and Hall), 217–243. doi: 10.1007/978-1-4613-1163-8_8

van der Heijden, G., Powers, J. S., and Schnitzer, S. A. (2015). Lianas reduce forest-level carbon accumulation and storage. *PNAS* 112, 13267–13271. doi: 10.1073/pnas.1504869112

van der Heijden, G. M., Schnitzer, S. A., Powers, J. S., and Phillips, O. L. (2013). Liana impacts on carbon cycling, storage and sequestration in tropical forests. *Biotropica* 45, 682–692. doi: 10.1111/btp.12060

Wyka, T. P., Oleksyn, J., Karolewski, P., and Schnitzer, S. A. (2013). Phenotypic correlates of the lianescent growth form: a review. *Ann. Botany* 112, 1667–1681. doi: 10.1093/aob/mct236

Yanoviak, S., and Schnitzer, S. (2013). "Functional roles of lianas for forest canopy animals," in *Tree Tops at Risk*, eds L. Devy and Ganesh, May, 209–214. doi: 10.1007/978-1-4614-7161-5_21

frontiers
in Forests and Global Change

ORIGINAL RESEARCH
published: 22 June 2021
doi: 10.3389/ffgc.2021.663291

Lianas Significantly Reduce Aboveground and Belowground Carbon Storage: A Virtual Removal Experiment

Félicien Meunier[1,2]*†, *Geertje M. F. van der Heijden*[3]†, *Stefan A. Schnitzer*[4,5]†, *Hannes P. T. De Deurwaerder*[6]† *and Hans Verbeeck*[1]†

[1] CAVElab – Computational and Applied Vegetation Ecology, Ghent University, Ghent, Belgium, [2] Department of Earth and Environment, Boston University, Boston, MA, United States, [3] School of Geography, University of Nottingham, Nottingham, United Kingdom, [4] Smithsonian Tropical Research Institute, Panama City, Panama, [5] Department of Biological Sciences, Marquette University, Milwaukee, WI, United States, [6] Department of Ecology and Evolutionary Biology, Princeton University, Princeton, NJ, United States

Lianas are structural parasites of trees that cause a reduction in tree growth and an increase in tree mortality. Thereby, lianas negatively impact forest carbon storage as evidenced by liana removal experiments. In this proof-of-concept study, we calibrated the Ecosystem Demography model (ED2) using 3 years of observations of net aboveground biomass (AGB) changes in control and removal plots of a liana removal experiment on Gigante Peninsula, Panama. After calibration, the model could accurately reproduce the observations of net biomass changes, the discrepancies between treatments, as well as the observed components of those changes (mortality, productivity, and growth). Simulations revealed that the long-term total (i.e., above- and belowground) carbon storage was enhanced in liana removal plots (+1.2 $\mathrm{kg_C\ m^{-2}}$ after 3 years, +1.8 $\mathrm{kg_C\ m^{-2}}$ after 10 years, as compared to the control plots). This difference was driven by a sharp increase in biomass of early successional trees and the slow decomposition of liana woody tissues in the removal plots. Moreover, liana removal significantly reduced the simulated heterotrophic respiration (−24%), which resulted in an average increase in net ecosystem productivity (NEP) from 0.009 to 0.075 $\mathrm{kg_C\ m^{-2}\ yr^{-1}}$ for 10 years after liana removal. Based on the ED2 model outputs, lianas reduced gross and net primary productivity of trees by 40% and 53%, respectively, mainly through competition for light. Finally, model simulations suggested a profound impact of the liana removal on the soil carbon dynamics: the simulated metabolic litter carbon pool was systematically larger in control plots (+51% on average) as a result of higher mortality rates and faster leaf and root turnover rates. By overcoming the challenge of including lianas and depicting their effect on forest ecosystems, the calibrated version of the liana plant functional type (PFT) as incorporated in ED2 can predict the impact of liana removal at large-scale and its potential effect on long-term ecosystem carbon storage.

Keywords: tropical lianas, liana removal experiment, vegetation modeling, carbon stocks and fluxes, ecosystem demography model 2

Edited by:
Jürgen Homeier,
University of Göttingen, Germany

Reviewed by:
Frans Bongers,
Wageningen University and Research,
Netherlands
Emilio Vilanova,
University of California, Berkeley,
United States
Florian Hofhansl,
International Institute for Applied
Systems Analysis (IIASA), Austria

Correspondence:
Félicien Meunier
felicien.meunier@gmail.com

†*ORCID:*
Félicien Meunier
orcid.org/0000-0003-2486-309X
Geertje M. F. van der Heijden
orcid.org/0000-0002-2110-5173
Stefan A. Schnitzer
orcid.org/0000-0002-2715-9455
Hannes P. T. De Deurwaerder
orcid.org/0000-0002-9287-2062
Hans Verbeeck
orcid.org/0000-0003-1490-0168

Specialty section:
This article was submitted to
Tropical Forests,
a section of the journal
Frontiers in Forests and Global
Change

Received: *02 February 2021*
Accepted: *31 May 2021*
Published: *22 June 2021*

Citation:
Meunier F, van der Heijden GMF,
Schnitzer SA, De Deurwaerder HPT
and Verbeeck H (2021) Lianas
Significantly Reduce Aboveground
and Belowground Carbon Storage:
A Virtual Removal Experiment.
Front. For. Glob. Change 4:663291.
doi: 10.3389/ffgc.2021.663291

INTRODUCTION

Lianas (woody vines) are an important yet overlooked component of tropical forests (Schnitzer, 2018). As structural parasites, they climb tree stems to reach the forest canopy (Stevens, 1987) and in doing so, avoid massive carbon investment in self-supporting tissues (Ewers et al., 2015). Lianas compete with their hosts for resources with an intensity that has been shown to be stronger than the regular tree-tree competition (Tobin et al., 2012). Although lianas contribute relatively little to forest-level biomass (van der Heijden et al., 2013), they profoundly impact forest dynamics and ecology: liana-infested forests are characterized by slower tree growth (Schnitzer et al., 2014), reduced tree survival (Ingwell et al., 2010) and fecundity (Martínez-Izquierdo et al., 2016), and an overall decline of primary productivity and carbon sequestration (van der Heijden et al., 2015).

In the past few decades, lianas have gained scientific interest as (i) lianas are increasing in abundance and biomass in the Neotropics (Phillips, 2002; Schnitzer and Bongers, 2011), and (ii) liana density is negatively correlated with forest carbon stocks (Durán and Gianoli, 2013). Understanding liana ecology requires observational and experimental assessments of their impact in tropical forests (Schnitzer and Bongers, 2002). Observational studies measure growth-form differences of observable traits (e.g., leaf nutrient content) or the effects of liana abundance on dynamic variables (e.g., tree growth) in undisturbed forests, while experimental studies aim to compare the biogeochemical cycles of control and manipulated plots. Experimental studies include CO_2 enrichment (Norby and Zak, 2011), nutrient addition (Schnitzer et al., 2020), and liana removal experiments.

Liana removal experiments are a powerful tool to assess the role that lianas play in the biogeochemical cycles of tropical forests (Estrada-Villegas and Schnitzer, 2018). They allow for a comprehensive comparison of forest demography and functioning in liana-free and unmanipulated control plots. Liana removal studies can also help link growth-form specific traits with mechanistic changes of forest-level variables (e.g., tree growth rate, recruitment or reproduction). However, liana removal studies present a suite of logistical challenges: they are time and labor demanding, costly to maintain, and as any experiment, limited in the number and types of possible observations. For instance, as measuring belowground carbon stocks and dynamics is challenging (Freschet et al., 2020), below-ground assessment of liana impacts is currently almost systematically overlooked in liana removal experiments.

Dynamic mechanistic modeling of liana-tree interactions has been recently identified as one of the four essential challenges for global change science relating to lianas (Marshall et al., 2020). Process-based vegetation models may mediate the logistical challenges of conducting liana removal experiments in-situ by extending their findings to exhaustively describe forest biogeochemical cycles, including these occurring belowground (Fisher et al., 2018). They can specifically help to predict the forest recovery response after a liana infestation or a liana removal experiment and the underlying response mechanisms (Marshall et al., 2020). Vegetation models can also serve as platforms to integrate trait measurements and/or observed impacts of an experimental design (Dietze and Latimer, 2011). Finally, they have the potential for upscaling in time and space with virtually no additional cost (Snell et al., 2014). Yet, to realistically simulate tropical forest dynamics, vegetation models need to mechanistically account for processes specific to the lianescent growth form (Verbeeck and Kearsley, 2015) and require extensive quality datasets for calibration and validation (Schnitzer et al., 2016).

Despite their importance, lianas have only recently been incorporated in vegetation models, specifically by the introduction of a liana plant functional type (PFT) into the Ecosystem Demography model, version 2 (ED2; di Porcia e Brugnera et al., 2019). Dynamic model simulations confirmed the negative impact of lianas on the ecosystem carbon sequestration capacity, especially in young and secondary forests (di Porcia e Brugnera et al., 2019). The liana PFT in ED2 was recently updated to include a mechanistic representation of water competition and to include the most up-to-date observations of liana traits (Meunier et al., 2020). Yet, so far, the vegetation model simulations have not pursued a virtual impact assessment of liana removal on tree competition and forest-level carbon dynamics.

This study presents the proof of concept that ED2 and its liana PFT can be calibrated against the field data of a removal experiment in order to (i) provide new insights into the mechanisms governing liana and tree competition, and (ii) extend the findings of such a liana removal experiment. More generally, this is an illustration of how experimental data and vegetation models can work synergistically to deliver more comprehensive results than those provided by either approach alone.

MATERIALS AND METHODS

Liana Removal Experimental Data

We tried to replicate and extend the results of an ongoing liana removal experiment on Gigante Peninsula in Panama (van der Heijden et al., 2015). Gigante Peninsula is located on a mainland peninsula within the Barro Colorado Nature Monument (BCNM) and supports a mix of early and late secondary seasonally moist lowland forest. The nearby weather station of Barro Colorado Island (BCI) fluxtower recorded an average temperature of 26°C and an average annual rainfall of 2,640 mm between 2004 and 2016 (Detto et al., 2018), with a pronounced dry season of 4 months (total rainfall between late-December and mid-April is about 175 mm on average). Sixteen 80 m × 80 m plots were established in 2008 within the then approximately 60 years old forest area of Gigante Peninsula. In 2011, all lianas and trees ($\geq$1 cm) within the central areas (60 m × 60 m) of these plots were inventoried. In March 2011, all lianas were cut in half of the plots and left on site for decomposition. These manipulated plots were kept liana-free by cutting resprouting lianas at regular time intervals (i.e., monthly for the first 2 months and bimonthly for the next 6 months).

The change in diameter at breast height (DBH) of all trees ($\geq$10 cm) was then monitored twice yearly, at the beginning of the dry and the wet season, using dendrometer bands and electronic calipers. The resulting tree diameters were converted into aboveground biomass (AGB) using the pantropical allometric equation of Chave et al. (2005) for tropical moist forest, wood density estimates, and a local DBH-height relationship (van der Heijden et al., 2015). Wood density estimates were assigned to every tree record, using first locally measured wood samples, then the Global Wood Density Database (Zanne et al., 2009), and finally a site-based average wood density value (van der Heijden et al., 2015) when local and global data were unavailable. The changes in diameter of lianas $\geq$ 5 cm were also tracked in the control plots and similarly converted into biomass through a liana-specific allometric equation (Schnitzer et al., 2006; van der Heijden et al., 2015). The measurements of tree and liana DBH increments and the successive inventories provided estimates of biomass change due to growth, recruitment, stem productivity (as the sum of growth and recruitment), and mortality in all control and removal plots. In addition, for 3 years (between 2011 and 2014 starting in the second month after liana cutting, to exclude the initial pulse of dead liana leaves after removal), 80 litterfall traps were deployed in the 16 forest plots. Their analysis provided estimates of the canopy productivity. Total aboveground productivity was then computed by summing up the canopy productivity and the stem productivity. A complete description of all methods and experimental results are available in the original publication (van der Heijden et al., 2015).

Vegetation Model

The Ecosystem Demography Model

The Ecosystem Demography model is a cohort-based terrestrial biosphere model that accounts for inter- and intra-growth-form diversity as well as the horizontal and vertical heterogeneity of the simulated ecosystem (Medvigy et al., 2009). In ED2, plants are grouped in cohorts that are defined by their size (DBH) and the plant functional type (PFT) to which they belong (Moorcroft et al., 2001). PFTs represent a set of physiological, morphological, and life-history traits that mechanistically define how different plant types utilize resources (Fisher et al., 2010). Each cohort grows in a forest patch, which represents the forest areas that share a similar forest disturbance history. These two hierarchical levels (cohorts and patches) are spatially implicit: neither the horizontal position of trees nor the spatial arrangement of patches are determined by the model. Instead, ED2 computes the plant density of all cohorts and the relative area of every single patch (i.e., the probability of finding a forest portion sharing the same disturbance history), as well as their dynamics (i.e., temporal changes in plant density of every cohort due to the simulated demographic processes, and in relative area of every patch due to new disturbance events and ageing).

Among other biophysical processes, ED2 simulates soil hydrology (Walko et al., 2000), plant hydraulics (Xu et al., 2016), leaf-level photosynthesis (Farquhar et al., 1980), land-atmosphere radiative transfers (Sellers, 1985; Liou, 2002), and soil carbon decomposition (Bolker et al., 1998). At the cohort level, the ED2 model uses DBH-dependent allometric equations to partition the carbon available from net assimilation into the different plant pools (leaf, stem woody biomass, sapwood, and fine and coarse roots). Cohort carbon balance is determined by the difference between the cohort gross productivity on one hand, and the respiration (leaf and fine-roots, storage turnover, growth and maintenance respiration) and turnover of tissue on the other hand (Longo et al., 2019a). A negative cohort carbon balance can lead to starvation and hence increased mortality, which adds to the background constant ageing (PFT-dependent) and treefall (PFT-independent) mortality rates. Tissue turnover and mortality, in turn, increase soil carbon stocks. Following a simplified version of the CENTURY model (Bolker et al., 1998), ED2 considers three soil carbon pools, defined by their characteristic lifetime: fast (metabolic litter and microbial hereafter referred to as FSC), intermediate (structural debris or StructSC), and slow (humified and passive soil carbon or SSC). Through mortality and turnover, lignified and non-lignified plant tissues, respectively, feed the fast and intermediate soil carbon pools (**Figure 1**, left). For more details, we refer to the complete model description (Longo et al., 2019a) and to **Supplementary Appendix A** for the soil carbon decomposition submodel.

The Liana Plant Functional Type

Recently, a new PFT was introduced in ED2 to mechanistically account for lianas (di Porcia e Brugnera et al., 2019). It was further developed by Meunier et al. (2020) to (i) include most recent model developments related to root water uptake and plant hydraulics, (ii) enable liana-included simulations starting from prescribed initial conditions (inventory), and (iii) parameterize it according to the latest literature. In short, lianas are the only PFT in the model that cannot grow freely in height, but need the structural support from neighbors (i.e., trees within the same patch). Liana cohorts can only outgrow the tallest free-standing plant cohort by a small height threshold (0.5 m) as they lack self-supporting tissues to grow beyond this height limit. In addition, the model simulates: (i) the liana propensity for vegetative reproduction by allocating more of the available carbon, once their maintenance and respiration costs are met, to reproduction as compared to trees; (ii) the enhanced survival of lianas to treefall and their ability to resprout from such disturbances events; and (iii) the liana-specific carbon allocation strategies. Details of implementation are available in the aforementioned publications.

Initial Conditions

Model simulations were initialized using the tree and liana inventories of 2011 that occurred immediately before liana removal. Trees were classified into the ED2 default tropical tree PFTs (i.e., early, mid, and late-successional tropical trees) using available species wood density estimates and the model default mid-range values (0.62 and 0.81 g cm^{-3}) as class-separators (Longo et al., 2019a). Doing so, 101 and 62 of the 171 identified species were, respectively, classified as early- and mid-successional tree species (**Supplementary Figure B1**). The choice of the ED2 default class breaks resulted in a majority of early- (56.3%) and mid-successional (40%) tree individuals. The tree classification led to no differences of tree density per size class and PFT between treatments (control *vs.* removal),

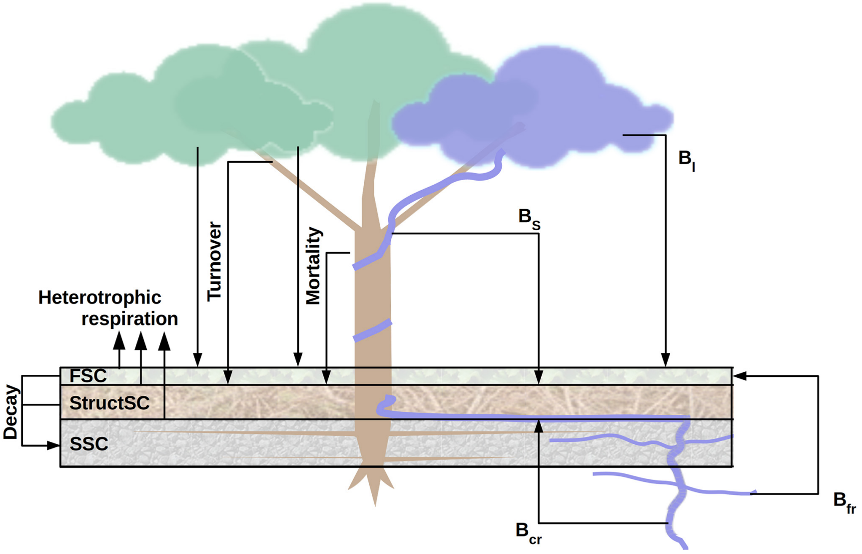

FIGURE 1 | Schematic overview of the carbon fluxes driving the soil carbon pools (left) and of the virtual liana removal experiment (right). In ED2, three soil carbon pools are simulated: the fast (FSC), the structural (StructSC) and the slow (SSC) carbon pools. The former two can decompose into the latter one and all three are partly responsible for heterotrophic respiration. Plant tissue turnover and mortality are direct inputs of the fast and structural soil carbon pools. To simulate the removal experiment, liana leaf (B_l) and fine root (B_{fr}) biomass was sent to the fast soil carbon pool while stem (B_s) and coarse root (B_{cr}) biomass was transferred into the structural soil carbon pool.

see **Supplementary Figure B2**. All lianas were allocated to a unique PFT (**Supplementary Figure B3**). All runs were initiated with eight 60 m × 60 m patches (either eight control or eight removal plots).

Soil carbon storage was initialized using the SoilGrids database (Hengl et al., 2017). Total soil carbon stocks from SoilGrids were split into the three soil pools required by ED2 using equilibrium fractions simulated by model spin up runs. In the removal simulations, liana leaf and fine root biomass were transferred to the fast soil carbon pool, whilst woody stem and coarse root biomass were transferred to the structural soil carbon pool (**Figure 1**, right).

Inventoried lianas were not included in the removal plots and the liana PFT was turned off in the removal runs, preventing their re-growth and the need for active virtual cutting after the initial removal. Following Meunier et al. (2020), liana initial height was determined by their size and the height distribution of the surrounding trees so that all lianas with a stem diameter > 3 cm reached the top of the forest canopy [based on Kurzel et al. (2006)].

Model Calibration

Parameter optimization was achieved within the Predictive Ecosystem Analyzer (PEcAn), an ecological workflow management software (LeBauer et al., 2013), using the Bayesian emulator framework developed by Fer et al. (2018). The emulator (or surrogate) approach is a statistical tool used to replace computationally expensive models such as ED2. Emulators are constructed by interpolating a response curve between the knots (i.e., points in the parameter/cost function space where the model has been previously run and its goodness of fit evaluated).

Ecosystem demography model predictions were calibrated against the final (2014) observation of net AGB changes reported by van der Heijden et al. (2015), using the residual sum of squares as the cost function. We made the decision to fit against the 2014 observation to avoid reproducing the earlier and potentially transitional effects of the process of liana removal itself. We calibrated the model using one type of data only, i.e., the net AGB changes and we were therefore able to validate the model predictions against the observed components of the AGB changes and the measurements of aboveground productivity.

To fit the observed net AGB changes, we optimized two types of PFT-specific parameters: the maximum rate of carboxylation (V_{cmax}) and the clumping factor (Ω). The former is a strong regulator of plant cohort primary productivity, while the latter mediates the amount of light that is transmitted through the canopy in the radiative transfer model of ED2. Ω can vary between 0 and 1. These values represent the two extreme situations of a perfectly clumped ($\Omega = 0$, infinite LAI over a tiny area and effectively zero LAI) and perfectly evenly spread canopy ($\Omega = 1$). Ω is an ED2 parameter that contributes a lot to the model uncertainty while being poorly constrained (Viskari et al., 2019). V_{cmax} is a parameter that is often targeted for calibration in vegetation models, including ED2, given its broad impact on the ecosystem functioning [see for instance Camino et al. (2019); Fer et al. (2018); and Rezende et al. (2013)]. We chose these two parameter types for this model calibration given (i) their nature and their contribution to model predictive uncertainty and (ii) the difficulty to constrain them with observational data when dealing with interspecific competition in ED2 (Meunier et al., 2020). Parameter priors were either uninformative (Ω), expert-informed (tree V_{cmax}) or defined by the meta-analysis of PEcAn (liana V_{cmax}), see **Table 1**. Lianas and trees were both assumed to share the same PFT-specific parameters in removal and control patches. All remaining plant and soil parameters were kept as standard in ED2 (Longo et al., 2019a).

Emulator calibration was run in three rounds, each with 100,000 iterations of three Markov chain Monte Carlo chains, using a total of 750 knots for a total of eight calibrated parameters (two per PFT). Calibrations were run for three simulation years between March 2011 and 2014 (the duration of the experiment).

Model Setup and Analyses

Model ensemble simulations (N = 100) were run with parameter values randomly sampled from the parameter posterior distributions determined by the emulator approach. The control and removal plots were simulated for 10 years starting in March 2011. Differences in biomass, productivity or flux estimates between the removal and control simulations were considered significant when the confidence intervals of the difference of the ensembles did not include zero (cf. van der Heijden et al., 2015). In addition to the discrepancies of carbon accumulation and productivities, we also compared additional model outputs between treatments, such as leaf water potential, seed biomass production or light interception.

The meteorological drivers of Powell et al. (2017) for the closeby BCI were used in all the simulations of this study. These drivers were specifically adjusted from the local fluxtower to the ED2 format, and include shortwave (direct and diffuse) and longwave downward irradiances, the zonal and meridional wind speeds, air temperature, pressure and specific humidity, as well as the precipitation rate.

To identify the environmental drivers of the liana-tree competition and the overall ecosystem growth, we evaluated the impact of the interannual variability of the meteorological forcing drivers on the model outputs. More specifically, we repeated the 10-years long virtual liana removal experiment described above using a single year of meteorological drivers which was then recycled for 10 years. We then compared the outputs of the 10 runs forced with a single year of drivers with the regular run (i.e., forced with 10 different years of drivers). In these runs, we used the most likely set of parameters, as determined by the emulator approach.

TABLE 1 | Liana and tree prior distributions used in the model calibration alongside with posterior medians.

PFT	Parameter	Prior(a, b)	Posterior median	$CV_{posterior}/CV_{prior}$
Early	V_{cmax}	unif(10, 30)	16.5	0.55
	Ω	unif(0.4, 0.9)	0.77	0.42
Mid	V_{cmax}	unif(5, 25)	12.7	0.65
	Ω	unif(0.4, 0.9)	0.76	0.59
Late	V_{cmax}	unif(1, 15)	5.6	0.91
	Ω	unif(0.4, 0.9)	0.62	0.96
Liana	V_{cmax}	norm(28, 5)	24.6	0.83
	Ω	unif(0.4, 0.9)	0.48	0.62

The values a and b are the constants of the prior distribution function (LeBauer et al., 2013) and represent the extremum values for the uniform (unif) distribution or the mean and the standard deviation for the normal (norm) distribution. Ω is unitless and V_{cmax} is defined at 15°C in μmol_C m^{-2} s^{-1}. CV, coefficient of variation.

The version of ED2 used in this study is the one developed by Meunier et al. (2020), which is available on Github at https://github.com/femeunier/ED2 (tag Liana_v.1). All functions, scripts, and inputs developed for this study were also uploaded on Github: https://github.com/femeunier/LianaRemoval.

RESULTS

Model Calibration

Targeted model parameters were successfully constrained by the model calibration: the coefficients of variation (CV) of the posterior distributions were all smaller than the CV of the prior distributions (**Table 1**). In the run with the lowest cost function, the net aboveground productivity and biomass changes during the third year of experiment reached on average 0.037 and 0.264 $\mathrm{kg_C}$ $\mathrm{m^{-2}}$ $\mathrm{yr^{-1}}$ in the control and removal plots respectively, which were similar to the observations from the liana removal experiment (0.037 and 0.261 $\mathrm{kg_C}$ $\mathrm{m^{-2}}$ $\mathrm{yr^{-1}}$). These results were obtained with lower maximum carboxylation rates and clumping factors closer to 1 for trees than for lianas (**Table 1**, see also **Supplementary Figure C1**). The higher V_{cmax} of lianas indicates higher primary leaf-level productivity for lianas while the smaller Ω (closer to 0) made their canopies more packed (horizontally clumped).

While not directly targeted by the calibration, the net biomass change and productivity components were also accurately estimated by the calibrated model runs (**Figure 2**). As observed empirically, simulated leaf productivity was significantly higher (p-value < 2e-16) in control patches than in removal patches (simulated: 0.42 vs. 0.33 $\mathrm{kg_C}$ $\mathrm{m^{-2}}$ $\mathrm{yr^{-1}}$, observed: 0.46 vs. 0.39 $\mathrm{kg_C}$ $\mathrm{m^{-2}}$ $\mathrm{yr^{-1}}$). By contrast, forest-level stem productivity significantly increased (p-value < 2e-16) *in silico* when lianas were removed, consistent with the experimental data (simulated: 0.29 vs. 0.42 $\mathrm{kg_C}$ $\mathrm{m^{-2}}$ $\mathrm{yr^{-1}}$; observed: 0.19 vs. 0.28 $\mathrm{kg_C}$ $\mathrm{m^{-2}}$ $\mathrm{yr^{-1}}$). These two contrasting significant findings cancelled each other out when aggregated to the total aboveground productivity in both the simulations and the observations (simulated: 0.71 *vs.* 0.75 $\mathrm{kg_C}$ $\mathrm{m^{-2}}$ $\mathrm{yr^{-1}}$ in control and removal patches respectively, observed: 0.65 vs. 0.67 $\mathrm{kg_C}$ $\mathrm{m^{-2}}$ $\mathrm{yr^{-1}}$).

Calibrated model runs also reproduced the direction of the liana removal impact for tree mortality (i.e., higher rates in control plots). Yet, the model overestimated mortality rates (0.27 *vs.* 0.16 $\mathrm{kg_C}$ $\mathrm{m^{-2}}$ $\mathrm{yr^{-1}}$ in control plots; 0.14 *vs.* 0.09 $\mathrm{kg_C}$ $\mathrm{m^{-2}}$ $\mathrm{yr^{-1}}$ in removal plots) and because of the very stochastic nature of mortality, the model could not reproduce its high interannual variability in either treatment. Simulated biomass recruitment in removal plots was underestimated (0.0032 vs. 0.023 $\mathrm{kg_C}$ $\mathrm{m^{-2}}$ $\mathrm{yr^{-1}}$). Yet, in both simulations and observations, recruitment contributed little to net biomass change: it represented between 6 and 8% of the stem productivity in the observational data and between 1 and 6% in the model outputs.

Because carbon accumulation was higher in removal plots, the difference in aboveground carbon stocks between control and removal patches reduced over time: the initial difference at

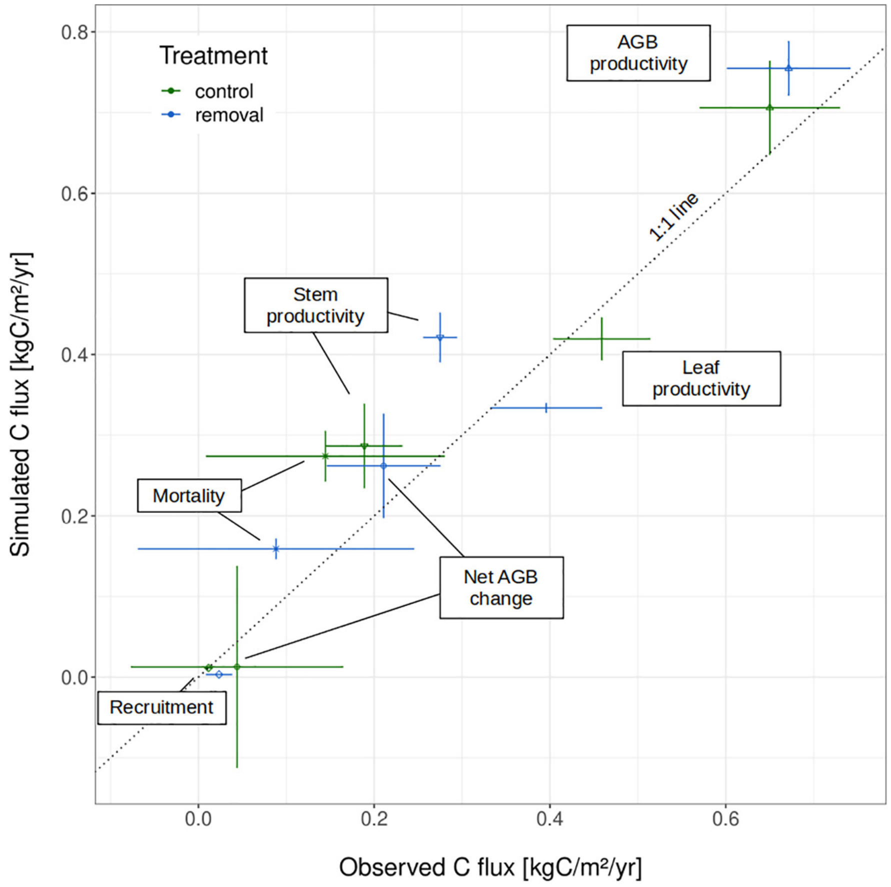

FIGURE 2 | Result of the model calibration: observed vs. simulated carbon fluxes as overaged over the 3 years of experiment (both observed and simulated) and the 100 posterior ensemble runs (simulated only). Liana and tree parameters were optimized to fit the net aboveground biomass (AGB) change during the last year only. The error bars represent the 95% confidence interval of the individual carbon fluxes/productivity components.

the onset of the experiment (+1.04 $\mathrm{kg_C\ m^{-2}}$ in control plot) decreased to +0.41 $\mathrm{kg_C\ m^{-2}}$ (simulations) or +0.52 $\mathrm{kg_C\ m^{-2}}$ (observations) after 3 years (**Figure 3**).

Causes and Consequences of the Liana-Tree Competition

In total, 0.19 $\mathrm{kg_C\ m^{-2}}$ and 1.9 $\mathrm{kg_C\ m^{-2}}$ of liana material were added to the fast and structural soil carbon pools due to removal (**Figure 3**). These transfers resulted in an initial larger belowground carbon stock in removal than in control plots (+1.6 $\mathrm{kg_C\ m^{-2}}$). Yet, in terms of initial total carbon storage, both treatments were indistinguishable from each other (19.7 ± 0.9 $\mathrm{kg_C\ m^{-2}}$ in control plots *vs.* 20.1 ± 0.9 $\mathrm{kg_C\ m^{-2}}$ in liana removal plots, see **Figure 3**). After 5 years of simulation, AGB in the liana removal plots reached that of the control plots (**Figure 4**), driven by a sharper increase of early successional tree biomass in liana-free patches (+1.1 $\mathrm{kg_C\ m^{-2}}$ in the liana removal plots, and only +0.1 $\mathrm{kg_C\ m^{-2}}$ in the control plots).

After 10 years of simulation, belowground carbon stocks were still larger in the liana removal plots. This was due in part because of faster increase in tree belowground biomass, but mostly because of the slow decomposition rates of the structural debris from the cut lianas (**Figure 3**). The decay of liana woody tissues led to a steep increase in simulated dissolved organic matter (**Figure 5**). The fast structural soil carbon pool rapidly became larger when lianas were simulated, after an initial transition due to the virtual removal (**Figure 5**). The increase in carbon of the FSC pool in control plots was driven by the faster leaf and fine root turnover of lianas and the increased mortality of trees in control plots. Slower soil carbon pools (StructSC and SSC) were relatively stable over time in control patches while the fast soil carbon pool rapidly reached a seasonal equilibrium in both treatments. All together, the soil carbon pools of both treatments slowly converged but the total soil carbon storage remained significantly lower in control plots during the 10 years of experiment (−1.74 $\mathrm{kg_C\ m^{-2}}$ after 3 years, −1.39 $\mathrm{kg_C\ m^{-2}}$ after 5, and −1.02 $\mathrm{kg_C\ m^{-2}}$ after 10 years). The higher soil carbon stocks combined with a sharp increase of the aboveground carbon accumulation in the liana-free plots led to significantly larger total carbon stocks in the liana removal plots after 3 (+1.2 $\mathrm{kg_C\ m^{-2}}$) and 10 (+1.8 $\mathrm{kg_C\ m^{-2}}$) years of simulation (**Figures 3**, **4**).

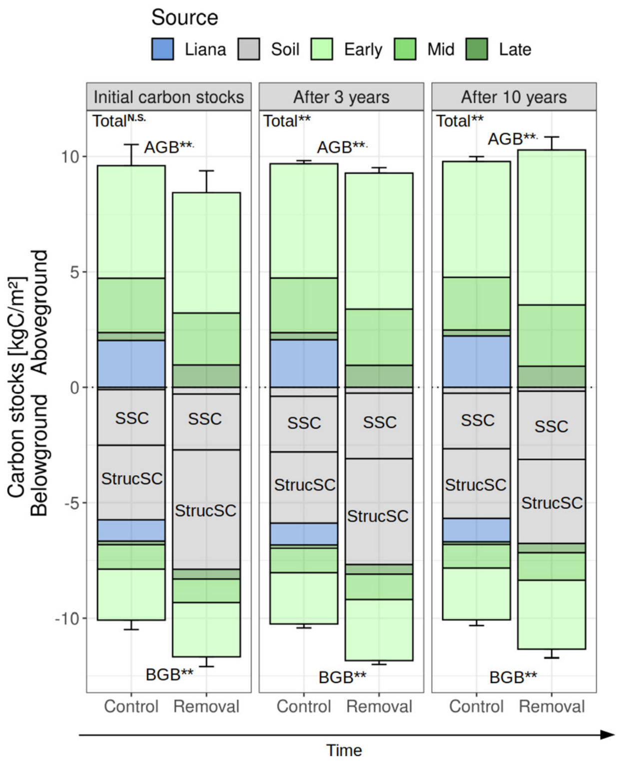

FIGURE 3 | Carbon stock changes over time in control and removal plots. Carbon stocks were splitted into their aboveground (>0) and belowground (<0) components as well as according to their source (PFT and/or soil). Soil carbon is divided into its three pools (SSC, slow soil carbon; StrucSC, structural soil carbon and the unannotated soil pool is the FSC or fast soil carbon pool). Bar plots and error bars denote median and 95% confidence intervals of the 100 members ensemble posterior runs (3 or 10 years of simulation) or the inter-patch variability (initial conditions). For the significance, we tested the difference between simulated control and removal plots for the aboveground (AGB), belowground (BGB), and total biomass at the 95% confidence level: $^{**}P \leq 0.05$; N.S. not significant ($P > 0.10$).

Overall, the carbon cycle of forest patches was profoundly impacted by the liana removal. Heterotrophic respiration was higher in control patches than in liana removal patches (1.75 vs. 1.37 $\text{kg}_\text{C}\ \text{m}^{-2}\ \text{yr}^{-1}$, **Figure 6**). This significantly affected the net ecosystem productivity (NEP), which increased by almost one order of magnitude when lianas were removed over the 10 years of the simulation (+0.066 $\text{kg}_\text{C}\ \text{m}^{-2}\ \text{yr}^{-1}$, on average). The liana removal effect on the NEP varies over the years and ranged between +0.04 and +0.16 $\text{kg}_\text{C}\ \text{m}^{-2}\ \text{yr}^{-1}$, depending on the incoming PAR radiation that significantly impacted GPP (**Figure 7**, R^2 of the linear model are 0.54 and 0.64 for the control and removal plots respectively). Because of the reduction in total leaf area, forest-level gross (GPP) and net (NPP) primary productivity remained on average smaller in liana removal plots over the 10 years of the virtual experiment (−0.56 $\text{kg}_\text{C}\ \text{m}^{-2}\ \text{yr}^{-1}$ and −0.34 $\text{kg}_\text{C}\ \text{m}^{-2}\ \text{yr}^{-1}$, respectively). However, this was the result of the large contribution of lianas to gross (39%) and net (48%) primary productivity. GPP and NPP of trees themselves increased by 40 and 53% in liana removal plots.

Liana removal triggered a strong increase in tree light interception. Controlling for the leaf area, the net PAR radiation intercepted by tree leaves increased by 42% in patches where lianas had been removed, leading to a strong increase in GPP for all tree PFTs (**Table 2**). This rise in photosynthesis was accompanied by a proportional increase in transpiration. Liana contribution to transpiration (40%) was not compensated by the increase in transpiration of all tree PFTs combined, so that overall ecosystem evapotranspiration decreased by 0.40 mm d^{-1} in removal plots (**Table 2**).

The contribution of lianas to the ecosystem LAI increased slightly during the simulation: they initially represented 24% of the total LAI and ended up contributing to 32% after 10 years (**Table 2**). The ecosystem LAI of both treatments converged rapidly: while the liana removal made the control plot total leaf area higher (+1.22 $\text{m}^2\ \text{m}^{-2}$), the difference disappeared over time (after 3 years: +0.24 ± 0.21 $\text{m}^2\ \text{m}^{-2}$; after 10 years: −0.03 ± 0.11 $\text{m}^2\ \text{m}^{-2}$).

DISCUSSION

In this study, we demonstrate that the ED2 model, once calibrated, could reproduce different aspects of the liana-tree competition, as well as the plot-level impact of liana removal. The calibrated version of the model could not only replicate the observations of net biomass change that were used for calibration but also their components and the leaf and wood productivities. The fact that the optimized parameter distributions are realistic (**Supplementary Figure C1**) increases the confidence in the model predictions. This work extends the successful use of ED2 in a variety of eco-climatic regions, ranging from boreal (Ise and Moorcroft, 2010) to tropical (Longo et al., 2019b) ecosystems, by simulating experimental conditions, such as the liana removal experiment described in van der Heijden et al. (2015).

Ecosystem-Level Effect of Liana Removal

Our model simulations showed that due to the removal of liana leaves, the photosynthetically active radiation that reached the ground increased on average by 15% in the liana-free plots during the first 2 years of the simulation. The sharp initial increase in understory light availability upon removal quickly decreased and after 4 years, both treatments were indistinguishable. These numerical results are very similar to the findings of Rodríguez-Ronderos et al. (2016) who measured a light attenuation of around 20% in control plots of the same experimental site that was replicated here. Yet, 4 years after the initial cutting, there were no more differences of light reaching the ground between liana-rich and liana-free plots (Rodríguez-Ronderos et al., 2016), which indicates that trees had fully compensated for the loss of liana leaves as in the model simulations. The rapid convergence of total leaf area in both treatments, as simulated by the model, was also observed in 17 natural treefall gaps that served for another liana removal experiment (Schnitzer and Carson, 2010) and through 30 forest stands in a landscape liana removal experiment (Estrada-Villegas et al., 2020), both in Panama. The strong impact

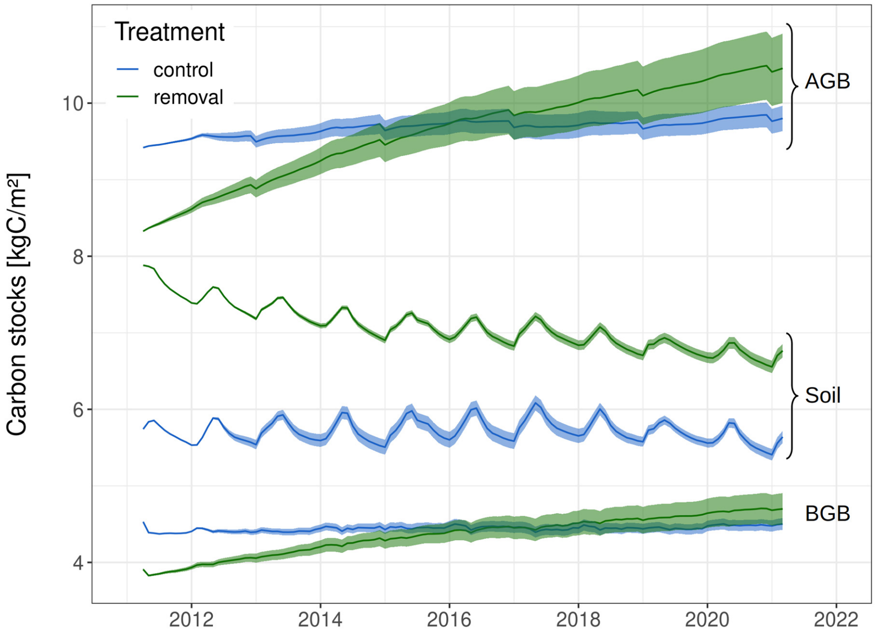

FIGURE 4 | Time Series of all carbon pools: total of all four PFT aboveground (AGB), and belowground (BGB) carbon biomass as well as total soil carbon stocks. Light envelopes represent the 95% confidence intervals of the 100 ensemble posterior runs.

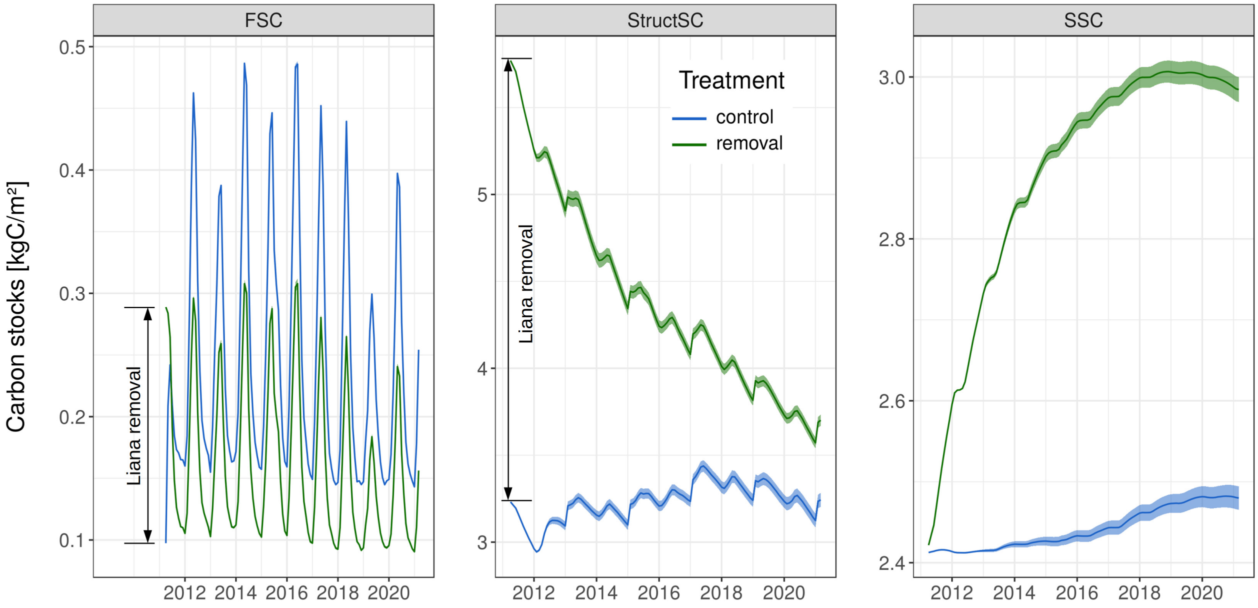

FIGURE 5 | Time series of the three soil carbon pools. Initial differences in the fast (FSC) and the structural (StructSC) soil carbon pools are due to the addition of liana living and woody tissues to these two respective pools during removal. The slow decomposition of liana woody tissues leads to a strong increase of the slow soil carbon (SSC) pool in removal plots. The shaded envelopes encompass the 95% confidence interval of the 100 ensemble members' posterior runs.

of lianas on light availability was also confirmed by measurements in an Amazonian dry forest in which light canopy transmission doubled after removal and remained significantly larger in liana-cut plots for 2 years (Gerwing, 2001). The release of the light competition intensity upon removal is compatible with larger canopy openness, enhanced light penetration, and hence faster growth rates of tree seedling observed once lianas were cut in dry forests of Bolivia and Brazil (Pérez-Salicrup, 2001; César et al., 2016).

Using the large-scale liana removal facility simulated in this study, Reid et al. (2015) found that liana removal significantly increased short-term (<4 months) surface (10 cm depth) water

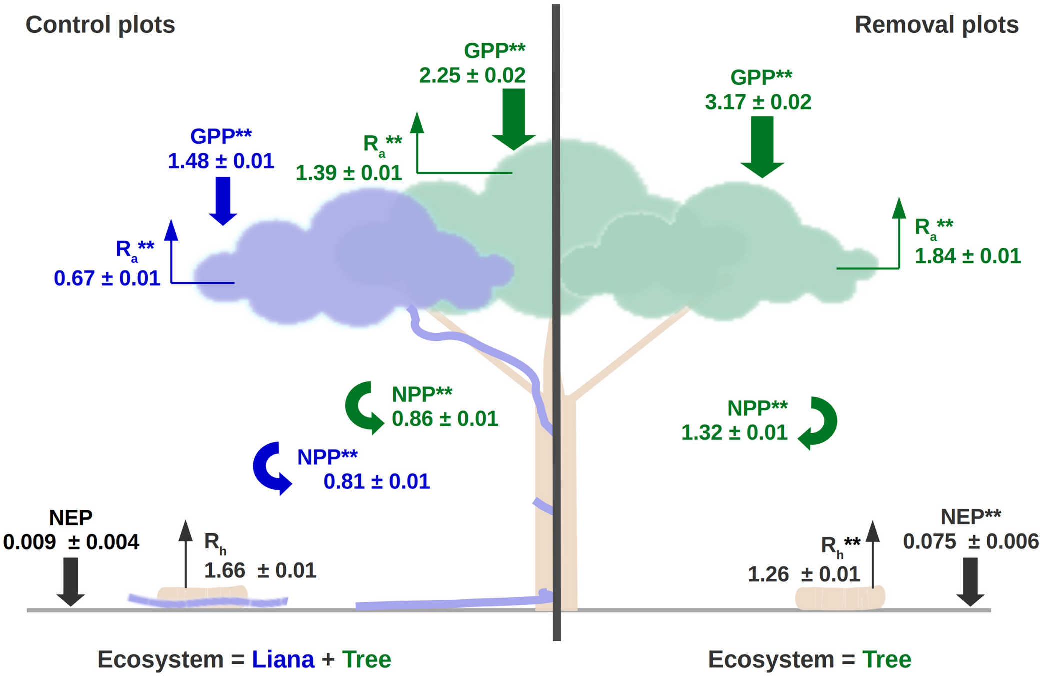

FIGURE 6 | Average carbon cycle of the control (left) and liana-removal (right) plots over the 10 years of simulation of the liana-removal experiment and the 100 posterior ensemble runs. Plant fluxes (GPP, NPP, and R_a) were divided into liana (blue) and self-supporting tree (green) components. We tested the impact of treatment (control vs. removal) on both the ecosystem (black, right hand-side) and the PFT variables (colors, left hand-side) at the 95% confidence level: $^{**}P \leq 0.05$; N.S. not significant ($P > 0.10$). Fluxes are summarized by their mean ± one standard deviation deviation and all have units of $kg_C\ m^{-2}\ yr^{-1}$. GPP, gross primary productivity; NPP, net primary productivity; R_a, autotrophic respiration; R_h, heterotrophic respiration; NEP, net ecosystem productivity.

TABLE 2 | Summary of the initial and final ecosystem states together with the changes due to liana removal in the manipulated plots, grouped by PFT.

			Plant functional type				
			Liana	**Early-successional tree**	**Mid-successional tree**	**Late-successional tree**	**Total**
Initial conditions (2011)	LAI ($m^2_{leaf}\ m^{-2}$)	Control	1.37	3.24	1.10	0.08	5.79
		Removal	–	3.36	1.04	0.17	4.57
	AGB ($kg_C\ m^{-2}$)	Control	1.79	4.59	2.24	0.34	8.96
		Removal	–	4.87	2.11	0.93	7.91
Final conditions (2021)	LAI ($m^2_{leaf}\ m^{-2}$)	Control	1.38	2.32	0.58	0.05	4.33
		Removal	–	3.40	0.81	0.15	4.36
	AGB ($kg_C\ m^{-2}$)	Control	2.20	4.98	1.84	0.26	9.28
		Removal	–	6.90	2.42	0.90	10.22
Changes after liana removal	Intercepted PAR ($10^6\ \mu mol\ m^{-2}_{leaf}\ s^{-1}$)		112	+26 (+41%)	+20 (+47%)	+31 (+64%)	+25 (+42%)
	Transpiration ($mm\ d^{-1}$)		0.97	+0.44 (+39%)	+0.1 (+40%)	+0.03 (+194%)	+0.57 (+40%)
	Midday leaf water potential (MPa)		− 1.02	− 0.17 (+16%)	− 0.08 (+7%)	− 0.24 (+24%)	− 0.15 (+14%)
	Gross primary productivity ($kg_C\ m^{-2}\ yr^{-1}$)		1.48	+0.71 (+39%)	+0.16 (+43%)	+0.05 (+196%)	+0.92 (+40%)
	Seed biomass ($kg_C\ m^{-2}$)		0.003	+0.005 (+83%)	+0.002 (+56%)	+0.001 (+102%)	+0.008 (+82%)

In the "changes after liana removal" rows, the liana contribution represents the average liana state variable in the control plots while the three tree columns sum up the absolute (and the relative) differences between removal and control plots for the 10 years of the virtual liana removal experiment. In those rows, the total column represents the absolute (and relative) changes in the state variables of the trees after removal.

availability and generated persistent (multi-years) wetter deep soil (40 cm depth) layers. In the simulations of the vegetation model, liana removal similarly increased the top- and subsoil water content, but only by 0.2 and 1.2%, respectively. These increases are smaller than those reported by Reid et al. (2015). However, not all experimental studies could detect an effect of lianas on soil moisture. For instance, Pérez-Salicrup (2001) showed that liana abundance did not affect soil water content on either the topsoil layer or at 1 m depth in a lowland forest in Bolivia. The lack of clear patterns in the water content discrepancies between treatments can be easily explained. In the model like in reality, trees begin to exploit immediately after liana removal the water resources that were otherwise used by lianas, which makes the detection of differences in soil moisture very challenging (Tobin et al., 2012; Alvarez-Cansino et al., 2015).

Despite their hardly visible impact on soil water content, lianas do alter the water balance of the forest, especially during seasonal drought (Toledo-Aceves, 2015). The increase of individual tree transpiration simulated by ED2 upon removal was also observed in 53 canopy trees by Alvarez-Cansino et al. (2015), and four canopy trees by Tobin et al. (2012). Liana removal has also been associated with a positive impact on tree leaf water potential (Pérez-Salicrup and Barker, 2000). In our simulations, tree leaf water potentials actually decreased when lianas were removed (**Table 2**) but it did not affect their drought water stress. This was due to an increase of the evaporative demand once lianas were cut combined with a satisfactory water supply, which allowed trees to significantly increase their evapotranspiration. Yet, as illustrated by another study in which liana removal had no effect on leaf water potentials (Barker and Pérez-Salicrup, 2000), the change of tree water status after liana cutting heavily depends on the intensity and the nature of the interspecific water competition.

Liana removal experiments have also evidenced a strong detrimental effect of lianas on tree reproduction (Estrada-Villegas and Schnitzer, 2018). In total, five liana removal experiments have demonstrated that lianas can reduce tree reproduction at both the population and the community levels that persisted for several years after the start of the experiment (Stevens, 1987; Kainer et al., 2006, 2014; César et al., 2017; García León et al., 2018). Our simulations revealed that the tree seed biomass pool increased by 82% over the 10 years of simulation (**Table 2**), with the rate of increase relatively constant over time. Those results corroborate the experimental findings of Kainer et al. (2014) who reported a fruit production increase of 77% in the liana removal treatment plots, up to 10 years after removal.

Empirical vs. Process-Based Models

After simulating 10 years of forest dynamics, our model forecasted a net increase in AGB that was 1.7 $\mathrm{kg_C\ m^{-2}}$ larger in patches where lianas were cut compared to control patches with lianas (i.e., 1.9 vs. 0.2 $\mathrm{kg_C\ m^{-2}}$). This is slightly lower than the 2.1 $\mathrm{kg_C\ m^{-2}}$ difference predicted by van der Heijden et al. (2015) based on an empirical model of the same system. The difference between the data-driven model of van der Heijden et al. (2015) and the process-based model used in this study originates from a faster deceleration of the net biomass increase simulated by the vegetation model. In ED2, the annual increase of total AGB in the liana removal plots rapidly dropped from 4% during the first 2 years to around 1.5% over the last 5 years. In the empirical model of van der Heijden et al. (2015), such annual net biomass change remained larger than 2% for 10 years.

The data-driven modeling approach of van der Heijden et al. (2015) is relatively simple compared to the ED2 model, which is a bigger, heavier to calibrate, and more complex machinery that yet offers multiple advantages. In ED2, it is possible to account for potential liana-induced shifts in forest composition, the increase in liana abundance over time (**Table 2**), and short- and long-term changes in meteorological drivers (**Figure 7**). Process-based model simulations like ED2 also allow for the examination of the mechanisms controlling the contrasting functioning of liana-rich and liana-free forests. Finally, process-based models offer the opportunity to extrapolate the observed AGB changes to unobserved carbon pools even if the conclusions necessarily rely on the model assumptions (di Porcia e Brugnera et al., 2019). For instance, the model showed that belowground plant biomass grew faster in liana removal plots (+0.7 $\mathrm{kg_C\ m^{-2}}$) compared to unmanipulated control plots (+0.05 $\mathrm{kg_C\ m^{-2}}$), while soil carbon remained larger 10 years after liana removal (+1.02 $\mathrm{kg_C\ m^{-2}}$) due to the slow decomposition of liana cut stems, which could not be estimated in the original study.

The model filled the unobserved gaps in the carbon cycle of forest plots in the presence and absence of lianas. Simulations demonstrated that lianas severely reduce both the carbon sink potential and the carbon storage capacity of tropical forests. This finding was due to a strong competition for light between liana and tree leaves (**Table 2**), and a more rapid turnover of carbon fixed in plant material to the atmosphere when lianas were present, as observed by van der Heijden et al. (2015). The higher investment in leaves in control plots (and the resulting lower allocation to woody tissues) generated higher autotrophic and heterotrophic respiration rates, which led to an 88% reduction of NEP compared to its potential value in liana removal plots. Tree productivity was reduced in liana-rich plots due to light competition, and liana removal resulted in a sharp increase in tree light interception (**Table 2**).

Study Limitations and Perspectives

The most important limitation of this study is the relatively short time period of the empirical study (3 years), which reduces our ability to model inter-annual variability. Longer-term monitoring of liana-removal experiments should allow a more thorough constraining of the model parameters and hence a significant reduction of the predictive uncertainties that currently increase with the extrapolation duration (**Figure 4**). Our model runs were limited to 10 years mainly because of this data availability issue, and hence did not simulate the full forest succession. In the model, the early-successional trees benefited the most from the liana removal (**Table 2**) as they share the most similar ecological niches (fast acquisitive, low wood density, high mortality rates). Extending the virtual removal simulations would further alter the carbon storage discrepancies between liana-removal and control plots in the long term but this necessitates longer-term observations of manipulated forests to calibrate or validate the model outputs.

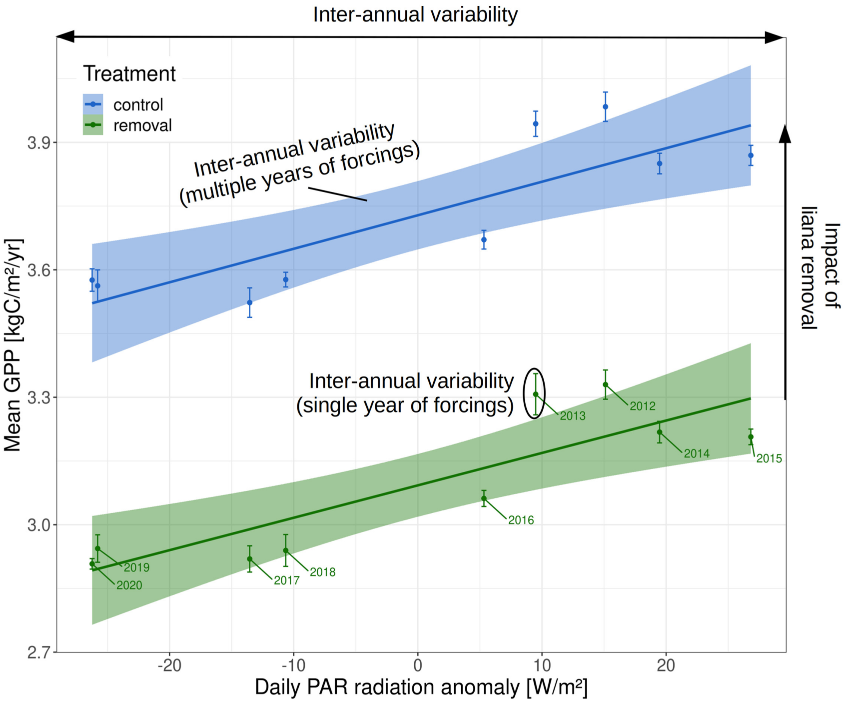

FIGURE 7 | Impact of the inter-annual variability of incoming PAR radiation on the ecosystem productivity in liana removal and control plots. In the plot, it is also possible to compare the magnitude of the model outputs with multiple years of meteorological drivers (linear fits and corresponding ranges) or a single year of meteorological forcing (vertical error bars).

At the start of the simulation, early successional trees were the most abundant PFT, as determined by the species classification based on the observed wood densities of the inventoried species and the default class separators of ED2 (see **Supplementary Figure B1**). A succession dominated by early-successional tree species is typically what ED2 simulates for a relatively young forest (0–75 years), see di Porcia e Brugnera et al. (2019), as this PFT is more broadly defined in ED2 than pioneering (sensu stricto) trees only. Yet, mid- and late-successional trees typically begin to emerge and dominate after a century in ED2 simulations (Longo et al., 2019a), and therefore their late emergence in the succession was not captured here. In this study, we did not quantify the impact of the specific choice of the class separators on the tree-liana quantification. Yet, it is an important variable as it determines the relative contribution of the different tree PFTs to the forest biomass and leaf area. Further analyses should focus on the variance decomposition of model outputs in order to estimate the relative contribution of model parameters, initial conditions, and processes to the overall model uncertainty.

Due to the lack of long-term experimental data, we also chose to calibrate the model only against the last year of net biomass change observation, where the difference between treatments was greatest. This led to an overestimation of the simulated carbon accumulation rate (stem productivity and hence aboveground productivity) in all (but especially in the removal) plots compared to observations in the first 2 years after removal.

Another limitation is that the empirical study was conducted at a single site. Extrapolation of the numerical findings generated here to all tropical forests globally should therefore be performed with caution, until additional data with more diverse origins have been collected and assimilated in the model. Here, the analysis of liana removal experiments in forests with different succession stages, and hence different light, growth and carbon storage responsiveness, seems particularly important. For instance, in the case of an old-growth forest that already reached an equilibrium phase in which lianas and early successional trees are far less abundant, we would expect a more limited impact of liana removal (di Porcia e Brugnera et al., 2019).

Model predictions are also limited by the structure of the model. For instance, plant carbon pools are determined by constant allocation repartition coefficients in ED2, rather than dynamic, resource-driven allocation schemes (Longo et al., 2019a). Simulated belowground woody biomass represents a PFT-specific fraction of the total woody biomass (fixed by default to 30% for all PFTs) just like living tissues are controlled by a user-defined, PFT-specific ratio between below- and AGB (by default, this ratio is fixed to 1). In the model, liana residues exhibit similar decomposition rates as tree residues despite likely different C:N ratios [see Tang et al. (2012)] as the model does not simulate the Nitrogen cycle and hence does not differentiate the soil carbon pools according to their origin (i.e., PFT). We also used the pantropical equation of Chave et al. (2005) coupled to a site-specific height allometry and estimates of woody density from e.g., the Global Wood Density Database (Zanne et al., 2009) to estimate above-ground biomass, which could affect the carbon stocks if species composition differed between the 16 experimental plots. To some extent, the model structure reflects the current state of knowledge on the forest demography and functioning as well as the liana ecology. For instance, it was shown that the ratio of below- to above-biomass production in the tropics is close to the default model parameter value (0.28 vs. 0.30), see Vicca et al. (2012). Yet, model structure and parameters could be updated, should new or site-specific empirical datasets bring contradictory evidence. In the absence of tissue composition, soil carbon and root biomass data, the results related to the impact of lianas on belowground carbon storage and sequestration remain speculative and as such mostly reflect model hypotheses.

This modeling framework provokes multiple additional hypotheses to be tested in future experimental analyses. First, model runs predicted larger amounts of soil organic matter as a result of liana removal, which persisted at least until 10 years after liana removal. This model prediction could still be validated in the field, since the liana-removal experiment on Gigante is ongoing (e.g., García León et al., 2018; Schnitzer and van der Heijden, 2019; van der Heijden et al., 2019). Second, larger litter pools were expected in control plots from the simulations, especially during the dry season (**Figure 5**, FSC pool). Establishing long term litterfall traps should enable a straightforward model validation of these seasonal and treatment effects. Third, the difference in simulated plant belowground biomass between treatments could also be evaluated through digging, sampling, and weighting root biomass in both treatments (Castellanos et al., 1991; Smith-Martin et al., 2020). More generally, the fine-root dynamics in the liana removal experiment and their seasonal fluctuations (Cordeiro et al., 2020) should be investigated in more detail in future experimental studies. Such experiments should allow disentangling two contrasting situations: there are either more (fine) roots in liana removal plots because of the faster tree growth (as simulated in ED2) or there are more (fine) roots in control plots because of the stronger ongoing competition for below ground resources (Cabal et al., 2020). These examples of model-enabled, field-testable hypotheses are a good illustration of an efficient model-data fusion approach: model simulations calibrated on field datasets generated research questions whose evaluation could help refine modeled plant and soil processes.

Such a validated model may allow prediction of the impact of liana infestation at large scale, or identification of the change of forest recovery potential due to lianas in secondary forests. In the future, especially when data from more sites is available, this model could also help to disentangle true liana feedback from driver-controlled thresholds, and parasitoid from bandage effects (Marshall et al., 2020).

CONCLUSION

Process-based models and experimental datasets are complementary tools that, combined, can extend the outcome of either approach used alone. Removal experiments remarkably demonstrated that lianas reduce carbon accumulation and storage in tropical forests (e.g., Schnitzer et al., 2014; van der Heijden et al., 2015, 2019; Estrada-Villegas et al., 2020). Yet, empirical studies do not permit the monitoring of every single carbon stock or flux for practical and financial reasons. Contrastingly, vegetation models can track the specific role of lianas in all forest biogeochemical cycles that they simulate including belowground components, but the accuracy of their prediction relies heavily on the model structure and the quality of the calibration datasets. In this proof-of-concept study, we illustrate how the process-based vegetation model ED2 and its liana plant functional type, calibrated with empirical field data from a liana removal experiment, can bring new insights into the mechanisms of liana-tree competition. A realistic parameter set reproduced the main field observations, i.e., faster aboveground carbon accumulation in removal plots, larger mortality and turnover rates in the control plots. The model further predicted larger net belowground biomass changes in removal plots due to a sharp increase in root biomass of mainly early successional trees, a slow decomposition of liana woody debris and a strong increase in soil organic content. Carbon stocks of removal plots were significantly larger both aboveground and belowground after 10 years of virtual experiment. These and many other testable predictions should now be further validated with longer-term empirical data and could lead to additional novel model developments.

DATA AVAILABILITY STATEMENT

The raw data supporting the conclusions of this article will be made available by the authors, without undue reservation.

AUTHOR CONTRIBUTIONS

FM, GMFvdH, and HV designed the study. FM implemented the workflow, ran the simulations, and analyzed the results with inputs and support from all co-authors. GMFvdH and SS processed the raw data of the liana removal experiment. All authors contributed to the manuscript writing.

FUNDING

This research was funded by the European Research Council Starting Grant 637643 (TREECLIMBERS). The computational resources and services used in this work were provided by the VSC (Flemish Supercomputer Center), funded by the Research Foundation – Flanders (FWO) and the Flemish Government – department EWI. During the preparation of this manuscript, FM was first funded by the BAEF and the WBI as a research fellow and then by the FWO (grant number: 1214720N) as a junior postdoc and is thankful to these organizations for their financial support. HDD was also a BAEF research fellow during the preparation of this manuscript and is grateful to this organization for its support. Financial support for the Gigante Peninsula liana removal study was provided by NSF-DEB 1019436, DEB 1822473, and DEB 2001799.

ACKNOWLEDGMENTS

We are grateful to the whole PEcAn group and the ED2 team for helpful discussions and support related to the functioning of PEcAn and ED2, in particular to Istem Fer for her great assistance in using the PDA for model calibration.

SUPPLEMENTARY MATERIAL

The Supplementary Material for this article can be found online at: https://www.frontiersin.org/articles/10.3389/ffgc.2021.663291/full#supplementary-material

Supplementary Appendix A | Soil carbon pools in ED2.

Supplementary Appendix B | Initial forest composition.

Supplementary Figure B1 | Wood density distribution of the tree individuals **(A)** and tree species **(B)** used to classify the initial tree census into the model PFTs. The vertical dashed lines mark the class separators between the early-, mid-, and late-successional PFTs.

Supplementary Figure B2 | Initial tree size distribution of the control (left) and removal (right) plots. Tree records were classified into the ED2 plant functional types according to their wood density. The error bars represent the inter-patch variability (one standard error) of the total tree density in each size class.

Supplementary Figure B3 | Initial liana size distribution of the liana control plots. The error bars represent the inter-patch variability (one standard error) of the total liana density in each size class. Lianas above 3 cm in size were initially located in the canopy.

Supplementary Appendix C | Supplementary results.

Supplementary Figure C1 | Posterior distributions of the calibrated model parameters. clumping_ factor is unitless and V_{cmax} is defined at 15°C in $\mu mol_C\ m^{-2}\ s^{-1}$. A larger clumping factor indicates a larger light interception per unit of leaf area.

REFERENCES

Alvarez-Cansino, L., Schnitzer, S. A., Reid, J. P., and Powers, J. S. (2015). Liana competition with tropical trees varies seasonally but not with tree species identity. *Ecology* 96, 39–45. doi: 10.1890/14-1002.1

Barker, M. G., and Pérez-Salicrup, D. (2000). Comparative water relations of mature mahogany (Swietenia macrophylla) trees with and without lianas in a subhumid, seasonally dry forest in Bolivia. *Tree Physiol.* 20, 1167–1174. doi: 10.1093/treephys/20.17.1167

Bolker, B. M., Pacala, S. W., and Parton, W. J. (1998). Linear analysis of soil decomposition: insights from the century model. *Ecol. Appl.* 8, 425–439. doi: 10.1890/1051-0761(1998)008[0425:laosdi]2.0.co;2

Cabal, C., Martínez-García, R., Aguilar, A., de, C., Valladares, F., and Pacala, S. W. (2020). The exploitative segregation of plant roots. *Science* 370, 1197–1199. doi: 10.1126/science.aba9877

Camino, C., Gonzalez-Dugo, V., Hernandez, P., and Zarco-Tejada, P. J. (2019). Radiative transfer Vcmax estimation from hyperspectral imagery and SIF retrievals to assess photosynthetic performance in rainfed and irrigated plant phenotyping trials. *Remote Sens. Environ.* 231: 111186.

Castellanos, J., Maass, M., and Kummerow, J. (1991). Root biomass of a dry deciduous tropical forest in Mexico. *Plant Soil* 131, 225–228. doi: 10.1007/bf00009452

César, R. G., Holl, K. D., Girão, V. J., Mello, F. N. A., Vidal, E., Alves, M. C., et al. (2016). Evaluating climber cutting as a strategy to restore degraded tropical forests. *Biol. Conserv.* 201, 309–313. doi: 10.1016/j.biocon.2016.07.031

César, R. G., Rother, D. C., and Brancalion, P. H. S. (2017). Early response of tree seed arrival after liana cutting in a disturbed tropical forest. *Tropical Conserv. Sci.* 10, 1–7.

Chave, J., Andalo, C., Brown, S., Cairns, M. A., Chambers, J. Q., Eamus, D., et al. (2005). Tree allometry and improved estimation of carbon stocks and balance in tropical forests. *Oecologia* 145, 87–99. doi: 10.1007/s00442-005-0100-x

Cordeiro, A. L., Norby, R. J., Andersen, K. M., Valverde-Barrantes, O., Fuchslueger, L., Oblitas, E., et al. (2020). Fine-root dynamics vary with soil depth and precipitation in a low-nutrient tropical forest in the Central Amazonia. *Plant-Environ. Interact.* 1, 3–16. doi: 10.1002/pei3.10010

Detto, M., Wright, S. J., Calderón, O., and Muller-Landau, H. C. (2018). Resource acquisition and reproductive strategies of tropical forest in response to the El Niño–Southern Oscillation. *Nat. Commun.* 9, 1–8.

di Porcia e Brugnera, M., Meunier, F., Longo, M., Moorthy, S. M. K., Deurwaerder, H. D., Schnitzer, S. A., et al. (2019). Modeling the impact of liana infestation on the demography and carbon cycle of tropical forests. *Global Change Biol.* 25, 3767–3780. doi: 10.1111/gcb.14769

Dietze, M. C., and Latimer, A. M. (2011). *Forest Simulators. In Sourcebook in Theoretical Ecology*. Berkeley, CA: University of California Press, 307–316.

Durán, S. M., and Gianoli, E. (2013). Carbon stocks in tropical forests decrease with liana density. *Biol. Lett.* 9, 1–4.

Estrada-Villegas, S., Hall, J. S., van Breugel, M., and Schnitzer, S. A. (2020). Lianas reduce biomass accumulation in early successional tropical forests. *Ecology* 101:e02989.

Estrada-Villegas, S., and Schnitzer, S. A. (2018). A comprehensive synthesis of liana removal experiments in tropical forests. *Biotropica* 50, 729–739. doi: 10.1111/btp.12571

Ewers, F. W., Rosell, J. A., and Olson, M. E. (2015). "Lianas as Structural Parasites," in *Functional and Ecological Xylem Anatomy*, ed. U. Hacke (Cham: Springer International Publishing), 163–188. doi: 10.1007/978-3-319-15783-2_6

Farquhar, G. D., von Caemmerer, S., and Berry, J. A. (1980). A biochemical model of photosynthetic CO2 assimilation in leaves of C3 species. *Planta* 149, 78–90. doi: 10.1007/bf00386231

Fer, I., Kelly, R., Moorcroft, P. R., Richardson, A. D., Cowdery, E. M., and Dietze, M. C. (2018). Linking big models to big data: efficient ecosystem model calibration through Bayesian model emulation. *Biogeosciences* 15, 5801–5830. doi: 10.5194/bg-15-5801-2018

Fisher, R., McDowell, N., Purves, D., Moorcroft, P., Sitch, S., Cox, P., et al. (2010). Assessing uncertainties in a second-generation dynamic vegetation model caused by ecological scale limitations. *New Phytol.* 187, 666–681. doi: 10.1111/j.1469-8137.2010.03340.x

Fisher, R. A., Koven, C. D., Anderegg, W. R. L., Christoffersen, B. O., Dietze, M. C., Farrior, C. E., et al. (2018). Vegetation demographics in earth system models: A review of progress and priorities. *Global Change Biol.* 24, 35–54. doi: 10.1111/gcb.13910

Freschet, G. T., Roumet, C., Comas, L. H., Weemstra, M., Bengough, A. G., Rewald, B., et al. (2020). Root traits as drivers of plant and ecosystem functioning: current understanding, pitfalls and future research needs. *New Phytol.* 2021:63.

García León, M. M., Martínez Izquierdo, L., Mello, F. N. A., Powers, J. S., and Schnitzer, S. A. (2018). Lianas reduce community-level canopy tree reproduction in a Panamanian forest. *J. Ecol.* 106, 737–745. doi: 10.1111/1365-2745.12807

Gerwing, J. J. (2001). Testing liana cutting and controlled burning as silvicultural treatments for a logged forest in the eastern Amazon. *J. Appl. Ecol.* 38, 1264–1276. doi: 10.1046/j.0021-8901.2001.00677.x

Hengl, T., de Jesus, J. M., Heuvelink, G. B. M., Gonzalez, M. R., Kilibarda, M., Blagotić, A., et al. (2017). SoilGrids250m: Global gridded soil information based on machine learning. *PLoS One* 12:e0169748. doi: 10.1371/journal.pone.0169748

Ingwell, L. L., Joseph Wright, S., Becklund, K. K., Hubbell, S. P., and Schnitzer, S. A. (2010). The impact of lianas on 10 years of tree growth and mortality on barro colorado Island, Panama. *J. Ecol.* 98, 879–887.

Ise, T., and Moorcroft, P. R. (2010). Simulating boreal forest dynamics from perspectives of ecophysiology, resource availability, and climate change. *Ecol. Res.* 25, 501–511. doi: 10.1007/s11284-009-0680-8

Kainer, K. A., Wadt, L. H. O., Gomes-Silva, D. A. P., and Capanu, M. (2006). Liana loads and their association with Bertholletia excelsa fruit and nut production, diameter growth and crown attributes. *J. Tropical Ecol.* 22, 147–154. doi: 10.1017/s0266467405002981

Kainer, K. A., Wadt, L. H. O., and Staudhammer, C. L. (2014). Testing a silvicultural recommendation: Brazil nut responses 10 years after liana cutting. *J. Appl. Ecol.* 51, 655–663. doi: 10.1111/1365-2664.12231

Kurzel, B. P., Schnitzer, S. A., and Carson, W. P. (2006). Predicting liana crown location from stem diameter in three Panamanian lowland forests. *Biotropica* 38, 262–266. doi: 10.1111/j.1744-7429.2006.00135.x

LeBauer, D. S., Wang, D., Richter, K. T., Davidson, C. C., and Dietze, M. C. (2013). Facilitating feedbacks between field measurements and ecosystem models. *Ecol. Monogr.* 83, 133–154. doi: 10.1890/12-0137.1

Liou, K. N. (2002). An Introduction to Atmospheric radiation. *Int. Geophys.* 84:583.

Longo, M., Knox, R. G., Medvigy, D. M., Levine, N. M., Dietze, M. C., Kim, Y., et al. (2019a). The biophysics, ecology, and biogeochemistry of functionally diverse, vertically- and horizontally-heterogeneous ecosystems: the Ecosystem Demography Model, version 2.2 — Part 1: Model description. *Geosci. Model Dev.* 12, 4309–4346. doi: 10.5194/gmd-12-4309-2019

Longo, M., Knox, R. G., Levine, N. M., Swann, A. L. S., Medvigy, D. M., Dietze, M. C., et al. (2019b). The biophysics, ecology, and biogeochemistry of functionally diverse, vertically- and horizontally-heterogeneous ecosystems: the Ecosystem Demography Model, version 2.2 &ndash Part 2: Model evaluation. *Geosci. Model Dev.* 12, 4347–4374.

Marshall, A. R., Platts, P. J., Chazdon, R. L., Seki, H., Campbell, M. J., Phillips, O. L., et al. (2020). Conceptualising the global forest response to liana proliferation. *Front. Forests Global Change* 3:35. doi: 10.3389/ffgc.2020.00035

Martínez-Izquierdo, L., García, M. M., Powers, J. S., and Schnitzer, S. A. (2016). Lianas suppress seedling growth and survival of 14 tree species in a Panamanian tropical forest. *Ecology* 97, 215–224. doi: 10.1890/14-2261.1

Medvigy, D., Wofsy, S. C., Munger, J. W., Hollinger, D. Y., and Moorcroft, P. R. (2009). Mechanistic scaling of ecosystem function and dynamics in space and time: ecosystem demography model version 2. *J. Geophys. Res. Biogeosci.* 114:G01002. doi: 10.1029/2008JG000812

Meunier, F., Verbeeck, H., Cowdery, B., Schnitzer, S. A., Smith-Martin, C. M., Powers, J., et al. (2020). Unraveling the relative role of light and water competition between lianas and trees in tropical forests. *J. Ecol.* 109, 519–540. doi: 10.1111/1365-2745.13540

Moorcroft, P. R., Hurtt, G. C., and Pacala, S. W. (2001). A method for scaling vegetation dynamics: the ecosystem demography model (ED). *Ecol. Monogr.* 71, 557–586. doi: 10.1890/0012-9615(2001)071[0557:amfsvd]2.0.co;2

Norby, R. J., and Zak, D. R. (2011). Ecological lessons from free-air CO2 Enrichment (FACE) Experiments. *Ann. Rev. Ecol. Evol. Syst.* 42, 181–203. doi: 10.1146/annurev-ecolsys-102209-144647

Pérez-Salicrup, D. R. (2001). Effect of liana cutting on tree regeneration in a liana forest in Amazonian Bolivia. *Ecology* 82, 389–396. doi: 10.1890/0012-9658(2001)082[0389:eolcot]2.0.co;2

Pérez-Salicrup, D. R., and Barker, M. G. (2000). Effect of liana cutting on water potential and growth of adult Senna multijuga (Caesalpinioideae) trees in a Bolivian tropical forest. *Oecologia* 124, 469–475. doi: 10.1007/pl00008872

Phillips, O. L. (2002). Increasing dominance of large lianas in Amazonian forests. *Nature* 418, 770–774. doi: 10.1038/nature00926

Powell, T., Kueppers, L., and Paton, S. (2017). *Seven years (2008-2014) of meteorological observations plus a synthetic El Nino drought for BCI Panama*.

Reid, J. P., Schnitzer, S. A., and Powers, J. S. (2015). Short and long-term soil moisture effects of liana removal in a seasonally moist tropical forest. *PLoS One* 10:e0141891. doi: 10.1371/journal.pone.0141891

Rezende, L. C., Arenque, B., von Randow, C., Moura, M. S., Aidar, S. D., Buckeridge, M. S., et al. (2013). *Calibration of the maximum carboxylation velocity (vcmax) for the Caatinga for use in dynamic global vegetation models (DGVMs)*. San Francisco, CA: AGU Fall Meeting, 0366.

Rodríguez-Ronderos, M. E., Bohrer, G., Sanchez-Azofeifa, A., Powers, J. S., and Schnitzer, S. A. (2016). Contribution of lianas to plant area index and canopy structure in a Panamanian forest. *Ecology* 97, 3271–3277. doi: 10.1002/ecy.1597

Schnitzer, S. A. (2018). Testing ecological theory with lianas. *New Phytol.* 220, 366–380. doi: 10.1111/nph.15431

Schnitzer, S. A., and Bongers, F. (2002). The ecology of lianas and their role in forests. *Trends Ecol. Evol.* 17, 223–230. doi: 10.1016/s0169-5347(02)02491-6

Schnitzer, S. A., and Bongers, F. (2011). Increasing liana abundance and biomass in tropical forests: emerging patterns and putative mechanisms. *Ecol. Lett.* 14, 397–406. doi: 10.1111/j.1461-0248.2011.01590.x

Schnitzer, S. A., and Carson, W. P. (2010). Lianas suppress tree regeneration and diversity in treefall gaps. *Ecol. Lett.* 13, 849–857.

Schnitzer, S. A., Dewalt, S. J., and Chave, J. (2006). Censusing and measuring lianas: a quantitative comparison of the common methods. *Biotropica* 38, 581–591. doi: 10.1111/j.1744-7429.2006.00187.x

Schnitzer, S. A., Estrada-Villegas, S., and Wright, S. J. (2020). The response of lianas to 20 yr of nutrient addition in a Panamanian forest. *Ecology* 101:e03190.

Schnitzer, S. A., and van der Heijden, G. M. F. (2019). Lianas have a seasonal growth advantage over co-occurring trees. *Ecology* 100:e02655. doi: 10.1002/ecy.2655

Schnitzer, S. A., van der Heijden, G. M. F., Mascaro, J., and Carson, W. P. (2014). Lianas in gaps reduce carbon accumulation in a tropical forest. *Ecology* 95, 3008–3017. doi: 10.1890/13-1718.1

Schnitzer, S. A., van der Heijden, G. M. F., and Powers, J. S. (2016). Reply to Verbeeck and Kearsley: Addressing the challenges of including lianas in global vegetation models. *PNAS* 113, E5–E6.

Sellers, P. J. (1985). Canopy reflectance, photosynthesis and transpiration. *Int. J. Remote Sens.* 6, 1335–1372. doi: 10.1080/01431168508948283

Smith-Martin, C. M., Xu, X., Medvigy, D., Schnitzer, S. A., and Powers, J. S. (2020). Allometric scaling laws linking biomass and rooting depth vary across ontogeny and functional groups in tropical dry forest lianas and trees. *New Phytol.* 226, 714–726. doi: 10.1111/nph.16275

Snell, R. S., Huth, A., Nabel, J. E. M. S., Bocedi, G., Travis, J. M. J., Gravel, D., et al. (2014). Using dynamic vegetation models to simulate plant range shifts. *Ecography* 37, 1184–1197. doi: 10.1111/ecog.00580

Stevens, G. C. (1987). Lianas as structural parasites: The bursera simaruba example. *Ecology* 68, 77–81. doi: 10.2307/1938806

Tang, Y., Kitching, R. L., and Cao, M. (2012). Lianas as structural parasites: A re-evaluation. *Chinese Sci. Bull.* 57, 307–312. doi: 10.1007/s11434-011-4690-x

Tobin, M. F., Wright, A. J., Mangan, S. A., and Schnitzer, S. A. (2012). Lianas have a greater competitive effect than trees of similar biomass on tropical canopy trees. *Ecosphere* 3, 1–11.

Toledo-Aceves, T. (2015). "Above-and belowground competition between lianas and trees," in *The Ecology of Lianas*, eds S. Schnitzer, F. Bongers, R. Burnham, and F. Putz (Hoboken, NJ: Wiley-Blackwell), 149–163.

van der Heijden, G., Powers, J. S., and Schnitzer, S. A. (2015). Lianas reduce forest-level carbon accumulation and storage. *PNAS* 112, 13267–13271. doi: 10.1073/pnas.1504869112

van der Heijden, G., Powers, J. S., and Schnitzer, S. A. (2019). Effect of lianas on forest-level tree carbon accumulation does not differ between seasons: results from a liana removal experiment in Panama. *J. Ecol.* 107, 1890–1900. doi: 10.1111/1365-2745.13155

van der Heijden, G. M., Schnitzer, S. A., Powers, J. S., and Phillips, O. L. (2013). Liana impacts on carbon cycling, storage and sequestration in tropical forests. *Biotropica* 45, 682–692. doi: 10.1111/btp.12060

Verbeeck, H., and Kearsley, E. (2015). The importance of including lianas in global vegetation models. *PNAS* 113:E4.

Vicca, S., Luyssaert, S., Peñuelas, J., Campioli, M., Chapin, F. S., Ciais, P., et al. (2012). Fertile forests produce biomass more efficiently. *Ecol. Lett.* 15, 520–526. doi: 10.1111/j.1461-0248.2012.01775.x

Viskari, T., Shiklomanov, A., Dietze, M. C., and Serbin, S. P. (2019). The influence of canopy radiation parameter uncertainty on model projections of terrestrial carbon and energy cycling. *PLoS One* 14:e0216512.

Walko, R. L., Band, L. E., Baron, J., Kittel, T. G. F., Lammers, R., Lee, T. J., et al. (2000). Coupled atmosphere–biophysics–hydrology models for environmental modeling. *J. Appl. Meteorol.* 39, 931–944. doi: 10.1175/1520-0450(2000)039<0931:cabhmf>2.0.co;2

Xu, X., Medvigy, D., Powers, J. S., Becknell, J. M., and Guan, K. (2016). Diversity in plant hydraulic traits explains seasonal and inter-annual variations of vegetation dynamics in seasonally dry tropical forests. *New Phytol.* 212, 80–95.

Zanne, A. E., Lopez-Gonzalez, G., Coomes, D. A., Ilic, J., Jansen, S., Lewis, S. L., et al. (2009). *Global Wood Density Database (Dryad Digital Repository).*

Conflict of Interest: The authors declare that the research was conducted in the absence of any commercial or financial relationships that could be construed as a potential conflict of interest.

The reviewer FB declared a past co-authorship with one of the author SS to the handling editor.

frontiers
in Forests and Global Change

ORIGINAL RESEARCH
published: 17 August 2021
doi: 10.3389/ffgc.2021.720813

Leaf Anatomical Traits of Lianas and Trees at the Canopy of Two Contrasting Lowland Tropical Forests in the Context of Leaf Economic Spectrum

*Dominica Harrison, J. Antonio Guzmán Q. and G. Arturo Sánchez-Azofeifa**

Centre for Earth Observation Science, Department of Earth and Atmospheric Sciences, University of Alberta, Edmonton, AB, Canada

OPEN ACCESS

Edited by:
Geertje M. F. Van Der Heijden,
University of Nottingham,
United Kingdom

Reviewed by:
Louis S. Santiago,
University of California, Riverside,
United States
Chris Chandler,
University of Nottingham,
United Kingdom

****Correspondence:***
G. Arturo Sánchez-Azofeifa
arturo.sanchez@ualberta.ca

Specialty section:
This article was submitted to
Tropical Forests,
a section of the journal
Frontiers in Forests and Global
Change

Received: *05 June 2021*
Accepted: *28 July 2021*
Published: *17 August 2021*

Citation:
Harrison D, Guzmán Q JA and
Sánchez-Azofeifa GA (2021) Leaf
Anatomical Traits of Lianas and Trees
at the Canopy of Two Contrasting
Lowland Tropical Forests
in the Context of Leaf Economic
Spectrum.
Front. For. Glob. Change 4:720813.
doi: 10.3389/ffgc.2021.720813

The leaf economic spectrum describes a comprehensive framework of how the surrounding environment modulates leaf functional traits (LFT) and how these are associated between them. This framework has traditionally focused on physiological, chemical, and biomass assignation traits, but rarely in leaf anatomical traits. Here we compare leaf anatomical metrics and traits of 40 liana and tree species from two lowland tropical forests in Panama with contrasting rainfall regimes: Parque Natural Metropolitano (dry-forest) and Parque Nacional San Lorenzo (wet-forest). Then we evaluate how anatomical traits are associated with well-established LFTs. Anatomical metrics were collected from leaf cross-section images estimating the area, thickness, cell count, and size of the upper and lower epidermis and palisade and spongy mesophyll. Ratios between metrics were performed as potential anatomical traits to reduce the leaf size effect between species. Our results suggest that anatomical changes between life forms are associated with increases in the palisade area and thickness of trees in comparison with lianas, while anatomical changes between forest type species are related to increases in the spongy area and thickness of wet-forest species than dry-forest. These differences could be associated with the high photosynthetic rates of trees or the need to enhance the gas exchange in humid environments. Our results also suggest that anatomical traits are related to well-established LFT; however, the degree of association between them may depend on the life forms and forest type. For example, our results suggest that reductions in the palisade and spongy cell density are associated with increases in leaf mass area and maximum photosynthetic capacity, but this association was not observed when we compared life forms or forest types. The use of leaf anatomical information may facilitate to describe the mechanism that drives the leaf economy, improving our understanding of the resource allocation strategies embedded in functional groups.

Keywords: life forms, functional traits, leaf mass per area, leaf anatomy, leaf economic spectrum

INTRODUCTION

Leaf economic spectrum (LES) provides a useful framework to describe how leaf traits are inter-correlated and how they are modulated by their surrounding environment (Wright et al., 2004). This theory attempts to transform discrete groups of plant functional types to a more continuum-oriented approach to assess plant functional diversity (Reich, 2014). Currently, the LES has been expanded towards other traits related to wood (Chave et al., 2009), organs such as roots or stems (Reich, 2014; Kong et al., 2019), plant structure (Verbeeck et al., 2019), or even to decomposition rates (Santiago, 2007). Overall, the traits founded in this spectrum are directly associated with the acquisition, processing, and conservation of resources (Reich, 2014); herein, the economic perspective. There are several traits that integrate the current economic spectrum, but those normalized by leaf area or mass have been used predominantly to group functional types based off of resource-investment strategies (Osnas et al., 2013). The most common traits used are leaf mass per area, nitrogen concentration, or maximum photosynthetic capacity that are strongly modulated by climate, latitude, or biome (Reich et al., 1997, 1999; Reich and Oleksyn, 2004; Wright et al., 2005; Reich, 2014). This modulation tends to be a consequence of internal adaptations of the leaf anatomy (upper epidermis, palisade mesophyll, spongy mesophyll, and lower epidermis) responsible for particular processes (i.e., protective cells, light capture, or conductance) (Villar et al., 2013).

The conceptual framework of the LES is rooted in the selective pressures associated with trade-off between the acquisition and conservation of carbon, water, and nutrients (Reich, 2014). Co-variances between the common functional traits, such as Leaf-Mass Area (LMA), leaf nitrogen concentration by mass (N) or photosynthetic capacity ($A_{\max}$), have been used to explore the broader implications of natural selection at the community level (Osnas et al., 2013; Reich, 2014). For instance, the positive relationships between the mass-based traits $\mathrm{N}_{\mathrm{mass}}$ and $A_{\max}$ (mass-based) are used to understand and equalize the productivity per leaf area or the unit of mass investment (Reich, 2014; John et al., 2017). This suggests there is a selective advantage of increased nitrogen leaf content to photosynthetic capacity across species and ecosystems. A deeper exploration of anatomical limitations and facilitations associated with resource acquisition to this spectrum-wide analysis could provide a structural and mechanical perspective of such generalized co-variances driven by selection.

Previous investigations have focused on specific functional traits' relationship and correlation with anatomy. For instance, Villar et al. (2013) and John et al. (2017) looked at co-variances between anatomy and LMA or Pyankov et al. (1999) compared anatomy to specific-leaf area and specific-leaf mass. There appears to be a gap in the literature that broadens the scope of multiple functional traits against multiple anatomical traits that relates to LES. Like the leaf, plant, or wood traits, leaf anatomy is likely to face physiological, structural, and defensive trade-offs (Javelle et al., 2011; Sack and Scoffoni, 2013; Somavilla et al., 2014; Onoda et al., 2017). At any given time, the variability of leaf anatomy depends on the species nature and the surrounding pressure on their growth and development (Tichá, 1985; Oguchi et al., 2003; Xiao et al., 2016). The lack of systematic anatomical deconstruction associated with leaf traits creates an incomplete representation of the mechanics by how the LES varies between plants and environments. For example, several anatomical features appear to be important for photosynthesis, such as the palisade thickness, mesophyll cell density, or air spaces that mediate photosynthetic rates, to mention some (Kenzo et al., 2004; Lehmeier et al., 2017). Currently, studies by Liu et al. (2019) suggest that anatomical traits tend to present a weak correlation with leaf economic traits in temperate and subtropical species. However, in tropical species, there is little information regarding how anatomical traits influence leaf traits in different growth forms and how these relationships vary according to ecosystems. The latter is crucial because as a theory LES must be applied equally to different species within the same ecosystem; even those that coexist together and present distinguishing physiological, biochemical, and optical traits such as the case of lianas and trees (Sánchez-Azofeifa et al., 2009; Asner and Martin, 2012; Slot and Winter, 2017; Werden et al., 2017; Guzmán et al., 2018; Guzmán and Sanchez-Azofeifa, 2021).

Lianas –woody vines– are non-self-supporting plants that use host trees to access canopy light, probably affecting the availability of resources around the tree host (Stewart and Schnitzer, 2017). Typically during their development, lianas produce a higher proportion of their biomass in foliage above their host affecting the tree growth, survival, and reproduction (Phillips et al., 2005; Peña-Claros et al., 2008; Ingwell et al., 2010; Wright et al., 2015; Martínez-Izquierdo et al., 2016). Many investigations throughout the tropics have revealed dramatic increases in liana abundance in recent decades, particularly in seasonal ecosystems and dry climatic conditions (Schnitzer and Bongers, 2011; Schnitzer, 2015; Wright et al., 2015). Moreover, some investigations have attributed this recent proliferation to the resource investment strategies of lianas, namely, light capture and growth traits (Asner and Martin, 2012; Wyka et al., 2013). This appears to be a viable investment without the burden of costs associated with self-supporting structures provided by their host tree. Conversely, trees have been reported to invest in traits associated with defence, maintenance, and metabolism (Asner and Martin, 2012; Wyka et al., 2013; Liu et al., 2021).

The aim of this study is to determine whether associations between anatomical and well-established leaf functional traits provide a mechanistic point of view to the trade-off theory of the LES. The associations between different anatomical traits and functional traits are the result of evolutionary and ecological pressures driving patterns along the spectrum as a continuous entity. Here we consider leaf functional traits as those morpho-physiological and structural traits that modulate the fitness of the individual (e.g., growth, reproduction, and survival) (Violle et al., 2007). The leaf anatomical traits studied here, which could also be functional, are focused on fractions of each tissue type and their density (i.e., epidermis, palisade, and spongy mesophyll) based on the cellular organization (i.e., number of cells, cell size, air spaces, and tissue cross area and thickness) in order to normalize the potential differences in leaf size. We attempt to address this by examining the LES using two perspectives: the spectrum as a single axis (i.e., investment patterns regardless of relatedness or climate) and a comparison of potential end members along the spectrum. Overall, the liana–tree co-existence and their contrasting traits make for a convenient comparison as contrasting endmembers of the spectrum. This is also explored at two different forest types (tropical wet forest and tropical dry forest) as a potential descriptor of environmental drivers that modulate the variation in leaf traits. Specifically, here we address two hypotheses: (i) liana and tree species present contrasting leaf anatomical traits exhibiting of resource acquisitive-conservative (fast-slow) strategies according to the forest type, and (ii) the trade-off investment strategies of the leaf anatomical traits are associated with those described in well-established leaf traits. For the first hypothesis, we expect that liana investment in leaf anatomical traits resemble those related to resource acquisitive strategies (fast), while trees to resource conservative (slow) (List of species **Table 1**). For the second hypothesis, we predict that the variability in leaf anatomical traits have a meaningful correlation, positive or negative, with the variability of well-establish traits, in accordance with investment payoff of a particular trait (**Table 2**). For example, as palisade cell density increases, A_{max} and R_{d} should also increase; this is because palisade anatomical traits which have light capture and growth strategies should exhibit positive relationships with A_{max} and R_{d} because they also exhibit light capture and growth functional strategies; or as spongy mesophyll density decreases nitrogen leaf content should increase because there two sets of traits have opposing strategic investments, maintenance and metabolism vs. light capture and growth, respectively (**Table 2**); The negative association is because there is an inherent energy requirement to maintain the leaf at the cost of resource acquisition ability. The anatomical traits studied here may represent the mechanism by which LES strategies are achieved, improving our understanding of the resource allocation hypothesis embedded in the LES framework.

MATERIALS AND METHODS

Study Area

This research took place at two canopy crane systems in Panama during the rainy season, August 2004: (i) Parque Natural Metropolitano (PNM, 8° 59′ 39.95″ N, 79° 32′ 34.68″ W, 150 m

TABLE 1 | List of species of lianas and trees collected at the Parque Natural Metropolitano and Parque Nacional San Lorenzo, Panama.

Parque Natural Metropolitano		Parque Nacional San Lorenzo	
Family	**Species**	**Family**	**Species**
Lianas			
Aristolochiaceae	*Aristolochia maxima* Jacq.	Apocynaceae	*Forsteronia myriantha* Donn. Sm.
Asteraceae	*Mikania leiostachya* Benth.		*Odontadenia puncticulosa* (Rich.) Pulle.
Bignoniaceae	*Arrabidaea candidans* DC.	Bignoniaceae	*Arrabidaea verrucose* Kranzl.
	Stizophyllum riparium (Kunth) Sandwith.		*Phryganocydia corymbosa* (Vent.) L.G. Lohmann
Convolvulaceae	*Bonamia maripoide* Hallier f.		*Pleonotoma variabilis* (Jacq.) Miers.
	Jacquemontia perryana Robertson.	Celastraceae	*Tontelea ovalifolia* (Miers.) A.C.
Papilionoideae	*Machaerium riparium* Brandegee.	Convolvulaceae	*Maripa panamensis* Hemsl.
Malpighiaceae	*Stigmaphyllon hypargyreum* Triana and Planch.	Dilleniaceae	*Doliocarpus multiflorus* Standl.
Passifloraceae	*Passiflora vitifolia* Triana and Planch.	Papilionoideae	*Dioclea wilsonii* Standl.
Rhamnaceae	*Gouania lupuloides* (L) Urb.		
Sapindaceae	*Serjania mexicana* (L) Willd.		
Vitaceae	*Vitis tiliifolia* Humb. and Bonpl.		
Trees			
Anacardiaceae	*Astronium graveolens* Jacq.	Apocynaceae	*Aspidosperma cruenta* Woodson
Annonaceae	*Annona spraguei* Saff.	Boraginaceae	*Cordia bicolor* A. DC.
Boraginaceae	*Cordia alliodora* (Ruiz and Pav.) Oken.	Clusiaceae	*Marila laxiflora* Rusby.
Tiliaceae	*Luehea seemannii* Triana and Planch.	Caesalpinioideae	*Tachigali versicolor* Standl. and L.O. Williams.
		Papilionoideae	*Lonchocarpus longifolium* Pitter.
		Meliaceae	*Carapa guianensis* Aubl.
		Moraceae	*Brosimum utile* (Kunth) Oken.
			Ficus insipida Willd.
			Ficus nymphaeifolia Mill.
		Myristicaceae	*Virola surinamensis* (Rol. ex Rottb.) Warb.
		Rubiaceae	*Tocoyena pittieri* Standl.
		Sapindaceae	*Matayba apetala* Radlk.
		Sapotaceae	*Manilkara bidentata* (A. DC.) A. Chev.
		Simaroubaceae	*Simarouba amara* Aubl.
		Urticaceae	*Porouma bicolor* Mart. (Standl.)

TABLE 2 | Functional strategy and primary resource invested of each anatomical tissue layer and LTF.

Tissue	Resource (Carbon, nutrients, and water)	Selective mechanism/functional strategy
Epidermis	Water	Structural and defensive
Palisade	Carbon	Photosynthetic capacity; light capture, and growth
Spongy	Water and gas exchange	Maintenance and metabolism
Air space	Water and gas exchange	Maintenance and metabolism
Trait	**Resource (Carbon, nutrients, and water)**	**Selective mechanism/functional strategy**
$A_{\max}$	Carbon	Photosynthetic capacity; light capture and growth
R_{dark}	Carbon	Light capture and growth
N	Nutrients	Light capture and growth
LMA	Carbon	Maintenance and metabolism; light capture and growth; Maintenance and metabolism
LT	Carbon	Structural and defensive; resource capture
LD	Carbon and water	Structural and defensive; resource capture
LL	Carbon and water and nutrients	Structural and defensive; Maintenance and metabolism

Acronyms represent the maximum photosynthetic capacity ($A_{\max}$), dark respiration (R_{dark}), leaf mass area (LMA), leaf thickness (LT), leaf density (LD), and leaf lifespan (LL).

a.s.l.), and (ii) Parque Nacional San Lorenzo (SL, 9° 16′ 51.71″ N, 79° 58′ 28.27″ W, 130 m a.s.l.). The PNM is located in Panama City on the Pacific coast of the Republic of Panama. This site presents a seasonally dry tropical forest with a mean annual temperature of 26.5°C and an annual rainfall of 1740 mm. The PNM contains a 265 ha of a natural reserve with an old secondary forest of 80–150 years with tree heights up to 40 m (Wright et al., 2003). The PNM site has a 42 m standing crane with a 51 m long jib with a suspended cage that can be used to access the top of the canopy. The crane covers approximately 0.85 ha of forest in which more than 60 species of trees and lianas can be reached (Wright et al., 2003). On the other hand, the SL is a wet evergreen forest located on the Caribbean coast of Panama with a mean annual temperature of 25.3°C and an annual rainfall of 3000 mm. This site presents a weak dry season from January to March with rainfalls below 45 mm per month. The SL contains a 12,000 ha of old forest (~300 years) that is part of the Mesoamerican Biological Corridor (Wright et al., 2003). This site also presents a standing crane of 52 m tall with a 54 m jib that can be used to access the top of the canopy. This crane provides access to 0.92 ha of the forest where more than 240 species of trees and lianas can be found (Wright et al., 2003).

Sample Collection and Leaf Histology

Three individuals (i.e., trees or lianas) were selected to collect three sun leaves from the top of the canopy using both cranes in the wet season of 2004; therefore, nine leaves per species were sampled. Leaves were collected from 40 species in total (**Table 1**). Twelve liana species and four tree species were collected from the PNM crane, while nine liana species and fifteen tree species were collected from the SL crane. Each leaf sample immediately upon clipping (early morning) was placed in a plastic bag with a moist paper towel and then transferred within 1-h to a dry ice cooler for transportation to a laboratory. Three small sections (5 mm in width and 20 mm in length) were cut from each leaf while avoiding the presence of prominent vascular areas. The cut-out sections were treated for 2 weeks with formalin aceto-alcohol in a vacuum oven. After the 2 weeks, the samples were run through an ethanol processing centre and transferred to a hot paraffin bath for embedding into paraffin blocks. A detailed description of the process can be found in Sánchez-Azofeifa et al. (2009).

Slides were prepared following Bancroft and Cook (1984) histological preparation protocols. On these samples, seven cross-sections were prepared with a Leica microtome from a paraffin block and mounted onto microscope slides. Each cross-section has a thickness of 7 μm and a width and height of 22 by 22 mm. The slides were placed in an oven at 37°C overnight for roughly 10–12 h. The following morning, slides were de-waxed with a series of diluted ethanol concentrations and then soaked in toluene for 2 min. The slides were then submerged in a toluene blue stain for 22 s. Coverslips were placed over stained samples using a DPX mounting medium. Slides were again placed in 37°C oven for 10–12 h to dry and set the DPX. Finally, cross-sectional photos were taken using a Zeiss M1 Axio Imager microscope at 400 times magnification. All samples had a field of view of 450 μm by 450 μm. For each species, nine leaves were mounted, stained, and photographed.

Estimation of Anatomical Metrics and Traits

The cross-section photographs previously obtained were used to derive metrics in order to quantify the anatomy of leaf tissues. Specifically, the used metrics are focused on describing the area, thickness, number of cells, and cell size of four-leaf sections: (i) upper epidermis (EU), (ii) lower epidermis (EL), (iii) palisade mesophyll (MP), and (iv) spongy mesophyll (MS). These anatomical metrics derived from photos that were previously enhanced by colour and contrast and transformed to black and white using ImageJ 1.46 (Schneider et al., 2012). The area and percentage of the blackened and non-blackened region were used to estimate the cell-occupied space and leaf airspace using the "analysed particles" tools. Likewise, the area and thickness of each leaf section were estimated, making a manual selection of each blackened section using the "region of interest" tool. The area and thickness of each section were calculated by taking the average of 5 measurements per sample. On the other hand, the number of cells was estimated using the edge effect rules with a counting frame (Mbf Bioscience, 2015). For this, a counting frame of 3,000 μm^2 central area was established from the centre of the photograph with a 1,500 μm^2 buffer zone surrounding the perimeter of the cross-section. Next, each cell at each layer was counted in the selected area. For cells to be included, they needed to be entirely encompassed in the central area and the buffer zone. Once the cell count was established, the number of cells was estimated per mesophyll layer (MP and MS). The estimated cell count was accomplished by multiplying the total area of the mesophyll layers by the estimates cell counts. Likewise, the individual cell size was then estimated with the cell count results. This was accomplished by dividing the cell counts by the area of the mesophyll layers. To eliminate pseudo-replication bias, the sample mean for the individual (three individuals per species) was used as a descriptor of the anatomical metrics.

Once the anatomical metrics were done, we calculated anatomical relationships between metrics to reduce the collinearity among them for future analysis. In general, these relationships are a group of ratios or fractions that can be used to normalize the variation of anatomical metrics, which could be affected by the leaf size. These anatomical relationships are called hereinafter as leaf anatomical traits. We calculated eight anatomical traits based on their potential significance to describe physiological, structural, and defensive trade-offs. Specifically, we calculated (**Table 3**): (i) palisade area fraction (fMParea), (ii) spongy area fraction ($f\mathrm{MS}_{\mathrm{area}}$), (iii) airspace area fraction ($f\mathrm{AIR}_{\mathrm{area}}$), (iv) palisade density ($\rho\mathrm{MP}_{\mathrm{cell}}$; number of cells per $\mu\mathrm{m}^2$), (v) spongy density ($\rho\mathrm{MS}_{\mathrm{cell}}$; number of cells per $\mu\mathrm{m}^2$), (vi) epidermis thickness fraction ($f\mathrm{E}_{\mathrm{thickness}}$), (vii) palisade thickness fraction ($f\mathrm{MP}_{\mathrm{thickness}}$), and (viii) palisade/spongy cell count ratio ($\mathrm{MP}_{\mathrm{count}}/\mathrm{MS}_{\mathrm{count}}$). For the following traits, $f\mathrm{MP}_{\mathrm{area}}$, $f\mathrm{MS}_{\mathrm{area}}$, $f\mathrm{AIR}_{\mathrm{area}}$, $f\mathrm{E}_{\mathrm{thickness}}$, $f\mathrm{MP}_{\mathrm{thickness}}$, and $\mathrm{MP}_{\mathrm{count}}/\mathrm{MS}_{\mathrm{count}}$ they do not have units because they are fractions. However, area and thickness are measured in μm and cell counts are the number of cells in a given area. Descriptions on how to derive these traits and their potential relevance are described in **Table 3**.

Well-Established Leaf Functional Traits

We used eight well-established LFTs for each species and forest type obtained from published records from Osnas et al. (2018). Specifically, we used: maximum net photosynthetic rate ($A_{\max}$, μmol CO_2 m^{-2} s^{-1}), dark respiration rate (R_{dark}, μmol CO_2 m^{-2} s^{-1}), nitrogen concentration (N, g m^{-2}), and phosphorus concentration (P, g m^{-2}), leaf mass per area (LMA, g m^{-2}), leaf thickness (LT, mm), leaf density (LD, g cm^{-3}) and leaf lifespan (LL, days). In general, these traits were collected at the same sites under two canopy positions (canopy and understory) from different species, including trees, treelets, lianas, vines, epiphytes, and hemi-epiphytes. For this research, only sun leaves were used to compare against leaf anatomical traits. A detailed description of the data collection and trait calculations can be found at Osnas et al. (2018).

TABLE 3 | Description of the leaf anatomical traits.

Leaf anatomical trait	Acronyms	Estimation
Palisade area fraction	$f\mathrm{MP}_{\mathrm{area}}$	Palisade cross-section area/total cross-section area
Spongy area fraction	$f\mathrm{MS}_{\mathrm{area}}$	Spongy cross-section area/total cross-section area
Air space area fraction	$f\mathrm{AIR}_{\mathrm{area}}$	Air space cross-section area/total cross-section area
Palisade cell density	$\rho\mathrm{MP}_{\mathrm{cell}}$	Palisade cell count/total cross-section area
Spongy cell density	$\rho\mathrm{MS}_{\mathrm{cell}}$	Spongy cell count/total cross-section area
Epidermis thickness fraction	$f\mathrm{E}_{\mathrm{thickness}}$	Epidermis thickness/total cross-section thickness
Palisade thickness fraction	$f\mathrm{MP}_{\mathrm{thickness}}$	Palisade thickness/total cross-section thickness
Palisade/Spongy cell count ratio	$\mathrm{MP}_{\mathrm{count}}/\mathrm{MS}_{\mathrm{count}}$	Palisade cell count/Spongy cell count

Data Analysis

We first compared the effect of life forms and forest type using MANOVAs at three levels of evaluation: (i) anatomical metrics, (ii) leaf anatomical traits, and (iii) well-established LFTs. For each MANOVA, we extracted the univariate analysis of variance (ANOVA) to describe the effects on each trait. For these analyses, we considered each species as the sample unit using the average of leaves per species, and thus meet the assumption of independent observations. In addition, for these analysis leaf traits variables were initially transformed using Box-Cox or log transformation in order to reach the univariate normality and homogeneity of variance assumptions. The application of the Mahalanobis distance tests did not reveal multivariate outliers at the three levels of evaluation. However, the multivariate normality assumption was not meet in all the cases; probably to the sample size. Therefore, Pillai trace was used as measure of variance given that it is relative robust to multivariate normality deviations, assumptions of homogeneity of the variance–covariance matrices across groups, and unbalanced datasets (Johnson and Field, 1993; Quinn and Keough, 2002). These analyses were performed following the recommendations of Quinn and Keough (2002). On the other hand, we performed bootstrapped pairwise Pearson's correlation analysis between the leaf anatomical traits and the well-established LFTs to see their association. These correlations were first performed using all the species, and then on separate by life forms and forest type. The previous analyses were conducted in R software version 3.6.1 (R Core Team, 2020) using the "manova" and "aov" functions to compute the MANOVAs and ANOVAs, respectively, the "corr.test" function of the *psych* package (Revelle, 2017) to estimate the Pearson correlations and their significance, and the *boot* package for bootstrapping (Canty and Ripley, 2019). Each trait was previously transformed using the logarithmic transformation when the normality of the data was not reached.

RESULTS

Anatomical Metrics

According to the MANOVA, the comparisons of the anatomical metrics between life forms, forest type, and their interactions suggested that the multivariate effect do not contribute to the differences between life forms (Pillai $\mathrm{trace}_{(15,21)} = 0.55$; $p = 0.12$), forest types (Pillai $\mathrm{trace}_{(15,21)} = 0.56$; $p = 0.11$), or the life form × forest type interaction (Pillai $\mathrm{trace}_{(15,21)} = 0.41$; $p = 0.53$). Despite this, the univariate analyses of these comparisons suggested the several anatomical metrics tend to differ between life forms as well as forest types (**Table 4**). Between life forms specially, the results revealed that liana leaves tend to have less cross-sectional area and are thinner than trees. Likewise, lianas presented lower palisade cross-section area and thickness than trees. However, at the cellular level, lianas seemed to have larger cells and fewer cells in the palisade and spongy leaf tissues. Between forest types on the other hand, species at PNM showed leaves with the less cross-sectional area and thinner that species at SL. Species at SL seemed to have higher spongy cross-section area and thickness than species at PNM. Likewise, the cross-section area of airspaces and the cell count of the spongy leaf tissue seemed to be higher in species at SL than PNM. The univariate comparisons did not reveal an effect of the interaction of life form and forest type in any anatomical metric.

Leaf Anatomical Traits

The comparisons on the anatomical traits between life forms, forest type, and their interactions using a MANOVA revealed that these traits tend to be affected by life form (Pillai trace$_{(8,28)}$ = 0.46; p = 0.01), but not by the forest type (Pillai trace$_{(8,28)}$ = 0.26; p = 0.31) or interaction of life form and forest type (Pillai trace$_{(8,28)}$ = 0.22; p = 0.45). The univariate comparisons showed that only ρMP_{cell} and ρMS_{cell} were affected by the life forms (**Table 5**), where lianas tended to present higher values than trees (**Figures 1D,E**). Likewise, the ρMS_{cell} is the only trait that seemed to be affected by forest type, where species at PNM presented higher values than species at SL (**Figure 1E**). Overall, lianas seemed to show higher values of fMS_{area}, $fAIR_{area}$, and $fE_{thickness}$ and lower values of fMP_{area}, $fMP_{thickness}$, and MP_{count}/MS_{count} than trees (**Figures 1A–C,F–H**); however, these differences did not appear to be statistically supported (**Table 5**).

TABLE 5 | Results of the ANOVA comparison of the effect of life forms, forest type, and their interaction on the derived leaf anatomical traits.

Traits	ANOVA		
	Life form	**Forest type**	**Life form × Forest type**
fMP_{area}	0.19	1.51	1.38
fMS_{area}	0.04	3.28	0.82
$fAIR_{area}$	0.18	3.38	2.37
ρMP_{cell}	11.59**	1.25	1.19
ρMS_{cell}	23.87***	6.10*	0.11
$fE_{thickness}$	2.56	2.26	0.56
$fMP_{thickness}$	0.67	3.84	0.25
MP_{count}/MS_{count}	0.02	1.37	0.06

*The ANOVA results represented by the F-ratios and the asterisks represent their significance: * $p < 0.05$; ** $p < 0.01$; *** $p < 0.001$.*

Well-Established Leaf Functional Traits

On the other hand, the comparisons of LFT between life forms, forest type, and their interactions revealed that the LFT were affected by the life forms (Pillai trace$_{(8,21)}$ = 0.66; $p < 0.01$), forest type (Pillai trace$_{(8,21)}$ = 0.69; $p < 0.001$), and their interaction (Pillai trace$_{(8,21)}$ = 0.58; $p < 0.05$). The univariate effects of this analysis suggest that only A_{max}, N, P, LMA, LD, and LL were affected by life forms, where lianas showed lower values than trees (**Table 6**). Likewise, the univariate effect of this analysis suggested that only P, LMA, and LT were affected by the forest type, where species at PNM showed higher values of P and lower values of LMA and LT than species at SL (**Table 6**). Despite the presence of multivariate interaction, the univariate analysis did not reveal statistically significant interaction within LFTs.

TABLE 4 | Comparison of anatomical metrics between lianas and trees summarized by forest type: seasonally dry forest (Parque Natural Metropolitano) and wet forest (Parque Nacional San Lorenzo).

Metrics	Region or tissue	Parque Natural Metropolitano		Parque Nacional San Lorenzo		ANOVA		
		Lianas	**Trees**	**Lianas**	**Trees**	**Life form**	**Site**	**Interaction**
Area (μm^2)	Leaf	51945.51 ± 9073.22	52971.91 ± 12256.89	69092.59 ± 15151.32	78999.87 ± 24544.74	5.74*	13.88***	0.32
	EU	6970.79 ± 2345.18	8518.13 ± 3355.51	8807.57 ± 3892.54	9988.36 ± 4022.03	3.42	2.29	0.06
	MP	19262.97 ± 4516.09	23051.87 ± 5863.77	24719.91 ± 11031.43	28319.36 ± 9080.87	5.93*	3.57	0.01
	MS	17481.74 ± 4691.01	16304.92 ± 6353.04	25404.92 ± 11373.29	29189.57 ± 10778.74	3.33	11.56**	0.93
	EL	5205.21 ± 1263.88	4079.67 ± 871.66	5414.98 ± 1197.84	5478.14 ± 1444.78	0.09	2.14	1.64
	Airspace	3024.80 ± 2624.25	1017.32 ± 1133.68	4745.21 ± 4117.84	6024.45 ± 6443.05	0.04	5.67*	2.21
Thickness (μm)	Leaf	299.93 ± 54.73	306.23 ± 67.97	402.91 ± 77.45	454.37 ± 138.04	5.82*	15.78***	0.22
	EU	19.95 ± 6.75	22.54 ± 9.14	25.32 ± 11.24	23.28 ± 7.90	0.20	1.64	0.50
	MP	55.94 ± 13.09	65.25 ± 7.87	66.58 ± 28.22	81.30 ± 22.71	8.94**	2.65	0.08
	MS	58.65 ± 20.92	53.05 ± 27.65	93.58 ± 37.85	101.73 ± 47.94	1.70	14.08***	0.52
	EL	13.88 ± 3.90	12.00 ± 2.58	15.99 ± 4.50	14.77 ± 4.47	0.22	2.63	0.05
Cell size (μm^2)	MP	261.75 ± 58.25	228.40 ± 99.92	353.89 ± 161.02	214.46 ± 81.50	7.40*	0.95	0.98
	MS	202.70 ± 41.91	135.09 ± 29.23	207.67 ± 60.27	164.57 ± 37.92	10.68**	0.84	0.58
Cell count	MP	80.57 ± 29.48	113.17 ± 37.46	98.79 ± 85.34	150.46 ± 67.17	10.28**	0.12	0.46
	MS	91.28 ± 27.25	130.14 ± 55.90	130.22 ± 53.43	179.90 ± 50.64	17.05***	7.25*	0.11

The regions or tissues refers to the upper epidermis (EU), lower epidermis (EL), palisade mesophyll (MP), and spongy mesophyll (MS). Leaf and airspaces refer to regions occupied or not occupied by cells in the leaves.

*The ANOVA values are represented by the F-ratios and the asterisks represent their significance: * $p < 0.05$; ** $p < 0.01$; *** $p < 0.001$.*

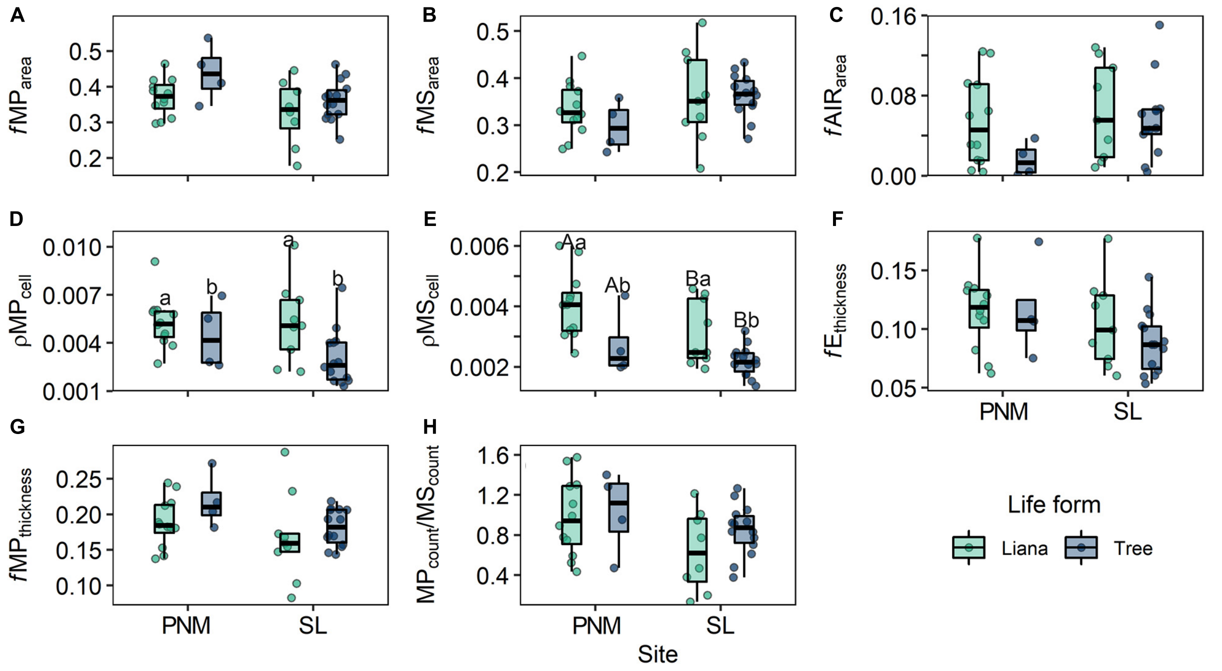

FIGURE 1 | Comparisons of the leaf anatomical traits of lianas and trees at Parque Natural Metropolitano (PNM) and Parque Nacional San Lorenzo (SL). Different capital letters represent a statistical difference between forest types, while different lowercase letters represent a statistical difference between life forms. Each point represents the mean value per species. Each fractional anatomical trait (fMP_{area}, fMS_{area}, $fAIR_{area}$, $fE_{thickness}$, $fMP_{thickness}$, and MP_{count}/MS_{count}) does not have units, however, area and thickness are measured in µm. While the units for, ρMP_{cell} and ρMS_{cell} are the number of cells per µm. ANOVA results are described in **Table 4**. See **Table 3** for abbreviations of traits.

TABLE 6 | Comparison of the well-established leaf traits between lianas and trees summarized by forest type: seasonally dry forest, Parque Natural Metropolitano, and wet forest, Parque Nacional San Lorenzo.

Traits	Parque Natural Metropolitano		Parque Nacional San Lorenzo		ANOVA		
	Lianas	Trees	Lianas	Trees	Life form	Site	Interaction
A_{max}	9.84 ± 3.25	16.43 ± 3.13	13.92 ± 2.26	14.95 ± 6.38	5.17*	0.65	2.54
R_{dark} (10^{-2})	1.02 ± 0.45	1.35 ± 1.50	1.22 ± 0.49	0.89 ± 0.57	0.23	0.36	1.60
N (10^{-2})	1.47 ± 0.38	1.99 ± 0.57	1.51 ± 0.23	2.02 ± 0.48	16.58***	0.18	0.31
P (10^{-2})	0.10 ± 0.02	0.14 ± 0.03	0.08 ± 0.02	0.11 ± 0.04	16.17***	8.04**	0.31
LMA	58.02 ± 17.45	82.26 ± 16.42	85.16 ± 13.78	120.15 ± 29.66	28.84***	8.64**	0.06
LT	0.23 ± 0.07	0.20 ± 0.06	0.28 ± 0.07	0.31 ± 0.08	2.22	5.63*	0.72
LD	0.27 ± 0.05	0.48 ± 0.16	0.32 ± 0.09	0.40 ± 0.08	16.44***	0.01	3.74
LL	146.09 ± 53.41	212.00 ± 42.98	286.00 ± 115.98	318.75 ± 136.90	6.18*	10.54**	0.76

*The ANOVA values are represented by the F-ratios and the asterisks represent their significance: * $p < 0.05$; ** $p < 0.01$; *** $p < 0.001$.*

Association Between Anatomical Traits and Well-Established Leaf Functional Traits

The correlations revealed that some leaf anatomical traits were associated with well-established traits (**Figure 2A**); however, the presence or degree of correlations seemed to be dependent on the life forms and forest type (**Figures 2B,C**). For instance, reductions in ρMP_{cell}, ρMS_{cell}, and $fE_{thickness}$ seemed to be associated with increases in LMA regardless of the life form or forest type (**Figure 2A**). Likewise, increases in $fE_{thickness}$ tended to be correlated with reductions in LD and LL. Increases in ρMP_{cell} also tended to be associated with reductions in N, while increases in ρMS_{cell} tended to be correlated with reductions of A_{max} and LT. Between life forms (**Figure 2B**), fMP_{area} and $fMP_{thickness}$ were positively correlated with N, P, and LD in trees, but not in lianas. On the other hand, in liana species increases in ρMP_{cell}, ρMS_{cell}, and $fE_{thickness}$ seemed to be correlated with reductions in N, LT, and LD, respectively, but not in trees species. When comparing forest types, the correlations revealed that reductions in ρMP_{cell}, ρMS_{cell} of PNM species seemed to be associated with increases in LT, but not for SL species. Likewise, increases of fMP_{area} of PNM species tended to be correlated with increases in LT. In SL species, reductions in $fE_{thickness}$ seemed

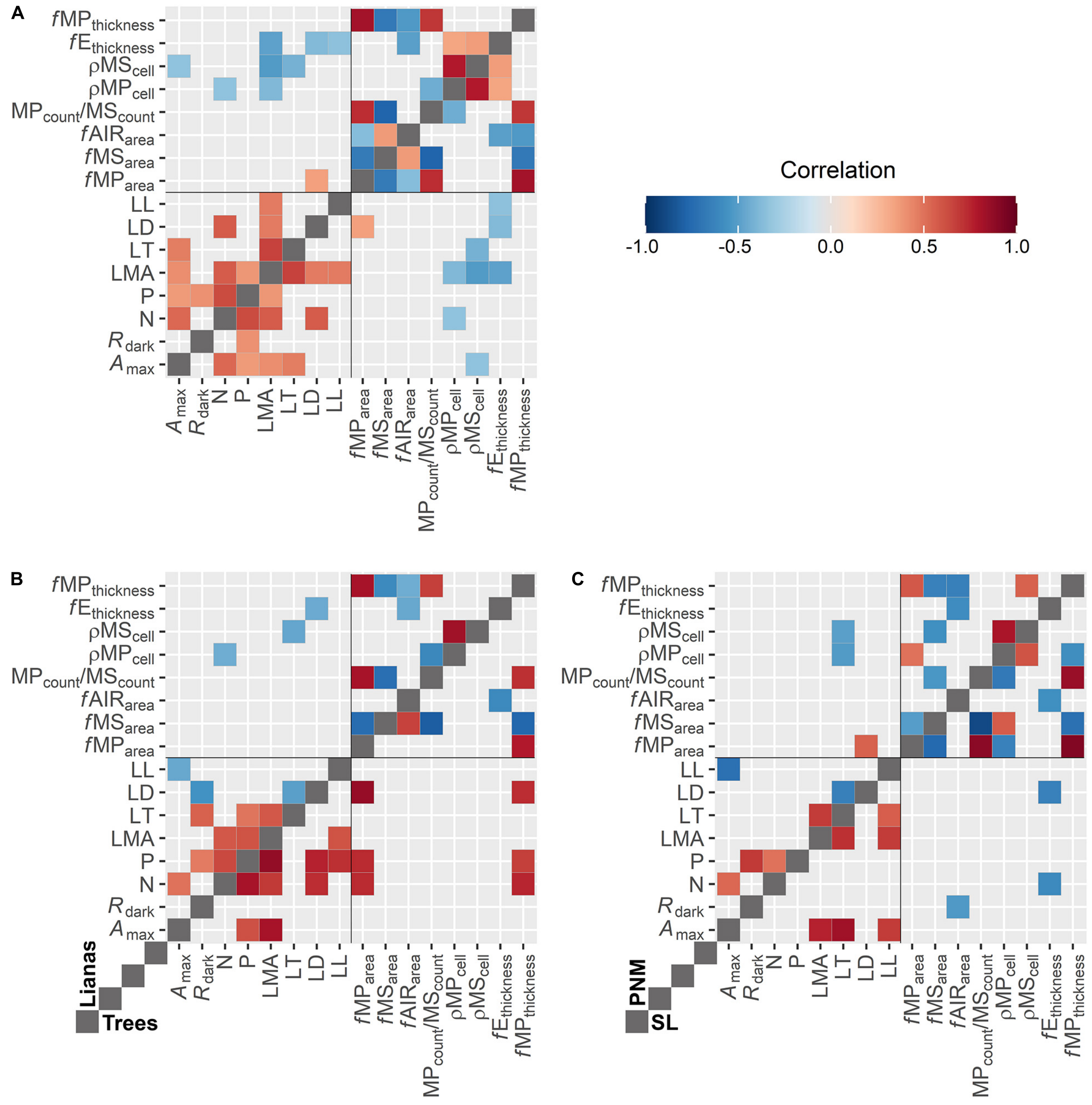

FIGURE 2 | Correlation analysis between leaf anatomical traits and well-established leaf functional traits. All species **(A)**, life forms **(B)**, and forest type (**C**; PNM: Parque Natural Metropolitano and, and SL: Parque Nacional San Lorenzo). The colours show the bootstrapped pairwise Pearson correlation that are significant ($p > 0.05$). The grey grid of the middle divides the upper and lower the correlation results between life forms **(A)** or forest type **(B)**. An extended figure with all the correlation was attached as **Supplementary Figure 1**.

to be associated with increases in N and LD, while reductions in $f\mathrm{AIR}_{\mathrm{area}}$ seemed to be associated with increases in R_{dark}. A complete figure with all the correlations (i.e., significant or not) was added in **Supplementary Figure 1**.

DISCUSSION

This research reveals several anatomical traits that tend to be contrasting between life forms and forest types as well as the mechanics that drive some of the well-established LFTs. Here, we focus on highlighting the interactions between anatomical traits and LFT, and how these differences reveal potential trade-off strategies between species and environments. Albeit the discussion regarding anatomy and LES has been had before, our finding advances this argument in that are cell and tissue mechanisms associated with morpho-physiological trait investment strategies. Moreover, our results also have merit to the idea that leaf anatomical traits, as an additional scientific exploration tool, can help us better understand the functional ecology of species. From these findings, we argue that anatomical traits could complement the framework of the LES.

End of Spectrum Case Study Comparison- Growth Form and Site

The objective of the endmember perspective of this investigation was to compare groups of species that exhibit fast vs. slow functional strategies. Therefore, our first hypothesis was supported by the association between anatomical traits and LFT may depend on the life forms and forest type. For example, species with higher LMA seem to be associated with reductions in ρMP_{cell}, ρMS_{cell}, and $fMP_{thickness}$, but this association is not observed when comparing life forms or forest types. Despite this, on some occasions, ρMP_{cell} and ρMS_{cell} and appear to have a negative association with the variation of LD and LT in lianas, and both forest types. These correlations interestingly mirror the breakdown of LMA as the product of LD and LT (LMA = Leaf volume area × Leaf density) (Poorter et al., 2009).

Trade-offs in investment strategies such as the conservative-acquisitive trade-off hypothesis between lianas and trees (Asner and Martin, 2012; Wyka et al., 2013) could be dissected with the correlative exploration between leaf anatomical traits and the well-established LFT. For example, trees tend to have more in N and P per unit leaf area and higher LD as a conservative strategy. These LFTs mentioned above seem to be positively correlated with fMP_{area} and $fMP_{thickness}$; probably to boost carbon assimilation for woody structures. On the other hand, with lower metabolic demand (compared to trees) of support structures, lianas traits are generally related to acquisitive strategies with low investment in nutrients and structures for fast growth and high light capture. This strategy appears to be reflected in the increasing cellular infrastructure (ρMP_{cell}, $\rho MS_{cell,}$ and $fE_{thickness}$) with high turnover of nutrients as investment and leaf volume demands (LT and LD). In addition, trade-offs in investment strategies between forest types may also reveal how species modify their leaf anatomy to deal with contrasting rainfall regimes. For example, it appears that species at the PNM tend to increase the density of palisade and spongy cells with lower LT which would suggest a loss of airspace. This strategy of dry-forest species may prevent to break the water tension between cells avoiding the leaf hydraulic failure. A negative pressure is formed between mesophyll cells when small menisci of water are formed through adhesion to the outside of the spongy mesophyll cells creating tension and suction as water is lost through the stomata. Conversely, species at the wet-forest seem to increase $fAIR_{area}$; to be more metabolically efficient to reduce of R_{dark}.

The LES as a Continuous Single Axis- an Anatomical Perspective

There is convincing evidence for leaf investment strategies along the LES to exhibit the same patterning of trait correlation across taxonomy and climatic gradients (Wright et al., 2004). The LES maps these universal patterns in which traits that are not energetically unfavourable are lost and thus allows for the LES to be placed along single axis. Our second perspective to the LES takes a closer look at these patterns and dissects the compositional origin. Broadly speaking, we find cellular mechanisms and organization associated with the function of a particular tissue. The anatomical traits that seem to have the most casual impacts are mesophyll densities and epidermal thickness (ρMP_{cell}, ρMS_{cell} and $fE_{thickness}$). For example, decreases in ρMP_{cell}, ρMS_{cell}, and $fE_{thickness}$ were found to be associated with an increase in LMA (**Figure 2**). This cellular structure demonstrates the trade off between metabolic function and the structural integrity of the leaf. Although LMA is thought to be a black box in the literature, John et al. (2017) complementarily found that an increase in cell size (thus decrease in density) drives greater LMA. Moreover, other compositional studies have found a breakdown of LMA by anatomy to be affected equally by protoplast and cell wall components (metabolism and structure, respectively; Shipley et al., 2006; John et al., 2017). A more specific example can be seen in the negative correlation between ρMP_{cell} and N. Given that nitrogen is an important component of chloroplast, more dense palisade results in lower N and thus there is a restriction on photosynthetic capacity. This is supported by Pyankov et al. (1999), who found that mesophyll size and numbers were negatively correlated and that leaves with large cells have more chloroplasts per cell.

When comparing investment strategies types, we found support for our second hypothesis. We found higher epidermal thickness with lower LD and LL. These correlations reflect the carbon allocation investment costs of structural defence. The cuticle and epidermis are considered the first line of defence in plants, this trade off can be seen regardless of phylogenetic and environmental factors. Simply put, this pattern arose from blanketed selective pressures on plants as stationary organisms and the of cost of protection. Moreover, Flexas et al. (2013) have found that across diverse range of species mesophyll conductance is strongly linked to gas exchange traits, stomatal conductance and leaf vein density. Supporting the idea that at the foliar traits can be linked to tissue-level dissection of these traits and there is evolution consistency in these trends.

Moreover, within the spongy mesophyll we found negative relationships between ρMS_{cell} and A_{max} which supports the trade-off hypothesis of different functional strategies (maintenance and metabolism against light capture and growth traits) (**Table 2**). Increasing spongy mesophyll density with lower A_{max} is indicative of increased gas diffusion resistance. Less intracellular space reduces the diffusion capacity of the spongy mesophyll and this shows photosynthesis capacity's limitation associated with the rate of gas diffusion. Liu et al. (2019) found high dry matter content with low SLA suggesting an increase diffusion resistance. Our findings take this one step further and show the allocation of spongy mesophyll tissue to come at a cost of decreased transpiration and photosynthetic capacity despite the wide variability around life form and site type. The application to the LES spectrum is that photosynthetic capacity is limited by its reactants' and products' the distance travelled and rate of travel across the spongy anatomy, quite literally, it is subjected to fast-slow continuum.

Future Perspectives of Leaf Anatomical Traits

Currently, there are a few studies that address the role of leaf anatomical traits on the functional ecology of the species or communities, however, they seem to focus on only snapshot perspectives of the LES; for instance solely discussing the usefulness of LMA (Pyankov et al., 1999; John et al., 2017), or finding a weak correlation between anatomical traits and economic and hydraulic traits (Liu et al., 2019).

The LES was a paradigm shift in plant ecology. This study provides further justification to add anatomical traits to the LES, however, we only focused on leaf traits. The future of this research should focus on anatomical deconstruction at all levels to match the grandiose nature of the LES: cellular, tissue, organ, and systems as well as root, stem, and leaf. Moreover, it seems clear that the degree of correlation of the anatomical traits depends on the different functional groups and environments. Therefore, the differentiation of the co-variation of anatomical traits between species, functional groups, or communities could reflect the different trade-off strategies of species in face to a given environment. Based on this, the use of anatomical decomposition of leaves may provide a deeper understanding of the leaf economy variation along ecological evolutionary and climatic gradients.

CONCLUSION

The discussion of traits as an explanation to the trade-off between growth and survival is long and continuous. Moreover, the discussion of including anatomy has been recited before, we have pushed this discussion in a direction that shows that leaf anatomy plays specific roles between growth and survival. The novel approach in this investigation was focusing on the LES as a spectrum, in a continuous vs. endmember dissection of the covariances of LFT and anatomy. These covariances are a result of ecological and evolutionary selective pressures. We found mesophyll density and epidermal thickness (ρMP_{cell}, ρMS_{cell}, and $fE_{thickness}$) have a more casual impact when summarizing the LES along singular axis. Mesophyll density is the proverbial stock to the currency of photosynthetic capacity traits as the currencies and epidermal thickness come at a cost of longevity and density. Such trade offs reflect unifying selective pressures along the LES: i-maintenance and metabolism for light capture and growth and ii- structure and defence for maintenance and metabolism, respectively. In contrast, our endmember case study found a group of traits selected for a specific life history. For example, lianas, resource acquisitive or at the "fast" end of the spectrum show positive covariance strategies both favourable to growth such as increase nutrients in their palisade mesophyll. The results where water was the comparative metric demonstrated that when resource was limited (water; PMN) the anatomy reflected this source of selective pressure by reducing thickness and ultimately airspaces. Future studies should investigate deeper in the harmonization of anatomical traits to better explain the leaf anatomy and current LFTs. Likewise, future studies should address the leaf anatomical trait co-variation of different taxonomic groups and how these are adapted to different environments.

DATA AVAILABILITY STATEMENT

Data collected by the authors of leaf anatomical metrics and traits per species and forest types are available at the Tropi-Dry dataverse through https://doi.org/10.7910/DVN/ESLKNT.

AUTHOR CONTRIBUTIONS

GS-A performed the leaf collection, helped to the interpretation of the results, editing of the manuscript, and got the funding. DH carried out the leaf histology and the measurements of anatomical metrics. JG analysed the data and performed the Figures. DH and JG drafted the manuscript. All the authors agreed with the final version of the manuscript.

FUNDING

This work was supported by the Natural Science and Engineering Research Council of Canada (NSERC) Discovery grant program. JG was a Vanier Scholar supported by NSERC.

ACKNOWLEDGMENTS

We are grateful to the Smithsonian Tropical Research Institute in Panama that provides the access to the canopy crane at both sites. Likewise, we thank S. Joseph Wright for previous discussions of the manuscript and the access to the well-established traits database. Our warm thanks to Janice Cooke for her guide and insights on the leaf anatomical measurements and results.

SUPPLEMENTARY MATERIAL

The Supplementary Material for this article can be found online at: https://www.frontiersin.org/articles/10.3389/ffgc.2021.720813/full#supplementary-material

REFERENCES

Asner, G. P., and Martin, R. E. (2012). Contrasting leaf chemical traits in tropical lianas and trees: implications for future forest composition. *Ecol. Lett.* 15, 1001–1007. doi: 10.1111/j.1461-0248.2012.01821.x

Bancroft, J., and Cook, H. (1984). *Manual of histological techniques*. Edinburgh: Churchill Livingstone.

Canty, A., and Ripley, B. (2019). *boot: Bootstrap R (S-Plus) Functions*. Cambridge: Cambridge University Press.

Chave, J., Coomes, D., Jansen, S., Lewis, S. L., Swenson, N. G., and Zanne, A. E. (2009). Towards a worldwide wood economics spectrum. *Ecol. Lett.* 12, 351–366. doi: 10.1111/j.1461-0248.2009.01285.x

Flexas, J., Scoffoni, C., Gago, J., and Sack, L. (2013). Leaf mesophyll conductance and leaf hydraulic conductance: an introduction to their measurement and coordination. *J. Exp. Bot.* 64, 3965–3981. doi: 10.1093/jxb/ert319

Guzmán, J. A., Rivard, B., and Sánchez-Azofeifa, G. A. (2018). Discrimination of liana and tree leaves from a Neotropical Dry Forest using visible-near infrared and longwave infrared reflectance spectra. *Remote Sens. Environ.* 219, 135–144. doi: 10.1016/j.rse.2018.10.014

Guzmán, J. A., and Sanchez-Azofeifa, G. A. (2021). Prediction of leaf traits of lianas and trees via the integration of wavelet spectra in the visible-near infrared and thermal infrared domains. *Remote Sens. Environ.* 259:112406. doi: 10.1016/j.rse.2021.112406

Ingwell, L. L., Joseph Wright, S., Becklund, K. K., Hubbell, S. P., and Schnitzer, S. A. (2010). The impact of lianas on 10 years of tree growth and mortality on Barro Colorado Island, Panama. *J. Ecol.* 98, 879–887. doi: 10.1111/j.1365-2745.2010.01676.x

Javelle, M., Vernoud, V., Rogowsky, P. M., and Ingram, G. C. (2011). Epidermis: the formation and functions of a fundamental plant tissue. *New Phytol.* 189, 17–39. doi: 10.1111/j.1469-8137.2010.03514.x

John, G. P., Scoffoni, C., Buckley, T. N., Villar, R., Poorter, H., and Sack, L. (2017). The anatomical and compositional basis of leaf mass per area. *Ecol. Lett.* 20, 412–425. doi: 10.1111/ele.12739

Johnson, C., and Field, C. (1993). Using fixed-effects model multivariate analysis of variance in marine biology and ecology. *Oceanogr. Mar. Biol. Annu. Rev.* 31, 177–221.

Kenzo, T., Ichie, T., Yoneda, R., Kitahashi, Y., Watanabe, Y., Ninomiya, I., et al. (2004). Interspecific variation of photosynthesis and leaf characteristics in canopy trees of five species of Dipterocarpaceae in a tropical rain forest. *Tree Physiol.* 24, 1187–1192. doi: 10.1093/treephys/24.10.1187

Kong, D., Wang, J., Wu, H., Valverde-Barrantes, O. J., Wang, R., Zeng, H., et al. (2019). Nonlinearity of root trait relationships and the root economics spectrum. *Nat. Commun.* 10:2203. doi: 10.1038/s41467-019-10245-6

Lehmeier, C., Pajor, R., Lundgren, M. R., Mathers, A., Sloan, J., Bauch, M., et al. (2017). Cell density and airspace patterning in the leaf can be manipulated to increase leaf photosynthetic capacity. *Plant J.* 92, 981–994. doi: 10.1111/tpj.13727

Liu, C., Li, Y., Xu, L., Chen, Z., and He, N. (2019). Variation in leaf morphological, stomatal, and anatomical traits and their relationships in temperate and subtropical forests. *Sci. Rep.* 9:5803. doi: 10.1038/s41598-019-42335-2

Liu, Q., Sterck, F. J., Zhang, J.-L., Scheire, A., Konings, E., Cao, M., et al. (2021). Traits, strategies, and niches of liana species in a tropical seasonal rainforest. *Oecologia* 196, 499–514. doi: 10.1007/s00442-021-04937-4

Martínez-Izquierdo, L., García, M. M., Powers, J. S., and Schnitzer, S. A. (2016). Lianas suppress seedling growth and survival of 14 tree species in a Panamanian tropical forest. *Ecology* 97, 215–224. doi: 10.1890/14-2261.1

Mbf Bioscience. (2015). *The edge effect with counting frame*. Available Online at: http://www.stereology.info/the-edge-effect-with-counting-frame/ [Accessed November 12, 2020]

Oguchi, R., Hikosaka, K., and Hirose, T. (2003). Does the photosynthetic light-acclimation need change in leaf anatomy? *Plant. Cell. Environ.* 26, 505–512. doi: 10.1046/j.1365-3040.2003.00981.x

Onoda, Y., Wright, I. J., Evans, J. R., Hikosaka, K., Kitajima, K., Niinemets, Ü, et al. (2017). Physiological and structural tradeoffs underlying the leaf economics spectrum. *New Phytol.* 214, 1447–1463. doi: 10.1111/nph.14496

Osnas, J. L. D., Katabuchi, M., Kitajima, K., Wright, S. J., Reich, P. B., Van Bael, S. A., et al. (2018). Divergent drivers of leaf trait variation within species, among species, and among functional groups. *Proc. Natl. Acad. Sci.* 115, 5480–5485. doi: 10.1073/pnas.1803989115

Osnas, J. L. D., Lichstein, J. W., Reich, P. B., and Pacala, S. W. (2013). Global leaf trait relationships: mass, area, and the leaf economics spectrum. *Science* 340, 741–744. doi: 10.1126/science.1231574

Peña-Claros, M., Fredericksen, T. S., Alarcón, A., Blate, G. M., Choque, U., Leaño, C., et al. (2008). Beyond reduced-impact logging: silvicultural treatments to increase growth rates of tropical trees. *For. Ecol. Manage.* 256, 1458–1467. doi: 10.1016/j.foreco.2007.11.013

Phillips, O. L., Vásquez Martínez, R., Monteagudo Mendoza, A., Baker, T. R., and Núñez Vargas, P. (2005). Large lianas are hyperdynamic elements of the tropical forest canopy. *Ecology* 86, 1250–1258. doi: 10.1890/04-1446

Poorter, H., Niinemets, Ü, Poorter, L., Wright, I. J., and Villar, R. (2009). Causes and consequences of variation in leaf mass per area (LMA): a meta-analysis. *New Phytol.* 182, 565–588. doi: 10.1111/j.1469-8137.2009.02830.x

Pyankov, V. I., Kondractchuk, A. V., and Shipley, B. (1999). Leaf structure and specific leaf mass: the alpine desert plants of the Eastern Pamirs, Tadjikistan. *New Phytol.* 143, 131–142. doi: 10.1046/j.1469-8137.1999.00435.x

Quinn, G., and Keough, M. (2002). *Experimental design and data analysis for biologists*. New York, USA: Cambridge University Press.

R Core Team. (2020). *R: A Language and Environment for Statistical Computing. R Found. Stat. Comput.* Available online at: https://www.r-project.org/ (accessed July 29, 2021).

Reich, P. B. (2014). The world-wide 'fast–slow' plant economics spectrum: a traits manifesto. *J. Ecol.* 102, 275–301. doi: 10.1111/1365-2745.12211

Reich, P. B., Ellsworth, D. S., Walters, M. B., Vose, J. M., Gresham, C., Volin, J. C., et al. (1999). Generality of leaf trait relationships: a test across six biomes. *Ecology* 80, 1955–1969.

Reich, P. B., and Oleksyn, J. (2004). Global patterns of plant leaf N and P in relation to temperature and latitude. *Proc. Natl. Acad. Sci. U S A.* 101, 11001–11006. doi: 10.1073/pnas.0403588101

Reich, P. B., Walters, M. B., and Ellsworth, D. S. (1997). From tropics to tundra: Global convergence in plant functioning. *Proc. Natl. Acad. Sci.* 94, 13730–13734.

Revelle, W. (2017). *psych: Procedures for Personality and Psychological Research*. Available Online at: https://cran.r-project.org/package=psych (accessed July 29, 2021).

Sack, L., and Scoffoni, C. (2013). Leaf venation: structure, function, development, evolution, ecology and applications in the past, present and future. *New Phytol.* 198, 983–1000. doi: 10.1111/nph.12253

Sánchez-Azofeifa, G. A., Castro, K., Wright, S. J., Gamon, J., Kalacska, M., Rivard, B., et al. (2009). Differences in leaf traits, leaf internal structure, and spectral reflectance between two communities of lianas and trees: Implications for remote sensing in tropical environments. *Remote Sens. Environ.* 113, 2076–2088. doi: 10.1016/j.rse.2009.05.013

Santiago, L. S. (2007). Extending the leaf economics spectrum to decomposition: evidence from a tropical forest. *Ecology* 88, 1126–1131. doi: 10.1890/06-1841

Schneider, C. A., Rasband, W. S., and Eliceiri, K. W. (2012). NIH Image to ImageJ: 25 years of image analysis. *Nat. Methods* 9, 671–675. doi: 10.1038/nmeth.2089

Schnitzer, S. (2015). *"Increasing liana abundance in neotropical forests: causes and consequences," in Ecology of Lianas*. Hoboken,NJ: John Wiley & Sons, Ltd, 451–464.

Schnitzer, S., and Bongers, F. (2011). Increasing liana abundance and biomass in tropical forests: emerging patterns and putative mechanisms. *Ecol. Lett.* 14, 397–406. doi: 10.1111/j.1461-0248.2011.01590.x

Shipley, B., Lechowicz, M., Wright, I., and Reich, P. (2006). Fundamental trade-offs generating the worldwide leaf economics spectrum. *Ecology* 87, 535–541. doi: 10.1890/05-1051

Slot, M., and Winter, K. (2017). In situ temperature response of photosynthesis of 42 tree and liana species in the canopy of two Panamanian lowland tropical forests with contrasting rainfall regimes. *New Phytol.* 214, 1103–1117. doi: 10.1111/nph.14469

Somavilla, N. S., Kolb, R. M., and Rossatto, D. R. (2014). Leaf anatomical traits corroborate the leaf economic spectrum: a case study with deciduous forest tree species. *Brazil. J. Bot.* 37, 69–82. doi: 10.1007/s40415-013-0038-x

Stewart, T. E., and Schnitzer, S. A. (2017). Blurred lines between competition and parasitism. *Biotropica* 49, 433–438. doi: 10.1111/btp.12444

Tichá, I. (1985). "Ontogeny of leaf morphology and anatomy," in *Photosynthesis during leaf development*, ed. Z. Šestăk (Dordrecht: Springer Netherlands), 16–50.

Verbeeck, H., Bauters, M., Jackson, T., Shenkin, A., Disney, M., and Calders, K. (2019). Time for a plant structural economics spectrum. *Front. For. Glob. Chang.* 2:43. doi: 10.3389/ffgc.2019.00043

Villar, R., Ruiz-Robleto, J., Ubera, J. L., and Poorter, H. (2013). Exploring variation in leaf mass per area (LMA) from leaf to cell: An anatomical analysis of 26 woody species. *Am. J. Bot.* 100, 1969–1980. doi: 10.3732/ajb.1200562

Violle, C., Navas, M.-L., Vile, D., Kazakou, E., Fortunel, C., Hummel, I., et al. (2007). Let the concept of trait be functional! *Oikos* 116, 882–892. doi: 10.1111/j.0030-1299.2007.15559.x

Werden, L. K., Waring, B. G., Smith-Martin, C. M., and Powers, J. S. (2017). Tropical dry forest trees and lianas differ in leaf economic spectrum traits but have overlapping water-use strategies. *Tree Physiol.* 38, 517–530. doi: 10.1093/treephys/tpx135

Wright, I. J., Reich, P. B., Cornelissen, J. H. C., Falster, D. S., Groom, P. K., Hikosaka, K., et al. (2005). Modulation of leaf economic traits and trait relationships by climate. *Glob. Ecol. Biogeogr.* 14, 411–421. doi: 10.1111/j.1466-822x.2005.00172.x

Wright, I. J., Reich, P. B., Westoby, M., Ackerly, D. D., Baruch, Z., Bongers, F., et al. (2004). The worldwide leaf economics spectrum. *Nature* 428, 821–827. doi: 10.1038/nature02403

Wright, S. J., Horlyck, V., Basset, Y., Barrios, H., Bethancourt, A., Bohlman, S. A., et al. (2003). "Tropical canopy biology program, Republic of Panama," in *Studying Forest Canopies from Above: The International Canopy Crane Network*, eds Y. Basset, V. Horlyck, and S. Wright (Balboa, Panama: Smithsonian Tropical Research Institute, Panama and the United Nations Environmental Programme), 137–155.

Wright, S. J., Sun, I.-F., Pickering, M., Fletcher, C. D., and Chen, Y.-Y. (2015). Long-term changes in liana loads and tree dynamics in a Malaysian forest. *Ecology* 96, 2748–2757. doi: 10.1890/14-1985.1

Wyka, T. P., Oleksyn, J., Karolewski, P., and Schnitzer, S. A. (2013). Phenotypic correlates of the lianescent growth form: a review. *Ann. Bot.* 112, 1667–1681. doi: 10.1093/aob/mct236

Xiao, Y., Tholen, D., and Zhu, X.-G. (2016). The influence of leaf anatomy on the internal light environment and photosynthetic electron transport rate: exploration with a new leaf ray tracing model. *J. Exp. Bot.* 67, 6021–6035. doi: 10.1093/jxb/erw359

Conflict of Interest: The authors declare that the research was conducted in the absence of any commercial or financial relationships that could be construed as a potential conflict of interest.

frontiers
in Forests and Global Change

SYSTEMATIC REVIEW
published: 11 February 2022
doi: 10.3389/ffgc.2021.812066

Lianas Significantly Reduce Tree Performance and Biomass Accumulation Across Tropical Forests: A Global Meta-Analysis

Sergio Estrada-Villegas[1,2,3]*, *Sara Sofia Pedraza Narvaez*[4], *Adriana Sanchez*[4] and *Stefan A. Schnitzer*[3,5]

[1] Yale School of the Environment, Yale University, New Haven, CT, United States, [2] The New York Botanical Garden, Bronx, NY, United States, [3] Smithsonian Tropical Research Institute, Balboa, Panama, [4] Department of Biology, Faculty of Natural Sciences, Universidad del Rosario, Bogotá, Colombia, [5] Department of Biological Sciences, Marquette University, Milwaukee, WI, United States

Edited by:
Nobuo Imai,
Tokyo University of Agriculture, Japan

Reviewed by:
Yajun Chen,
Xishuangbanna Tropical Botanical Garden (CAS), China
Patrick Addo-Fordjour,
Kwame Nkrumah University of Science and Technology, Ghana

***Correspondence:**
Sergio Estrada-Villegas
estradavillegassergio@gmail.com

Specialty section:
This article was submitted to Tropical Forests, a section of the journal Frontiers in Forests and Global Change

Received: 09 November 2021
Accepted: 29 December 2021
Published: 11 February 2022

Citation:
Estrada-Villegas S, Pedraza Narvaez SS, Sanchez A and Schnitzer SA (2022) Lianas Significantly Reduce Tree Performance and Biomass Accumulation Across Tropical Forests: A Global Meta-Analysis.
Front. For. Glob. Change 4:812066.
doi: 10.3389/ffgc.2021.812066

Lianas are a quintessential tropical plant growth-form; they are speciose and abundant in tropical forests worldwide. Lianas compete intensely with trees, reducing nearly all aspects of tree performance. However, the negative effects of lianas on trees have never been combined and quantified for multiple tropical forests. Here, we present the first comprehensive standardized quantification of the effect of lianas on trees across tropical forests worldwide. We used data from 50 liana removal experiments and quantified the effect size of lianas on tree growth, biomass accretion, reproduction, mortality, leaf water potential, sap flow velocity, and leaf area index (LAI) across different forest types. Using a three-level mixed-effect meta-analysis, we found unequivocal evidence that lianas significantly reduce tree growth and biomass accretion in ecological, logging, and silvicultural studies. Lianas also significantly reduce tree reproduction, recruitment, and physiological performance. The relative detrimental effect of lianas on trees does not increase in drier forests, where lianas tend to be more abundant. Our results highlight the substantial liana-induced reduction in tree performance and biomass accumulation, and they provide quantitative data on the effects of lianas on trees that are essential for large-scale plant demographic and ecosystem models that predict forest change and carbon dynamics.

Keywords: liana-tree interactions, competition, tropical forests, removal experiments, experimental ecology, forestry, biomass reduction

INTRODUCTION

Lianas (woody vines) are a diverse polyphyletic guild of woody climbing plants that add substantially to forest structure, complexity, diversity, and dynamics. Lianas can contribute up to 35% of the woody species and up to 25% of all woody stems in lowland tropical forests, respectively (Schnitzer et al., 2012). Lianas use trees (apically-dominant, self-supporting woody plants) for structural support to climb to the top of the forest canopy (Stevenson, 1927; Trimble and Tryon, 1974), where they deploy their foliage above that of their tree hosts (Kira and Ogawa, 1971; Putz, 1984; Medina-Vega et al., 2020), thus reducing the amount of light that would have been otherwise available for trees (Avalos et al., 1999; Clark et al., 2008). Indeed, liana-removal studies have shown that lianas reduce forest leaf area index (LAI) by up to 20% (Schnitzer and Carson, 2010; Rodríguez-Ronderos et al., 2016; Estrada-Villegas et al., 2020). Lianas also compete with trees for belowground resources, such as soil water and nutrients (Dillenburg et al., 1995). By reducing light and belowground resources, lianas significantly reduce tree survival (Ingwell et al., 2010), fecundity (García León et al., 2018), recruitment (Schnitzer and Carson, 2010), and growth (Pérez-Salicrup, 2001; Van Der Heijden and Phillips, 2009; Álvarez-Cansino et al., 2015).

The detrimental effect of lianas goes beyond individual trees; lianas reduce forest-level biomass sequestration and storage, and can reduce tree species diversity and alter tree species composition (Schnitzer, 2018). Lianas significantly reduce forest biomass sequestration, from 52% (César et al., 2016) up to 180% (Schnitzer et al., 2014). Lianas also modify where biomass is allocated; forest plots where lianas were removed allocated 44% of their biomass to woody tissues and 33% in leaves. By contrast, control plots where lianas were present allocated 29% of their biomass to woody tissues and an impressive 53% to leaves (Van Der Heijden et al., 2015). Therefore, lianas both reduce biomass accumulation and influence where biomass is stored, shifting biomass turnover toward leaves, which increases carbon and nutrient cycling (Van Der Heijden et al., 2015). Lianas also influence forest composition by reducing tree species richness in gaps (Schnitzer and Carson, 2010), and by decreasing population growth rates of some tree species more than others (Visser et al., 2018).

The detrimental effects of lianas on individual trees and forest communities may be stronger at sites where lianas are more abundant. Thus, in areas such as seasonal forests, where mean annual precipitation is low and month rainfall variability is high, liana communities are abundant and diverse (Schnitzer, 2005; Dewalt et al., 2015; Parolari et al., 2020) and can severely decrease tree growth and performance. In other words, lianas likely have a stronger detrimental effect on trees in areas where they are more abundant, assuming that their effect on trees scales with their abundance. Given that there are now 16 studies indicating that liana density, productivity, and biomass are all increasing relative to trees in tropical forests (Pandian and Parthasarathy, 2016; Ceballos and Malizia, 2017; Hogan et al., 2017; Venegas-González et al., 2020; Schnitzer et al., 2021), it is paramount to determine the magnitude at which lianas reduce tree performance and forest biomass, and how these effects change along important environmental gradients.

A recent review of 64 published liana removal experiments by Estrada-Villegas and Schnitzer (2018) provided strong support for the capacity of lianas to reduce tree growth, survival, recruitment, fecundity, and physiological performance. These experiments were conducted at a variety of temporal and spatial scales; from removals around targeted tree individuals from a single species and spanning a few days, to liana removals with thousands of trees comprising many species and spanning nearly three decades (Okali and Ola-Adams, 1987; Tobin et al., 2012; Kainer et al., 2014; César et al., 2016). The main conclusion, in accordance with that of other reviews (Isnard and Silk, 2009; Paul and Yavitt, 2011; Durán and Sánchez-Azofeifa, 2015), is that lianas reduce nearly all aspects of tree performance.

Despite the numerous reviews, no study up to date has quantified the direction and magnitude of the effect of lianas on trees for multiple liana removal experiments. While reviews from published literature have shown clear general trends on how lianas affect tree performance and forest ecosystem processes, there has not been an accurate quantification of such effects in a standardized fashion using multiple studies. In other words, there has been no previous attempt to combine data and use a meta-analytic approach to quantify the strength and direction of liana removal after accounting for the variability within and across experiments. Such quantification is critical to understand the role of lianas in tropical forests, as well as provide the essential parameters for global vegetation models (e.g., Di Porcia E Brugnera et al., 2019). Furthermore, lianas can have large negative effects on valuable tropical timber trees, but there has been no large-scale, standardized quantification of the effects of lianas in conjunction with other forms of forest manipulation common in forestry and silvicultural practices.

In this study, we standardized and combined data from 50 published ecological, forestry, and silvicultural liana-removal experiments from 16 countries in the African, American, and Asian tropics and subtropics to quantify the magnitude by which lianas reduce tree growth, biomass accumulation, and reproduction, as well as alter tree water potential, sap flow velocity, and LAI. By calculating the effect size for each experiment and combining these data, we provide the most accurate mean quantification of the direction and strength of the effect of lianas on tropical tree performance, as well as extrapolate these findings to tropical forest ecosystem functioning. Specifically, we addressed the following three main questions: (1) What is the combined standardized effect of lianas on tree performance (growth, biomass accumulation, reproduction, mortality, leaf water potential, sap flow velocity, and LAI) for ecological studies? (2) How strong is the negative effect of lianas on trees in logging and silvicultural practices? (3) Does the effect of lianas vary across forest with different levels of rainfall or among ecosystem types (i.e., life zone)?

METHODS

Literature Selection

To conduct the meta-analysis, we used an extensive list of published literature on liana removal experiments assembled by Estrada-Villegas and Schnitzer (2018), and added six more experiments that were either missed by, or published after, the 2018 review. We assembled this list of papers using Google Scholar, the LianaEcologyProject.com, and Web of Science (for more details on the search methods see Estrada-Villegas and Schnitzer, 2018). We included only tropical and subtropical *in situ* experiments, and excluded greenhouse experiments and observational studies.

We categorized the studies according to their goal (ecology or forestry), and whether the liana manipulation was paired with another manipulation, such as tree removal and canopy thinning. We divided the literature in three categories of liana removal: (1)

ecological; (2) logging; and (3) silvicultural (following Estrada-Villegas and Schnitzer, 2018). Ecological studies were those with a clear distinction between the liana removal and control (no liana removal) treatments across a range of forest types (from dry to seasonal to wet forests, and both old-growth and secondary forests). Logging studies were those where liana removal had been done in conjunction with logging treatments, such as tree girdling or poisoning; thus, the effect of liana removal was compounded with that of tree removal. Silvicultural studies included those where a liana removal manipulation was imposed either before or after logging operations. Silvicultural studies, for example, often include liana cutting as part of experimental treatments either before or after logging, and sought to determine whether logging damage or future logging yield was affected by liana removal. By contrast, the goal of ecological studies was typically to quantify the effect of liana removal on the performance of trees and on emergent ecosystem processes, while not explicitly accounting for previous land use (Estrada-Villegas and Schnitzer, 2018).

We further classified the selected studies according to response variables at the tree-level (tree biomass accretion, growth, leaf water potential, mortality, reproduction, sap flow) and plot-level (tree seedling and sapling recruitment, forest canopy openness, and LAI) (Rodríguez-Ronderos et al., 2016). For each study, we noted the ecosystem type (i.e., life zone) where the experiments were conducted (Holdridge, 1964) (Tropical Dry Forest, Tropical Moist Forest, Tropical Wet Forests, Subtropical Moist Forest, Subtropical Marsh), the mean annual precipitation, and the length of the study period when available. We excluded studies that omitted a measure of the variability around a measure of central tendency for the response variables (with a few exceptions, see "Data collection" below). We also omitted studies that did not specify data from a control treatment and studies that used unique response variables that precluded comparisons with other experiments.

Data Collection

We found a total of 50 studies that met our criteria. From each study and response variable, we extracted data on the sample size, the mean value from the liana removal experiment (with or without co-occurring forestry treatment), and mean value of the control treatment (no liana removal and no co-occurring forestry treatment). From each study, we also extracted the standard deviations of the response variables from both the liana removal and the control treatments. We used WebPlotDigitizer Version 4.3 (Rohatgi, 2020) to extract the necessary data from published figures. Standard errors were transformed into standard deviations, and when medians and quantiles were reported, we used the methods from Wan et al. (2014) to calculate means and standard deviations.

We extracted data that were aggregated across size classes and species. However, if the data were not aggregated in the original study, we extracted the values per species or size class. In a few cases, when variances were not reported, we obtained means and standard deviations by averaging the means of several size classes (e.g., Pinard and Putz, 1996), or averaging means among replicates of the same logging treatment (e.g., Dekker and De Graaf, 2003). Given that many studies had multiple censuses over time, we included all observations each time a mean and a deviation were reported (i.e., multiple observations). Noting multiple observations per study allowed us to incorporate the dynamic responses of trees and forests to liana removal through time within studies without losing important data by averaging responses across time (Cheung, 2019). We accounted for these non-independent repeated measurements in our data analyses. Data stored as **Supplementary Material 1** in a digital repository (https://doi.org/10.6084/m9.figshare.14770095.v1).

Data Analysis

To determine the effect size of each observation, we calculated standardized mean differences using Hedges' *g* (Hedges and Olkin, 1985). Standardized mean differences express the magnitude of the response of the liana removal manipulation minus the unmanipulated controls, divided by the pooled standard deviation of both treatments. Standardized mean differences corrects for small sample sizes, and are suitable when there are negative values, such as leaf water potentials (Gurevitch et al., 2001; Koricheva et al., 2013). Positive standardized mean differences indicate that trees were benefited by liana removal.

We calculated the standardized mean difference and the variance for every observation (i.e., time interval) of every study with the function "escalc" from the R package metafor (Viechtbauer, 2010). We used these values in a series of three-level mixed effect meta-analytic models (Konstantopoulos, 2011; Midolo and Wellstein, 2020) employing the function "rma.mv." Many studies reported multiple measurements through time; therefore, we used time nested within study as a random effect. This random structure accounts for the non-independence of multiple measurements across time within a study (Konstantopoulos, 2011; Cheung, 2019). These models allowed us to calculate a standardized mean difference and 95% confidence intervals for each response variable within each category.

To investigate what is the combined standardized effect of lianas on tree performance and how strong is the effect of lianas on trees, we ran separate models for each response variable within each study category to capture the direction and magnitude of the liana effect. To determine whether lianas have a stronger effect in more seasonal sites, where they tend to be more abundant (Dewalt et al., 2015), we used mean annual precipitation and life zone separately as moderators in the meta-analytic models. Forty-six studies reported mean annual precipitation, so we used WorldClim data (Fick and Hijmans, 2017) to obtain mean annual precipitation for the remaining four studies. We used an omnibus test to evaluate the effect of the moderators but only for those response variables that were significantly affected by liana removal (Viechtbauer, 2010).

We evaluated whether there is evidence of potential publication bias in the liana removal literature where studies have selectively and systematically reported significant results in the same direction and magnitude as the available literature (Koricheva et al., 2013). Assessing publication bias gave us the capacity to incorporate the influence of that bias in the inference made from the meta-analysis. To assess publication bias, we

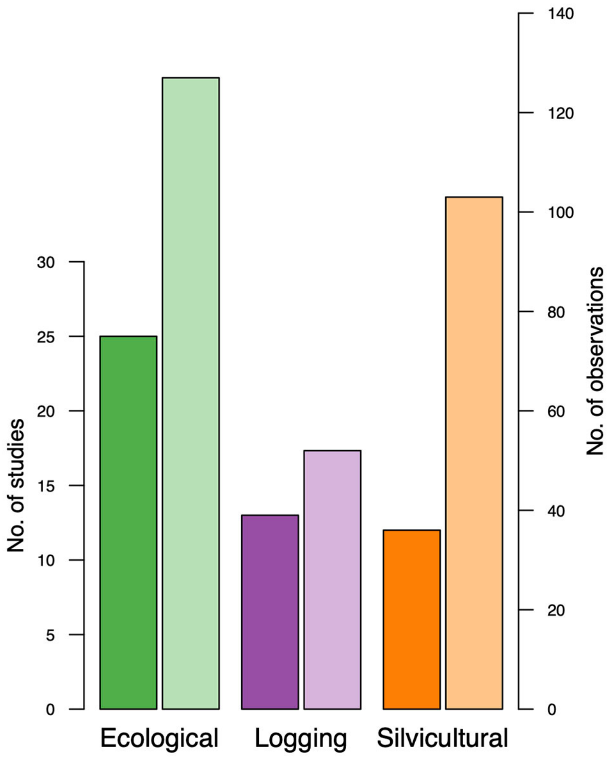

FIGURE 1 | Number of liana removal studies and observations within studies used to conduct three-level meta-analyzes for ecological, logging, and silvicultural experiments. Number of studies in darker colors, number of observations in lighter shades.

first created a funnel plot for every meta-analytic model, and tested its symmetry with an Egger's regression test. We ran the tests with the "rma.mv" function, and used the inverse of the sampling variance as a moderator (Nakagawa and Santos, 2012). A significant effect of the moderator indicated a potential publication bias.

RESULTS

We identified 282 observations from the 50 studies published from 1968 to 2021 (**Supplementary Material 1**). Seventeen of the 50 studies reported responses to liana removal over time, and 37 reported a single response variable regardless of category. We found more ecological studies, followed by logging and silvicultural experiments (**Figure 1**), with more observations in silvicultural than logging studies (**Figure 1**). The most commonly assessed response variables across categories were tree growth, mortality and biomass accretion (**Table 1**). Across all categories, 12 studies were conducted in Panama, 10 in Brazil, 8 in Bolivia, 4 in Indonesia, 2 studies in each of the following countries: Argentina, Cameroon, Costa Rica, and Malaysia, and 1 study in: CÃťte d'Ivoire, Mexico, Nigeria, Suriname, Tanzania, Uganda, USA, and Venezuela (**Supplementary Material 1**).

For ecological studies, we found that liana removal had strong and significant positive effects on tree growth, biomass accretion, leaf water potential, recruitment of seedlings or saplings, and tree reproduction (**Figure 2**; **Table 1**). Liana removal had a marginally significant positive effect on tree sap flow (**Figure 2**; **Table 1**). However, there was a significant decrease in forest LAI, indicating that lianas contribute an important proportion of the foliage in the canopy. By contrast, liana removal did not influence tree mortality nor canopy openness (**Figure 2**; **Table 1**). For logging and silvicultural studies, lianas significantly decreased tree growth and biomass accretion (**Figure 2**; **Table 1**). Silvicultural liana removal had a marginally positive effect on tree growth. Mortality was not affected by liana removal for logging or silvicultural studies (**Figure 2**; **Table 1**). Across all three study categories, lianas significantly reduced tree biomass accretion, growth, reproduction, and decreased physiological performance in terms of water status.

The strength of liana removal effects did not increase in dryer ecosystems, and none of the response variables increased in magnitude as mean annual precipitation declined (**Table 2**). Egger's regression tests indicate a probable publication bias for studies that assessed LAI, canopy openness and reproduction, in the ecological literature, and for studies that assessed growth and biomass accretion in the logging and silvicultural literature, respectively (**Table 1**).

DISCUSSION

This study is the first standardized comparative quantification of the effect of lianas on tropical ecosystems worldwide. Our findings unambiguously show that lianas have a strong negative effect on tree growth, biomass accretion, water status, and reproductive output. Previous reviews reported results based on trends across data (e.g., Toledo-Aceves, 2015; Marshall et al., 2017; Estrada-Villegas and Schnitzer, 2018), but they did not use rigorous quantitative methods to compare between experimental treatments. The meta-analytic approach allowed us to incorporate the effect of sample sizes and variances within and across studies to quantitatively evaluate the effect of lianas on trees and on tropical and subtropical forest growth and performance. Our findings provide an unequivocal result: lianas have a strong negative effect on tree performance and reproduction, regardless of forest type or the goals of the study (i.e., ecological, logging, or silvicultural).

Effects of Lianas on Tree Growth and Biomass Accretion

Studies in all three categories (ecological, logging, and silvicultural) consistently showed that lianas had a negative effect on tree growth and biomass accumulation that scaled up to the whole-forest level. In fact, their effects on tree growth and biomass were more than one standard deviation greater in some of the comparisons, attesting to the strength by which lianas negatively affect trees. Trees grow less in the presence of lianas, and forests that have more lianas allocate more biomass to leaves than to stems (Van Der Heijden et al., 2015), indicating that lianas can have serious detrimental consequences for biomass accumulation and carbon cycling in tropical forests. In fact,

TABLE 1 | The number of studies, observations per study, and results from a meta-analysis and assessment of publication bias of 50 liana removal experiments in tropical and subtropical forests worldwide.

Category	Response variable	Three-level meta-analytic model			Publication bias (Egger's test)		
		No. of studies	No. of observations	*P*-value	Intercept	*z*	*P*-value
Ecological	Biomass accretion	8	25	0.041	0.0141	0.5	0.617
	Canopy openness	4	19	0.675	−1.1592	−4.6290	<0.0001
	Growth	8	26	0.0002	−0.0124	−0.5051	0.614
	LAI	2	8	0.004	0.6713	4.3988	<0.0001
	Mortality	4	13	0.97	0.3037	0.6070	0.544
	Recruitment	4	13	0.011	−0.6440	−1.7880	0.074
	Reproduction	4	18	0.007	−0.0413	−5.4221	<0.0001
	Sap flow	2	5	0.05	−0.6854	−1.3642	0.173
	Leaf water potential	2	4	<0.0001	0.0487	0.1925	0.847
Logging	Canopy openness	3	4	0.099	−0.0255	−2.4630	0.014
	Growth	8	24	0.024	−0.0058	−11.1805	<0.0001
	Mortality	3	15	0.159	0.2338	3.4897	0.001
	Recruitment	4	8	0.187	0.0160	0.6141	0.539
Silvicultural	Biomass accretion	2	23	0.002	−2.8697	−4.9715	<0.0001
	Growth	5	44	0.081	−0.0078	−1.0230	0.306
	Mortality	9	29	0.146	0.0210	0.6610	0.509

Studies are grouped in three categories: ecological, logging, and silvicultural.

recent removal experiments have shown that lianas can reduce up to 1.462 Mg of carbon per hectare per year, or 51.7% with respect to controls, and the effect is significant up to 6 years after experimental removal (Van Der Heijden et al., 2019).

Our results have important implications for global models of carbon sequestration. Current vegetation models usually incorporate differential tree growth and mortality among functional groups (Aleixo et al., 2019). These models, however, may fail to account the strength by which lianas reduce tree growth and biomass accretion, and probably overestimate how much biomass tropical forests will accumulate in the future. A recent vegetation model showed that forest net productivity was 2.6% lower when lianas were incorporated in the calculations compared to models that excluded them (Di Porcia E Brugnera et al., 2019). The reduction in productivity found in this model was mostly driven by the capacity of lianas to strongly compete for water and light (Meunier et al., 2021). Given that climate change may be accelerating tree mortality (Mcdowell et al., 2018), and that lianas increase in density and basal area in disturbed areas created by tree falls (Ledo et al., 2016; Schnitzer et al., 2021), it is necessary to include the detrimental effects that lianas exert on forest growth and biomass accretion we quantified in this meta-analysis in future vegetation models.

Effects of Lianas on Tree Reproduction

Lianas significantly reduce tree reproduction, which may have substantial effects on tree species demography. Trees bearing lianas accrue less resources, which may limit the amount of carbohydrates that can be allotted to flowers or fruits compared to trees without lianas in their canopies (Staudhammer et al., 2013; Kainer et al., 2014). Therefore, lianas can have the capacity to modify tree population dynamics and community turnover due to a reduction in tree reproduction (Schnitzer, 2018). Nevertheless, the number of studies assessing the effect of lianas on tree reproduction is low; there are only four studies that have reported species-specific cases and community-wide results that document the magnitude by which lianas affect tree reproduction. For example, studies have shown that flower and fruit production increases following liana removal for only three species: *Bursera sminaruba, Chrysophyllum lucentifolium,* and *Bertholletia excelsa* (Stevens, 1987; Fonseca et al., 2009). One set of experiments examined the 10-year effect of lianas on individuals of the Brazil Nut tree (*Bertholletia excelsa*), demonstrating that they significantly decrease fruit yield compared to trees without lianas (Staudhammer et al., 2013; Kainer et al., 2014). Studies that pool flowering and fruiting data across the tree community have also shown significant changes in tree reproduction after removal. For example, in a lowland moist forest in Panama, the number of tree species with fruits increased by 169% in liana removal plots compared to unmanipulated plots. Moreover, the number of fruiting trees was 173% higher in removal plots compared to unmanipulated plots (García León et al., 2018). While the limited data indicate that lianas strongly reduce tree reproduction, more species-specific experiments and community-wide manipulations are necessary to determine, for example, if a reduction in flowering or fruiting is coupled with a decrease in tree seed size and germination success when lianas are present in the forest canopy.

Effects of Lianas on Tree Recruitment and Water Status

Lianas often climb small trees as they begin their ascent to the forest canopy (Putz, 1984) and, by doing so, lianas can smother small trees, thus decreasing their recruitment. The negative

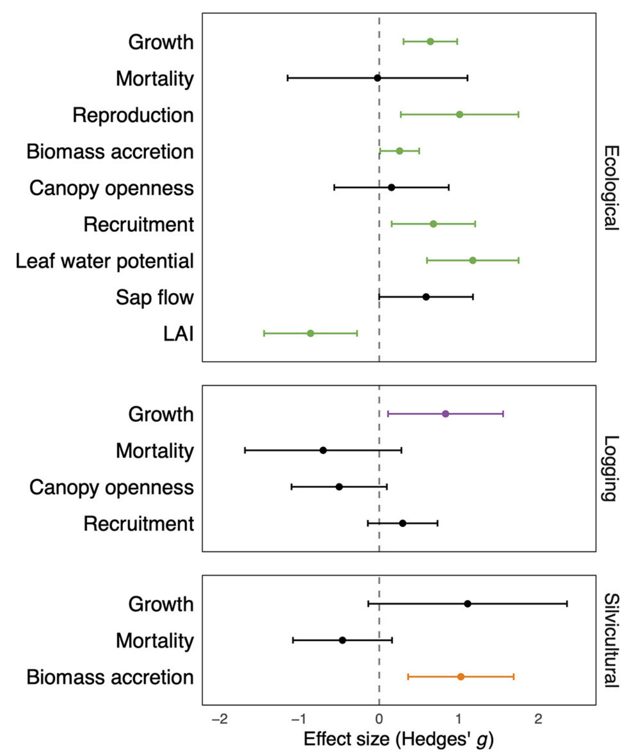

FIGURE 2 | Tree responses to liana removal experiments conducted in tropical and subtropical forests in published ecological, logging, and silvicultural studies. Values are standardized effect sizes (Hedges' *g*) and their 95% confidence intervals estimated by three-level meta-analytic models. Values greater than zero indicate positive effects of liana removal. Green, purple, and orange values represent significant differences from zero; black values represent non-significant differences from zero.

effects of lianas on tree recruitment is especially prevalent in forest gaps, where lianas recruit rapidly and in high density (Schnitzer and Carson, 2010). Nevertheless, there are nuances on how lianas affect tree recruitment. In an experiment to compare the competitive effect of lianas and trees, Wright et al. (2015) removed similar amounts of tree and liana biomass in a moist forest in Panama. They found that seedling recruitment of the shade-tolerant species *Dipteryx oleifera* was greater in the liana removal treatment compared to the tree biomass treatment, but only during the dry season. In a separate study, the removal of tree saplings during the wet season had a stronger effect on recruitment compared to the removal of an equal mass of lianas (Venegas-González et al., 2020). Therefore, the liana effect on tree seedling recruitment may vary seasonally and across tree species.

The limited number of removal experiments that have assessed tree physiological performance have shown that lianas significantly reduce water availability for trees (Barker and Pérez-Salicrup, 2000; Pérez-Salicrup and Barker, 2000; Tobin et al., 2012; Álvarez-Cansino et al., 2015). Specifically, lianas reduce tree leaf water content and sap flow. Water drawdown by lianas, which is necessary to fuel their "fast and furious" physiological strategy (Schnitzer, 2018; Smith-Martin et al., 2019), may diminish water availability for trees (Reid et al., 2015). The reduction in water availability results in lower sap flow and, ultimately, in decreased tree growth (Álvarez-Cansino et al., 2015). Additional experiments are required to elucidate the extent and the mechanisms by which lianas reduce tree physiological performance and the cascading effects on tree growth and reproduction.

Liana-removal experiments have also shown that lianas contribute substantially to canopy foliage despite their relatively low basal area (Kira and Ogawa, 1971). Two manipulations from tropical moist forest in Panama reported that lianas contributed approximately 20% of the foliage in the canopy (Rodríguez-Ronderos et al., 2016; Estrada-Villegas et al., 2020). The 20% contribution is remarkable because lianas contribute <5% of the total forest basal area (Clark et al., 2008). Moreover, liana leaves displace tree leaves on a 1-to-1 mass ratio (Kira and Ogawa, 1971), which explains the increase in tree growth and biomass accretion following liana-removal, as tree foliage rapidly seizes the space vacated by lianas (Rodríguez-Ronderos et al., 2016; Van Der Heijden et al., 2019; Estrada-Villegas et al., 2020). In sum, lianas significantly reduce tree reproduction, recruitment, and water status. Moreover, the reduction of liana foliage matched an increase in tree foliage, which followed a marked increase in tree growth and biomass accretion.

Effect of Lianas Across Forest Types

The effect of lianas on tree growth and biomass accretion was expected to be greater in areas with lower mean annual precipitation and high rainfall variability, areas where lianas are usually more abundant and speciose (Schnitzer, 2005, 2018; Parolari et al., 2020). However, this was not the case. Lianas seem to have a similarly strong negative effect on trees in both wet and dry seasons, or sometimes not evidenced aboveground. For example, in a 5-year study of seasonal liana and tree growth in central Panama, lianas grew mostly during the dry season and less during the wet season, whereas trees grew poorly in the dry season and mostly in the wet season (Schnitzer and Van Der Heijden, 2019). Due to these differences in the optimal periods for liana and tree growth, the negative effects of lianas on trees were similar throughout the year. Indeed, a liana removal experiment in central Panama showed that over a 5-year period, lianas reduced biomass accretion similarly (by 46.9 and 48.5%, respectively) in the dry and wet seasons (Van Der Heijden et al., 2019). Moreover, a recent removal experiment in a Panamanian dry forest showed that lianas did not reduce above ground biomass accumulation (Estrada-Villegas et al., 2021), suggesting that the competitive effect of lianas is lower where water stress is greater despite high liana richness or abundance. Thus, the combined standardized data suggest that the relative strength of liana competition among forests that differ in rainfall or ecosystem type may not scale with liana density *per se* because as liana abundance increases with decreasing precipitation, drought lessens the per-capita competitive effect of lianas on trees.

Publication Bias

For ecological studies that showed a significant detrimental effect of lianas on trees, we found a probable publication bias for

TABLE 2 | Results from omnibus tests to evaluate the effect of mean annual precipitation and Holdridge life zone on response variables that showed a significant effect of liana removal.

		Mean annual precipitation			Holdridge life zone		
Category	**Response variable**	Q_M	*df*	*P*-value	Q_M	*df*	*P*-value
Ecology	Biomass accretion	0.198	1	0.657	7.368	3	0.061
	Growth	2.265	1	0.132	4.602	2	0.1
	LAI	0.463	1	0.496	NA	NA	NA
	Recruitment	1.875	1	0.171	0.477	1	0.49
	Reproduction	0.416	1	0.519	0.114	2	0.945
Logging	Growth	0.371	1	0.542	0.416	2	0.812
Silvicultural	Biomass accretion	2.262	1	0.133	2.261	1	0.133

Leaf water potential and leaf area index (LAI) could not be evaluated because of low sample size.

experiments assessing LAI and reproduction. This bias may be attributable to low sample size within response variables across study categories, heterogeneity across studies due to differences not accounted by the random effects of the statistical models, or high variability across observations within studies (Nakagawa and Santos, 2012; Koricheva et al., 2013). These potential causes for bias are not mutually exclusive. Perhaps there have been too few published experiments to elucidate the true magnitude and variability of the effect of lianas on these response variables.

The publication bias for experiments assessing growth and biomass accretion in logging and silvicultural studies may be due to high variability among observations within studies or high heterogeneity across studies. To evaluate whether variability among observations for biomass accretion in silvicultural studies is a potential cause of bias, we conducted a *post hoc* test and calculated the median response across observations within studies, and recalculated effect sizes and confidence intervals. This analysis corroborated the finding that lianas significantly decreased biomass accretion in silvicultural studies (Hedge's $g = 1.208$; 95%CI = 0.568–1.847; p-value $= 0.0002$), but Egger's regression test for plot asymmetry remained significant (Intercept $= -2.679$, z score $= -2.65$, p-value $= 0.008$). This finding indicates that factors other than variability across observations may be driving plot asymmetry (i.e., publication bias). Logging and silvicultural experiments have high heterogeneity across studies in terms of forest types, forest ages, and intensity or timing of liana removal that were not accounted in our analyzes (Estrada-Villegas and Schnitzer, 2018). Future manipulations in forestry-oriented studies will help elucidate whether the bias is an artifact of sample size, heterogeneity across studies, or variability within studies over time.

In conclusion, this study represents the first comprehensive meta-analysis of the experimental effects of lianas on tree growth and performance. The combined standardized effect sizes used in this study demonstrate unequivocally that lianas reduce tree growth, biomass accretion, reproduction, recruitment, and leaf water potential. At the forest level, lianas reduce biomass accumulation and shift carbon pools from stems to leaves. The standardized quantitative results we provide here can be used to parameterize global vegetation models so as to improve our understanding of the global carbon cycle and tropical forests dynamics.

DATA AVAILABILITY STATEMENT

The original contributions presented in the study are included in the article/**Supplementary Material**, further inquiries can be directed to the corresponding author/s.

AUTHOR CONTRIBUTIONS

SE-V and SS conceived the study. SE-V and SP collected the data. SE-V analyzed the data. SE-V, SP, AS, and SS interpreted the data and wrote the manuscript. All authors approved the final version of the manuscript.

FUNDING

This work was supported by a fellowship to SE-V from the Departamento Administrativo de Ciencia, Tecnología e Innovación COLCIENCIAS, and by the Cullman Fellowship from the School of the Environment at Yale University and the New York Botanical Garden. SS was funded by the US National Science Foundation (NSF IOS-1558093, DEB-1822473, and DEB-2001799).

ACKNOWLEDGMENTS

We thank MaryRose Weatherton, who helped us compile a first version of the data set. We thank two reviewers for their comments on the manuscript.

SUPPLEMENTARY MATERIAL

The Supplementary Material for this article can be found online at: https://www.frontiersin.org/articles/10.3389/ffgc.2021.812066/full#supplementary-material

Supplementary Material 1 | Data to conduct three-level mixed effect meta-analytic models to determine the direction and magnitud of the effect of lianas on tree growth, growth, biomass accumulation, reproduction, mortality, leaf water potential, sap flow velocity in ecological, silvicultural and logging studies. The information for the column headings are here: https://doi.org/10.6084/m9.figshare.14770095.v1.

REFERENCES

Aleixo, I., Norris, D., Hemerik, L., Barbosa, A., Prata, E., Costa, F., et al. (2019). Amazonian rainforest tree mortality driven by climate and functional traits. *Nat. Clim. Chang.* 9, 384–388. doi: 10.1038/s41558-019-0458-0

Álvarez-Cansino, L., Schnitzer, S. A., Reid, J. P., and Powers, J. S. (2015). Liana competition with tropical trees varies seasonally but not with tree species identity. *Ecology* 96, 39–45. doi: 10.1890/14-1002.1

Avalos, G., Mulkey, S. S., and Kitajima, K. (1999). Leaf optical properties of trees and lianas in the outer canopy of a tropical dry forest. *Biotropica* 31, 517–520. doi: 10.1111/j.1744-7429.1999.tb00395.x

Barker, M. G., and Pérez-Salicrup, D. (2000). Comparative water relations of mature mahogany (*Swietenia macrophylla*) trees with and without lianas in a subhumid, seasonally dry forest in Bolivia. *Tree Physiol.* 20, 1167–1174. doi: 10.1093/treephys/20.17.1167

Ceballos, S. J., and Malizia, A. (2017). Liana density declined and basal area increased over 12 y in a subtropical montane forest in Argentina. *J. Trop. Ecol.* 33, 241–248. doi: 10.1017/S0266467417000153

César, R. G., Holl, K. D., Girão, V. J., Mello, F. N. A., Vidal, E., Alves, M. C., et al. (2016). Evaluating climber cutting as a strategy to restore degraded tropical forests. *Biol. Conserv.* 201, 309–313. doi: 10.1016/j.biocon.2016.07.031

Cheung, M. W. L. (2019). A guide to conducting a meta-analysis with non-independent effect sizes. *Neuropsychol. Rev.* 29, 387–396. doi: 10.1007/s11065-019-09415-6

Clark, D. B., Olivas, P. C., Oberbauer, S. F., Clark, D. A., and Ryan, M. G. (2008). First direct landscape-scale measurement of tropical rain forest Leaf Area Index, a key driver of global primary productivity. *Ecol. Lett.* 11, 163–172. doi: 10.1111/j.1461-0248.2007.01134.x

Dekker, M., and De Graaf, N. R. (2003). Pioneer and climax tree regeneration following selective logging with silviculture in Suriname. *For. Ecol. Manage.* 172, 183–190. doi: 10.1016/S0378-1127(01)00801-5

Dewalt, S. J., Schnitzer, S. A., Alves, L. F., Bongers, F., Burnham, R. J., Cai, Z., et al. (2015). "Biogeographical patterns of liana abundance and diversity," in *Ecology of Lianas*, eds S. A. Schnitzer, F. Bongers, R. J. Burnham, and F. E. Putz (Oxford: John Wiley and Sons), 131–146.

Di Porcia E Brugnera, M., Meunier, F., Longo, M., Krishna Moorthy, S. M., De Deurwaerder, H., Schnitzer, S. A., et al. (2019). Modeling the impact of liana infestation on the demography and carbon cycle of tropical forests. *Glob. Change Biol.* 25, 3767–3780. doi: 10.1111/gcb.14769

Dillenburg, L. R., Teramura, A. H., Forseth, I. N., and Whigham, D. F. (1995). Photosynthetic and biomass allocation responses of *Liquidambar styraciflua* (Hamamelidaceae) to vine competition. *Am. J. Bot.* 82, 454–461. doi: 10.2307/2445691

Durán, S. M., and Sánchez-Azofeifa, G. A. (2015). "Liana effects on carbon storage and uptake in mature and secondary tropical forests," in *Biodiversity of Lianas,* ed N. Parthasarathy (Cham: Springer International Publishing), 43–55.

Estrada-Villegas, S., Hall, J. S., Van Breugel, M., and Schnitzer, S. A. (2020). Lianas reduce biomass accumulation in early successional tropical forests. *Ecology* 101, e02989. doi: 10.1002/ecy.2989

Estrada-Villegas, S., Hall, J. S., Van Breugel, M., and Schnitzer, S. A. (2021). Lianas do not reduce tree biomass accumulation in young successional tropical dry forests. *Oecologia*. 195, 1019–1029. doi: 10.1007/s00442-021-04877-z

Estrada-Villegas, S., and Schnitzer, S. A. (2018). A comprehensive synthesis of liana removal experiments in tropical forests. *Biotropica* 50, 729–739. doi: 10.1111/btp.12571

Fick, S. E., and Hijmans, R. J. (2017). WorldClim 2: new 1-km spatial resolution climate surfaces for global land areas. *Int. J. Climatol.* 37, 4302–4315. doi: 10.1002/joc.5086

Fonseca, M. G., Vidal, E., and Maës Dos Santos, F. A. (2009). Intraspecific variation in the fruiting of an amazonian timber tree: implications for management. *Biotropica* 41, 179–185. doi: 10.1111/j.1744-7429.2008.00480.x

García León, M. M., Martínez Izquierdo, L., Mello, F. N. A., Powers, J. S., and Schnitzer, S. A. (2018). Lianas reduce community-level canopy tree reproduction in a Panamanian forest. *J. Ecol.* 106, 737–745. doi: 10.1111/1365-2745.12807

Gurevitch, J., Curtis, P. S., and Jones, M. H. (2001). Meta-analysis in ecology. *Adv. Ecol. Res.* 32, 199–247. doi: 10.1016/S0065-2504(01)32013-5

Hedges, L. V., and Olkin, I. (1985). *Statistical Methods for Meta-Analysis.* San Diego, CA: Academic Press.

Hogan, J. A., Mayorquín, S., Rice, K., Thompson, J., Zimmerman, J. K., and Brokaw, N. (2017). Liana dynamics reflect land-use history and hurricane response in a Puerto Rican forest. *J. Trop. Ecol.* 33, 155–164. doi: 10.1017/S0266467417000049

Holdridge, L. R. (1964). *Life Zone Ecology.* San José: Centro Científico Tropical.

Ingwell, L. L., Joseph Wright, S., Becklund, K. K., Hubbell, S. P., and Schnitzer, S. A. (2010). The impact of lianas on 10 years of tree growth and mortality on Barro Colorado Island, Panama. *J. Ecol.* 98, 879–887. doi: 10.1111/j.1365-2745.2010.01676.x

Isnard, S., and Silk, W. K. (2009). Moving with climbing plants from Charles Darwin's time into the 21st century. *Am. J. Bot.* 96, 1205–1221. doi: 10.3732/ajb.0900045

Kainer, K. A., Wadt, L. H. O., and Staudhammer, C. L. (2014). Testing a silvicultural recommendation: Brazil nut responses 10 years after liana cutting. *J. Appl. Ecol.* 51, 655–663. doi: 10.1111/1365-2664.12231

Kira, T., and Ogawa, H. (1971). "Productivity of forest ecosystems assessment of primary prodution in tropical and equatorial forests," in *Production of Forest Ecosystems: Proc. Brussels Symp. Organized by UNESCO and IBP* (27–31 Oct. 1969), ed P. Duvigneaud (Czechoslovakia: UNESCO), 309–321.

Konstantopoulos, S. (2011). Fixed effects and variance components estimation in three-level meta-analysis. *Res. Synth. Methods* 2, 61–76. doi: 10.1002/jrsm.35

Koricheva, J., Gurevitch, J., and Mengersen, K. (2013). *Handbook of Meta-Analysis in Ecology and Evolution.* Princeton, NJ: Princeton University Press.

Ledo, A., Illian, J. B., Schnitzer, S. A., Wright, S. J., Dalling, J. W., and Burslem, D. F. R. P. (2016). Lianas and soil nutrients predict fine-scale distribution of above-ground biomass in a tropical moist forest. *J. Ecol.* 104, 1819–1828. doi: 10.1111/1365-2745.12635

Marshall, A. R., Coates, M. A., Archer, J., Kivambe, E., Mnendendo, H., Mtoka, S., et al. (2017). Liana cutting for restoring tropical forests: a rare palaeotropical trial. *Afr. J. Ecol.* 55, 282–297. doi: 10.1111/aje.12349

Mcdowell, N., Allen, C. D., Anderson-Teixeira, K., Brando, P., Brienen, R., Chambers, J., et al. (2018). Drivers and mechanisms of tree mortality in moist tropical forests. *New Phytol.* 219, 851–869. doi: 10.1111/nph.15027

Medina-Vega, J. A., Bongers, F., Schnitzer, S. A., and Sterck, F. J. (2020). Lianas explore the forest canopy more effectively than trees under drier conditions. *Funct. Ecol*. 35, 318–329. doi: 10.1111/1365-2435.13717

Meunier, F., Verbeeck, H., Cowdery, B., Schnitzer, S. A., Smith-Martin, C. M., Powers, J. S., et al. (2021). Unraveling the relative role of light and water competition between lianas and trees in tropical forests: a vegetation model analysis. *J. Ecol.* 109, 519–540. doi: 10.1111/1365-2745.13540

Midolo, G., and Wellstein, C. (2020). Plant performance and survival across transplant experiments depend upon temperature and precipitation change along elevation. *J. Ecol.* 108, 2107–2120. doi: 10.1111/1365-2745.13387

Nakagawa, S., and Santos, E. S. A. (2012). Methodological issues and advances in biological meta-analysis. *Evol. Ecol.* 26, 1253–1274. doi: 10.1007/s10682-012-9555-5

Okali, D. U. U., and Ola-Adams, B. A. (1987). Tree population changes in treated rain forest at Omo Forest Reserve, south-western Nigeria. *J. Trop. Ecol.* 3, 291–313. doi: 10.1017/S0266467400002297

Pandian, E., and Parthasarathy, N. (2016). Decadal (2003–2013) changes in liana diversity, abundance and aboveground biomass in four inland tropical dry evergreen forest sites of peninsular India. *J. For. Res.* 27, 133–146. doi: 10.1007/s11676-015-0146-5

Parolari, A. J., Paul, K., Griffing, A., Condit, R., Perez, R., Aguilar, S., et al. (2020). Liana abundance and diversity increase with rainfall seasonality along a precipitation gradient in Panama. *Ecography* 43, 25–33. doi: 10.1111/ecog.04678

Paul, G. S., and Yavitt, J. B. (2011). Tropical vine growth and the effects on forest succession: a review of the ecology and management of tropical climbing plants. *Bot. Rev.* 77, 11–30. doi: 10.1007/s12229-010-9059-3

Pérez-Salicrup, D. R. (2001). Effect of liana cutting on tree regeneration in a liana forest in Amazonian Bolivia. *Ecology* 82, 389–396. doi: 10.2307/2679867

Pérez-Salicrup, D. R., and Barker, M. G. (2000). Effect of liana cutting on water potential and growth of adult *Senna multijuga* (Caesalpinioideae) trees in a Bolivian tropical forest. *Oecologia* 124, 469–475. doi: 10.1007/pl00008872

Pinard, M. A., and Putz, F. E. (1996). Retaining forest biomass by reducing logging damage. *Biotropica* 28, 278–295. doi: 10.2307/2389193

Putz, F. E. (1984). The natural history of lianas on Barro Colorado Island, Panama. *Ecology* 65, 1713–1724. doi: 10.2307/1937767

Reid, J. P., Schnitzer, S. A., and Powers, J. S. (2015). Short and long-term soil moisture effects of liana removal in a seasonally moist tropical forest. *PLoS ONE* 10, e0141891. doi: 10.1371/journal.pone.0141891

Rodríguez-Ronderos, M. E., Bohrer, G., Sanchez-Azofeifa, A., Powers, J. S., and Schnitzer, S. A. (2016). Contribution of lianas to plant area index and canopy structure in a Panamanian forest. *Ecology* 97, 3271–3277. doi: 10.1002/ecy.1597

Rohatgi, A. (2020). "*WebPlotDigitizer". 4.3 ed*. Pacifica, CA.

Schnitzer, S. A. (2005). A mechanistic explanation for global patterns of liana abundance and distribution. *Am. Nat.* 166, 262–276. doi: 10.1086/431250

Schnitzer, S. A. (2018). Testing ecological theory with lianas. *New Phytol.* 220, 366–380. doi: 10.1111/nph.15431

Schnitzer, S. A., and Carson, W. P. (2010). Lianas suppress tree regeneration and diversity in treefall gaps. *Ecol. Lett.* 13, 849–857. doi: 10.1111/j.1461-0248.2010.01480.x

Schnitzer, S. A., Defilippis, D. M., Visser, M., Estrada-Villegas, S., Rivera-Camaña, R., Bernal, B., et al. (2021). Local canopy disturbance as an explanation for long-term increases in liana abundance. *Ecol. Lett*. 24, 2635–2647. doi: 10.1111/ele.13881

Schnitzer, S. A., Mangan, S. A., Dalling, J. W., Baldeck, C. A., Hubbell, S. P., Ledo, A., et al. (2012). Liana abundance, diversity, and distribution on Barro Colorado Island, Panama. *PLoS ONE* 7, e52114. doi: 10.1371/journal.pone.0052114

Schnitzer, S. A., and Van Der Heijden, G. M. F. (2019). Lianas have a seasonal growth advantage over co-occurring trees. *Ecology* 100, e02655. doi: 10.1002/ecy.2655

Schnitzer, S. A., Van Der Heijden, G. M. F., Mascaro, J., and Carson, W. P. (2014). Lianas in gaps reduce carbon accumulation in a tropical forest. *Ecology* 95, 3008–3017. doi: 10.1890/13-1718.1

Smith-Martin, C. M., Bastos, C. L., Lopez, O. R., Powers, J. S., and Schnitzer, S. A. (2019). Effects of dry-season irrigation on leaf physiology and biomass allocation in tropical lianas and trees. *Ecology* 100, e02827. doi: 10.1002/ecy.2827

Staudhammer, C., Wadt, L. H. O., and Kainer, K. (2013). Tradeoffs in basal area growth and reproduction shift over the lifetime of a long-lived tropical species. *Oecologia* 173, 45–57. doi: 10.1007/s00442-013-2603-1

Stevens, G. C. (1987). Lianas as structural parasites: the *Bursera simaruba* example. *Ecology* 68, 77–81. doi: 10.2307/1938806

Stevenson, N. S. (1927). Silvicultural treatment of mahogany forests in British Honduras. *Emp. Forest. J.* 6, 219–227. doi: 10.2307/42591669

Tobin, M. F., Wright, A. J., Mangan, S. A., and Schnitzer, S. A. (2012). Lianas have a greater competitive effect than trees of similar biomass on tropical canopy trees. *Ecosphere* 3, 1–11. doi: 10.1890/ES11-00322.1

Toledo-Aceves, T. (2015). "Above- and belowground competition between lianas and trees," in *Ecology of Lianas,* eds S. A. Schnitzer, F. Bongers, R. J. Burnham, and F. E. Putz (Oxford: John Wiley and Sons), 147–163.

Trimble, G. R. J., and Tryon, E. H. (1974). Grapevines a serious obstacle to timber production on good hardwood sites in Appalachia. *Northern Logger* 23, 22–44.

Van Der Heijden, G. M. F., and Phillips, O. L. (2009). Liana infestation impacts tree growth in a lowland tropical moist forest. *Biogeosciences* 6, 2217–2226. doi: 10.5194/bg-6-2217-2009

Van Der Heijden, G. M. F., Powers, J. S., and Schnitzer, S. A. (2015). Lianas reduce carbon accumulation and storage in tropical forests. *Proc. Natl. Acad. Sci. U.S.A.* 112, 13267–13271. doi: 10.1073/pnas.1504869112

Van Der Heijden, G. M. F., Powers, J. S., and Schnitzer, S. A. (2019). Effect of lianas on forest-level tree carbon accumulation does not differ between seasons: results from a liana removal experiment in Panama. *J. Ecol.* 107, 1890–1900. doi: 10.1111/1365-2745.13155

Venegas-González, A., Mello, F. N. A., Schnitzer, S. A., César, R. G., and Tomazello-Filho, M. (2020). The negative effect of lianas on tree growth varies with tree species and season. *Biotropica* 52, 836–844. doi: 10.1111/btp.12796

Viechtbauer, W. (2010). Conducting meta-analyses in R with the metafor package. *J. Stat. Softw*. 36, 1–48. doi: 10.18637/jss.v036.i03

Visser, M. D., Schnitzer, S. A., Muller-Landau, H. C., Jongejans, E., Kroon, H., Comita, L. S., et al. (2018). Tree species vary widely in their tolerance for liana infestation: a case study of differential host response to generalist parasites. *J. Ecol.* 106, 781–794. doi: 10.1111/1365-2745.12815

Wan, X., Wang, W., Liu, J., and Tong, T. (2014). Estimating the sample mean and standard deviation from the sample size, median, range and/or interquartile range. *BMC Med. Res. Methodol.* 14, 135. doi: 10.1186/1471-2288-14-135

Wright, A., Tobin, M., Mangan, S., and Schnitzer, S. A. (2015). Unique competitive effects of lianas and trees in a tropical forest understory. *Oecologia* 177, 561–569. doi: 10.1007/s00442-014-3179-0

Conflict of Interest: The authors declare that the research was conducted in the absence of any commercial or financial relationships that could be construed as a potential conflict of interest.

frontiers in Forests and Global Change

ORIGINAL RESEARCH
published: 25 February 2022
doi: 10.3389/ffgc.2022.836711

Two Co-occurring Liana Species Strongly Differ in Their Hydraulic Traits in a Water-Limited Neotropical Forest

Kasper Coppieters[1,2,3]*, Hans Verbeeck[1], Simon Dequeker[1,2,3], Jennifer S. Powers[3,4], German Vargas G.[4,5], Chris M. Smith-Martin[6], Kathy Steppe[2] and Félicien Meunier[1,7]

[1] CAVElab—Computational and Applied Vegetation Ecology, Department of Environment, Faculty of Bioscience Engineering, Ghent University, Ghent, Belgium, [2] Laboratory of Plant Ecology, Department of Plants and Crops, Faculty of Bioscience Engineering, Ghent University, Ghent, Belgium, [3] Department of Ecology, Evolution, and Behavior, University of Minnesota, St. Paul, MN, United States, [4] Department of Plant and Microbial Biology, University of Minnesota, St. Paul, MN, United States, [5] School of Biological Sciences, The University of Utah, Salt Lake City, UT, United States, [6] Department of Ecology, Evolution, and Evolutionary Biology, Columbia University, New York, NY, United States, [7] Department of Earth and Environment, Boston University, Boston, MA, United States

OPEN ACCESS

Edited by:
Nobuo Imai,
Tokyo University of Agriculture, Japan

Reviewed by:
Zafar Siddiq,
Government College University,
Lahore, Pakistan
Shidan Zhu,
Guangxi University, China

****Correspondence:***
Kasper Coppieters
kasper.coppieters@UGent.be

Specialty section:
This article was submitted to
Tropical Forests,
a section of the journal
Frontiers in Forests and Global
Change

Received: *15 December 2021*
Accepted: *31 January 2022*
Published: *25 February 2022*

Citation:
Coppieters K, Verbeeck H,
Dequeker S, Powers JS, Vargas G. G,
Smith-Martin CM, Steppe K and
Meunier F (2022) Two Co-occurring
Liana Species Strongly Differ in Their
Hydraulic Traits in a Water-Limited
Neotropical Forest.
Front. For. Glob. Change 5:836711.
doi: 10.3389/ffgc.2022.836711

Lianas are a key growth form in tropical forests. They are believed to be strong competitors for water, thanks to their presumed efficient vascular systems. However, despite being a large polyphyletic group, they are currently often considered as a functionally homogeneous entity. In this study, we challenged this assumption by estimating the variability in hydraulic traits of two common, co-occurring liana species in a water-limited environment, namely, a seasonally dry tropical forest in Costa Rica. We measured vulnerability to embolism at the leaf and branch levels using two different methods (optical and acoustic vulnerability) and found that both species had very different hydraulic properties. Compared to reported P_{50} values in literature, we found two extreme P_{50} values: a low value for *Bignonia diversifolia* (−4.30 ± 0.54 MPa at the leaf level; −7.42 ± 0.54 MPa at the branch level) and a high value for *Cissus microcarpa* (−1.07 ± 0.14 at the leaf level; −1.20 ± 0.05 MPa at the branch level). Furthermore, *B. diversifolia* had a higher apparent modulus of elasticity in the radial direction (556.6 ± 401.0 MPa) and a variable midday water potential. On the other hand, *C. microcarpa* had a low apparent modulus of elasticity in the radial direction (37.8 ± 26.3 MPa) and a high branch water content, which enabled the species to keep its water potential stable during the dehydration experiments and during a drought period in the field. This mechanism may enable this species to coexist with species that are more resistant to drought-induced embolisms such as *B. diversifolia*. Although only two species were studied, considerable overlap was found between the range of hydraulic properties of trees growing in the same location and trees and lianas growing in two forests in Panama. These findings demonstrate that lianas cannot be considered as a homogeneous group and call for further research into the intra-growth form diversity of liana properties.

Keywords: drought tolerance, lianas, tropical dry forest, vulnerability to embolism, optical vulnerability, acoustic vulnerability

INTRODUCTION

Tropical forests are one of the most important ecosystems on Earth. They are responsible for almost one third of the carbon uptake by terrestrial plants (Beer et al., 2010), they store more than half of the terrestrial biomass (Pan et al., 2011) and support approximately 50% of the described species (Dirzo and Raven, 2003). Dry forests make up a significant part of tropical forests as they encompass 42% of the tropical forest region (Miles et al., 2006). By definition, they are characterized by at least 3 months with less than 100 mm precipitation and 50% drought-deciduous species (Sánchez-Azofeifa et al., 2005).

A key growth form in tropical forests is lianas (woody vines). Here, lianas represent on average 24% of the woody stems (Putz and Mooney, 1991) and substantially contribute to forest leaf area (Schnitzer, 2015). Unlike most other growth forms, liana density increases with increasing seasonality and with decreasing mean annual precipitation, which makes them more abundant in tropical dry forests (Schnitzer, 2005). Through intense competition for resources with self-standing plants, lianas reduce tree growth, increase tree mortality (Ingwell et al., 2010), and reduce forest-level carbon accumulation and storage (van der Heijden et al., 2015). In addition, abundance and basal area of large lianas were shown to be increasing in the Neotropics (Phillips et al., 2002). While the mechanistic understanding of this proliferation remains unclear, it could be related to the water competition between growth forms (Schnitzer, 2005, 2018; Smith-Martin et al., 2019).

Lianas were indeed found to have a strong competitive advantage over trees during the dry season, when light is abundant and water is limiting: during that period, they were shown to have larger growth rates and water use efficiency than their host trees (Schnitzer, 2015; Schnitzer and van der Heijden, 2019; Smith-Martin et al., 2019) as well as higher predawn water potentials and higher transpiration rates (Chen et al., 2015; Ichihashi et al., 2017). Under dry conditions, lianas also explore the forest canopy more effectively than trees, showing stronger apical dominance, higher stem slenderness, and fewer leaf layers (Medina-Vega et al., 2021). Among the trait growth-form differences, one of the discrepancies between lianas and trees is their respective hydraulic architecture, which could explain such contrasting behavior between lianas and trees during the dry season. Lianas are typically associated with longer and wider vessels than co-occurring trees (Ewers et al., 1990), resulting in a higher maximum sapwood-specific hydraulic conductivity (Zhu and Cao, 2009; De Guzman et al., 2017), but also a higher vulnerability to drought (Chen et al., 2017; De Guzman et al., 2017). In contrast, van der Sande et al. (2019) found that hydraulic efficiency was decoupled from hydraulic safety in lianas, indicating that they potentially have high water conductivity while limiting their vulnerability to drought.

Despite their abundance and their overall impact on tropical ecosystems, studies on lianas are scarce. Lianas are often overlooked in inventory and modeling studies, and when they are taken into account, they are often considered as a functionally homogeneous entity (di Porcia e Brugnera et al., 2019). However, lianas form a large polyphyletic group (Gentry, 1992; Schnitzer and Bongers, 2002), and some pioneer studies indicate that they can exhibit heterogeneous traits, even within a single site (Meunier et al., 2020). One of the reasons for the scarcity of hydraulic trait data is the difficulty related to measuring these variables in the field. Several methods commonly used to quantify the vulnerability to embolism (often expressed as P_{50}), including the bench dehydration method, which is considered as the gold standard, are time-consuming or require a large input of plant material (Venturas et al., 2017). However, understanding water competition in tropical forests is key, as hydraulic failure during droughts may be one of the most critical processes in water-limited environments (Choat et al., 2018; Brodribb et al., 2020; Powers et al., 2020), especially in a climate change context where future droughts may be longer and more intense (Trenberth et al., 2014). In this respect, the optical (Brodribb et al., 2016b) and acoustic (Vergeynst et al., 2015) methods are real advances, as they can be easily applied in the field.

To contribute to this knowledge gap, we estimated the variability in liana hydraulic properties in a water-limited, seasonally dry tropical forest located in Costa Rica. More specifically, we determined the drought susceptibility of two contrasting liana species by measuring their vulnerability curves using two different methods, covering the leaf and branch organs. Vulnerability curves are at the heart of much of plant hydraulic studies and characterize plant losses in conductivity as xylem pressure decreases (Venturas et al., 2017, 2019). Next, we measured predawn and midday leaf water potentials. The regulation of the water potential on short time scales is determined by the water-use strategy of the plant. Two main water-use strategies exist: isohydric species keep their water potential almost constant throughout the day through a strong stomatal regulation, while anisohydric species maintain their stomata open, with the consequence of low and variable water potential throughout the day (Tardieu and Simonneau, 1998; McDowell et al., 2008). We further measured key hydraulic variables including maximum vessel length, wood specific gravity, fresh wood water content, and apparent modulus of elasticity. These hydraulic traits are important for the characterization of the functioning of species regarding plant water use (Sterck et al., 2011; Cosme et al., 2017) and indicate the response of species to drought (Anderegg et al., 2016; Powers et al., 2020). As water is the most limiting resource during at least part of the year, we hypothesized that an evolutionary convergence could be expected within a functional group at a single site, and thus that liana species from a single site would exhibit similar hydraulic traits.

MATERIALS AND METHODS

Site Description

All samples were collected in Estación Experimental Forestal Horizontes (Horizontes), which is part of Área de Conservación Guanacaste in Northwestern Costa Rica (10.714 N, 85.596 W) in 2019. Horizontes contains a mosaic of secondary forest in various stages of succession and tree plantations (Werden et al., 2018). According to the historical observations of the nearby weather station in Liberia between 1957 and 2017,[1] the mean annual temperature and mean annual precipitation of this site are 27.2°C and 1,585 mm, respectively. There is a 5–6 months long dry season with little to no precipitation (< 100 mm). The wet season, during which there is usually a short but distinctive dry period, typically starts in May and ends in December (Allen et al., 2017). In this study, all experiments were conducted in Horizontes, except for the acoustic vulnerability curves (see below) and the wood specific gravity, which were measured in Ghent, Belgium (Ghent University, Faculty of Bioscience Engineering, Laboratory of Plant Ecology).

In 2019, the wet season started in May, with a total monthly rainfall of 268 mm. The next 4 months (June–September) were relatively dry compared to the long-term averages, with a total monthly rainfall of 47, 71, 59, and 141 mm, respectively. From 22/08/2019 to 13/09/2019, no precipitation was registered. From 14/09/2019 onward, 141 mm precipitation was registered. Therefore we divided the field campaign into three periods: a relatively dry (07/08-21/08), dry (22/08-13/09), and wet (14/09-30/09) period, hereafter referred to as the “early dry,” “dry,” and “wet” periods (**Figure 1A**).

Species Selection and Harvest

We selected the two liana species based on the accessibility of target individuals along roads and their local abundance in the forest and on a preliminary analysis of water potentials in the field. The latter showed that liana species could be divided into two different groups: one with constant and high water potentials and the other one with variable and low water potentials. From these two groups, the most abundant species were retained for the study, namely, *Cissus microcarpa* Vahl (Vitaceae) and *Bignonia diversifolia* Kunth (Bignoniaceae), two drought-deciduous species. Smith-Martin (2018) identified 57 liana species during an inventory in 18 permanent plots established in the same region as the experimental forest in Horizontes. Based on the relative stem number, *B. diversifolia* was the second most common liana species (12.07%) across all plots whereas *C. microcarpa* was the 9th (4.27%). Based on the relative basal area, *B. diversifolia* was also the second most abundant liana species (10.31%), while *C. microcarpa* was the 13th most abundant species (2.10%). In another study conducted in the 40-year-old tree plantations in Horizontes, 1084 lianas were found in 385 out of 748 surveyed trees. 25% of the lianas stems belonged to the genus Cissus, 2% of the stems belonged to *B. diversifolia* (Powers et al., 2020).

Collected leaves and branches were in direct sunlight most of the day and the collected specimen could be considered mature, as they were climbing and growing across the tops of their host trees, an approach similar to Smith-Martin et al. (2020). To minimize embolism induction, all branches were harvested predawn, between 4:00 and 5:30 a.m. Whenever possible, the branches were cut at a length of at least 2 times their maximum vessel length (see below), after which a second piece was cut under water to remove embolisms induced by the cutting. As in Gorel et al. (2019), the cut end of the branches was immediately put in a vial filled with water, and the branches were enclosed in a humidified black plastic bag for transport to the lab.

Maximum Vessel Length

The maximum vessel length (MVL, cm) was determined using the air injection method (Ewers and Fisher, 1989) on 5 and 6 individual branches of *C. microcarpa* and *B. diversifolia*, respectively, whereby a syringe was used to create pressure. No measurements of hydraulic conductivity were performed in this study.

Water Potential Measurements

Water potential measurements were conducted with gas pressure chambers (Model 600, 1,000, and 1505D, PMS Instrument Company, Corvallis, OR, United States), which can measure leaf water potential down to −4, −7, and −14 MPa, respectively. Both in the field and in the lab, leaves were cut using a razor blade and directly put in the pressure chamber.

Predawn and midday water potentials were frequently measured *in situ* on three leaves of the same three specimens per species, using the Model 600 gas pressure chamber. Sampling height ranged between 1 and 3 m. Predawn measurements (Ψ_{pd}) were conducted between 4:30 and 5:30 a.m. As full darkness was assured, it was assumed that the leaf water potential (Ψ_{leaf}) was in balance with the stem water potential (Ψ_{stem}). Midday water potential measurements (Ψ_{md}) were conducted between 11:15 a.m. and 1:15 p.m., close to the local solar noon which varied from 11:32 a.m. to 11:48 a.m. throughout the field campaign. To equilibrate Ψ_{leaf} with Ψ_{stem}, all leaves to be measured were wrapped in a plastic bag surrounded by aluminum foil, at least 1 h before measurement (Trifilò et al., 2014). The bag was placed in such a way that there was still enough exchange of air to avoid condensation.

Optical Vulnerability Curves

Optical Vulnerability (OV) measurements were conducted on 6 leaves of each species starting from 26/08 to 09/09 (**Figure 1A**; Brodribb et al., 2016b). Per measurement cycle, three branches were harvested predawn and one leaf of each of the three

---

[1] www.imn.ac.cr/inicio

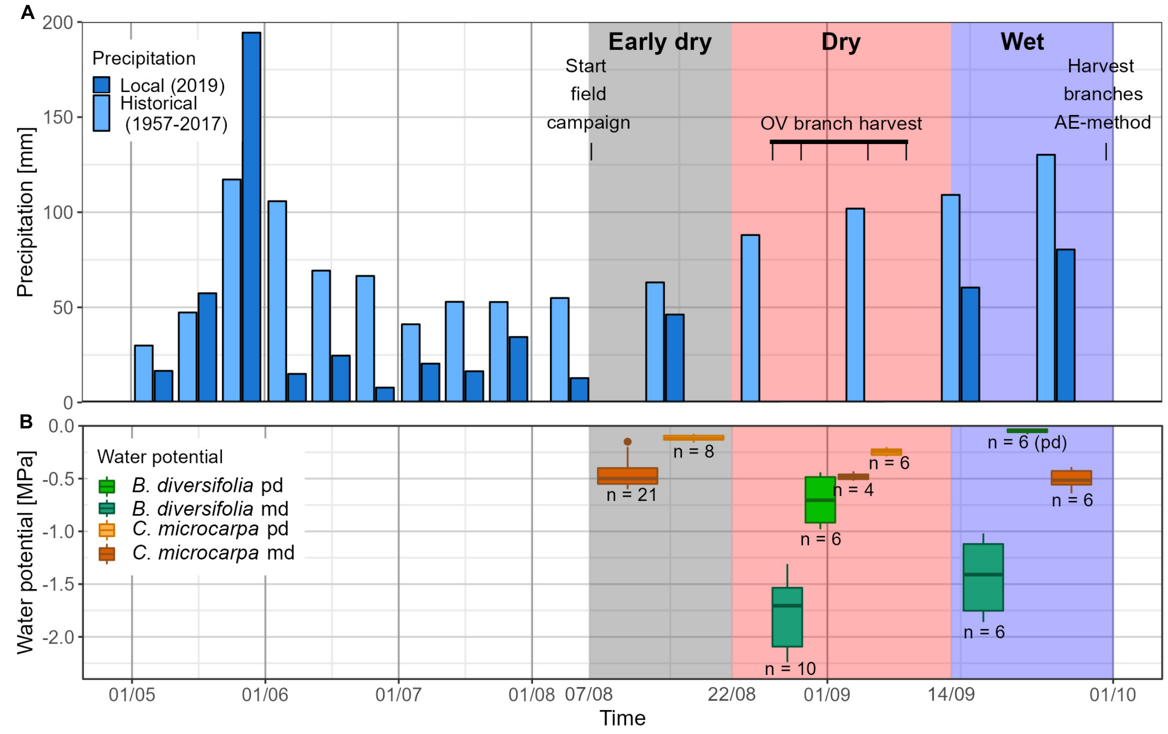

FIGURE 1 | Overview of the field campaign. In **(A)**, precipitation is plotted on 10 day intervals (11 days for the last period of the month if the month has 31 days). Light blue bars represent the average precipitation between 1957 and 2017 as measured by a nearby weather station in Liberia. Dark blue bars indicate the precipitation measured in 2019 in Horizontes. The precipitation was used to divide the field campaign (07/08–30/09) into three periods: the first period was relatively dry, with some precipitation (Early dry); in the second period, no precipitation occurred (Dry) and during the last period, large quantities of precipitation were observed (Wet). **(B)** Shows the measured predawn and midday water potentials for the two species. Measurements took place throughout the field campaign and are here grouped per period.

branches was placed onto a scanner (Epson Perfection V800 Photo Color Scanner, Epson America, Inc.) while still connected to its parent branch. Leaves were carefully placed between two microscope slides, allowing to have the same focal point on the whole scan and to reduce vertical movement due to shrinking. Every leaf was captured in a ten-minute interval until no new embolism event occurred in a 4-h time interval and the leaf appeared crispy dry. In total, the experiments lasted between 1.26 and 2.32 days. During the desiccation process, Ψ_{stem} measurements were carried out on the other leaves of the same branches every 0.5–2 h, except from 8:00 p.m. to 7:00 a.m., using the Model 1505D gas pressure chamber. Additionally, low stem water potentials were also measured using the WP4C dewpoint potentiameter (Decagon Devices, Inc., Pullman, Washington, United States) following the METER group protocol.[2] In brief, a selected leaf was gently abraded with a 600 grit sandpaper with a drop of distilled water in between to remove the cuticle and allow faster moisture exchange. After this, moisture was removed with a lint-free tissue, a circle was cut out of the leaf and inserted into the device after which the measurement was started. The device was calibrated daily before use.

This measurement process was repeated twice for each species. Data processing was executed as described by OpenSourceOV[3] using the Fiji-ImageJ processing software (Schindelin et al., 2012). To obtain a continuous water potential curve, water potential measurements were plotted against time, and a linear regression was derived for each species. In all cases, we also tested a piecewise linear model (i.e., two linear models with a single inflection point), and only the best model according to the model adjusted r-square was retained. By converting the time of the scan to its respective water potential, we could derive the optical vulnerability curve for each leaf. $P_{50,\mathrm{OV}}$ (MPa) was defined as the water potential at which 50% of the embolized vessel area (EVA) was reached.

Acoustic Vulnerability Curves

For the acoustic vulnerability (AV) method, six branches of each species were harvested the night prior to transport to Belgium, between 1:00 and 4:00 a.m. Wet clothes were added to the transport bags to prevent desiccation of the branches and the cut end was put in a vial with water to ensure that the plants would survive the 26 h journey. Upon arrival in Belgium and until the start of the experiment, the plants were kept out of direct sunlight

---

[2] www.metergroup.com/environment/articles/measurement-leaf-water-potential-using-wp4c/

[3] http://www.opensourceov.org for more details

in a cool environment with an average temperature of 10°C for approximately 10 h. During the experiment, four branches of each species were used. Branch selection for the AV method was based on visual inspection.

Sensor installation and data registration were carried out as in De Baerdemaeker et al. (2019a). In short, all leaves were wrapped in aluminum foil, after which a dendrometer (DD-S, Ecomatik, Dachau, Germany) and a broadband point-contact acoustic emission (AE) sensor (KRNBB-PC, KRN Services, Richland, United States) were attached to the branches at least one time the MVL from the cut end. During dehydration, water potential measurements were conducted every 0.5–2 h using the Model 1,000 gas pressure chamber, until the water potential dropped below −7 MPa. After that, the sensors continued to measure diameter shrinkage and AE signals, respectively, to ensure that the activity peak had been reached before ending the experiment. In total, the experiment lasted for 4 days.

The P_{50} values for the AV method (defined as AE_{50} in Steppe et al., 2022) were determined by using two different procedures. First, the endpoint of embolism formation (AE_{100}) was determined as in Vergeynst et al. (2016). In short, AE_{100} was determined as the point at which the decrease in AE activity, following the AE activity peak, decreases most strongly, which corresponds to the local maximum of the third derivative after the peak in the AE activity (Vergeynst et al., 2016; Steppe et al., 2022). The time interval used to calculate the third derivative was dependent on the timespan at which the AE-activity peaks (Steppe et al., 2022), and varied between 6.1 and 10.1 h. An estimation of the continuous water potential series was obtained by establishing a pooled linear relationship between the relative radial shrinkage of the branch (μm mm^{-1}, strain) and the water potential measurements (MPa, stress) (De Baerdemaeker et al., 2019a). Again, a linear regression and a piecewise linear model were constructed, after which the model with the highest adjusted r-squared was retained. To plot the acoustic vulnerability curves, the cumulative AE signals between the start of the experiment and AE_{100} were re-scaled between 0 and 100. AE_{50} was then determined as the water potential at 50% of the cumulative AEs (Steppe et al., 2022), and will henceforth be referred to as $P_{50,AV}$ in this study. Second, $P_{50,AV}$ was determined as the water potential at the peak of the activity curve, which is the first derivative of the cumulative AE-curve (Nolf et al., 2015a). The apparent modulus of elasticity in the radial direction (E_r, MPa) was calculated as the slope of the stress-strain relationship (Nobel, 2012; Vergeynst et al., 2015). Hydraulic safety margin at the branch level (HSM_{AV}, MPa) was defined as the difference between the lowest stem water potential measured in the field on 1 day (Ψ_{min}) and $P_{50,AV}$ (Meinzer et al., 2009).

Wood Specific Gravity and Branch Water Fraction

Wood specific gravity (WSG, g cm^{-3}) was determined for branch segments collected before the start of the acoustic experiment and calculated as the ratio of dry weight to green volume. The wet volume was calculated from two diameters measured perpendicularly to each other at both ends, and the length of the sample, assuming a cylindrical shape for both species. The dry weight of the samples was determined after the samples were oven-dried at 80°C for 48 h (ML104T/00, Mettler-Toledo GmbH, Switzerland, with 0.1 mg accuracy). The water fraction of the branches (unitless) was calculated as fresh weight minus dry weight divided by the fresh weight.

Data Analysis

For the construction of the vulnerability curves, four fitting models (Weibull, Lopez et al. (2005), sigmoidal, Pammenter and Van der Willigen (1998), and two polynomial models Scoffoni et al. (2012); Manzoni et al. (2013); **Supplementary Table 1**) were fitted to the data for all branches. The model with the best fit was

TABLE 1 | Summary of the hydraulic properties of *B. diversifolia* and *C. microcarpa* measured in this study.

	B. diversifolia	***C. microcarpa***	***p*-value**
MVL [cm]	113.4 ± 49.3 (*n* = 6)	233.2 ± 49.6 (*n* = 5)	**4.33 E-03**
$\Psi_{pd,earlydry}$ [MPa]	–	−0.12 ± 0.03 (*n* = 8)	–
$\Psi_{md,earlydry}$ [MPa]	–	−0.45 ± 0.13 (*n* = 21)	–
$\Psi_{pd,dry}$ [MPa]	−0.71 ± 0.26 (*n* = 6)	−0.25 ± 0.04 (*n* = 6)	**2.17 E-03**
$\Psi_{md,dry}$ [MPa]	−1.78 ± 0.33 (*n* = 10)	−0.48 ± 0.04 (*n* = 4)	**2.00 E-03**
$\Psi_{pd,wet}$ [MPa]	−0.05 ± 0.02 (*n* = 6)	–	–
$\Psi_{md,wet}$ [MPa]	−1.43 ± 0.38 (*n* = 6)	−0.51 ± 0.10 (*n* = 6)	**5.00 E-03**
$P_{50,OV}$ [MPa]	−4.30 ± 0.54 (*n* = 6)	−1.07 ± 0.14 (*n* = 5)	**4.33 E-03**
$P_{50,AV}$ [MPa]	−7.42 ± 0.54 (*n* = 4)	−1.20 ± 0.05 (*n* = 3)	**1.53 E-04**
Ψ_{min} [MPa]	−1.88 ± 0.43 (*n* = 5)	−0.52 ± 0.11 (*n* = 6)	**0.002**
HSM_{AV} [MPa]	5.54 ± 0.69	0.68 ± 0.12	**3.26 E-4**
$ax_{50,OV}$ [%]	−409.6 ± 829.3 (*n* = 6)	−2068.6 ± 1762.6 (*n* = 5)	0.106
$ax_{50,AV}$ [%]	−55.2 ± 25.7 (*n* = 4)	−1208.3 ± 1773.6 (*n* = 3)	0.057
$P_{12,OV}$–$P_{88,OV}$ [MPa]	1.54 ± 1.1 (*n* = 6)	0.18 ± 0.21 (*n* = 5)	**0.017**
$P_{12,AV}$–$P_{88,AV}$ [MPa]	2.17 ± 1.11 (*n* = 4)	0.36 ± 0.29 (*n* = 3)	**0.042**
$E_{r,1}$ [MPa]	556.6 ± 401.0 (*n* = 4)	37.8 ± 26.3 (*n* = 4)	**0.029**
WSG [g cm^{-3}]	0.54 ± 0.07 (*n* = 5)	0.25 ± 0.05 (*n* = 5)	**1.64 E-04**
Water fraction [-]	0.56 ± 0.05 (*n* = 5)	0.78 ± 0.03 (*n* = 5)	**6.63 E-05**

Values shown are the mean ± one standard deviation. Numbers between brackets represent the number of samples. Significant p-values are indicated in bold. Pd, predawn; md, midday; early dry, period from 07/08 to 21/08; dry, period from 22/08 to 13/09; wet, period from 14/09 to 30/09; OV, optical vulnerability; AV, acoustic vulnerability; MVL, maximum vessel length; $P_{50,OV}$*, water potential at 50% embolized vessel area;* $P_{50,AV}$*, water potential at 50% of cumulative acoustic emissions;* Ψ_{min} *minimum stem water potential measured in the field on 1 day;* HSM_{AV}*, hydraulic safety margin at the branch level;* ax_{50}*, slope of the vulnerability curve at* P_{50}*;* P_{12}*–*P_{88}*, difference between onset and ending of embolism formation; WSG, wood specific gravity;* $E_{r,1}$*, apparent modulus of elasticity in the radial direction of the first regression segment.*

selected based on the minimal RMSE criterion. Next, the process was repeated using a bootstrapping method (n = 10,000), and VC-related variables, such as P_{12}, P_{50}, P_{88}, and ax_{50} [respectively the water potential at 12, 50, and 88% embolism (MPa) and the slope at P_{50} (%)] were determined. After bootstrapping, averages per branch were calculated for all variables and the species average was calculated as the average of all branches. To plot the vulnerability curves, the mean was plotted as the mean of all bootstrapped values, the 95% confidence interval was generated by disregarding the 2.5% highest and lowest values for each water potential value.

The normality of the data was checked using the Shapiro–Wilk test. Differences between two groups were tested with a two-sample t-test and a Mann–Whitney U-test for parametric and non-parametric data, respectively. To calculate differences between species for the HSM_{AV}, the average Ψ_{min} was subtracted from all $P_{50},_{AV}$ values, and these values were then used to perform the statistical analysis. A linear mixed model (nlme package in R, Pinheiro et al., 2013) was used to analyze the potential difference in water potential of the species between the different periods (early dry, dry, and wet). The period was used as a fixed effect, and the timing of the measurement (pd or md) was used as a random effect. Statistical analyses were executed in RStudio (version 1.3.959) (RStudio Team, 2020) with R version 4.0.2.

RESULTS

Maximum Vessel Length and Water Potential Measurements

The MVL of *C. microcarpa* (233.2 ± 49.6 cm) was more than twice as large as that of *B. diversifolia* (113.4 ± 49.3 cm, p-value = 0.004, **Table 1**). There was a significant difference between the water potentials of both species in all periods where measurements were available for both species (**Table 1**). *C. microcarpa* had systematically higher water potentials throughout the field campaign (**Figure 1B**). The most significant differences between the two species occurred during the dry period when Ψ_{pd} and Ψ_{md} of *C. microcarpa* were, respectively, −0.45 MPa and −1.3 MPa lower than that of *B. diversifolia* (**Table 1** and **Figure 1B**). Moreover, the water potential of *C. microcarpa* was not significantly different between periods (p = 0.06), whereas that of *B. diversifolia* was (p-value < 0.001).

Vulnerability Curves

The two different procedures for determining $P_{50},_{AV}$ did not show significant differences (paired wilcoxon test, p-value = 0.12 and 0.25 for *B. diversifolia* and *C. microcarpa*, respectively, **Supplementary Figure 1**). For this reason in the following, we systematically use the method of Vergeynst et al. (2015) to plot the acoustic vulnerability curves and calculate the $P_{50},_{AV}$ value.

While the course of the species-specific vulnerability curves was similar between methods, the comparison between the two species showed a clear difference (**Figure 2**). *C. microcarpa* had a steeper curve at the P_{50} value (ax_{50}) for both methods (**Table 1**). This steeper curve was not significant (p-value = 0.11) for the OV method because one branch of *B. diversifolia* had fewer data points and consequently a steeper curve (**Figure 2**). For the AV method, the effect was also not significant (p-value = 0.057), however, no outliers were found here. The onset of embolism was significantly different between species for both methods: P_{12} = −0.97 ± 0.08 and −1.02 ± 0.12 MPa for *C. microcarpa* and −3.58 ± 0.98 and −6.32 ± 0.83 MPa for *B. diversifolia* for the OV and AV method, respectively (p-value < 0.001 and 0.004, respectively). The difference between the onset (P_{12}) and the ending (P_{88}) of embolism was significantly different, with the smallest difference found for *C. microcarpa* (**Table 1**). These differences translated into

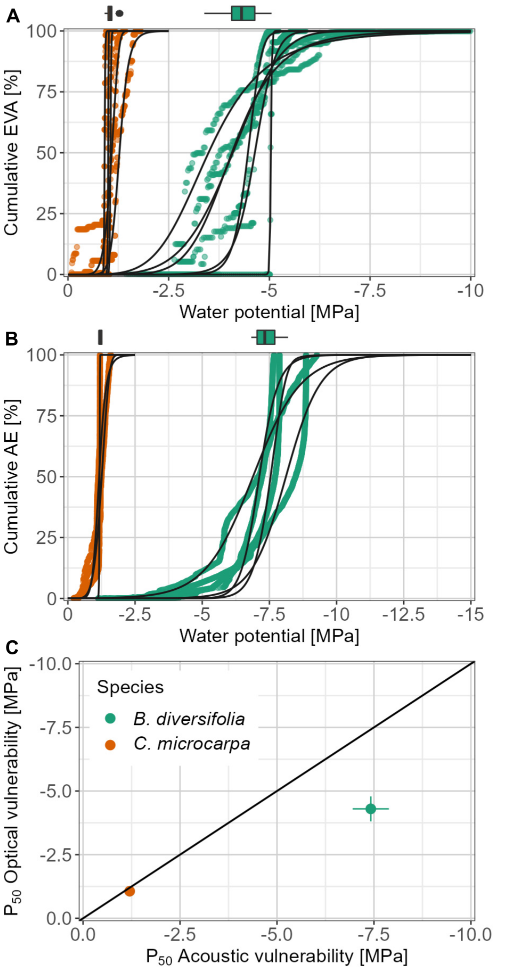

FIGURE 2 | Vulnerability curves for *B. diversifolia* and *C. microcarpa*, obtained by the OV method **(A)** and the AV method **(B)**. Vulnerability curves for the AV method are plotted using the results of the Vergeynst et al. (2015) procedure only. Dots represent the data points collected during the experiment, the black curves represent the vulnerability curves fitted to the data points with their 95% confidence interval, as derived from bootstrapping. The boxplots on top of each subplot show the respective P_{50} values, obtained from the bootstrapping. Subplot **(C)** compares the $P_{50,AV}$ and $P_{50,OV}$ values for the studied species. Horizontal and vertical error bars indicate the species standard deviation. EVA, embolized vessel area; AE, acoustic emission.

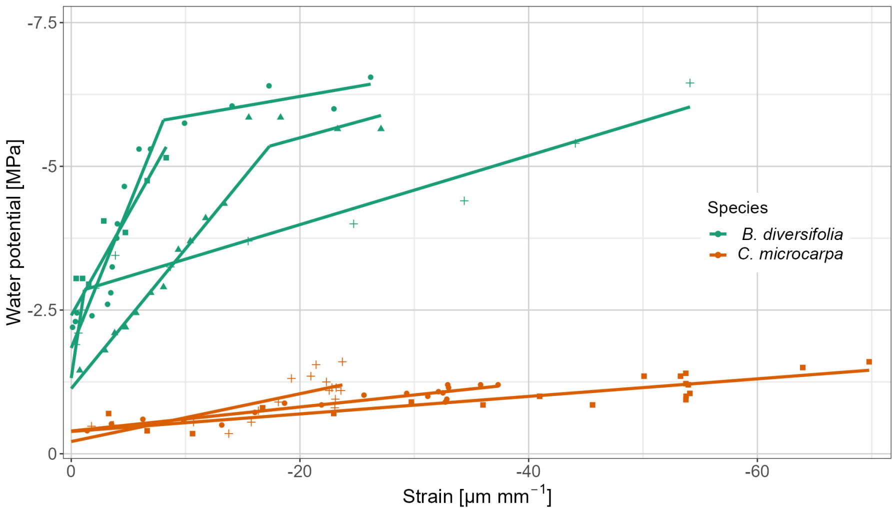

FIGURE 3 | Pooled linear stress-strain relations between the point measurements of stem water potential and the strain for the measured branches of *B. diversifolia* and *C. microcarpa*. For some branches, a linear relationship was established, while others had a segmented course. Different symbols indicate different branches. The slope of the curves represents E_r.

distinctly different P_{50} for the two species: for *C. microcarpa*: $P_{50,OV} = -1.07 \pm 0.14$ MPa and $P_{50,AV} = -1.20 \pm 0.05$ MPa, and for *B. diversifolia*: $P_{50,OV} = -4.30 \pm 0.54$ MPa and $P_{50,AV} = -7.42 \pm 0.54$ MPa for the OV and AV methods, respectively (**Table 1**). These values are significantly different between species for each method (*p*-value = 0.004 and < 0.001) and between the two methods for *B. diversifolia* (*p*-value < 0.001). Both species have a significantly higher (less negative) P_{50} value at leaf level than at branch level (**Figure 2**). Ψ_{min} for *C. microcarpa* and *B. diversifolia* were -0.52 ± 0.11 MPa and -1.88 ± 0.43 MPa, respectively. Combined with the $P_{50,AV}$, Ψ_{min} resulted in a positive hydraulic safety margin at the branch level for both species: 0.68 ± 0.12 MPa and 5.54 ± 0.69 MPa, for *C. microcarpa* and *B. diversifolia*, respectively (*p*-value < 0.001).

The E_r value differed between species, but intra-species variability was also important (**Figure 3**). Both linear and segmented relationships emerged for the data, the slope of the first segment is shown in **Table 1**, inflection points and slopes of the second segment can be found in **Supplementary Table 2**. *C. microcarpa* had a significantly lower $E_{r,1}$-value (*p*-value = 0.029) and mostly had a linear course. On the other hand, *B. diversifolia* had a higher E_r-value and had more segmented curves. For both species, the E_r-value after the inflection point was systematically lower than the E_r-value before the inflection point (**Figure 3**).

Wood Specific Gravity and Water Fraction

The wood specific gravity of *C. microcarpa* (0.25 ± 0.05 g/cm^3) was less than half that of *B. diversifolia* (0.54 ± 0.07 g/cm^3, *p*-value < 0.001) and its water fraction was significantly larger (0.78 ± 0.03 *vs.* 0.56 ± 0.05, respectively, *p*-value < 0.001) (**Table 1**).

DISCUSSION

Hydraulic Traits

In this study, we showed that liana species found in the same environment can have contrasting hydraulic traits, which refutes our hypothesis that lianas from a single site would exhibit similar hydraulic traits due to evolutionary convergence. Both investigated liana species are abundant in the studied forest as compared to other liana species, which points at the potential ecological importance/impact of the two studied species in the ecosystem.

The two species we studied differed substantially in hydraulic traits. The vulnerability curves resulted in a similar course for both methods, albeit with a difference between the species. *C. microcarpa* had the highest P_{50} values of the two species and had a very steep increase in vulnerability for both methods once a certain water potential "threshold" was reached. However, these embolisms did not happen at one moment in time. After reaching the water potential "threshold," *C. microcarpa* kept its water potential more or less stable, causing the embolisms to occur at the same water potential, but spread over time. It is possible that this species could keep its water potential constant due to a combination of a large initial water content (78% of its fresh weight), a high elasticity (small E_r values), i.e., only a limited drop in water potential when water is released during branch shrinkage, and a high shrinkage of the branch during desiccation. The ability to keep its water potential constant was also found in the field, where the Ψ_{md} showed little variation throughout the field campaign (**Figure 1B**). On the other hand, this species could also have deep roots and thus have access to deeper water. As no plants were excavated in this study, no conclusion can be drawn about the rooting depth of this species. However, in a study in the same forest, Smith-Martin et al. (2020) found that studied lianas had the shallowest root systems when compared to deciduous and evergreen trees. Because the species was also able to keep its water potential constant during the desiccation experiments, i.e., without roots and access to water, it can be assumed that deep roots are not the primary cause of this mechanism. The ability to keep its water potential constant may enable this species to coexist with species that are more resistant to drought-induced embolism, such as *B. diversifolia* (De Guzman et al., 2021). Indeed, *B. diversifolia* was more drought tolerant, with a smaller slope at P_{50}, later onset of embolism, lower water content, and a more variable Ψ_{md} in the field. However, both species had in common that they never reached water potential levels that lead to significant embolism during the field campaign.

In a study conducted at the same site, Werden et al. (2018) found that lianas and trees have overlapping water-use strategies. They measured predawn and midday water potentials of 12 tree species and seven liana species, including *B. diversifolia* and *C. microcarpa*. They found that both lianas and trees fell along a continuum of water-use strategies, from isohydric (drought-avoider) to anisohydric (drought-tolerator). In this study, we found similar results, with *C. microcarpa* leaning toward the isohydric strategy, and *B. diversifolia* toward the anisohydric strategy. However, our results for *B. diversifolia* differed from theirs, in the sense of a higher Ψ_{pd} and a lower Ψ_{md}, as considered over the whole field campaign (data not shown). Additionally, our Ψ_{min} values corresponded to what was expected for both water-use strategies: a high value for the drought-avoiding *C. microcarpa* (-0.52 ± 0.11 MPa) and a low value for *B. diversifolia* (-1.88 ± 0.43 MPa), which is characteristic for drought-tolerant species. This is also in line with the findings of Meinzer et al. (2009), who showed that Ψ_{min} measured when soil water deficits are non-extreme are positively correlated with P_{50} and P_{12} values.

Two indirect techniques were used to construct the vulnerability curves at branch and leaf level, namely, the AV method and OV method. Both of them have been validated several times using other methods (see e.g., Nolf et al., 2015b; De Baerdemaeker et al., 2019b; Steppe et al., 2022 for the AV method and Skelton and Diaz, 2020 for the OV method), so it was decided not to repeat this validation in this study. The AV method was, for example, validated by Vergeynst et al. (2015) comparing the AV results with simultaneously acquired X-ray micro-computed tomography (μCT) images. Both methods showed a similar pattern, and no significant trend in the diameters of the embolized vessels was found over time, indicating that AEs are valid as an indirect estimation of the percent loss of conductivity of the branch. As this validation was performed on the vine *Vitis vinifera* L. "Johanniter," it is assumed that it will also be valid for other long-vesseled species. Brodribb et al. (2016b) applied the OV technique on four angiosperm species and found strong agreement between the dynamics of the recorded embolism by the OV method and the decline of whole leaf hydraulic conductance.

The P_{50} values differed markedly between species and methods. The vulnerability at leaf level, measured by the OV method, always resulted in higher values than the vulnerability at branch level, measured by the AV method, suggesting a vulnerability segmentation between the two organs. With increasing drought at the start of the dry season, this segmentation could ensure that the stem and branches are spared from embolism until leaves have dropped, and keep them functional throughout the dry season (Zimmermann, 1983). Because the area studied has a distinctly dry period, this observation is also consistent with that of Zhu et al. (2016), who showed that vulnerability segmentation occurs more often in species that occur in drier areas.

To our knowledge, this paper is, together with Smith-Martin et al. (unpublished)[4], the first to report leaf-level P_{50} values for lianas using the optical method. Two studies that determined P_{50} at leaf level using other methods reported rather divergent values: Tan et al. (2020) used the rehydration kinetics method described by Brodribb and Holbrook (2003) and reported a mean value of -2.21 ± 0.21 MPa for four liana species in a tropical karst forest during the dry season, whereas Medina-Vega et al. (2021) used the evaporative flux method as described in Sack and Scoffoni (2012) and reported a mean value of -0.19 ± 0.1 MPa for 16 liana species in two tropical forests in Panama, where most samples were collected during the wet season. Compared to these values, the result of *B. diversifolia* was low, however, recently, Smith-Martin et al. (unpublished) measured $P_{50,OV}$ values down to -4.62 MPa on lianas in two forests in Panama which confirmed that our value is not an isolated value. P_{50} values at branch level, on the other hand, have been reported more frequently for lianas. Here, however, the value of *B. diversifolia* deviated considerably from reported values, while that of *C. microcarpa* was in line with other studies. For example, Chen et al. (2021) recently found P_{50} values at branch level of -3.86 and -3.93 MPa using the bench dehydration method for two liana species, representing one of the most negative P_{50} values for lianas in literature. Most other studies reported P_{50} values at branch level between -1 and -2 MPa. Even compared to trees, which generally have a higher resistance to embolism (e.g., De Guzman et al., 2017), our value for *B. diversifolia* remained low. Despite the large difference with values from the literature, we argue that the results can still be used as an indicative value, as the acoustic vulnerability curve showed a similar course as the optical vulnerability curve for both species, and the two procedures to determine P_{50},$_{AV}$ did not give a significant difference.

The timing of the OV measurements, i.e., during a dry year, most likely had no impact on the results of the method. Brodribb et al. (2016a) found that embolisms in leaf veins follow a size-dependent embolism pattern, with embolisms starting in the largest veins, which we also observed. If the leaves were already partially embolized, this would no longer be detectable using the OV method, as this method can only detect embolisms as the difference in light transmission between two successive scans (Brodribb et al., 2016b). Since multiple embolism events can take place in the same vessel, we cannot exclude that no embolisms occurred before the start of the scanning. However, if this were the case, it would only have a small effect on the P_{50} value, which would become slightly higher. Furthermore, no signs of extreme drought stress were found in either species during the field campaign: Ψ_{min} never reached or came close to the P_{12} value of the two species, suggesting that no or only very limited

---

[4] Smith-Martin, C. M., Jansen, S., Brodribb, T. J., Medina-Vega, J. A., Lucani, C. J., Huppenberger, A., et al. (2022). Tropical lianas and trees differ in their xylem anatomical traits in a seasonally dry forest but not in a wet forest. *Front. For. Glob. Change**.

embolisms occurred during the measurement period. As it was drier than average during this period (**Figure 1A**), it could be assumed that these species will continue to thrive in this forest in a context of climate change, where future droughts may be longer and more intense (Trenberth et al., 2014). However, since these measurements were only made during a dry period in the wet season, lower water potentials could potentially occur during other parts of the growing season, which could still lead to embolisms. Because both species are drought-deciduous, it is not expected that they would have an advantage over trees in the dry season.

We found positive safety margins for both species, ranging from a relatively small value for *C. microcarpa* (0.68 ± 0.12 MPa), to a large value for *B. diversifolia* (5.54 ± 0.69 MPa). Few studies had examined hydraulic safety margins (HSM) for lianas, and when they were, different definitions were used, which made comparison with our results difficult (Tan et al., 2020). Nevertheless, the HSM value found for *B. diversifolia* was very large compared to values in the literature. A possible explanation for this is that Ψ_{min} measured during this field campaign does not correspond to the lowest water potential that the species could reach in the field. For example, in a tropical dry Karst forest, Ψ_{min} of *Lasiococca comberi* was independently measured in multiple studies in multiple years, resulting in very diverse values, ranging from −2.92 MPa in Chen et al. (2021) over −3.77 MPa in Fu et al. (2012) to −6.58 MPa in Chen et al. (2015). Tan et al. (2020) also found strong differences between minimum water potentials measured in a normal dry season and in an extreme dry season. The difference between the HSM values that we found and those of other previous studies could also be due to the different methods used, as our results align with those found by Smith-Martin et al. (unpublished), who also found a range of mostly positive HSMs for lianas (−0.88 to 3.00 MPa) using the OV method.

Yet, it is not only the safety margin that determines the vulnerability of a species, but also the rate of drying during drought periods (Brodribb et al., 2020). As *C. microcarpa* was able to maintain its high Ψ_{md} during the whole field campaign, it is likely that despite its smaller safety margin, it is able to withstand drought periods. This shows that two species with contrasting hydraulic traits can both survive in a water-limited environment, demonstrating that lianas are a heterogeneous group, contrasting to our initial expectations.

Comparison With Local Tree Data

In a study conducted in the same region, Powers et al. (2020) determined P_{50} of 23 tree species using the OV method at leaf level, as well as other hydraulic traits such as the wood specific gravity. The mean $P_{50,OV}$ of the tree species was close to what we measured on lianas in this study (mean ± standard deviation for trees and lianas are −3.69 ± 1.19 MPa (n = 23) and −2.69 ± 2.28 MPa (n = 2), respectively). The range we measured for lianas overlapped for 62.5% with the range of tree $P_{50,OV}$ values, and had a higher maximum (minimum, maximum for trees and lianas are −6.72, −1.55, and −4.30, −1.07, respectively). For wood specific gravity, our values overlapped for 41.8% with the specific wood specific gravity values for trees (n = 60). It is clear that despite the low number of liana species samples, they overlapped to a considerable extent with the values measured for the most abundant tree species in the same location. Additionally, the $P_{50,OV}$ values from both liana species are located at both extremes of $P_{50,OV}$ values found by Smith-Martin et al. (unpublished) for trees in two tropical forests with different rainfall patterns in Panama (**Supplementary Figure 2**), and the difference between the $P_{50,OV}$ values of the lianas is greater than the difference between the most extreme trees. This shows that it is important to consider lianas not as a homogenous group, as is often done to this day, but as a heterogeneous group, just like trees.

CONCLUSION

In this study, we showed that two common, co-occurring liana species exhibit very different hydraulic properties in a water-limited environment. The two species studied showed a similar course of embolism at leaf and branch level, albeit with different susceptibility to embolism for both organs. Other hydraulic characteristics, such as branch water content, Ψ_{min}, MVL, and the course of the water potential in the field were also significantly different between the two species. Although only two species were studied, considerable overlap was found between the range of hydraulic properties of trees and lianas growing in the same location. These findings show that lianas are not a homogeneous group, at least for some hydraulic properties. These results call for further research into the differences in properties between liana species, as this data could substantially contribute to the understanding of liana ecology and their interactions with trees in tropical ecosystems.

DATA AVAILABILITY STATEMENT

The raw data supporting the conclusions of this article will be made available by the authors, without undue reservation.

AUTHOR CONTRIBUTIONS

HV, KS, FM, JP, KC, SD, and CS-M designed the research. KC and SD collected data in the field with contributions from GV. KC and SD analyzed the data. KC wrote the manuscript with substantial input from FM. All authors complemented the article writing and read and agreed to the published version of the manuscript.

FUNDING

This research was funded by the European Research Council Starting Grant 637643 (TREECLIMBERS), FWO grant V401018N ("krediet aan navorsers"), FWO senior research project G002321N. Funding was provided by the Research Foundation Flanders (FWO) under research program G094115N granted to KS. JP thanks the US Department of Energy Grant DE-SC0020344. During the preparation of this manuscript, FM was first funded by the BAEF and the WBI as a research fellow and then by the FWO as a junior postdoc (fellowship 1214720N) and is thankful to these organizations for their financial support.

ACKNOWLEDGMENTS

We are very thankful to D. Perez-Aviles for assistance with species identification and F. Lauriks for assistance with the AV data collection.

SUPPLEMENTARY MATERIAL

The Supplementary Material for this article can be found online at: https://www.frontiersin.org/articles/10.3389/ffgc.2022.836711/full#supplementary-material

REFERENCES

Allen, K., Dupuy, J. M., Gei, M. G., Hulshof, C., Medvigy, D., Pizano, C., et al. (2017). Will seasonally dry tropical forests be sensitive or resistant to future changes in rainfall regimes? *Environ. Res. Lett.* 12:023001.

Anderegg, W. R. L., Klein, T., Bartlett, M., Sack, L., Pellegrini, A. F. A., Choat, B., et al. (2016). Meta-analysis reveals that hydraulic traits explain cross-species patterns of drought-induced tree mortality across the globe. *Proc. Natl. Acad. Sci.* 113, 5024–5029. doi: 10.1073/pnas.1525678113

Beer, C., Reichstein, M., Tomelleri, E., Ciais, P., Jung, M., Carvalhais, N., et al. (2010). Terrestrial Gross Carbon Dioxide Uptake: Global Distribution and Covariation with Climate. *Science* 329, 834–838. doi: 10.1126/science.1184984

Brodribb, T. J., Bienaimé, D., and Marmottant, P. (2016a). Revealing catastrophic failure of leaf networks under stress. *Proc. Natl. Acad. Sci.* 113, 4865–4869. doi: 10.1073/pnas.1522569113

Brodribb, T. J., Skelton, R. P., McAdam, S. A. M., Bienaimé, D., Lucani, C. J., and Marmottant, P. (2016b). Visual quantification of embolism reveals leaf vulnerability to hydraulic failure. *New Phytol.* 209, 1403–1409. doi: 10.1111/nph.13846

Brodribb, T. J., and Holbrook, N. M. (2003). Stomatal Closure during Leaf Dehydration. *Correlation with Other Leaf Physiological Traits. Plant. Physiol.* 132, 2166–2173. doi: 10.1104/pp.103.023879

Brodribb, T. J., Powers, J., Cochard, H., and Choat, B. (2020). Hanging by a thread? *Forests and drought. Science* 368, 261–266.

Chen, Y.-J., Cao, K.-F., Schnitzer, S. A., Fan, Z.-X., Zhang, J.-L., and Bongers, F. (2015). Water-use advantage for lianas over trees in tropical seasonal forests. *New Phytol.* 205, 128–136. doi: 10.1111/nph.13036

Chen, Y.-J., Maenpuen, P., Zhang, Y.-J., Barai, K., Katabuchi, M., Gao, H., et al. (2021). Quantifying vulnerability to embolism in tropical trees and lianas using five methods: can discrepancies be explained by xylem structural traits? *New Phytol.* 229, 805–819. doi: 10.1111/nph.16927

Chen, Y.-J., Schnitzer, S. A., Zhang, Y.-J., Fan, Z.-X., Goldstein, G., Tomlinson, K. W., et al. (2017). Physiological regulation and efficient xylem water transport regulate diurnal water and carbon balances of tropical lianas. *Funct. Ecol.* 31, 306–317.

Choat, B., Brodribb, T. J., Brodersen, C. R., Duursma, R. A., López, R., and Medlyn, B. E. (2018). Triggers of tree mortality under drought. *Nature* 558, 531–539. doi: 10.1038/s41586-018-0240-x

Cosme, L. H. M., Schietti, J., Costa, F. R. C., and Oliveira, R. S. (2017). The importance of hydraulic architecture to the distribution patterns of trees in a central Amazonian forest. *New Phytol.* 215, 113–125. doi: 10.1111/nph.14508

De Baerdemaeker, N. J. F., Stock, M., Van den Bulcke, J., De Baets, B., Van Hoorebeke, L., and Steppe, K. (2019a). X-ray microtomography and linear discriminant analysis enable detection of embolism-related acoustic emissions. *Plant. Methods* 15:153. doi: 10.1186/s13007-019-0543-4

De Baerdemaeker, Niels, J. F., Arachchige, K. N. R., Zinkernagel, J., Van den Bulcke, J., Van Acker, J., et al. (2019b). The stability enigma of hydraulic vulnerability curves: addressing the link between hydraulic conductivity and drought-induced embolism. *Tree Physiol.* 39, 1646–1664. doi: 10.1093/treephys/tpz078

De Guzman, M. E., Acosta-Rangel, A., Winter, K., Meinzer, F. C., Bonal, D., and Santiago, L. S. (2021). Hydraulic traits of Neotropical canopy liana and tree species across a broad range of wood density: implications for predicting drought mortality with models. *Tree Physiol.* 41, 24–34. doi: 10.1093/treephys/tpaa106

De Guzman, M. E., Santiago, L. S., Schnitzer, S. A., and Álvarez-Cansino, L. (2017). Trade-offs between water transport capacity and drought resistance in neotropical canopy liana and tree species. *Tree Physiol.* 37, 1404–1414. doi: 10.1093/treephys/tpw086

di Porcia e Brugnera, M., Meunier, F., Longo, M., Moorthy, S. M. K., Deurwaerder, H. D., Schnitzer, S. A., et al. (2019). Modeling the impact of liana infestation on the demography and carbon cycle of tropical forests. *Glob. Change Biol.* 25, 3767–3780. doi: 10.1111/gcb.14769

Dirzo, R., and Raven, P. H. (2003). Global State of Biodiversity and Loss. *Annu. Rev. Environ. Resour.* 28, 137–167.

Ewers, F. W., and Fisher, J. B. (1989). Techniques for Measuring Vessel Lengths and Diameters in Stems of Woody Plants. *Am. J. Bot.* 76, 645–656.

Ewers, F. W., Fisher, J. B., and Chiu, S.-T. (1990). A survey of vessel dimensions in stems of tropical lianas and other growth forms. *Oecologia* 84, 544–552. doi: 10.1007/BF00328172

Fu, P.-L., Jiang, Y.-J., Wang, A.-Y., Brodribb, T. J., Zhang, J.-L., Zhu, S.-D., et al. (2012). Stem hydraulic traits and leaf water-stress tolerance are co-ordinated with the leaf phenology of angiosperm trees in an Asian tropical dry karst forest. *Ann. Bot.* 110, 189–199. doi: 10.1093/aob/mcs092

Gentry, A. H. (1992). "The distribution and evolution of climbing plants," in *The Biology of Vines*, eds F. E. Putz and H. A. Mooney (Cambridge: Cambridge University Press), 3–50. doi: 1.1017/CBO9780511897658.003

Gorel, A.-P., Steppe, K., Beeckman, H., De Baerdemaeker, N. J. F., Doucet, J.-L., Ligot, G., et al. (2019). Testing the divergent adaptation of two congeneric tree species on a rainfall gradient using eco-physio-morphological traits. *Biotropica* 51, 364–377.

Ichihashi, R., Chiu, C.-W., Komatsu, H., Kume, T., Shinohara, Y., Tateishi, M., et al. (2017). Contribution of lianas to community-level canopy transpiration in a warm-temperate forest. *Funct. Ecol.* 31, 1690–1699. doi: 10.1111/1365-2435.12881

Ingwell, L. L., Wright, S. J., Becklund, K. K., Hubbell, S. P., and Schnitzer, S. A. (2010). The impact of lianas on 10 years of tree growth and mortality on Barro Colorado Island. *Panama. J. Ecol.* 98, 879–887. doi: 10.1111/j.1365-2745.2010.01676.x

Lopez, O. R., Kursar, T. A., Cochard, H., and Tyree, M. T. (2005). Interspecific variation in xylem vulnerability to cavitation among tropical tree and shrub species. *Tree Physiol.* 25, 1553–1562. doi: 10.1093/treephys/25.12.1553

Manzoni, S., Vico, G., Katul, G., Palmroth, S., Jackson, R. B., and Porporato, A. (2013). Hydraulic limits on maximum plant transpiration and the emergence of the safety–efficiency trade-off. *New Phytol.* 198, 169–178. doi: 10.1111/nph.12126

McDowell, N., Pockman, W. T., Allen, C. D., Breshears, D. D., Cobb, N., Kolb, T., et al. (2008). Mechanisms of plant survival and mortality during drought: why do some plants survive while others succumb to drought? *New Phytol.* 178, 719–739. doi: 10.1111/j.1469-8137.2008.02436.x

Medina-Vega, J. A., Bongers, F., Schnitzer, S. A., and Sterck, F. J. (2021). Lianas explore the forest canopy more effectively than trees under drier conditions. *Funct. Ecol.* 35, 318–329.

Meinzer, F. C., Johnson, D. M., Lachenbruch, B., McCulloh, K. A., and Woodruff, D. R. (2009). Xylem hydraulic safety margins in woody plants: coordination of stomatal control of xylem tension with hydraulic capacitance. *Funct. Ecol.* 23, 922–930.

Meunier, F., Krishna Moorthy, S. M., De Deurwaerder, H. P. T., Kreus, R., Van den Bulcke, J., Lehnebach, R., et al. (2020). Within-Site Variability of Liana Wood Anatomical Traits: A Case Study in Laussat. *French Guiana. Forests* 11:523.

Miles, L., Newton, A. C., DeFries, R. S., Ravilious, C., May, I., Blyth, S., et al. (2006). A global overview of the conservation status of tropical dry forests. *J. Biogeogr.* 33, 491–505.

Nobel, P. S. (2012). *Physicochemical and Environmental Plant Physiology*. Cambridge: Academic Press.

Nolf, M., Beikircher, B., Rosner, S., Nolf, A., and Mayr, S. (2015a). Xylem cavitation resistance can be estimated based on time-dependent rate of acoustic emissions. *New Phytol.* 208, 625–632. doi: 10.1111/nph.13476

Nolf, M., Creek, D., Duursma, R., Holtum, J., Mayr, S., and Choat, B. (2015b). Stem and leaf hydraulic properties are finely coordinated in three tropical rain forest tree species. *Plant Cell Environ.* 38, 2652–2661. doi: 10.1111/pce.12581

Pammenter, N. W., and Van der Willigen, C. (1998). A mathematical and statistical analysis of the curves illustrating vulnerability of xylem to cavitation. *Tree Physiol.* 18, 589–593. doi: 10.1093/treephys/18.8-9.589

Pan, Y., Birdsey, R. A., Fang, J., Houghton, R., Kauppi, P. E., Kurz, W. A., et al. (2011). A Large and Persistent Carbon Sink in the World's Forests. *Science* 333, 988–993. doi: 10.1126/science.1201609

Phillips, O. L., Vásquez Martínez, R., Arroyo, L., Baker, T. R., Killeen, T., Lewis, S. L., et al. (2002). Increasing dominance of large lianas in Amazonian forests. *Nature* 418, 770–774. doi: 10.1038/nature00926

Pinheiro, J., Bates, D., DebRoy, S., Sarkar, D., and R CoreTeam. (2013). *nlme: Linear and Nonlinear Mixed Effects Models*.Vienna, Aus;R Foundation for Statistical Computing

Powers, J. S., Vargas, G. G., Brodribb, T. J., Schwartz, N. B., Pérez-Aviles, D., Smith-Martin, C. M., et al. (2020). A catastrophic tropical drought kills hydraulically vulnerable tree species. *Glob. Change Biol.* 26, 3122–3133. doi: 10.1111/gcb.15037

Putz, F. E., and Mooney, H. A. (1991). *The Biology of Vines*. Cambridge: Cambridge University Press.

RStudio Team (2020). *RStudio: Integrated Development for R. RStudio*. Boston, MA: PBC.

Sack, L., and Scoffoni, C. (2012). Measurement of leaf hydraulic conductance and stomatal conductance and their responses to irradiance and dehydration using the Evaporative Flux Method (EFM). *J. Vis. Exp.*70, 4179. doi: 10.3791/4179

Sánchez-Azofeifa, G. A., Quesada, M., Rodríguez, J. P., Nassar, J. M., Stoner, K. E., Castillo, A., et al. (2005). Research Priorities for Neotropical Dry Forests1. *Biotropica* 37, 477–485.

Schindelin, J., Arganda-Carreras, I., Frise, E., Kaynig, V., Longair, M., Pietzsch, T., et al. (2012). Fiji: an open-source platform for biological-image analysis. *Nat. Methods* 9, 676–682. doi: 10.1038/nmeth.2019

Schnitzer, S., and Bongers, F. (2002). The Ecology of Lianas and Their Role in Forests. *Trends Ecol. Evol.* 17, 223–230.

Schnitzer, S. A. (2005). A Mechanistic Explanation for Global Patterns of Liana Abundance and Distribution. *Am. Nat.* 166, 262–276. doi: 10.1086/431250

Schnitzer, S. A. (2015). "Increasing liana abundance in neotropical forests: causes and consequences," in *Ecology of Lianas*, eds A. S. Stefan, F. Bongers, J. B. Robyn, and E. P. Francis (Hoboken, NJ: John Wiley & Sons, Ltd), 451–464. doi: 1.1002/9781118392409.ch30

Schnitzer, S. A. (2018). Testing ecological theory with lianas. *New Phytol.* 220, 366–380. doi: 10.1111/nph.15431

Schnitzer, S. A., and van der Heijden, G. M. F. (2019). Lianas have a seasonal growth advantage over co-occurring trees. *Ecology* 100:e02655. doi: 10.1002/ecy.2655

Scoffoni, C., McKown, A. D., Rawls, M., and Sack, L. (2012). Dynamics of leaf hydraulic conductance with water status: quantification and analysis of species differences under steady state. *J. Exp. Bot.* 63, 643–658. doi: 10.1093/jxb/err270

Skelton, R., and Diaz, J. (2020). Quantifying losses of plant hydraulic function: seeing the forest, the trees and the xylem. *Tree Physiol.* 40, 285–289. doi: 10.1093/treephys/tpz141

Smith-Martin, C.M. (2018). *Liana Survey May 2018 (Unpublished raw data)*. Horizontes.

Smith-Martin, C. M., Bastos, C. L., Lopez, O. R., Powers, J. S., and Schnitzer, S. A. (2019). Effects of dry-season irrigation on leaf physiology and biomass allocation in tropical lianas and trees. *Ecology* 100:e02827. doi: 10.1002/ecy.2827

Smith-Martin, C. M., Xu, X., Medvigy, D., Schnitzer, S. A., and Powers, J. S. (2020). Allometric scaling laws linking biomass and rooting depth vary across ontogeny and functional groups in tropical dry forest lianas and trees. *New Phytol.* 226, 714–726. doi: 10.1111/nph.16275

Steppe, K., Aggelis, D. G., and Grosse, C. U. (2022). "AE in Biological Materials," in *Acoustic Emission Testing: Basics for Research – Applications in Engineering*, eds C. U. Grosse, M. Ohtsu, D. G. Aggelis, and T. Shiotani (Cham: Springer Tracts in Civil Engineering. Springer International Publishing), 583–619. doi: 1.1007/978-3-030-67936-1_20

Sterck, F., Markesteijn, L., Schieving, F., and Poorter, L. (2011). Functional traits determine trade-offs and niches in a tropical forest community. *Proc. Natl. Acad. Sci.* 108, 20627–20632. doi: 10.1073/pnas.1106950108

Tan, F.-S., Song, H.-Q., Fu, P.-L., Chen, Y.-J., Siddiq, Z., Cao, K.-F., et al. (2020). Hydraulic safety margins of co-occurring woody plants in a tropical karst forest experiencing frequent extreme droughts. *Agric. For. Meteorol.* 292-293:108107.

Tardieu, F., and Simonneau, T. (1998). Variability among species of stomatal control under fluctuating soil water status and evaporative demand: modelling isohydric and anisohydric behaviours. *J. Exp. Bot.* 49, 419–432.

Trenberth, K. E., Dai, A., van der Schrier, G., Jones, P. D., Barichivich, J., Briffa, K. R., et al. (2014). Global warming and changes in drought. *Nat. Clim. Change* 4, 17–22.

Trifilò, P., Raimondo, F., Lo Gullo, M. A., Barbera, P. M., Salleo, S., and Nardini, A. (2014). Relax and refill: xylem rehydration prior to hydraulic measurements favours embolism repair in stems and generates artificially low PLC values. *Plant Cell Environ.* 37, 2491–2499. doi: 10.1111/pce.12313

van der Heijden, G. M. F., Powers, J. S., and Schnitzer, S. A. (2015). Lianas reduce carbon accumulation and storage in tropical forests. *Proc. Natl. Acad. Sci.* 112, 13267–13271. doi: 10.1073/pnas.1504869112

van der Sande, M. T., Poorter, L., Schnitzer, S. A., Engelbrecht, B. M. J., and Markesteijn, L. (2019). The hydraulic efficiency–safety trade-off differs between lianas and trees. *Ecology* 100:e02666. doi: 10.1002/ecy.2666

Venturas, M. D., Pratt, R. B., Jacobsen, A. L., Castro, V., Fickle, J. C., and Hacke, U. G. (2019). Direct comparison of four methods to construct xylem vulnerability curves: Differences among techniques are linked to vessel network characteristics. *Plant Cell Environ.* 42, 2422–2436. doi: 10.1111/pce.13565

Venturas, M. D., Sperry, J. S., and Hacke, U. G. (2017). Plant xylem hydraulics: What we understand, current research, and future challenges. *J. Integr. Plant Biol.* 59, 356–389. doi: 10.1111/jipb.12534

Vergeynst, L. L., Dierick, M., Bogaerts, J. A. N., Cnudde, V., and Steppe, K. (2015). Cavitation: a blessing in disguise? New method to establish vulnerability curves and assess hydraulic capacitance of woody tissues. *Tree Physiol.* 35, 400–409. doi: 10.1093/treephys/tpu056

Vergeynst, L. L., Sause, M. G. R., De Baerdemaeker, N. J. F., De Roo, L., and Steppe, K. (2016). Clustering reveals cavitation-related acoustic emission signals from dehydrating branches. *Tree Physiol.* 36, 786–796. doi: 10.1093/treephys/tpw023

Werden, L. K., Waring, B. G., Smith-Martin, C. M., and Powers, J. S. (2018). Tropical dry forest trees and lianas differ in leaf economic spectrum traits but have overlapping water-use strategies. *Tree Physiol.* 38, 517–530. doi: 10.1093/treephys/tpx135

Zhu, S.-D., and Cao, K.-F. (2009). Hydraulic properties and photosynthetic rates in co-occurring lianas and trees in a seasonal tropical rainforest in southwestern China. *Plant Ecol.* 204, 295–304.

Zhu, S.-D., Liu, H., Xu, Q.-Y., Cao, K.-F., and Ye, Q. (2016). Are leaves more vulnerable to cavitation than branches? *Funct. Ecol.* 30, 1740–1744.

Zimmermann, M. H. (1983). *Xylem Structure and the Ascent of Sap. Springer Science & Business Media*. Heidelberg: Springer.

Conflict of Interest: The authors declare that the research was conducted in the absence of any commercial or financial relationships that could be construed as a potential conflict of interest.

frontiers
in Forests and Global Change

ORIGINAL RESEARCH
published: 11 March 2022
doi: 10.3389/ffgc.2022.803194

Linking Drone and Ground-Based Liana Measurements in a Congolese Forest

Begüm Kaçamak[1,2]*, Nicolas Barbier[1], Mélaine Aubry-Kientz[1], Eric Forni[2], Sylvie Gourlet-Fleury[2], Daniel Guibal[3], Jean-Joël Loumeto[4], Sasha Pollet[5], Vivien Rossi[2,6], Nick Rowe[1], Yorick van Hoef[2] and Maxime Réjou-Méchain[1]*

[1] AMAP, Univ. Montpellier, IRD, CNRS, CIRAD, INRAE, Montpellier, France, [2] Cirad, UPR Forêts et Sociétés, Montpellier, France, [3] Cirad-PERSYST-UPR BioWooEB, Montpellier, France, [4] Faculté des Sciences et Techniques, Université Marien Ngouabi, Brazzaville, Republic of Congo, [5] Gembloux Agro-Bio Tech, University of Liège, Gembloux, Belgium, [6] Plant Systematic and Ecology Laboratory, Department of Biology, Higher Teachers' Training College, University of Yaoundé I, Yaoundé, Cameroon

Edited by:
Félicien Meunier,
Ghent University, Belgium

Reviewed by:
Sruthi M. Krishna Moorthy,
University of Maryland, College Park, United States
Margaret Kalacska,
McGill University, Canada
J. Antonio Guzmán Q.
University of Minnesota Twin Cities, United States

***Correspondence:**
Begüm Kaçamak
bkacamak@gmail.com
Maxime Réjou-Méchain
maxime.rejou@ird.fr

Specialty section:
This article was submitted to Tropical Forests, a section of the journal Frontiers in Forests and Global Change

Received: *27 October 2021*
Accepted: *10 February 2022*
Published: *11 March 2022*

Citation:
Kaçamak B, Barbier N, Aubry-Kientz M, Forni E, Gourlet-Fleury S, Guibal D, Loumeto J-J, Pollet S, Rossi V, Rowe N, van Hoef Y and Réjou-Méchain M (2022) Linking Drone and Ground-Based Liana Measurements in a Congolese Forest. Front. For. Glob. Change 5:803194. doi: 10.3389/ffgc.2022.803194

Lianas are abundant and diverse in tropical forests and impact forest dynamics. They occupy part of the canopy, forming a layer of leaves overtopping tree crowns. Yet, their interaction with trees has been mainly studied from the ground. With the emergence of drone-based sensing, very high-resolution data may be obtained on liana distribution above canopies. Here, we assessed the relationship between common liana ground measurements and drone-determined liana leaf coverage over tree crowns, tested if this relationship is mediated by liana functional composition, and compared the signature of liana patches and tree crowns in our drone images. Using drone platforms, we acquired very high resolution RGB and multispectral images and LiDAR data over two 9-ha permanent plots located in northern Republic of Congo and delineated liana leaf coverage and individual tree crowns from these data. During a concomitant ground survey, we focused on 275 trees infested or not by lianas, for which we measured all lianas $\geq$ 1 cm in diameter climbing on them (n = 615) and estimated their crown occupancy index (COI). We additionally measured or recorded the wood density and climbing mechanisms of most liana taxa. Contrary to recent findings, we found significant relationships between most ground-derived metrics and the top-of-view liana leaf coverage over tree crowns. Tree crown infestation by lianas was primarily explained by the load of liana climbing on them, and negatively impacted by tree height. Liana leaf coverage over individual tree crowns was best predicted by liana basal area and negatively mediated by liana wood density, with a higher leaf area to diameter ratio for light-wooded lianas. COI scores were concordant with drone assessments, but two thirds differed from those obtained from drone measurements. Finally, liana patches had a higher light reflectance and variance of spectral responses than tree crowns in all studied spectra. However, the large overlap between them challenges the autodetection of liana patches in canopies. Overall, we illustrate that the joint use of ground and drone-based data deepen our understanding of liana-infestation pathways and of their functional and spectral diversity. We expect drone data to soon transform the field of liana ecology.

Keywords: Central Africa, woody vines, strategy, canopy, competition, UAV systems, remote sensing

INTRODUCTION

Lianas are essential components of tropical forests. They may represent up to 20% of woody plant diversity and 40% of stem density in Neotropical forests (Dalling et al., 2012). Because they do not invest into structural support at the adult stage, often using trees to rise to the forest canopy, lianas tend to exhibit a large leaf area-stem diameter ratio compared to trees (Hegarty and Caballé, 1991; Medina-Vega et al., 2021). They can invade more than half of canopy tree crowns (Ingwell et al., 2010), forming a monolayer of leaves overtopping trees and limiting their light acquisition (Avalos et al., 1999; Visser et al., 2018). They are also suspected to better explore and capture soil resources than trees (Collins et al., 2016; Smith-Martin et al., 2019). They thus are in direct competition with trees for both below-ground and above-ground resources (Avalos et al., 1999; De Deurwaerder et al., 2018), reducing forest tree diversity, growth and carbon storage and strongly limiting forest resilience (Schnitzer and Carson, 2010; Laurance et al., 2014; van der Heijden et al., 2015; Tymen et al., 2016). Therefore, accurately estimating liana infestation is important to quantify its effects on forest functions and predict tropical forests dynamics.

Lianas have mostly been studied through ground-level observations, using common measurements such as stem diameters, following international standardized protocols (Clark and Clark, 1990; Gerwing et al., 2006; Schnitzer et al., 2008). However, while they typically represent less than 5% of woody stem biomass, they can occupy up to 30% of the forest leaf area (van der Heijden et al., 2013). To our knowledge, only one study has looked into the relationship between estimates derived from classical ground measurements (i.e., liana stem density, basal area and biomass) and the top-of-view liana leaf coverage over tree crowns, measured by a canopy crane (Cox et al., 2019). This study found no significant correlations between ground-derived estimates and the liana leaf coverage, raising important questions about the conclusions drawn from ground-based measurements on the aboveground impact of lianas on trees. Understanding the relationship between ground-based measurements and the top-of-view liana leaf coverage over tree crowns is thus important to better interpret the conclusions drawn from classical ground measurements and to better understand liana impact and proliferation in tropical forests.

One mechanism that could blur the relationship between ground-based measurements and the top-of-view liana leaf coverage on tree crowns is that lianas do not constitute a homogenous functional group. A recent study has indeed shown that liana trait variations are comparable in magnitude to tropical tree trait variations, within and across studies (Meunier et al., 2020). Indeed, lianas possess a wide range of strategies for climbing and colonizing trees, allowing them to adapt to different environments (Darwin, 1875; Hegarty, 1991; Putz and Holbrook, 1991; Rowe and Speck, 2015). For instance, physiologically, different wood densities may enable lianas to have different growth-survival strategies. As shown for trees, low wood densities tend to characterize acquisitive species, with high growth rates, large and thin leaves, high photosynthesis rates, large wood vessels and high hydraulic conductance (Van Gelder et al., 2006; Chave et al., 2009; Baraloto et al., 2010; Poorter et al., 2010; Werden et al., 2018; Buckton et al., 2019). These characteristics may in turn impact the patterns of biomass allocation between foliage and woody structures in liana species, as shown for trees where the biomass allocated to the foliage decreases with wood density (Mensah et al., 2016). Furthermore, different climbing mechanisms enable lianas to have different exploration strategies to reach the canopy (Darwin, 1875; Putz, 1984; Isnard and Silk, 2009). Active climbers, such as lianas with tendrils or twining species, exhibit a support-seeking behavior through circumnutation, whereas other climbers, for example climbing with hooks, spines or root climbing attachment, have developed entirely different mechanisms to attach and climb (Melzer et al., 2010). Attachment modes and climbing behaviors have been long known to be of key interest for understanding liana ecology (Putz, 1984). For instance, Bongers et al. (2020) recently found that climbing strategies was significantly related to the recruitment rates of lianas in Central Africa.

With the development of new emerging remote sensing tools such as unmanned aerial vehicles (hereafter referred to as drones), we can now acquire very high-resolution data in which patches of liana leaves can be visually detected on individual trees (Waite et al., 2019). These high-resolution images provide us with accurate estimations of liana leaf distribution above individual tree crowns and allow us to assess the accuracy of commonly used ground-based liana infestation estimates such as the Crown Occupancy Index (COI). This index is a semiquantitative ground-based assessment of relative liana leaf cover over trees (Clark and Clark, 1990). Some studies have looked into the accuracy of the COI to estimate liana loads through its relationship with metrics derived from common ground liana measurements (density, basal area), with positive conclusions (van der Heijden et al., 2010). As a consequence, liana-infestation has been monitored through time using the COI, as it is much less time-expensive than classical dendrometric measurements (Ingwell et al., 2010; Wright et al., 2015). However, using high resolution drone data in Malaysia, Waite et al. (2019) showed that even if a significant positive correlation between the COI and the relative liana leaves coverage over tree crowns exists, ground-based COI estimates were prone to errors, with more than 25% of trees incorrectly classified from the ground. Most of these errors occurred for low infestation levels, representing nearly half of the wrongly classified trees. Given the importance of the COI in current liana studies, the accuracy of this index should be further evaluated in different forest contexts.

One important condition for detecting liana leaves in remote sensing products is the existence of different spectral responses between liana and tree leaves. Lianas tend to have different leaf chemical properties than trees, resulting in higher reflectance across the solar spectrum, with higher differences between trees and lianas observed around 550 nm (green domain; Castro-Esau, 2004; Asner and Martin, 2012; Li et al., 2018; Chandler et al., 2021) and in the near infrared (NIR; 780–1,400 nm; Li et al., 2018) and shortwave infrared (SWIR; 1,400–3,000 nm; Chandler et al., 2021; Visser et al., 2021). Some studies have used these differences in spectral responses to detect liana infested trees and monitor infestation rates at the scale of the canopy (Marvin et al., 2016; Li et al., 2018; Chandler et al., 2021). For instance, Li et al. (2018) obtained an accurate classification of liana infested and non-infested trees using a deep self-encoding network at the scale of the canopy, using high-resolution multi-spectral [475 nm (blue) to 840 nm (NIR)] drone data. However, as most previous studies, they solely focused on the presence or absence of lianas and did not quantify the degree of infestation of trees. All studies aiming at quantifying the degree of liana infestation found reliable results only for highly infested trees (>50 or 75% of infestation by lianas) and could not accurately estimate nor detect low liana infestation rates (Marvin et al., 2016; Chandler et al., 2021). A recent study even showed that lianas and trees do not differ significantly in their spectral signatures at the leaf level (Visser et al., 2021). Nevertheless, radiative transfer modeling has suggested that lianas display a lower light absorption and greater projected leaf area, due to flatter leaf angles. This results in a higher reflectance at the canopy scale, especially in the near and shortwave infrared regions and when liana leaves are aggregated within large patches (Visser et al., 2021). Most of these studies were, however, conducted in Neotropical forests while much less is known about the spectral properties of lianas in the paleotropics. Given that lianas are present in more than 133 families of angiosperms (Gentry et al., 1991), probably generating a large range of spectral signatures as observed for trees (Féret and Asner, 2012; Rocchini et al., 2016) and that spectral signatures partly depend on local environmental conditions (Asner and Martin, 2012; Medina-Vega et al., 2021), the extent to which liana leaves can be detected from their spectral signatures should be further investigated, especially with the use of very high-resolution drone data and focusing in other tropical regions than the Neotropics. Furthermore, with the recent advances in processing Light Detection and ranging (LiDAR) data, we now can semi-automatically delineate individual tree crowns thanks to dedicated algorithms (Aubry-Kientz et al., 2019) and thus better disentangle the spectral response of tree crowns from that of liana patches.

In this study, we investigated the relationship between ground-based liana measurements and liana leaf coverage over tree crowns quantified through high-resolution drone images. More specifically, we assessed whether ground-based measurements accurately predict liana leaf coverage over tree crowns and whether these two measurements are mediated by liana functional composition. We also separated the signatures of liana patches and tree crowns both in the visible and non-visible domain to evaluate the extent to which they overlap. We hypothesize that (i) classical ground-based liana measurements are significantly correlated with drone-based liana leaf coverage estimates; (ii) liana wood density and climbing mechanisms both influence liana leaf coverage over tree crowns; (iii) the COI is not an accurate measure of liana leaf coverage for low infested trees, as found by Waite et al. (2019); and (iv) spectral responses of liana patches and tree crowns significantly differ in multispectral data, with higher reflectances of lianas both in the green and near infrared domain, as previously found in the Neotropics.

MATERIALS AND METHODS

Study Site

Our study took place in Central Africa, in the north of the Republic of Congo, in the Likouala province (2°27′11.87″ N and 17°02′32.17″ E). Mean annual rainfall is 1,605 mm/year (unpublished data obtained from 2003 to 2017 using a local station at Pokola, 140 km away from our study site). The climate is characterized by two dry seasons with a short one from June to August and a long one from December to February. The Loundoungou site is located on a plateau, the geological substrate consists of limestone and alluvium from the Quaternary. Soils can be classified as Xanthic Acrisols, sandy-clay to clay-sandy, representative of the highest and lowest elevations of the plateau (Freycon, 2014). The studied landscape is generally low and flat, between 395 and 470 m asl (Freycon, 2014). The vegetation is a semi deciduous forest characterized by the abundance of trees belonging to the Fabaceae, Annonaceae, and Malvaceae families (Réjou-Méchain et al., 2021).

The experimental study site was settled in 2013–2014 in the Forest Management Unit (UFA) of Loundoungou-Toukoulaka, in a concession managed by the logging company CIB-Olam. The experimental design aims at comparing different silvicultural treatments among four 9-ha plots that were established in similar soil, topography and initial vegetation conditions (using preliminary inventories). In the present study, we focused on two 9-ha permanent plots that experienced highly selective logging operations at the end of 2018 (0.3 trees logged per ha on average). Other human activities are unlikely to have induced major disturbances in the recent decades. Inside each plot, all trees $\geq$ 10 cm dbh (diameter at breast height) have been identified, located, and their diameter measured each year since 2015 following international standards (Picard and Gourlet-Fleury, 2008), for a total of 6,380 trees $\geq$ 10 cm dbh measured in 2019.

Drone-Based Data and Pre-field Inventories Analyses

Drone-based acquisitions were performed at three different periods: in June 2018, April 2019 and in February 2020. In 2018 and 2019, Red Green Blue (RGB) images were acquired over the experimental site using an EBEE 03-907 drone, from the manufacturer SENSEFLY, operated by a private company (Sylvafrica). In 2020, we acquired three drone datasets: Red Green Blue (RGB), multispectral and LiDAR data. All flights were conducted under homogeneous sunlit conditions. RGB data were acquired with a Mavic 2 Pro drone, using an integrated three-waveband (RGB) camera (20MP Hasselblad L1D-20c gimbal). The flight trajectory was calculated and conducted with the UGCS software. The acquisitions were made in three flights covering the whole study site in less than 1-h between 7 and 8 a.m., on the 14th of February, with an overlap of 90% between flight lines. This short time of acquisition of all RGB data allowed us to obtain Digital Numbers (DN) values under homogeneous sunlight and atmospheric conditions, and were hereafter assumed as a proxy of relative radiometric responses (radiometric corrections were not possible in our study). Multispectral data were acquired in the red (660 nm ± 40 nm), green (550 nm ± 40 nm), red-edge (735 nm ± 10 nm) and near-infra red (790 nm ± 40 nm) regions using a Parrot Sequoia camera mounted on a DJI Matrice 600 drone. The flight trajectory was also calculated and conducted using UGCS. The acquisitions were made in two overlapping flights over the studied area, on the 13th of February, the first at 8 am and the second at 15 pm, with an overlap of 90% within flight lines. Data from an incident light sensor located above the drone was used for conversion of DN values into bottom-of-atmosphere (BoA) reflectance in the Pix4D software.[1] However, as the Pix4D routine did not yield satisfactory results, analyses based on the BoA reflectance values of trees versus lianas were restricted to 60% of the studied area, i.e., using only the first flight to minimize atmospheric effects and avoid inter flight radiometric corrections.

All drone imagery data were processed through Pix4D to produce orthomosaics at spatial resolutions of 10 cm (2018), 5 cm (2019), 3 cm (2020 RGB), and 17 cm (2020 Multispectral). Pix4D used structure from motion algorithms, and other algorithms, to build a dense point cloud from which a digital surface model (DSM) was derived and used to produce an orthomosaic. In all cases, pixels were represented by a minimum of five overlapping images, with a total of 1095 images over 1292 ha (2018), 248 images over 80 ha (2019), 1153 images over 56 ha (2020 RGB) and 2011 images over 450 ha (2020 Multispectral). We used both the Pix4D algorithms of noise filtering, to remove outliers in the generated points cloud, and of surface smoothing (type Sharp), to flatten erroneous small bumps in the DSM.

Finally, very high-resolution LiDAR data were acquired on the 9th of February 2020 over the whole study site. A Yellowscan Surveyor Ultra sensor (combining a Velodyne Ultra Puck, 600 kHz, 905 nm wavelength LiDAR scanner and an Applanix 15 IMU) was flown mounted on the DJI Matrice 600 UAV platform at 60 m above SRTM elevation at a speed of 8 m/s, with an interline distance of 50 m. A multiple return acquisition resulted in a point density of 372 points/m^2. We used a Reach RS2 GNSS base station for PPK differential positioning with a global accuracy of less than 4 cm on the X and Y axis (average accuracy of 3.7 cm on all trajectories) and less than 7 cm on the Z axis (average accuracy of 6.3 cm on all trajectories). Trajectories were post-processed in PosPac UAV v9 and point clouds were processed in LASTools (Isenburg, 2014) to derive a 1-m resolution Digital Terrain Model (DTM) using the lasground (with the wilderness option) and las2dem functions. We then normalized the point clouds (using the lasheight function) and assessed the maximum height values with a 1m-grid in the normalized point cloud (lascanopy function) to create a Canopy Height Model (CHM), representing the top-of-canopy height above the ground.

Prior to the field inventory (see next section), we conducted preliminary analyses on the 2018 and 2019 drone datasets in order to facilitate our upcoming fieldwork. Through a visual interpretation of RGB mosaics, we manually delineated what was seemingly liana leaf cover patches over individual tree crowns, using the QGIS open source software (version 3.10). We then validated the presence of lianas in these tree crowns using binoculars in the field to assess the accuracy of these preliminary delineations from the ground. This assessment also both helped our tree selection and liana delineation afterward on the 2020 drone images (see section "Liana Delineation and Spectral Signatures of Lianas").

Field Inventories

We conducted a field campaign concomitantly with the third drone acquisition in February 2020. Using the field application of QGIS, Qfield,[2] we validated and corrected (if needed) the delineation of individual tree crowns and the presence of liana leaf coverage observed on the 2019 RGB images, and recorded the corresponding tree field inventory number for each tree crown. In almost all cases the preliminary delineations of lianas were validated with the presence of liana leaf coverage patches over tree crowns, with only a few errors due to the occurrence of hemi-parasite and hemi-epiphyte plants. Because the number of liana-infested trees was much smaller than that of non-infested ones, we focused our field investigations on trees that were identified as liana-infested in our preliminary analyses and measured non-infested trees in an opportunistic way. It enabled us to optimize our time during our 3-week field mission and to ensure the measurement of numerous liana-infested trees. In total, we were able to link individual tree crowns delineated on drone images with tree ground survey numbers for a total of 275 trees, infested or not by lianas, with diameters ranging from 12.9 to 170.7 cm dbh (median of 55.7 cm dbh). All studied trees had a crown entirely visible from drone images, as estimated from the field.

For each tree, we estimated the liana leaf coverage from the ground using the widely used Crown Occupancy Index (COI; Clark and Clark, 1990; van der Heijden et al., 2010). This semi-quantitative index expresses the relative coverage of liana leaves in the tree crown using five categories: (0) no liana leaves in the crown, (1) 1–25%, (2) 26–50%, (3) 51–75%, and (4) > 75% of the tree crown covered by liana leaves. For each tree, the COI was systematically assessed by two observers, equipped with binoculars, who observed tree crowns from every visible and accessible angle, discussed their estimates and agreed on the final COI score.

All woody lianas $\geq$ 1 cm in diameter climbing on the studied trees, or visibly entering or leaving the tree crown, were identified by vernacular name and their diameters were measured following international protocols using a manual caliper for small lianas and a tape for large ones (Gerwing et al., 2006; Schnitzer et al., 2008). In total, we measured 615 lianas belonging to 54 vernacular taxa climbing on 104 trees. For each tree, we computed four stand level liana measurements: liana stem number (N_L), liana basal area (BA_L), liana maximum diameter ($Dmax_L$), liana mean quadratic diameter (QMD_L).

We measured or recorded two functional traits: the stem wood infradensity and the climbing mechanism. For stem wood infradensity, we collected stem cylinders of more than 2 cm in diameter at 1.3 m from the stem root, out of the permanent plot

---

[1] https://www.pix4d.com/

[2] https://qfield.org/

to avoid destructive measurements within the plots. In total, we collected stems belonging to the most abundant 20 vernacular taxa, representing 83% of the 615 liana stems inventoried. Wood samples of approximately 2 cm of length were debarked and saturated with water under pressure and the Archimedes thrust was measured following the protocol described by Birouste et al. (2014). Wood samples were first dried in an oven at 45°C for a week to avoid damaging the water saturated materials with sudden extreme temperatures. Then, we rose the temperature to 103°C for 24 h to eliminate all water residuals. Finally, the anhydrous masses of wood samples were measured, to assess the wood infradensity, hereafter named wood density.

Liana climbing mechanisms were recorded for 34 vernacular taxa, representing 92% of the 615 liana stems inventoried. Climbing mechanisms were assigned to each vernacular name following the classification proposed by Sperotto et al. (2020). We classified as "active" climbing mechanisms twining lianas, lianas with tendrils, prehensible branches and lianas with angular branches. We classified as "passive" climbing mechanisms lianas with hooks, spines, adhesive roots and simple scrambling lianas.

Data Analysis

Geospatial Analysis

Tree Crown Segmentation

We used the LiDAR data to delineate tree crowns on the two 9-ha plots. After normalizing the point cloud with the DTM, we removed the ground points and reduced randomly the density of the point cloud to 40 points/m^2 to limit computing time. We then used the Adaptative Mean Shift approach (AMS3D; Ferraz et al., 2012) implemented in the open Computree software (Piboule et al., 2013). This approach composes a normalized point cloud into 3D clusters, corresponding to individual tree crowns, by finding local maxima giving a certain cylinder size. We deliberately parameterized the model to over-segment tree crowns (**Figures 1A,B**) because it is then easier to manually merge over-segmented crowns than to segment under-segmented crowns. After extracting the projected shapes from Computree, we manually cleaned the segmentation in QGIS, using our field observations and high resolution RGB and multispectral images (**Figures 1C,D**). In total, we delineated 1626 individual canopy tree crowns over the 18-ha study area. We finally assigned to each tree its maximum height using the LiDAR-derived CHM model built at 1-m resolution.

Liana Delineation and Spectral Signatures of Lianas

In all the studied trees validated from the ground, liana leaves were clearly distinguished visually from leaves of their host trees in the visible (RGB) and/or non-visible (Red-Edge and Near Infrared) domain (**Figure 2**). We thus delineated all visible liana leaf coverage over the two 9-ha plots, manually from QGIS, combining our specialized field observations and a careful visual interpretation using the different 2020 spectral bands available.

Using the 2020 RGB images, we then selected pixels that were likely dominated by leaves, either from trees or lianas, to quantify the photosynthetic surface of trees and lianas. To do this, we first only selected pixels belonging to a segmented tree crown (see previous section), ignoring canopy gaps and below-canopy vegetation. We then filtered out woody pixels (in our case DN values $>$ 190 in the blue waveband) and pixels corresponding to small gaps in the tree crown (DN values $\leq$ 100 in the green waveband). Using this dataset, we finally estimated the relative area of liana leaves over the total canopy photosynthetic surface.

To test whether liana leaves expressed a singular spectral response, we averaged pixel DN (RGB data) and reflectance (multispectral data) values for each individual liana patch and liana-free tree crown for all bands independently to minimize the noise associated with pixel-level information. We submitted object-level averaged DN and reflectance values to a Principal Coordinate Analysis (PCA) and compared the liana and tree leaves responses along the first two PCA axes using Wilcoxon tests, to test for difference in signal average, and *F*-test, to test for difference in signal variance. As mentioned earlier, this analysis was conducted on only 60% of the study area to minimize atmospheric and radiometric bias in multispectral data. Considering multispectral data in DN values instead of reflectance values in the PCA led to the same results (not shown).

Statistical Analyses

Relationship Between the Crown Occupancy Index and Liana Leaf Coverage Over Tree Crowns

We used the whole dataset (275 trees) to study the relationship between the COI determined from the ground and the proportion of photosynthetic surface of lianas on tree crowns determined by drone-based data. We modeled with an ordinal probit regression the relationship between the different ground-determined COI categories (0, 1, 2, 3, or 4) and the proportion of photosynthetic surface of lianas (aka drone-determined liana leaf coverage) on tree crowns.

Relationship Between Stem Ground Measurements and Liana Leaf Coverage Over Tree Crowns

We performed all statistical analyses at the scale of individual trees. We divided our dataset in four categories by the type of infestation of the host tree:

(i) trees that were not infested by lianas. These trees did not have any visible liana climbing on them or coming from adjacent trees from the ground (COI of zero), and did not have any liana leaves visible on the crown from the drone images (*n* = 161 trees);

(ii) trees that were identified as infested by lianas. These trees were identified as infested either from ground measurements or/and drone observations;

(ii)-a trees that were identified as infested from both ground measurements and drone observations (*n* = 87 trees);

(ii)-b trees that were identified as infested only from ground measurements, with no visible liana leaves on the crown from drone images (*n* = 17 trees);

(ii)-c trees that were identified as infested only from drone observations, with no visible lianas climbing on them or coming from adjacent trees from the ground (*n* = 10 trees).

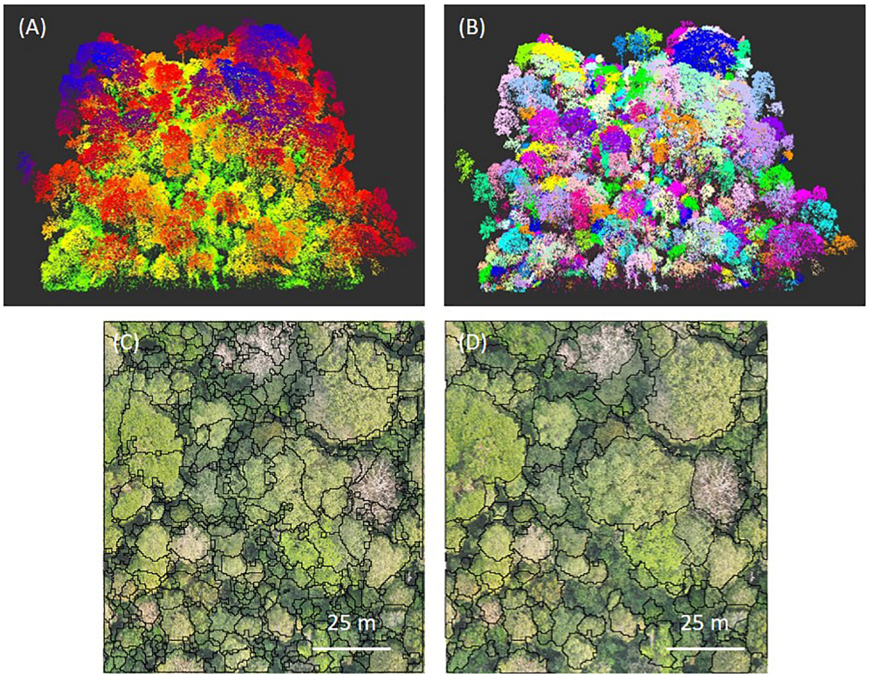

FIGURE 1 | An example of tree crowns segmentation of a 1-ha subplot, with the AMS3D approach. **(A)** The point cloud before the segmentation, colored by height (green to blue) and **(B)** after the segmentation, colored by individual tree. The projected 2D shapes of individual tree crowns (in black) before manual cleaning in **(C)** and after in **(D)** over an RGB image.

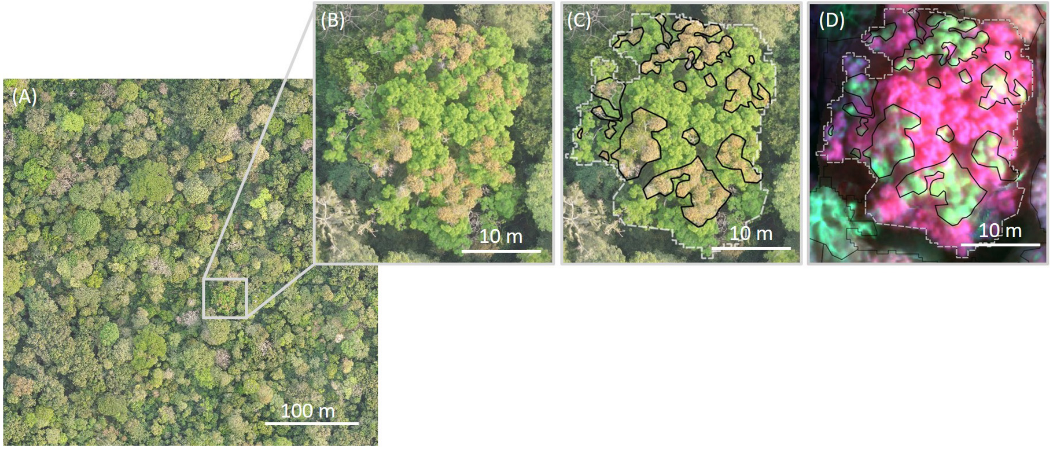

FIGURE 2 | Example of the manual delineation of liana leaves using RGB and multispectral data. **(A)** RGB mosaic of one of the two 9-ha plots. A liana-infested tree crown is illustrated before **(B)** and after **(C,D)** the manual delineation of lianas (in black lines) and the LiDAR segmentation of the tree crown with the AMS3D approach (in white dotted lines) on RGB **(C)** and multispectral **(D)** images.

Because including category (i) may lead to an overestimation of model performance, with an inflation of zero values, we only considered infested trees of category (ii) when analysing the relationship between ground measurements and liana leaf coverage. We also discarded infested trees of the category (ii)-c because we either failed to find the corresponding lianas rooted point in the ground or the leaves most probably belonged to epiphytes (see section "Discussion"). Thus, ground measurements and liana leaf coverage comparison were done on a total of 104 trees (categories (ii)-a and (ii)-b). Our infested tree selection was the same as Cox et al. (2019) except that, here, we also included trees with lianas climbing on them without any visible leaves from above.

First, we modeled with a Bernoulli probit-regression, the probability that a tree infested from ground measurements had visible liana leaves on the crown from drone images. This model was calibrated on the 104 trees of [categories (ii)-a and (ii)-b]. Second, we modeled with a log-linear regression, the liana leaf coverage for trees infested from ground measurements and with visible liana leaves on the crown from drone images. This model was calibrated on the 87 trees of [categories (ii)-a].

For the two models, the predictors were selected among the four tree-level liana measurements calculated at the tree level (N_L, BA_L, $Dmax_L$, QMD_L), the LiDAR-derived total tree height (H) and the interactions between N_L* QMD_L and H* QMD_L. We selected the predictors using a stepwise approach (backward/forward) based on the Bayesian Information Criterion (BIC; the best model has the lowest BIC).

Hence, the products of these two models could lead to a model of the liana leaf coverage for trees defined as infested from ground measurements.

Influence of Liana Functional Traits on Liana Leaf Coverage

To study the influence of growth strategies on liana leaf coverage, we analyzed the relationship between the residuals of the selected linear log-log regression model and two liana functional traits averaged at the tree level: the basal-area weighted wood density of lianas (WD_L) and the climbing mechanisms of lianas ($Mecha_L$). WD_L was estimated for every infested tree for which we knew the wood density of liana individuals for more than 80% of the total liana basal area (n = 57 trees) using the equation as follows:

$$\frac{WD_L \;=\; \sum_{i=1}^{n}(WD_i * BA_{Li})}{\sum_{i=1}^{n} BA_{Li}}$$

With n the total number of liana stem climbing on the host tree, WD_i the wood density for liana species i and BA_{Li} the total liana basal area for individuals belonging to the liana species i. on the host tree We calculated the climbing mechanism index ($Mecha_L$) indicating the mean liana growth strategy through the following equation:

$$Mecha_L \;=\; \frac{\sum_{i=1}^{n_a} BA_{i_a}}{\sum_{i=1}^{n_a} BA_{i_a} + \sum_{i=1}^{n_b} BA_{i_b}}$$

With n_a the total number of liana stems with active climbing mechanisms, $n_b$the total number of liana stems with passive climbing mechanisms and BA_{i_a} and BA_{i_b} the basal area of all lianas having an active and passive climbing mechanism, respectively. We calculated $Mecha_L$ for every infested tree for which we knew the climbing mechanism of more than 80% of the total liana basal area (n = 70 trees).

We did not include directly functional traits variables into the regression models but decided to look at their relationship with the residuals of the models (response minus fitted values), because we did not have trait data information for the whole dataset.

All analyses were conducted on R version 4.0.3 (R Core Team, 2020), using the libraries sf (Pebesma et al., 2018), raster (Hijmans, 2021), lidR (Roussel et al., 2020), MASS (Venables and Ripley, 2002), reshape2 (Wickham, 2007), ggplot2 (Villanueva et al., 2016), DescTools (Signorell et al., 2021), dplyr (Wickham et al., 2021), and RcmdrMisc (Fox et al., 2020).

RESULTS

Amount of Liana Infestation Estimated From the Ground and From Drone Data

Drone- and ground-based measurements indicated that 35 and 38% of the selected 275 trees were infested by lianas, respectively. These numbers are unlikely to be representative because we deliberately sampled a higher proportion of liana-infested trees than non-infested trees. However, at the scale of the study sites (the two 9-ha plots), drone-based measurements indicated that 16.6% of canopy trees (n = 270) were infested by lianas and that liana leaves covered 6.2% of the total canopy photosynthetic surface (n = 594 patches). At the scale of the 275 trees dataset, ground-based measurements indicated that liana-infested trees were infested by an average of 5.9 lianas (range of 1–20) with a mean quadratic diameter of 3.5 cm (range of 0.7–22.8 cm) and an average basal area of 157.8 cm^2 (range of 1.6–1027.5 cm^2). Using herbariums, we identified a total of 54 liana taxa, although this estimate might be underestimated because some vernacular names cannot yet be assigned to a single species (work in progress). Wood density also varied markedly among liana taxa, ranging from 0.29 to 0.52 g cm^{-3} (mean of 0.42 g cm^{-3}), and the basal-area weighted wood density of lianas at the scale of an individual tree, WD_L, ranged from 0.37 to 0.52 g cm^{-3} (mean of 0.44 g cm^{-3}). Finally, the dominant climbing mechanisms was active (64% of individuals), with 47% of the total stems belonging to twining lianas.

Link Between Drone and Ground-Based Liana Measurements

Eighty four percent of the trees hosting lianas had visible liana leaves on their tree crowns in drone images [category (ii)-a; red dots in **Figure 3**]. Thus, 16% of the trees observed as infested from the ground did not have any visible leaf coverage on their crowns when drone data were acquired [category (ii)-b; green dots in **Figure 3**]. Most of these trees consistently had a COI score of 0 (n = 5) or 1 (n = 11), except one tree that had a COI score of 3. For this tree, our field note indicated that the COI score was uncertain due to the co-existence of a hemi-epiphyte (*Ficus* sp.) and a mix of old and young liana leaves. Finally, we observed liana leaves in the crown of 10 trees [4%; category (ii)-c; blue dots in **Figure 3**] for which we failed to assign any corresponding liana stems on the ground.

Link Between Liana Leaf Coverage and Classical Ground-Based Liana Measurements

For trees identified as infested either from the ground or drone data (category (ii)), we found that ground-derived liana stand metrics were significantly correlated with the liana leaf coverage measured on drone data (Spearman's ρ = 0.43–0.58; $p < 0.001$; **Figure 3**), except for liana mean quadratic diameter (p = 0.97).

The infestation status of tree crowns (infested or not) was first best predicted by liana basal area and total tree height, with a predominant positive effect of liana basal area and a negative effect of tree height (**Table 1**). The selected model classified 86% of the 275 trees accurately but tended to overestimate the

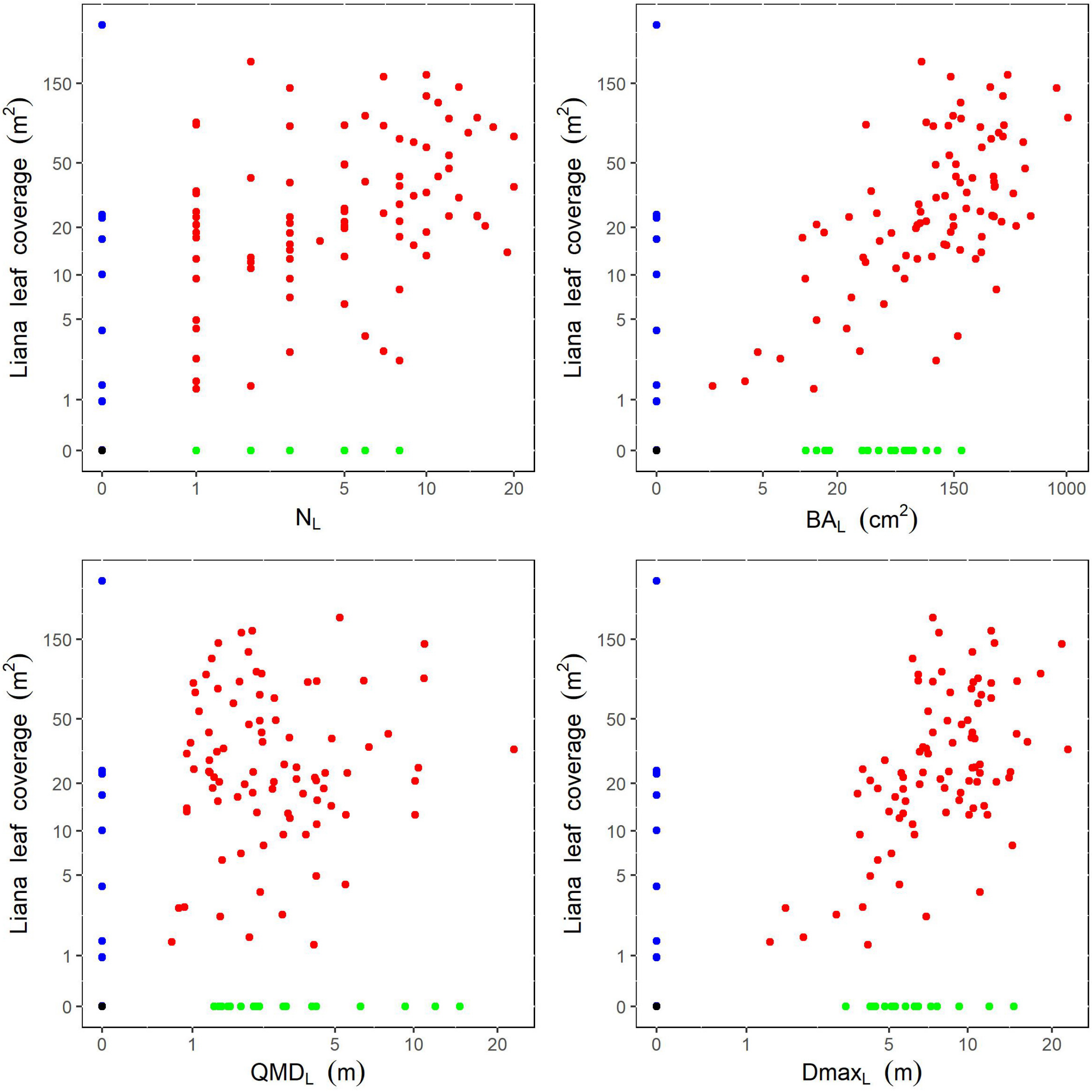

FIGURE 3 | Relationships between liana ground measurements and liana leaf coverage estimated from drone data for the 275 studied trees. Colors illustrate the different infestation categories, black for category (i), red for (ii)-a, green for (ii)-b, and blue for (ii)-c. Axes are shown in log scale. For N_L, Spearman's $\rho = 0.43$, $p < 0.001$; for BA_L, Spearman's $\rho = 0.58$, $p < 0.001$; for QMD_L, Spearman's $\rho = 0.004$, $p = 0.97$; for $Dmax_L$, Spearman's $\rho = 0.48$, $p < 0.001$.

number of tree crowns infested by liana leaves using ground-based measurements as predictors (**Table 2**).

When focusing on trees being interpreted as liana-infested from both ground and drone observations [category (ii)-a; $n = 87$], our BIC selection procedure only retained the total liana basal area per tree as a predictor of liana leaf coverage over tree crowns, with a significant positive effect, explaining 43% of the total variance (intercept = 0.42; slope = 0.60; $p < 0.001$; **Figure 4**).

We then found a significant, albeit weak, negative effect of liana basal area weighted wood density on the residuals of the selected model predicting liana leaf coverage (intercept = 2.18; slope = -5.10; $p = 0.048$; **Figure 5**). Trees hosting lianas with lower wood densities thus tend to have a larger liana leaf coverage over their crowns. By contrast, we did not detect any significant effect of liana climbing mechanisms on the model residuals ($p = 0.96$).

Link Between Liana Leaf Coverage and the Crown Occupancy Index

COI scores estimated from the ground and from drone data were significantly concordant (Kendall's W = 0.94, $p < 0.001$,

TABLE 1 | Estimates of parameters of the model selected to predict liana infestation status (tree crowns infested or not).

	Estimate	Std. Error	*z*-value	Pr(>|z|)
(Intercept)	1.4791	0.2754	5.371	<0.0001***
BA_L	1.3630	0.4258	3.201	0.0001**
Height	−0.4791	0.1937	−2.474	0.01337*

Parameters associated with variables that were not selected by the BIC step procedure are not reported.
$*p < 0.05$; $**p < 0.01$; $***p < 0.001$.

TABLE 2 | Error matrix showing the number of tree crowns predicted to be infested by liana leaves using ground-based measurements as predictors and drone observations as reference data.

		Drone observations	
		Not infested	**Infested**
Predictions from ground measurements	**Not infested**	**5**	2
	Infested	12	**85**

Agreements between predictions and observations are represented in bold.

$N = 275$), with the same classification for 72% of the studied trees (**Table 3**). However, most of these agreements were due to trees identified as non-infested by the two approaches (95% of the trees identified as non-infested from the ground were also identified as non-infested by drone measurements). When the comparison was restricted to trees observed as infested from the ground, only 32% of them were assigned to the same COI category using both approaches, with an overestimation of the ground-based compared to the drone-based estimates (**Table 3**). For 22% of the trees, the classification varied by one class and, for 6% of the trees, it varied by two or more classes. The probit model confirmed that a large overlap exists between the probabilities of belonging to the different categories along the gradient of infestation, even if the ranks were fairly well-preserved among categories on average (**Figure 6**).

Spectral Signatures of Lianas and Trees in Drone Images

The PCA performed on liana patches and liana-free tree crowns signal averages resulted in a first dominant axis (76% of the inertia) negatively correlated with signal intensity in all bands (**Figure 7**). The second axis, expressing 16% of the variance, tended to oppose invisible (near-infrared and red-edge) from visible bands. Despite a large overlap, we found that liana patches had significantly lower scores (higher DN and reflectance values) than tree crowns on the first axis (Wilcoxon's $W = 82{,}447$, $p < 0.0001$) but exhibited no significant difference along the second axis ($W = 141{,}893$, $p = 0.21$). On the two PCA axes, the variance of the scores of individual lianas patches was significantly larger than that of trees (PCA Axis 1: $F = 1.2$, $p = 0.05$; PCA Axis 2: $F = 1.6$, $p < 0.0001$). Analyses conducted at the band level (**Supplementary Figure 1**) confirmed that liana patches tend to have greater DN and reflectance values than tree crowns in all the bands with a marked difference in the red and green domain compared to the other bands.

DISCUSSION

In this study, we used a combination of high-resolution drone images and field ground surveys to understand the links between below- and above-canopy liana distribution. We showed that the ability of lianas to reach the canopy depends mostly on their basal area and, to a less extent, on the total height of their host. Once the canopy is reached, lianas expand their leaves over tree crowns proportionally to their basal area, even though large variability in liana leaf cover exists for a given basal area. Some of this variability was explained here by a differential investment in leaf versus wood biomass with a larger leaf cover observed for liana species with lighter wood. We further showed that the widely used COI provides reliable information on the liana infested status but that, in our case, this index tends to provide lower estimates of infestation levels compared to drone-determined liana leaf coverage. Finally, our results suggest that liana patches display a stronger light reflectance than tree crowns in all the studied bands but that their spectral signatures largely overlap with that of trees. The mechanisms underlying these results and their implications are discussed below.

Liana Drone-Based Measurements Can Be Linked to Classical Ground Measurements, in Most Cases

Our results indicate that drone and ground data led to similar estimates of the number of liana-infested trees. The infestation status of tree crowns was indeed well predicted from ground data with 90% of the drone-based infested trees identified as such from a model using ground-derived estimates as predictors. This suggests that both methods are suited to study the number of tree crowns infested by lianas. We also found a significant correlation between classical ground measurements of lianas and drone-determined liana leaf coverage over tree crowns. This result is contradictory to that found by the only other study which has analyzed the link between above and below canopy liana measurements, using a canopy crane to determine liana leaf coverage over tree crowns (Cox et al., 2019). This study surprisingly indicated that liana leaf coverage was unrelated to liana stem count, basal area, aboveground biomass or tree diameter at breast height and the authors interpreted this negative result by the fact that lianas tended to mostly spread through neighboring tree crowns in their site. In our case, as discussed in the next section, we found strong significant correlations between the top-of-view liana leaf coverage and the ground-derived liana stem count, basal area, maximum diameter and tree height. This constitutes a reassuring result because liana infestation on trees has been extensively studied through ground measurements and estimations (Phillips et al., 2005; van der Heijden and Phillips, 2009; Ingwell et al., 2010; Wright et al., 2015). However, liana leaf cover was highly variable for a given range of ground-based measurements, keeping in mind that we studied the relationship between both measurements

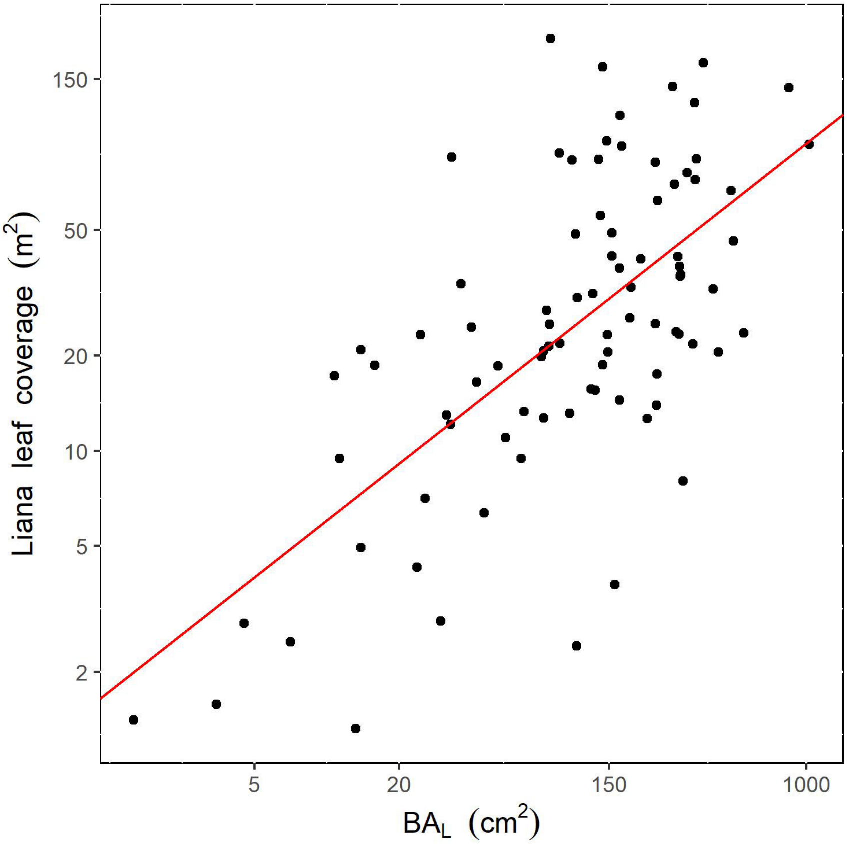

FIGURE 4 | Relationship between total liana basal area measured from the ground and leaf coverage estimated from drone data for 87 tree crowns. The red line illustrates the predicted linear log-log model. Axes are shown in log scale.

in log-transformed scale. This indicates that a large variance in aboveground competition between lianas and trees cannot be captured by ground measurements.

Some liana-infested trees were not identified as such from the ground [10 trees, category (ii)-c]. For one of these trees, the crown of which was heavily infested by lianas, our field notes indicated that it was impossible to follow any of the liana stems coming out or into the crown and measure them with certainty due to a poor visibility. For the other trees, a careful reanalysis of the drone images suggested that (i) five of them were infested by hemi-epiphytes or epiphytes that we did not detect during our fieldwork; (ii) four of them were trees with lianas coming from adjacent tree crowns, with probably remote rooting points of lianas that we missed from the ground. Once they reach the canopy, lianas can progress horizontally from crown to crown (Putz, 1984), sometimes up to relatively large distances (Ingwell et al., 2010), making the link between above and below-canopy views difficult to establish in some cases. Conversely, some trees identified with lianas climbing on them during the ground survey did not have liana leaf coverage over their crowns [17 trees; category (ii)-b]. Four of these trees were trees with lianas climbing on them but which did not reach the canopy either because they still were at an early stage of development or because they appeared to have fallen at the time of the inventory, due to tree branch falls. For the other trees, lianas appeared to reach the canopy from the ground but were still invisible in drone images. One potential explanation is that these lianas were either deciduous or dying at the time of the 2020 drone acquisition. However, for all trees of this category, we did not find any visible leaves on the older drone data, up to two years before (2018 and 2019; **Figure 8**). Even if these lianas are not currently in competition with trees for light, they still may compete with trees for below-ground resources and induce significant mechanical stress on host trees (Ingwell et al., 2010), decreasing tree growth and survival rates (Schnitzer et al., 2005). This well illustrates that if most of the drone and ground measurements can be paired with confidence, exhaustive links are unlikely to be made due to the complexity of some liana infestation pathways and that both measurements can bring complementary information on the impact of liana on forest dynamics.

The Allometry Between Liana Leaf Coverage and Ground Measurements Is Mediated by Liana Wood Density

We found that the probability of tree crowns to be infested by lianas depends strongly on the size of lianas and tree height.

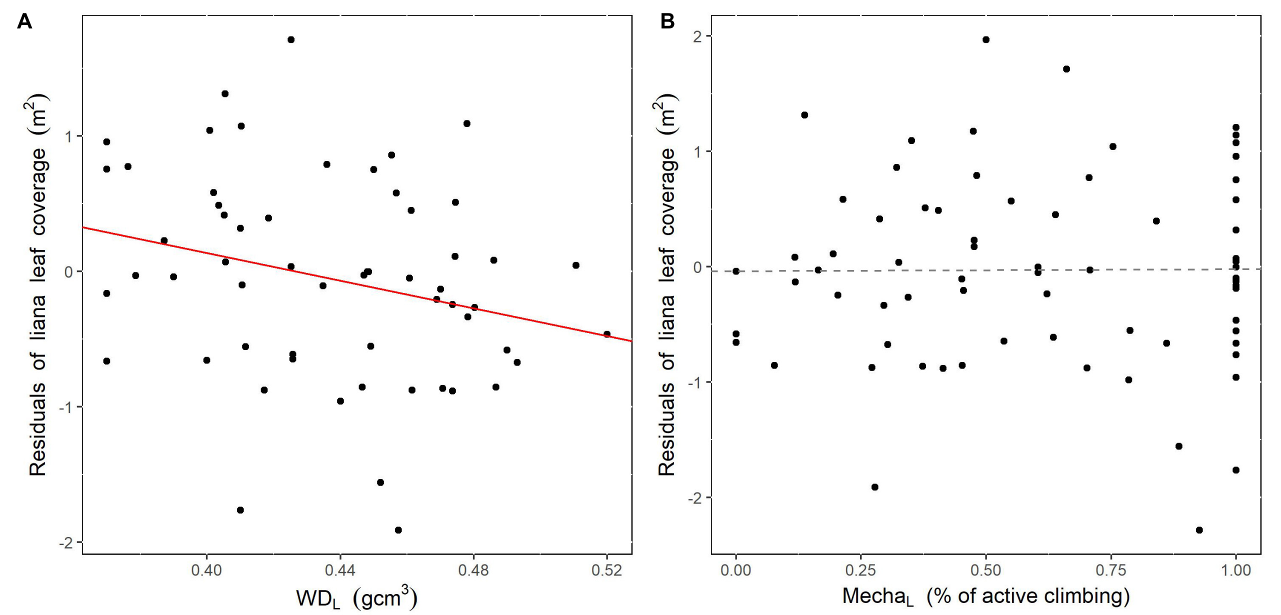

FIGURE 5 | Relationship between the basal area weighted liana wood density **(A)**, or the percentage of active climbing mechanism **(B)**, and the residuals of the selected linear model predicting liana leaf coverage from total liana basal area. The red (significant slope) or dotted gray (non-significant slope) lines illustrate the predicted linear model between the two variables.

Larger lianas are developmentally older and have thus, on average, had more time to reach the canopy. However, the length-diameter allometry is known to be weak in lianas (Smith-Martin et al., 2019) with individuals of only 2 cm in diameter already reaching the canopy (Kurzel et al., 2006). Consistently, the total liana basal area was identified as the best predictor of tree crown infestation status (infested or not by lianas). Tree height also had a significant, yet smaller, effect on the probability of infestation of a tree crown in our statistical model. This result is consistent with previous studies where liana loads tended to be higher on smaller trees or lower canopy forests (Wright et al., 2015; Tymen et al., 2016). However, these results may originate from two non-exclusive mechanisms: lianas can more easily colonize small trees and/or liana infestation can lead to smaller tree heights by limiting their growth. By contrast, Marvin et al. (2016) found no strong associations between liana leaf coverage and canopy height but, as discussed in section "Lianas Display (Not Enough) Specific Spectral Signatures," their remote sensing approach only enabled them to account for severe and high liana infestation levels, for which they had the lowest prediction error. Our findings also showed that if several ground-derived estimates can be successfully linked to liana leaf coverage, liana basal area was the best predictor, explaining 43% of the variance in the log-transformed space. This result is consistent with other studies that focused on the relationship between liana basal area and liana loads estimated from the ground (Ingwell et al., 2010; van der Heijden et al., 2010).

TABLE 3 | Confusion matrix showing the number of trees classified into the five COI classes from ground and drone-based measures.

		Ground data COI				
		0	**1**	**2**	**3**	**4**
Drone data COI	**0**	**166**	11	0	1	0
	1	8	**10**	11	7	1
	2	1	0	**9**	14	5
	3	0	0	2	**11**	11
	4	0	0	1	3	**3**

Agreement between the two approaches are illustrated in bold.

Our findings revealed that the large variability of liana leaf coverage for a given liana basal area can be partly explained by the functional composition of lianas. We indeed found a significant negative relationship between the drone-determined liana leaf coverage and mean wood density indicating that, for a given diameter, light-wooded lianas tend to invest in wider liana leaf coverages than hard-wooded lianas. As introduced earlier, variations of wood density are well-known to express different growth strategies in trees (Van Gelder et al., 2006; Chave et al., 2009; Baraloto et al., 2010; Poorter et al., 2010; Werden et al., 2018; Buckton et al., 2019) but the implication of wood density variation on liana ecology has been much less studied. Our results show that wood density significantly vary among taxa and that this variation entails ecological trade-offs among lianas, with greater biomass allocation to leaves for lianas with softer wood, as previously found for trees (Mensah et al., 2016). This pattern suggests that light-wooded lianas allocate more resources into leaves, and thus to light acquisition, at the expense of wood material, which may entail a greater mortality, as observed for trees (Chave et al., 2009). By contrast, no significant effect of liana climbing mechanism

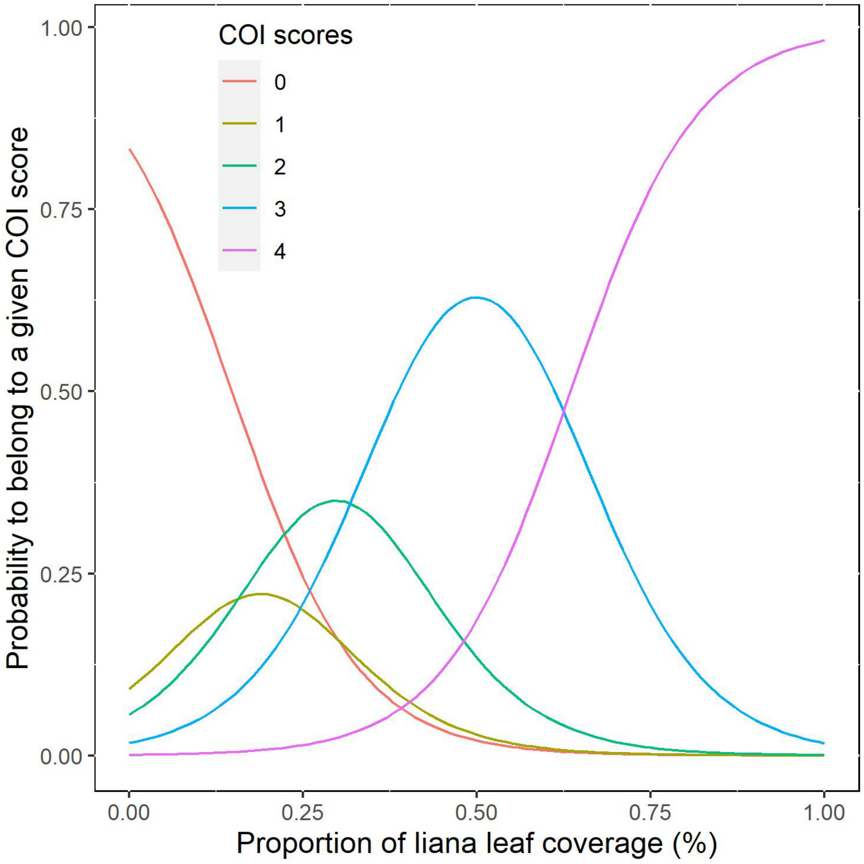

FIGURE 6 | Probabilities that a tree belong to a given COI score determined from the ground according to the level of infestation measured with drone data.

was found on liana leaf coverage. Some studies have shown that climbing mechanisms have an effect on liana recruitment and distribution across different forest structures (Dewalt et al., 2000; Bongers et al., 2020). Indeed, it is expected that climbing mechanism has a primary role in the early life of lianas and may thus constitute a central trait to understand the spatial (horizontal) liana distribution (Dias et al., 2021). For instance, Dewalt et al. (2000) showed that lianas with tendrils were more abundant in low canopy forests. The absence of an effect of climbing mechanisms on liana leaf coverage may be due to the fact that the early-life influence of climbing mechanisms on liana ecology may vanish when lianas reach the canopy. In this study, we divided our dataset between active and passive climbing mechanisms following Sperotto et al. (2020). Further investigations using different classifications, such as the one used by Dewalt et al. (2000), may provide different insights on the role of liana climbing mechanisms in liana structure and dynamics.

The Crown Occupancy Index Should Be Used Carefully

The COI is widely used to estimate liana leaf coverage over tree crowns and is now routinely used in international protocols such as in the RAINFOR network (Lopez-Gonzalez et al., 2011). We found a significant concordance between the ground-determined COI scores and the drone-determined liana leaf coverage. This supports that the COI is a quite reliable estimate of liana infestation over tree crowns, and is an alternative worth considering against time-consuming dendrometric liana measurements (van der Heijden et al., 2010), at least when substantial time is dedicated to this measurement, as done in the present study. However, we found that two thirds of the infested trees were attributed to a (generally neighboring) different infestation level from that determined by drone. This mismatch between categories raises questions about the reliability of the use of the COI to monitor liana infestation over time (Ingwell et al., 2010; Wright et al., 2015). One clear difference between the ground-determined COI and the extent of the drone-determined liana leaf coverage over tree crowns was the overestimation of infestation levels from the ground. This result is expected not to be specific to our study case because, from the ground, tree crowns are rarely entirely visible, and thus the proportion of the tree crown covered by liana leaves could easily be over-estimated (but see Waite et al. (2019)). Moreover, the results of our probit model supports the idea that dividing the COI in five infestation levels is too ambitious given the large variability of the ground estimates for a given drone-determined relative liana leaf

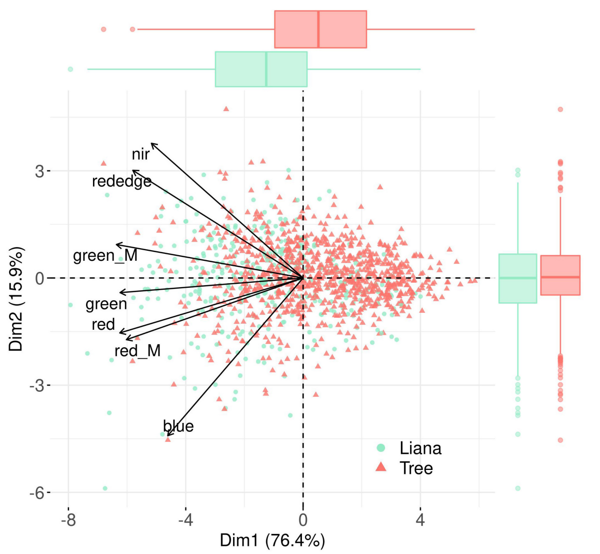

FIGURE 7 | Plan 1–2 of a Principal Coordinate Analysis performed on RGB (red, green, blue) and multispectral (red_M, green_M, rededge, nir) bands. Tree and liana objects are represented in green and red, respectively, boxplots illustrate the differences between the scores of liana patches and tree crowns along the two first PCA axes.

coverage (**Figure 6**). Our model indeed suggests that separating, or aggregating, infestation levels in three categories, as done by Rutishauser et al. (2011), is a more conservative approach. To summarize, if the COI might be a reliable estimate of the spatial distribution of liana load on trees, it should be interpreted carefully when used to detect changes of liana infestation over time. For the latter objective, multi-temporal drone acquisition appears as a more reliable and accurate approach.

Lianas Display (Not Enough) Specific Spectral Signatures

The emergence of new remote sensing approaches and data, such as the use of high spatial and spectral resolution products, appeared as a promising way to monitor canopy liana infestation in space and time over large scales (Marvin et al., 2016; Chandler et al., 2021). A prerequisite to map liana distribution over tree crowns is that lianas should display a detectable signature over tree crowns (Visser et al., 2021). In our study site, our results suggest that liana patches exhibit significantly higher light reflectance than trees on average in all studied spectral bands, as found and predicted by Visser et al. (2021), who accounted for several parameters that were unavailable in our study, such as chemical and architectural leaf traits. Thus, the origin of these higher DN and reflectance values should be further investigated as it may be due to several non-exclusive origins, such as a higher leaf reflectance, lower gap fraction or flatter leaf angles, as shown in the neotropics by Visser et al. (2021). Note also that, in our study, we were unable to explicitly or accurately radiometrically calibrate our data due to a lack of reference data, such as those obtained with white panels or from *ex situ* physical measurements. To minimize this aspect, we focused on data acquired during a single flight or within 1 h, limiting the spatial extent of our analyses. Future works should thus provide more efforts to improve this calibration step to both enable the investigation of larger areas and to minimize the potential problems associated with illumination artifacts. Contrary to Chandler et al. (2021) and Visser et al. (2021), we did not find that the near-infrared region provided additional information for the discrimination of lianas versus trees (non-significant differences along the second PCA axis; **Figure 7**), suggesting that visible bands already contained most of the information, even if our studied bands were limited to only two invisible bands. Interestingly, the variances of the scores along the two first PCA axes were significantly higher than those of trees, suggesting a higher spectral diversity and/or a higher variability in leaf optical properties (e.g., leaf area in vertical profiles and leaf angles; see Visser et al., 2021) among lianas than among trees. Indeed, liana species have different leaf structure, pigment concentration or water content, resulting in a wide range of spectral responses (Sánchez-Azofeifa and Castro-Esau, 2006; Visser et al., 2021). Importantly, we found that the PCA scores of lianas versus

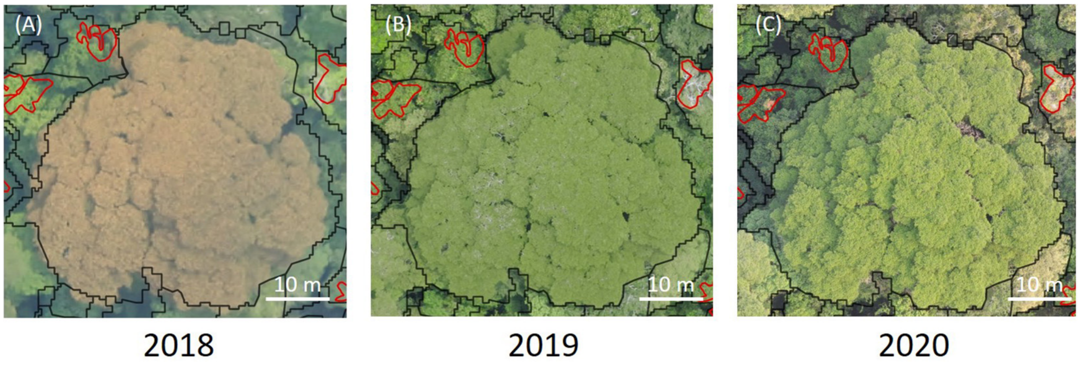

FIGURE 8 | Example of a time series of photographs made by drone of a tree hosting a large liana of 6.3 cm dbh but that lacks any visible liana leaves in its crown. Black lines illustrate the tree crown limit and the red lines some delineated liana leaves belonging to other liana stems, as observed from the field. **(A)** Image at a resolution of 10 cm GSD from 2018. **(B)** Image at a resolution of 5 cm GSD from 2019. **(C)** Image at a resolution of 3 cm GSD from 2020.

trees largely overlapped, as acknowledged by previous studies (Chandler et al., 2021; Visser et al., 2021), potentially leading to a high rate of confusion in predictive models. It partly explains why reliable remote sensing predictions were obtained only for highly infested trees (>50% of infestation; Marvin et al., 2016; Chandler et al., 2021; Visser et al., 2021). If the probability of identifying liana pixels among a set of pixels is rather low, the probability that the spectral signature of a given liana does not overlap with that of its host tree is much higher, as illustrated in **Figure 2**. Thus, developing approaches that classify pixels based on their contrast with surrounding pixels, and accounting for tree crown segmentation information, might be more promising than adopting a pixel-based approach. The rapid development of deep learning approaches on very high-resolution images, that specifically account for texture, thus constitutes a promising avenue (Li et al., 2018). Another efficient strategy has been recently adopted by Visser et al. (2021), who combined observations, trait measurements and radiative transfer modeling to understand the promise and limitations of monitoring liana infestation from remote sensing data. Finally, with the low cost associated with drone acquisitions, it is today possible to acquire drone data at a high frequency level, typically on a monthly basis. Assuming that the leaf phenology of a given liana and its host tree are decoupled in time, repeated drone acquisitions have the potential to better discriminate liana leaf patches over tree crows using approaches accounting for intra-annual co-variability in spectral signals.

CONCLUSION

Combining drone-based and ground-based measurements has the potential to approximate the complex infestation pathways of lianas and their consequences on forest dynamics. Ground-based data on liana distributions and structure have been acquired for decades in tropical forests, providing key insights on liana ecology and on their impact on forest dynamics. However, as shown here, ground-based data approximate the above canopy distribution of lianas with important uncertainties, limiting our ability to understand tree-liana interactions in what is often considered as the most important forest layer for ecosystem dynamics. The emergence of easy-to-acquire drone-data can make a difference on this aspect, providing a very-high resolution view of liana distribution above the canopy, thus improving our ability to integrate explicitly light competition between lianas and trees in ecological models. Drone-based determinations also open new opportunities to study liana infestation over large extents and over time, e.g., accounting for leaf phenology when acquisitions are done with a high frequency. However, drone-data also have serious drawbacks, especially when not paired with ground data. Given that current automatic approaches are not yet fully satisfactory due to a large overlap in the spectral signatures of lianas and trees, delineating manually liana patches in drone data requires significant time and a certain level of expertise. Furthermore, as seen in this paper, the functional composition of lianas can mediate the dynamics of infestation, something that would not have been seen using only drone data. Thus, we here advocate that combining ground- and drone-based data have the potential to take a major step forward in liana ecology, especially if the dynamics of lianas through time and space are studied in relation to their diverse ecological strategies.

DATA AVAILABILITY STATEMENT

The raw data supporting the conclusions of this article will be made available by the authors, without undue reservation.

AUTHOR CONTRIBUTIONS

BK and MR-M: conceptualization and writing (original draft). BK, SP, YH, and MR-M: ground data collection. NB and EF: drone data collection and pre-processing. BK, MA-K, VR, and MR-M: formal analysis. BK and DG: wood trait measurements. All authors: writing (review and editing).

FUNDING

This project has received funding from the European Union's Horizon 2020 Research and Innovation Programme under grant agreement no. 824074 in form of a prize awarded to BK. It also benefited from financial support from the French National Research Institute for Sustainable Development. The studied experimental site has been settled within the DynAfFor project (French Fund for the Global Environment; grant nos. CZZ1636.01D and CZZ1636.02D), the International Foundation for Science (grant no. D/5822-1), F.R.S-FNRS (grant no. 2017/v3/5/332 – IB/JN – 9500), Nature+ (asbl, Belgium) and the Republic of Congo (OGES-Congo). MR-M was supported by the DESSFOR ANR project (grant no. ANR-20-CE32-0010).

ACKNOWLEDGMENTS

We thank the CIB-Olam logging company that host and greatly facilitates the work conducted in this site. Last but not least, we are thankful to Isaac Zombo, Marien Fongo, Patchely Mbondo, Ati Ngouabi, Fred Ngouabi and Cyril Dzebou for their invaluable help during the field missions.

SUPPLEMENTARY MATERIAL

The Supplementary Material for this article can be found online at: https://www.frontiersin.org/articles/10.3389/ffgc.2022.803194/full#supplementary-material

SUPPLEMENTARY FIGURE S1 | Distribution of the mean DN and reflectance values per tree crown or liana patch for each RGB (red, gree, blue) and multispectral (red_M, green_M, rededge, nir) bands. Liana patches and tree crowns are represented in red and green boxplots respectively.

REFERENCES

Asner, G. P., and Martin, R. E. (2012). Contrasting leaf chemical traits in tropical lianas and trees: implications for future forest composition. *Ecol. Lett.* 15, 1001–1007. doi: 10.1111/j.1461-0248.2012.01821.x

Aubry-Kientz, M., Dutrieux, R., Ferraz, A., Saatchi, S., Hamraz, H., Williams, J., et al. (2019). A comparative assessment of the performance of individual tree crowns delineation algorithms from ALS Data in tropical forests. *Remote Sens.* 11:1086. doi: 10.3390/rs11091086

Avalos, G., Mulkey, S. S., and Kitajima, K. (1999). Leaf optical properties of trees and lianas in the outer canopy of a tropical Dry Forest1. *Biotropica* 31, 517–520. doi: 10.1111/j.1744-7429.1999.tb00395.x

Baraloto, C., Timothy Paine, C. E., Poorter, L., Beauchene, J., Bonal, D., Domenach, A.-M., et al. (2010). Decoupled leaf and stem economics in rain forest trees: decoupled leaf and stem economics spectra. *Ecol. Lett.* 13, 1338–1347. doi: 10.1111/j.1461-0248.2010.01517.x

Birouste, M., Zamora-Ledezma, E., Bossard, C., Pérez-Ramos, I. M., and Roumet, C. (2014). Measurement of fine root tissue density: a comparison of three methods reveals the potential of root dry matter content. *Plant Soil* 374, 299–313.

Bongers, F., Ewango, C. E. N., Sande, M. T., and Poorter, L. (2020). Liana species decline in Congo basin contrasts with global patterns. *Ecology* 101:e03004. doi: 10.1002/ecy.3004

Buckton, G., Cheesman, A. W., Munksgaard, N. C., Wurster, C. M., Liddell, M. J., and Cernusak, L. A. (2019). Functional traits of lianas in an Australian lowland rainforest align with post-disturbance rather than dry season advantage. *Austral Ecol.* 44, 983–994. doi: 10.1111/aec.12764

Castro-Esau, K. (2004). Discrimination of lianas and trees with leaf-level hyperspectral data. *Remote Sens. Environ.* 90, 353–372. doi: 10.1016/j.rse.2004.01.013

Chandler, C. J., Van Der Heijden, G. M., Boyd, D. S., Cutler, M. E., Costa, H., Nilus, R., et al. (2021). Remote sensing liana infestation in an aseasonal tropical forest: addressing mismatch in spatial units of analyses. *Remote Sens. Ecol. Conserv.* 7, 397–410.

Chave, J., Coomes, D., Jansen, S., Lewis, S. L., Swenson, N. G., and Zanne, A. E. (2009). Towards a worldwide wood economics spectrum. *Ecol. Lett.* 12, 351–366. doi: 10.1111/j.1461-0248.2009.01285.x

Clark, D. B., and Clark, D. A. (1990). Distribution and effects on tree growth of Lianas and Woody Hemiepiphytes in a Costa Rican Tropical Wet Forest. *J. Trop. Ecol.* 6, 321–331. doi: 10.1017/s0266467400004570

Collins, C. G., Wright, S. J., and Wurzburger, N. (2016). Root and leaf traits reflect distinct resource acquisition strategies in tropical lianas and trees. *Oecologia* 180, 1037–1047. doi: 10.1007/s00442-015-3410-7

Cox, C. J., Edwards, W., Campbell, M. J., Laurance, W. F., and Laurance, S. G. W. (2019). Liana cover in the canopies of rainforest trees is not predicted by local ground-based measures. *Austral Ecol.* 44, 759–767. doi: 10.1111/aec.12746

Dalling, J. W., Schnitzer, S. A., Baldeck, C., Harms, K. E., John, R., Mangan, S. A., et al. (2012). Resource-based habitat associations in a neotropical liana community: habitat associations of lianas. *J. Ecol.* 100, 1174–1182. doi: 10.1111/j.1365-2745.2012.01989.x

Darwin, C. (1875). *The Movements and Habits of Climbing Plants*. London: John Murray.

De Deurwaerder, H., Hervé-Fernández, P., Stahl, C., Burban, B., Petronelli, P., Hoffman, B., et al. (2018). Liana and tree below-ground water competition—Evidence for water resource partitioning during the dry season. *Tree Physiol.* 38, 1071–1083. doi: 10.1093/treephys/tpy002

Dewalt, S. J., Schnitzer, S. A., and Denslow, J. S. (2000). Density and diversity of lianas along a chronosequence in a central Panamanian lowland forest. *J. Trop. Ecol.* 16, 1–19.

Dias, A. S., Oliveira, R., Martins, F., Bongers, F., Anten, N., and Sterck, F. (2021). *Climbing Mechanisms as a Central Trait to Understand the Ecology of Lianas—A Global Synthesis.* Available online at: https://d197for5662m48.cloudfront.net/documents/publicationstatus/62374/preprint_pdf/6068759b4d003f91e6a0bf0cfb4c9f6f.pdf (accessed September 05, 2021).

Féret, J.-B., and Asner, G. P. (2012). Tree species discrimination in tropical forests using airborne imaging spectroscopy. *IEEE Trans. Geosci. Remote Sens.* 51, 73–84. doi: 10.1109/tgrs.2012.2199323

Ferraz, A., Bretar, F., Jacquemoud, S., Gonçalves, G., Pereira, L., Tomé, M., et al. (2012). 3-D mapping of a multi-layered Mediterranean forest using ALS data. *Remote Sens. Environ.* 121, 210–223. doi: 10.1016/j.rse.2012.01.020

Fox, J., Muenchen, R., and Putler, D. (2020). *RcmdrMisc: R Commander Miscellaneous Functions (2.7-0)[Computer software]*. Available online at: https://cran.r-project.org/web/packages/RcmdrMisc/RcmdrMisc.pdf (accessed September 05, 2021).

Freycon, V. (2014). *Caractérisation des sols de Loundoungou et de Mokabi (Congo)*. Montpellier: CIRAD.

Gentry, A. H., Putz, F. E., and Mooney, H. A. (1991). *The Biology of Vines*. Cambridge: Cambridge University Press.

Gerwing, J. J., Schnitzer, S. A., Burnham, R. J., Bongers, F., Chave, J., DeWalt, S. J., et al. (2006). A standard protocol for liana censuses ^{1}: short communications. *Biotropica* 38, 256–261. doi: 10.1111/j.1744-7429.2006.00134.x

Hegarty, E. E. (1991). "Vine-host interactions," in *The Biology of Vines*, eds F. E. Putz and H. A. Mooney (Cambridge: Cambridge University Press), 357–375.

Hegarty, E. E., and Caballé, G. (1991). "Distribution and abundance of vines in forest communities," in *The Biology of Vines*, eds F. E. Putz and H. A. Mooney (New York, NY: Cambridge University Press), 313-334.

Hijmans, R. J. (2021). *Geographic Data Analysis and Modeling [R package raster version 3.4-10]*. Available online at: http://cran.stat.unipd.it/web/packages/raster/ (accessed June 9, 2021).

Ingwell, L. L., Joseph Wright, S., Becklund, K. K., Hubbell, S. P., and Schnitzer, S. A. (2010). The impact of lianas on 10 years of tree growth and mortality on Barro Colorado Island, Panama: impact of lianas on 10 years of tree growth and mortality. *J. Ecol.* 98, 879–887. doi: 10.1111/j.1365-2745.2010.01676.x

Isenburg, M. (2014). *LAStools-Efficient LiDAR Processing Software.* Available online at: Lastools.Org (accessed October 10, 2017).

Isnard, S., and Silk, W. K. (2009). Moving with climbing plants from Charles Darwin's time into the 21st century. *Am. J. Bot.* 96, 1205–1221. doi: 10.3732/ajb.0900045

Kurzel, B. P., Schnitzer, S. A., and Carson, W. P. (2006). Predicting liana crown location from stem diameter in three panamanian lowland forests 1. *Biotropica* 38, 262–266. doi: 10.1111/j.1744-7429.2006.00135.x

Laurance, W. F., Andrade, A. S., Magrach, A., Camargo, J. L. C., Valsko, J. J., Campbell, M., et al. (2014). Long-term changes in liana abundance and forest dynamics in undisturbed Amazonian forests. *Ecology* 95, 1604–1611. doi: 10.1890/13-1571.1

Li, W., Campos-Vargas, C., Marzahn, P., and Sanchez-Azofeifa, A. (2018). On the estimation of tree mortality and liana infestation using a deep self-encoding network. *Int. J. Appl. Earth Observ. Geoinform.* 73, 1–13. doi: 10.1016/j.jag.2018.05.025

Lopez-Gonzalez, G., Lewis, S. L., Burkitt, M., and Phillips, O. L. (2011). *ForestPlots. Net: A Web Application and Research Tool to Manage and Analyse Tropical Forest Plot Data.* New York, NY: Wiley Online Library.

Marvin, D. C., Asner, G. P., and Schnitzer, S. A. (2016). Liana canopy cover mapped throughout a tropical forest with high-fidelity imaging spectroscopy. *Remote Sens. Environ.* 176, 98–106. doi: 10.1016/j.rse.2015.12.028

Medina-Vega, J. A., Bongers, F., Schnitzer, S. A., and Sterck, F. J. (2021). Lianas explore the forest canopy more effectively than trees under drier conditions. *Funct. Ecol.* 35, 318–329.

Melzer, B., Steinbrecher, T., Seidel, R., Kraft, O., Schwaiger, R., and Speck, T. (2010). The attachment strategy of English ivy: a complex mechanism acting on several hierarchical levels. *J. R. Soc. Interface* 7, 1383–1389. doi: 10.1098/rsif.2010.0140

Mensah, S., Kakaï, R. G., and Seifert, T. (2016). Patterns of biomass allocation between foliage and woody structure: the effects of tree size and specific functional traits. *Ann. For. Res.* 59, 49–60.

Meunier, F., Krishna Moorthy, S. M., De Deurwaerder, H. P. T., Kreus, R., Van den Bulcke, J., Lehnebach, R., et al. (2020). Within-site variability of liana wood anatomical traits: a case study in Laussat, French Guiana. *Forests* 11:523. doi: 10.3390/f11050523

Pebesma, E., Bivand, R., Racine, E., Sumner, M., Cook, I., and Keitt, T. (2018). *sf: Simple Features for R. R Package Version 0.6-1*. Available online at: https://cran.r-project.org/web/packages/sf/index.html (accessed September 05, 2021).

Phillips, O. L., Vásquez Martínez, R., Monteagudo Mendoza, A., Baker, T. R., and Núñez Vargas, P. (2005). Large lianas as hyperdynamic elements of the tropical forest canopy. *Ecology* 86, 1250–1258.

Piboule, A., Krebs, M., Esclatine, L., and Hervé, J. C. (2013). "Computree: a collaborative platform for use of terrestrial lidar in dendrometry," in *Proceedings of the International IUFRO Conference MeMoWood*, Nancy, 1–4.

Picard, N., and Gourlet-Fleury, S. (2008). *Manuel de Référence Pour L'installation de Dispositifs Permanents en Forêt de Production Dans le Bassin du Congo*. Yaoundé: COMIFAC.

Poorter, L., McDonald, I., Alarcón, A., Fichtler, E., Licona, J.-C., Peña-Claros, M., et al. (2010). The importance of wood traits and hydraulic conductance for the performance and life history strategies of 42 rainforest tree species. *New Phytol.* 185, 481–492. doi: 10.1111/j.1469-8137.2009.03092.x

Putz, F. E. (1984). The Natural History of Lianas on Barro Colorado Island, Panama. *Ecology* 65, 1713–1724. doi: 10.2307/1937767

Putz, F. E., and Holbrook, N. M. (1991). "Biomechanical studies of vines," in *The Biology of Vines*, eds F. E. Putz and H. A. Mooney (Cambridge: Cambridge University Press), 73–97.

R Core Team (2020). *R: A Language and Environment for Statistical Computing. R Package Version 4.0.3*. Available online at: https://www.R-project.org/ (accessed September 05, 2021).

Réjou-Méchain, M., Mortier, F., Bastin, J.-F., Cornu, G., Barbier, N., Bayol, N., et al. (2021). Unveiling African rainforest composition and vulnerability to global change. *Nature* 593, 90–94. doi: 10.1038/s41586-021-03483-6

Rocchini, D., Boyd, D. S., Féret, J.-B., Foody, G. M., He, K. S., Lausch, A., et al. (2016). Satellite remote sensing to monitor species diversity: Potential and pitfalls. *Remote Sens. Ecol. Conserv.* 2, 25–36. doi: 10.1002/rse2.9

Roussel, J.-R., Auty, D., Coops, N. C., Tompalski, P., Goodbody, T. R., Meador, A. S., et al. (2020). LidR: an R package for analysis of Airborne Laser Scanning (ALS) data. *Remote Sens. Environ.* 251:112061.

Rowe, N. P., and Speck, T. (2015). "Biomechanics of lianas," in *The Ecology of Lianas*, eds S. A. Schnitzer, F. Bongers, R. J. Burnham, and F. E. Putz (Chichester: John Wiley & Sons, Ltd), 323–341.

Rutishauser, E., Barthélémy, D., Blanc, L., and Eric-André, N. (2011). Crown fragmentation assessment in tropical trees: method, insights and perspectives. *For. Ecol. Manage.* 261, 400–407.

Sánchez-Azofeifa, G. A., and Castro-Esau, K. (2006). Canopy observations on the hyperspectral properties of a community of tropical dry forest lianas and their host trees. *Int. J. Remote Sens.* 27, 2101–2109. doi: 10.1080/01431160500444749

Schnitzer, S. A., and Carson, W. P. (2010). Lianas suppress tree regeneration and diversity in treefall gaps: lianas suppress tree diversity. *Ecol. Lett.* 13, 849–857. doi: 10.1111/j.1461-0248.2010.01480.x

Schnitzer, S. A., Kuzee, M. E., and Bongers, F. (2005). Disentangling above-and below-ground competition between lianas and trees in a tropical forest. *J. Ecol.* 93, 1115–1125.

Schnitzer, S. A., Rutishauser, S., and Aguilar, S. (2008). Supplemental protocol for liana censuses. *For. Ecol. Manage.* 255, 1044–1049. doi: 10.1016/j.foreco.2007.10.012

Signorell, A., Aho, K., Alfons, A., Anderegg, N., Aragon, T., and Arppe, A. (2021). *DescTools: Tools for descriptive statistics. R Package Version 0.99.42*, *28*, 17. Available online at: https://cran.r-project.org/web/packages/DescTools/index.html (accessed September 05, 2021).

Smith-Martin, C. M., Bastos, C. L., Lopez, O. R., Powers, J. S., and Schnitzer, S. A. (2019). Effects of dry-season irrigation on leaf physiology and biomass allocation in tropical lianas and trees. *Ecology* 100:e02827. doi: 10.1002/ecy.2827

Sperotto, P., Acevedo-Rodríguez, P., Vasconcelos, T. N., and Roque, N. (2020). Towards a standardization of terminology of the climbing habit in plants. *Bot. Rev.* 86, 180–210.

Tymen, B., Réjou-Méchain, M., Dalling, J. W., Fauset, S., Feldpausch, T. R., Norden, N., et al. (2016). Evidence for arrested succession in a liana-infested Amazonian forest. *J. Ecol.* 104, 149–159. doi: 10.1111/1365-2745.12504

van der Heijden, G. M., Feldpausch, T. R., de la Fuente Herrero, A., van der Velden, N. K., and Phillips, O. L. (2010). Calibrating the liana crown occupancy index in Amazonian forests. *For. Ecol. Manage.* 260, 549–555. doi: 10.1016/j.foreco.2010.05.011

van der Heijden, G. M., Schnitzer, S. A., Powers, J. S., and Phillips, O. L. (2013). Liana impacts on carbon cycling, storage and sequestration in tropical forests. *Biotropica* 45, 682–692.

van der Heijden, G. M. F., and Phillips, O. L. (2009). Liana infestation impacts tree growth in a lowland tropical moist forest. *Biogeosciences* 6, 2217–2226. doi: 10.5194/bg-6-2217-2009

van der Heijden, G. M. F., Powers, J. S., and Schnitzer, S. A. (2015). Lianas reduce carbon accumulation and storage in tropical forests. *Proc. Natl. Acad. Sci. U.S.A.* 112, 13267–13271. doi: 10.1073/pnas.1504869112

Van Gelder, H. A., Poorter, L., and Sterck, F. J. (2006). Wood mechanics, allometry, and life-history variation in a tropical rain forest tree community. *New Phytol.* 171, 367–378. doi: 10.1111/j.1469-8137.2006.01757.x

Venables, W. N., and Ripley, B. D. (2002). *Modern Applied Statistics with S*, 4th Edn. New York, NY: Springer.

Villanueva, R. A. M., Chen, Z. J., and Wickham, H. (2016). *ggplot2: Elegant Graphics for Data Analysis Using the Grammar of Graphics*. New York, NY: Springer-Verlag.

Visser, M. D., Detto, M., Meunier, F., Wu, J., Bongalov, B., Coomes, D., et al. (2021). Why can we detect lianas from space? *bioRxiv* [Preprint]. doi: 10.1101/2021.09.30.462145

Visser, M. D., Schnitzer, S. A., Muller-Landau, H. C., Jongejans, E., de Kroon, H., Comita, L. S., et al. (2018). Tree species vary widely in their tolerance for liana infestation: a case study of differential host response to generalist parasites. *J. Ecol.* 106, 781–794. doi: 10.1111/1365-2745.12815

Waite, C. E., Heijden, G. M. F., Field, R., and Boyd, D. S. (2019). A view from above: unmanned aerial vehicles (UAV s) provide a new tool for assessing liana infestation in tropical forest canopies. *J. Appl. Ecol.* 56, 902–912. doi: 10.1111/1365-2664.13318

Werden, L. K., Waring, B. G., Smith-Martin, C. M., and Powers, J. S. (2018). Tropical dry forest trees and lianas differ in leaf economic spectrum traits but have overlapping water-use strategies. *Tree Physiol.* 38, 517–530. doi: 10.1093/treephys/tpx135

Wickham, H. (2007). Reshaping data with the reshape package. *J. Stat. Softw.* 21, 1–20.

Wickham, H., Francois, R., Henry, L., and Müller, K. (2021). *dplyr: A Grammar of Data Manipulation. R Package Version 1.0.5, 3*. Available online at: https://cran.r-project.org/web/packages/dplyr/index.html (accessed September 05, 2021).

Wright, S. J., Sun, I.-F., Pickering, M., Fletcher, C. D., and Chen, Y.-Y. (2015). Long-term changes in liana loads and tree dynamics in a Malaysian forest. *Ecology* 96, 2748–2757. doi: 10.1890/14-1985.1

Conflict of Interest: The authors declare that the research was conducted in the absence of any commercial or financial relationships that could be construed as a potential conflict of interest.

frontiers | Frontiers in Forests and Global Change

ORIGINAL RESEARCH
published: 05 April 2022
doi: 10.3389/ffgc.2022.836247

Mind the Gap: Reach and Mechanical Diversity of Searcher Shoots in Climbing Plants

Tom Hattermann, Laureline Petit-Bagnard, Christine Heinz, Patrick Heuret† and Nick P. Rowe†*

UMR AMAP, Université de Montpellier, CIRAD, CNRS, INRAE, IRD, Montpellier, France

Climbing plants need to reach supports and position their leaves for light capture. Vines and lianas develop a large diversity of self-supporting shoots among diverse species and different kinds of attachment. A searcher's reach is a crucial trait for colonising supports in complex three-dimensional spaces. We explore the reach capacity and diversity of searcher shoots among representative temperate and tropical climbing plants. We investigate the overall range of variation between short- and long-reach searchers; the mechanical and anatomical organisations underlying reach capacities; how searcher architectures are linked to different climbing strategies such as stem twining, tendril climbing, root climbing, and branch-angle-hook climbing. We investigated reach and mechanical and anatomical organisations (stem rigidity and stiffness, stem and tissue geometry) in 29 climbing plant species from temperate and tropical habitats. Searchers show a wide range of maximal reach per species from 0.1 to 2.5 m. Flexural rigidity (*EI*) at the base of searchers increased with reach length; overall this increase was proportional although some longest-reaching shoots develop proportionally thinner searcher bases with higher stiffness [structural Young's modulus (E_{str})] than shorter-reach shoots. Bases of short-reach searchers rely more on primary tissues compared to long-reach shoots, which rely more on wood production. We identified different mechanical architectures for a given reach capacity across all species. These are linked to different kinds of attachment mechanisms, support foraging, and possibly leaf display. Plants attaching by twining of the main stem showed a wide range of reach capacity. They also developed lighter, more slender, less rigid, but generally relatively stiff (higher E_{str}) shoots compared with tendril climbers and branch-angle-hook climbers. Differences in the mechanical architecture of searcher shoots in climbing plants are informative for understanding how diverse climbing plant species explore and colonise different kinds of three-dimensional spaces. This is a key feature that distinguishes different habitat preferences. We discuss how such knowledge is not only important for understanding functional biology and ecology of climbing plants but is also of interest for developing new technologies in soft robotics that mimic climbing plants that can navigate through unstructured environments.

Keywords: biomechanics, climbing plants, liana, searcher shoot, self-supporting anatomy, support foraging, three-dimensional space

Edited by:
Félicien Meunier,
Ghent University, Belgium

Reviewed by:
Hao Ran Lai,
University of Canterbury, New Zealand
Friederike Gallenmüller,
University of Freiburg, Germany

***Correspondence:**
Tom Hattermann
tom.hattermann@gmail.com

†These authors share senior authorship

Specialty section:
This article was submitted to Tropical Forests, a section of the journal Frontiers in Forests and Global Change

Received: *15 December 2021*
Accepted: *21 February 2022*
Published: *05 April 2022*

Citation:
Hattermann T, Petit-Bagnard L, Heinz C, Heuret P and Rowe NP (2022) Mind the Gap: Reach and Mechanical Diversity of Searcher Shoots in Climbing Plants. Front. For. Glob. Change 5:836247. doi: 10.3389/ffgc.2022.836247

INTRODUCTION

Many land plants such as trees mechanically sustain their entire aerial system for their entire life history (Givnish, 1995; Niklas, 1999b; Moulia et al., 2006; Read and Stokes, 2006). Climbing plants are well known for their highly flexible older stems and their reliance on host trees for support. Vines and lianas are also becoming increasingly better understood in terms of the functional biology of young stages of growth as self-supporting shoots and searchers. Searcher shoots or "searchers" represent a key developmental phase of climbing plants. In many natural conditions, young shoots of climbing plants must navigate an obstacle course of gaps, hindrances, potential supports, movements caused by wind and rain as well as moving, oscillating leaves and stems. Such shoots have been referred to as: rising shoots (Darwin, 1875), searcher shoots (Putz, 1984), erect leaders shoots (Hegarty, 1991), searchers (Rowe and Speck, 1996), stiff young shoots (Rowe et al., 2006) and erect leafless shoots (Gianoli, 2015). The climbing habit potentially saves energy by reducing investment in mechanical support. It is often characterised by slender stems and high leaf productivity and turn-over compared with self-supporting plants of similar stem biomass (Wyka et al., 2013). Slender stems, rapid growth, searching mechanisms, and movements combined with reliable attachment are all key adaptations for the climbing habit. These features facilitate exploration, and occupation of the forest understory, the canopy, and disturbed environments such as treefall gaps and forest margins (Putz, 1984; Nabe-Nielsen and Hall, 2002; Ledo and Schnitzer, 2014; Mori et al., 2018). Self-supporting phases of growth may be prolonged under certain environmental conditions such as water, light, or support availability (Gartner, 1991; Cai et al., 2008). In some species, young stages of self-supporting growth can even develop as small treelets and reach sexual maturity (Ménard et al., 2013). Self-supporting phases of growth are most often expressed during younger phases of development (Caballé, 1998). But are also expressed during episodes of vegetative growth and renewal of shoots (Peñalosa, 1984; Rowe and Speck, 1996; Baret et al., 2003; Gianoli, 2003; Rowe et al., 2006). We explore the functional significance of self-supporting properties in climbing plants in terms of three interrelated properties that are determined by bending experiments in the field. The reader is referred to two excellent sources that discuss these parameters in detail (Ennos, 2011; Niklas and Spatz, 2012) and a further source that details a more hands-on application of the experimental protocols (Rowe et al., 2006).

(i) stem rigidity, this is a measure of the resistance of a stem to a bending force (*EI*) in units of (N.mm^2). It is a measure of the combined influence of the stem's combined tissue's stiffness (*E*) and the stem's second moment of area (*I*), which is a measure of the stem's size and geometry. Stem rigidity and the properties, which contribute to it are crucial traits for functional and ecological studies. A plant stem can change its flexural rigidity during development by either changing the stiffness of the material comprising the stem or increasing or decreasing the diameter of the stem or both.

(ii) Stem stiffness, this is a measure of the elastic mechanical resistance of a tissue or a combination of tissues that comprise a plant stem. It is measured by placing the material under compression, tension or bending and determining how much deformation is observed for a given force applied. It is normally referred to as Young's modulus (*E*) in units of MNm^{-2} (units of force per units of area). A "soft" tissue that is low in stiffness such as parenchyma typically has a "low" Young's modulus. "hard" tissue that is high in stiffness such as dense lignified wood typically has a high Young's modulus. In some studies, the term "structural" Young's modulus E_{str} is used to emphasise that we are referring to a combination of tissues comprising the materials under study. In this case, most searcher shoots comprise a mixture of different tissues with different Young's moduli.

(iii) Stem second moment of area, this is a measure of the cross-sectional size and shape of a stem when under bending. It refers to the distribution of material(s) (tissues) in the stem cross-section relative to the neutral axis. This exists at the centroid and along the length of a structure under bending and at 90° to the direction of the applied force. It is referred to as second moment of area (*I*) and is measured in units of mm or m to the power of four (m^4 or mm^4). We refer to second moment of area in terms of a whole stem as well as in terms of single tissue areas. A large tree trunk will have an exponentially larger second moment of area than a small sapling. In terms of the organisation of tissues in a cross section, a centrally positioned pith will have a low second moment of area. A peripherally placed layer of sclerenchyma, for example, will have a high second moment of area.

For a given stem the product of stem stiffness (*E*) and stem second moment of area (*I*) result in the flexural rigidity of a stem in bending (*EI*). Approaches that measure and explore these three terms are an excellent way of revealing how different plant stems develop and optimise rigidity and stiffness and have a great potential for comparative studies in ecology. In this study, we explore the patterns of stiffness, rigidity, and second moment of area for diverse searcher shoots and their abilities to cross gaps between supports. In climbing plants these mechanical and geometrical features are linked to other complex attributes. These include circumnutatory movements, nastic movements, and a wide range of attachment mechanisms. All of these must work together to cross gaps and find and attach to supports especially in unstructured, unpredictable three-dimensional spaces. Rigid self-supporting stems and their length and reach capacity are possibly linked to complex movements and anchorage mechanisms. This combination of "static properties" and "movements" — what we might call "searcher behaviour" is much less well known but is of considerable interest.

Searching and Foraging

Different species of searcher shoots can locate new hosts in different ways. In many species, there is a basal rigid component of the searcher shoot constructed of stiff tissues that ensures mechanical stability. More apical parts of the searcher shoot are often capable of movement. These can be either "active" such as circumnutations or nastic movements or more "passive" mechanisms such as off-vertical leaning and swaying toward potential supports. Some searcher shoots undergo extreme elastic buckling and collapsing under their own weight onto host branches below. Many species undergo what can be referred to as scrambling and roving forward by apical growth. Such forms can grow through complex three-dimensional environments without "targeting" specific host structures. Most climbers develop searchers that deploy attachment organs. These can comprise highly modified leaves, stems, petioles, branches and roots as well as smaller scale textured surfaces that stick or hook onto host surfaces. Searcher shoots and their attachment organs are often highly adapted for attaching to different supports in many different "active" and "passive" ways. These include twining on supports and tendril attachment to twigs and leaves. Hooks, branches, and petiole angle attachments can anchor more passively to host structures but need to remain in tension to stay reliably attached. Searchers can also attach and anchor themselves to supports via growth processes and thigmomorphogenetic responses induced by proximity or continuous or repeated contacts. Uninduced mechanisms exist such as preformed coiling and hook differentiation and deployment prior to any direct contact with a support (Gerbode et al., 2012; Guerra et al., 2019; Sousa-Baena et al., 2021). Support foraging behaviours can involve different mechanisms acting in concert such as stem elongation, self-supporting mechanics, searching by active and/or passive movement, attachment organ deployment, and anchorage (Baillaud, 1962; Millet et al., 1988; Stolarz, 2009; Simonetti et al., 2021). Searching and attaching mechanisms have been popularly studied in terms of the attachment organ itself. Rather less is known about how the searchers deploy combined searching and attachment behaviours. Furthermore, little is known about how deployment mechanisms vary according to the distance between supports, which is a crucial factor in colonising different habitats.

Reach Capacity

Searcher shoots are well known for developing relatively high stiffness compared to the older more compliant stems (Rowe and Speck, 1996; Isnard et al., 2003; Rowe et al., 2006). This allows them to span distances up to several metres in length (Putz, 1984). The reach capacity of searcher shoots has been shown to vary considerably between species. This is likely linked to the developmental constraints that limit rigidity for sustaining mechanical stability (Coudurier, 1992; Lahaye et al., 2005). Some authors have suggested that tendril-climbers span shorter distances than climbers with other modes of attachment such as twiners or scramblers. This difference might be related to tendril climbers being restricted mostly to only slender supports (Darwin, 1875; Putz, 1984; Gianoli, 2015). According to optimal foraging theory (e.g., Charnov, 1976; Pyke, 1984; Bartumeus and Catalan, 2009; Gianoli, 2015), selection should favour economising biomass investment for self-supporting searchers. This would potentially enhance support location and light acquisition at the level of the whole plant (Gianoli, 2015). Reaching a longer distance potentially comes at the expense of proportionally higher constructional costs via stem thickening and stiffening. This will likely influence different biomass and tissue development patterns of the stem. Furthermore, different climbing behaviours are likely adapted to differences in three-dimensional distances and support geometries. There is therefore a large potential for understanding climbing performances between different species and different climbing habits by considering how mechanical properties, anatomical organisation, and supported biomass are related to the gap spanning capacity of searcher stems.

Functional Implications at the Shoot Level

Attachment to a support is believed to influence a change in shoot development from being stiff (high Young's modulus) to being flexible (capable of deforming-bending or twisting-a lot without breaking). Flexible stems that are resistant to breaking are typical of many old stages of growth (Ewers et al., 1991; Putz and Holbrook, 1991). Transitions from stiff to flexible properties can involve changes in tissue organisation at several hierarchical levels. These can include the proportions and radial organisations of stiff versus compliant tissues, to changes in cell wall thickness and lumen diameter (Rowe and Speck, 1996; Rowe et al., 2004; Isnard et al., 2005) to changes in microfibril angle (Ménard et al., 2009) and cell wall chemistry (Chabbert et al., 1997; Hoffmann et al., 2003). The stiff to flexible transition also involves profound changes in biomass allocation, hydraulic conductivity, light capture as well as stem toughness (the resistance to fracture). One highly visible trait among shoots of many vines and lianas is delayed leaf expansion. This has been considered to be important for stem twiners and tendril climbers, since the presence of large foliage leaves are believed to physically hinder foraging for supports (Raciborski, 1900; French, 1977). Some architectural shifts known as "axialization" (growth and development of stems) and "foliarization" (growth and development of leaves) are well known for trees (Lauri, 1988; Lauri and Kelner, 2001) and also play important strategic roles in the growth of climbing plants (Peñalosa, 1982, 1984; Baret et al., 2003). Despite knowledge of many morphological strategies during the development of searcher shoots, the anatomical and mechanical features underlying stem development during leaf display, stem movements, and diverse support-foraging strategies remain little known.

Aims

We investigate how reach capacity in climbing plants varies between species and how it is linked to different attachment mechanisms. Second, we explore how reach capacities of different species are related to stem properties of the searcher base – the part that mechanically supports the entire searcher shoot. This includes searcher rigidity (EI), searcher stiffness structural Young's modulus (E_{str}), cross-sectional area (A), and second moment of area and (I). We measure all these parameters for the basal whole stem cross section, and furthermore, we explored values of (A) and (I) for the different tissues of the load-bearing searcher base. For example, some searcher stem bases might employ a wide central pith as a geometrical spacer to optimise the contribution of stiff tissues at the outside. Other species rely on a central wood cylinder and others on an outer band of stiff primary fibre tissues. Some species might integrate all of these patterns for optimising stem properties and reach. Third, we discuss how divergent mechanical and anatomical organisations vary between short- and long-reach searcher shoots and how such differences might vary with overall fresh mass and dry mass of searcher shoots. In other words, how might climbing plants optimise the trade-off between maintaining long reaches but minimising mass and construction costs. Fourth, we analyse how divergent organisations vary for a given reach capacity and how these are related to attachment modes and leaf development.

In this paper, we use a working definition for a searcher shoot as an axial self-supporting part of a climbing plant having a growing apex that may show one or more characteristics linked to support foraging and attachment. These latter can include elongated internodes, attachment organs, and commonly, a segment of the stem (normally distal to median) that undergoes circumnutatory or nastic movement. This definition is not that straightforward across diverse climbers. However, it is necessary to identify in the field "true searcher shoots" that functionally locate and attach to supports. This is not always easy since some species of climber do not develop noticeably specialised climbing organs but achieve true climbing via modified branch angles (Gallenmüller et al., 2004, 2009; Ménard et al., 2009). Furthermore, vines and lianas can develop different kinds of self-supporting stems other than searcher shoots. For example, shoots of the same individual or species that are adapted for light capture and which differ markedly from self-supporting, support foraging (truly searching) searchers. The latter can differ in the presence of fully expanded leaves, shorter internodes, and absence of climbing organs and specialised circumnutatory movements.

MATERIALS AND METHODS

In this study our approach was to include species from both tropical and temperate regions, thus including diverse searcher shoots from different climatic zones. We collected the longest searcher shoots for each species that still maintained an erect or self-supporting posture from a vertical to horizontal orientation but not downward pointing orientation and that were still unattached to a support. Our aim was to analyse how this maximal reach of a given species was related to the mechanical properties and anatomy of the crucial load bearing segment at the base of the searcher long- and short-reach searchers.

Biological Material and Study Sites

We sampled 190 searcher shoots in 29 species from 21 families to represent a wide range of climbing habits (**Table 1**). For most species, we were able to sample searcher shoots derived from mature individuals in wooded, marginal to open habitats. A few species were only accessible in early stages of growth as young individuals (genets) because they were difficult to find free of any support as searcher shoots of older stages (i.e., *Machaerium quinquinatum* and *Bauhinia guianensis*). One species of a climbing Cactaceae was sampled from a common garden collection at the AMAP lab, Montpellier. Tropical species from natural habitats were sampled during a 2-month field season at the beginning of the rainy season from November 2020 to January 2021. Shoots were sampled in French Guiana from their natural habitats in two sites in the vicinity of Sinnamary. One site included the Paracou experimental station (5°16′26″ N, 52°55′26″ W) and the second included stations in forest margins accessible along the road known as the "Piste de St-Elie" (5°16′59″ N, 53°03′15″ W). Temperate species were sampled during the summer season from July to August 2020. Shoots were sampled in urban and natural habitats in the vicinity of Montpellier, South of France (43°39′7″ N, 3°51′41″ E).

Morphological Descriptions

Numerous approaches exist for categorising climbing plants based on (i) the degree of wood development of the stem (Gentry, 1991); (ii) the degree of strength of attachment with supports (Caballé, 1986); (iii) the kind of attachment mechanism (e.g., Darwin, 1875; Schenck, 1892; Menninger, 1970; Putz, 1984) and (iv) the morphological origin of the organ involved in the attachment process (Sousa-Baena et al., 2018). We sampled searchers of different species grouping them by their main kind of deployment and attachment. We identified four broad working categories for the study: (i) Stem twiners: searchers that attach by twining of the main searcher stem. (ii) Tendril climbers: searchers that attach by modified, determinate growth of lateral organs (leaves, stems, petioles) of the searcher stem that are highly modified into sensitive tendrillar organs. (iii) Branch-hook-angle climbers: searchers that attach by branch angles, petiole angles, preformed open hooks, epidermal spines, and prehensile branches. (iv) Root climbers: searchers that attach by adventitious roots deploying active adhesive and attachment development.

Plant Functional Traits

Twelve main traits were selected to investigate functional attributes of different searcher shoots (**Table 2**).

Morphological Traits

In order to estimate the reach of a searcher shoot, we measured *in situ* the distance in a straight line from the base to the apex of the searcher shoot (here called the "reach"). Searcher shoots were cut at the base and temporary stored in a plastic bag before measurements. In our field laboratory, all the leaves were removed by cutting the petiole/rachis as close as possible to the insertion point with the lamina(s). Laminae were digitised using a 300 dpi-imaging scanner (Epson Perfection V800; Epson America Inc., Long Beach, CA, United States and Canon CanoScan LiDE 400; Canon Japan Inc., Tokyo, Japan), and areas were extracted using the leafarea R package (Katabuchi, 2015). Fresh masses of the searcher stem and all appendages (branches, petioles, and laminae) were measured within 3 h after the shoot was sampled. Dry masses of each were measured using a precision balance (to 0.1 mg) after

TABLE 1 | Species information.

Taxa	Family	Biomes	N	Attachment modes	Attachment organs	Group
Clematis vitalba L.	Ranunculaceae	temperate	15	Twining petioles	Rachis	Tendril climber
Elaeagnus umbellate Thunb.	Elaeagnaceae	temperate	5	Scrambling + Hooks or grapnels	Axilary stem	Branch-hook-angle climber
Fallopia dumetorum (L.) Holub	Polygonaceae	temperate	12	Twining	Main stem apex	Stem twiner
Hedera helix L.	Araliaceae	temperate	10	Adhesive roots	Adventicious roots	Root-climber
Lonicera japonica Thunb.	Caprifoliaceae	temperate	5	Twining	Main stem apex	Stem twiner
Pereskia aculeata Mill.	Cactaceae	tropical	1	Twining + Hooks or grapnels	Main stem apex	Branch-hook-angle climber
Rubus ulmifolius Schott	Rosaceae	temperate	11	Scrambling + Spines	Epicuticular structures	Branch-hook-angle climber
Smilax aspera L.	Smilacaceae	temperate	13	Twining + Tendrils + Spines	Main stem apex + petiole + epicuticular structures	Tendril climber
Trachelospermum jasminoides (Lindl.) Lem.	Apocynaceae	temperate	6	Twining	Main stem apex	Stem twiner
Vitis vinifera L.	Vitaceae	temperate	12	Tendrils	Axilary stem	Tendril climber
Aegiphila laevis (Aubl.) J.F.Gmel	Lamiaceae	tropical	3	Twining	Main stem apex	Stem twiner
Bauhinia guianensis Aubl.	Fabaceae	tropical	1	Hooks or grapnels	Petiole	Branch-hook-angle climber
Byttneria cordifolia Sagot	Malvaceae	tropical	8	Twining + Hooks or grapnels	Main stem apex + petiole	Stem twiner
Cissus haematantha Miq.	Vitaceae	tropical	5	Tendrils	Axilary stem	Tendril climber
Condylocarpon guianense Desf.	Apocynaceae	tropical	5	Twining	Main stem apex	Stem twiner
Croton pullei Lanj.	Euphorbiaceae	tropical	2	Hooks or angled-petiole	Petiole	Branch-hook-angle climber
Davilla nitida (Vahl) Kubitzki	Dilleniaceae	tropical	10	Twining	Main stem apex	Stem twiner
Dioscorea sagittata Poir.	Dioscoreaceae	tropical	10	Twining + Hooks or grapnels	Main stem apex + petiole + epicuticular structures	Stem twiner
Gouania blanchetiana Miq.	Rahmnaceae	tropical	1	Angled-branches + Tendrils	Axilary stem (2nd and 3rd order)	Tendril climber
Machaerium floribundum Benth.	Fabaceae	tropical	2	Prehensile branches + Spines	Axilary stem + stipules	Branch-hook-angle climber
Machaerium quinata (Aubl.) Sandwith	Fabaceae	tropical	1	Prehensile branches + Spines	Axilary stem + stipules	Branch-hook-angle climber
Mesechites trifidus (Jacq.) Müll. Arg.	Apocynaceae	tropical	10	Twining	Main stem apex	Stem twiner
Odontadenia perrottetii (A. DC.) Woodson.	Apocynaceae	tropical	5	Twining	Main stem apex	Stem twiner
Paullinia caloptera Radlk.	Sapindaceae	tropical	1	Tendrils	Axilary stem	Tendril climber
Sabicea cinerea Aubl.	Rubiaceae	tropical	10	Twining	Main stem apex	Stem twiner
Serjania membranacea Splitg.	Sapindaceae	tropical	4	Tendrils	Axilary stem	Tendril climber
Stigmaphyllon sinuatum (DC.) A.Juss.	Malpighiaceae	tropical	10	Twining	Main stem apex	Stem twiner
Styzophyllum riparium (HBK) Sandw.	Bignoniaceae	tropical	10	Tendrils + Hooks or grapnels	Terminal leaflet	Tendril climber
Uncaria guianensis (Aubl.) J.F.Gmel.	Rubiaceae	tropical	3	Angled-branches + Hooks or grapnels	Axilary stems (2nd and 3rd order)	Branch-hook-angle climber

at least 72 h in the oven at 70° and constant mass. Stem diameters were measured using digital callipers with a stated precision of 0.01 mm.

Biomechanical Traits

Bending properties of the basal part of the searcher shoot were measured using four-point bending tests (Ennos, 2011). Flexural rigidity (*EI*) and Young's modulus (*E*) were calculated from regression lines resulting from plots of the applied bending forces plotted against the maximum deflections (Rowe et al., 2006). Up to five weights were applied in sequence at 30 s intervals and deflections were measured with a dissecting microscope equipped with a calibrated eyepiece graticule. Weight increments were selected according to the bending resistance of each sample. Weights were made up of stainless-steel nuts and machined brass weights ranging from 1 g to 200 g. The exact mass of weights was measured to 0.001 gram before field work using a precision balance in the lab. Span distances were defined as proportional to the mean elliptical diameter of the stem segment. The span support was 40 times greater than the diameter and ranged from 30 mm to 447 mm for the longest stems. The load span was set at between one-half and two-thirds of the span support and ranged from 11 mm to 255 mm. For the shortest stem segments, we used customised panniers made of wood and aluminium profiles,

TABLE 2 | Functional traits measured at the searcher shoots level.

Trait	Abbreviation	Unit	Formula	Related function
Reach	R	cm	/	Gap-spanning capacity
Basal diameter	D	mm	$D = \frac{D_{\text{vertical}} + D_{\text{horizontal}}}{2}$	Growth rate, mechanical reinforcement
Whole shoot freshmass	$\text{Shoot}_{\text{freshmass}}$	g	/	Supported mass
Lamina area	A_{lamina}	cm^2	/	Energy balance, hydraulic demand
Lamina freshmass	$\text{Lamina}_{\text{freshmass}}$	g	/	Weight of photosynthetic function
Lamina drymass	$\text{Lamina}_{\text{drymass}}$	g	/	Cost of construction of photosynthetic function
Shoot water content	SWC	%	$SWC = \frac{(Shoot_{\text{freshmass}} - Shoot_{\text{drymass}})}{Shoot_{\text{freshmass}}} * 100$	Capacitance; Growth rate; Searcher mobility capacity (pers. Cons.)
Flexural rigidity	EI	$N.mm^2$	$a = \frac{L-l}{2}$ $EI_{4pt} = (b) * \left(\frac{L^3}{48}\right) * \left(\frac{3*a}{L}\right) - 4 * \left(\frac{a}{L}\right)^3$ See Section "Biomechanical Traits" for the definition of the terms	Mechanical support
Structural young modulus	E_{str}	$MN.m^{-2}$	$E_{\text{str}} = \frac{EI}{I}$	Stiffness parameter of flexural rigidity
Second moment of area	I	mm^4	$I_{\text{rectangular}} = \frac{D^3_{\text{vertical}} * D_{\text{horizontal}}}{12}$ $I_{\text{elliptic}} = \frac{\pi}{4} * \left(\frac{D_{\text{vertical}}}{2}\right)^3 * \left(\frac{D_{\text{horizontal}}}{2}\right)$ With D for mean diameter in 3 positions for both orientations (vertical and horizontal).	Geometrical parameter of flexural rigidity
Cross sectional area of tissues	A_{tissues}	mm^2	/	Structural composition of the stem
Contribution of tissues to cross-section second moment of area	$I\%_{\text{tissues}}$	%	$I_{\text{tissue,i}} = \frac{\left(I_{\text{c-tissue}} + A_{\text{tissue}} * a^2\right)}{I_{\text{section}}}$ With $I_{\text{tissue,i}}$ corresponding to the proportion of the ith tissue in terms of second moment of area of the entire stem section. With $I_{\text{c-tissue}}$ corresponding to the second moment of area of the i_{th} tissue as measured with respect to the centre of gravity of the tissue itself. With A_{tissue} corresponding to the cross-sectional area of the i_{th} tissue. With a corresponding to the distance from the centre of gravity of the i_{th} tissue to the neutral axis in bending. The neutral axis passes through the centre of gravity of the stem cross section and is parallel to the direction of bending. With I_{section} corresponding to the second moment of area of the entire stem section.	Mechanical role of tissues

and for the longer stems, we used customised panniers made of stainless steel.

Flexural rigidity EI ($N.mm^2$) was calculated via the formula present in **Table 2**, where l is the load support (i.e., the distance between two internal supports), L is the support span (i.e., the distance between the two outside supports) and b is the slope of the force-deflection curve (N/mm). Stem diameters were measured at three positions along the searcher shoot (basal, medial, apical) in the vertical direction of the applied load and that orthogonal to it in order to calculate the second moment of area. We used the different formulas depending on whether the stem was ellipsoidal (e.g., *Condylocarpon guianense* and *Trachelospermum jasminoides*) or rectangular (i.e., *Cissus haematantha*). Some searcher stems had star-shaped or undulating cross-sectional shape (i.e., *Serjania membraceae*, *Rubus ulmifolius*, and *Clematis vitalba*). These were approximated as an ellipse. Since flexural rigidity (EI) is the product of stiffness (E) and second moment of area (I) we calculated the structural Young's modulus at the base of the searcher shoot (E_{str}) (MNm^{-2}) from measured values of EI and calculated values of I (Niklas, 1999b; Rowe et al., 2006).

Anatomical Traits

Anatomical samples were taken from the segment used for the bending test from near the base of the shoot. 190 cross sections ranging from 0.59 to 13.74 mm of diameter were embedded in paraffin before sectioning at a thickness of 8 to 10 μm with a semi-automated rotary microtome (Leica Biosystems Rm2245). Sections were stained with Safranin/Astra blue to distinguish unlignified cells (blue) and lignified cells (red). Images were taken with a digital microscope (Keyence VHX-700F) with a magnification of X100 to X300. Multiple images were taken at different depths of focus and position to obtain a panorama of stacked pictures of the cross-section. Thick-walled lignified cells observed in cross section might represent elongated fibre cells or foreshortened sclereid tissue (Niklas, 1999a; Clair et al., 2019). We therefore prepared longitudinal sections on one individual per species to distinguish fibres from sclereids (Lehnebach et al., 2020) and thus interpret their putative mechanical significance to stem stiffness.

To characterise anatomical organisations of different species, we distinguished up to 9 types of tissue per species from the following tissue categories: (i) medullary parenchyma, (ii) medullary fibres, (iii) xylem (including primary and secondary xylem), (iv) phloem (including primary and secondary phloem), (v) cortical parenchyma, (vi) cortical sclereids, (vii) cortical fibres, (viii) cortical collenchyma and (iv) periderm. We manually delineated tissues from digitised cross-sections with a graphics tablet and created layers with the GIMP software (version 2.10.12[1]). Masks of layers were used to calculate cross-sectional areas and second moments of the entire stem and each area of each tissue with a customised macro using ImageJ software (v.1.43u[2]).

The orientation of the cross-section is critical for calculating the second moment of area of the entire stem and tissue proportions. An oval cross-section positioned with its long axis in the vertical plane would have a higher second moment of area than if it would be placed in the horizontal plane. We therefore aligned each cross section and its masks with the long-axis of the stem arranged vertically. We then measured the second moment of area in this vertical position (I_x) and at 90° (I_y) to it for both the entire section and the individual tissues. We then calculated proportions of each tissue in terms of second moment of area based on the mean values calculated from the vertical and horizontal orientations.

Statistical Analysis

All statistical analyses and data graphics were performed with R software[3]. We applied a one-way ANOVA on a subset data frame with 170 searcher shoots accounting for 22 species represented by at least 3 replicates to test how reach capacity varies between species.

We used standardised major axis regression (SMA) via the SMATR package (Warton et al., 2012) to observe absolute and relative changes of mechanical properties, anatomical organisations, and functional traits with reach capacity. Since power functions were linked to most traits and reach capacity, we used log-log graphs to plot the data and log-transformed the data via the sma function. The assumptions of linearity and equal variance of all fitted values and assumption of normally distributed residuals were graphically checked for all variables. We interpreted correlation coefficients to estimate the strength linking functional features with reach distance. We also compared regression slopes (beta) to interpret whether there were proportional or disproportional changes with increasing reach distance. Proportionality was defined according to an expected slope defined by the power function linking both variable units. If the observed slope is statistically equivalent to the expected one, we assume that both variables are proportionally related. If the observed slopes differ from the expected one, we assume that both variables are disproportionally related (Warton et al., 2012).

For exploring the different patterns of tissue organisation across different searchers, we grouped tissues into four categories according to their developmental origin and mechanical properties. These included pith, xylem, stiff bark, and soft bark. From a mechanical perspective, delimiting the pith is important since it maximises second moment of area of lignified tissues for petioles and stems of self-supporting plants (Mahley et al., 2018; Olson et al., 2018; Pittermann and Olson, 2018; Levionnois et al., 2020, 2021). Medullary fibres were not considered separately as a mechanical tissue for the regression analyses. This was because of their scarcity among species and low contributions to second moment of area (central positioning close to the neutral axis in bending) of the whole cross section. We considered the “xylem” component as a single tissue combining xylem fibres, vessels, and rays without regard to their primary or secondary origins. For more peripheral tissues, for simplicity, we defined outer tissues as “bark” (following the definition of Esau, See Evert, 2006) which included all tissues outside the xylem cylinder in both young and older developmental stages. For this category we differentiated the main supportive bark tissues (cortical fibres and collenchyma; Leroux, 2012; Mahley et al., 2018; Lehnebach et al., 2020) from the compliant ones (phloem, cortical parenchyma and periderm) and none-supportive one (cortical sclereids).

RESULTS

Morphological Diversity

All sampled species could be grouped into one of four broad groups of attachment mode. These included stem twiners, tendril climbers, root climbers, and branch-hook angle climbers (**Figure 1** and **Table 1**). There was a large morphological diversity within these groups apart from the root climbers which included only English Ivy (*Hedera helix*) (**Figure 1**). All searchers included a main axis, but species varied in terms of branching, presence of leaves, and secondary axes. The main axis of some searchers developed branches with tendrillar structures (e.g., *Cissus haematantha* and *Serjania membranaceae*) or prehensile branches (e.g., *Machaerium quinata* and *floribundum*). Other species developed branches producing attachment via wide angled-branches (e.g., *Gouania blanchetiana*) or developed photosynthetic leafy branches (e.g., *Uncaria guianensis*).

Attachment Mechanisms

Stem twiners often exhibited a hook-shaped distal part of the searcher, which underwent circumnutatory movements (e.g., *Stigmaphyllon sinuatum*), particularly among tropical species (**Figures 1D,F,J,N**). Hook-shaped apices, were not present in all twining species (e.g., *Condylocarpon guianense* or *Aegiphila laevis*). Different species possessed tendrillar attachment structures that are derived from different morphological organs. These included modifications of second-order axillary axes (e.g., *Paullinia caloptera*), 3rd order axilary axes (e.g., *Gouania blanchetiana*), as well as terminal axes resulting from sympodial branching at the phytomer level (e.g., *Vitis vinifera*), leaf sheath (e.g., *Smilax aspera*), rachis (e.g., *Clematis vitalba*), or leaflet level (e.g., *Styzophyllum riparium*). Branch-hook angle attachment

---

[1] https://www.gimp.org

[2] http://imagej.nih.gov/ij/

[3] https://cran.r-project.org/

FIGURE 1 | (Continued)

FIGURE 1 | Morphological diversity of searcher shoots: **(A)** *Elaeagnus umbellata*; **(B)** *Cissus haematantha*; **(C)** *Condylocarpon guianense*; **(D)** *Fallopia dumetorum*; **(E)** *Croton pullei*; **(F)** *Davilla nitida*; **(G)** *Gouania blanchatiana*; **(H)** *Machaerium quinata*; **(I)** *Rubus ulmifolius*; **(J)** *Stigmaphyllon sinuatum*; **(K)** *Hedera helix*; **(L)** *Uncaria guianensis*; **(M)** *Sabicea cinerea*; **(N)** *Mesechites trifidus*; **(O)** *Smilax aspera*; **(P)** *Bauhinia guianensis*; **(Q)** *Aegiphila laevis*; **(R)** *Dioscorea sagittata*; **(S)** *Serjania membranacea*; **(T)** *Styzophyllum riparium*; **(U)** *Vitis vinifera.* Different searcher shoots vary significantly in terms of stem shape, degree of branching, kind of attachment organ and presence of leaves in addition to the length of the gap across which a species can reach. Many species show straight searcher stems **(A,G,P,Q)**, but others, especially twiners develop conspicuously curved apical portions that undergo circumnutatory movements **(C,D,F,J,N,M).** Some searchers produce woody branches capable of attachment as sensitive prehensile structures **(H)**, others develop sensitive, tendrillar attachment organs **(B,G,O,S,T,U)**, while still others develop recurved spines, hooks and prickles acting as grappling attachment structures **(P,I,L)**. Presence of leaves on searchers is highly variable; developmental patterns vary considerably from no leaves at all to basally developed leaves and to leaves all along the searcher stem. In some species leaf petioles can act as hook like anchoring structures **(E)**.

mechanisms included attachment by reflexed lateral branches (e.g., *Gouania blanchetiana*; *Uncaria guianense*) petiole angles (e.g., *Croton pullei, Dioscorea sagittata, Byttneria cordifolia*). Hooks, grapnels and prickles were observed as modified 3rd order axes (e.g., *Uncaria guianensis*), modified stipules (e.g., *Machaerium quinata* and *M. floribundum*) and epicuticular structures (e.g., *Rubus ulmifolius*). *Uncaria guianensis* is commonly considered to be a hook climber. We observed that hooks are modified 3rd order stems borne by 2nd order lateral branches and that these may also function as angle attachment devices. Moreover, the 3rd order stems take the shape of spines when they are initiated in the adaxial position of the bearing branch. Different degrees of branching and branch modification can therefore produce combinations of different attachment mechanisms. *Uncaria guianensis* can be seen as hook climber, spine climber, and branch angle climber. The brief morphological survey underlined the fact that many climbing plants deploy more than one attachment mechanism. Even further attachment organ complexity was seen in *Smilax aspera* which has epicuticular structures modified into prickles, stipules modified into tendrils as well as weak stem-twining behaviour.

Leaf Expansion on Searcher Shoots

Leaf development on searcher shoots was extremely variable across species. Searcher shoots of some species developed fully expanded leaves from the beginning of the self-supporting phase such as *Croton pullei, Hedera helix,* and *Aegiphila laevis* (**Figures 1E,K,Q**). Other species such as *Davilla nitida, Machaerium quinnata,* and *Odontadenia perotteti* did not bear expanded leaves at all (**Figures 1H,J**). Leaf development on self-supporting searcher shoots was variable among species. It varied from leaves that were fully expanded only at the base (e.g., *Styzophyllum riparium*) (**Figure 1T**) to being fully expanded all along the searcher shoot during the self-supporting phase (e.g., *Aegiphila laevis*) (**Figure 1Q**). Some species showed delayed leaf development where only leaf primordia are present with small unexpanded laminas during the self-supporting phase (e.g., *Fallopia dumetorum; Stigmaphyllon sinuatum; Condylocarpon guianense; Serjania membranaceae).* Following the retention of leaves as primordia several developmental variations were seen: leaf expansion occurred following attachment to a support or also when a support was not found and the searcher became pendulous (**Figure 2A**). In other species, leaf primordia are rapidly aborted if the internode bearing them does not come in contact with a support (e.g., *Odontadenia perotteti*). In other species, expanded leaves are only produced via short leafy shoots from axilary or terminal meristems in growth episodes after the searching and support foraging phase (e.g., *Davilla nitida* and *Machaerium quinata*) (**Figure 2B**).

Reach Variation

Among 190 searcher shoots sampled we observed a maximal reach capacity that varied from 10.5 cm in the stem twiner *Fallopia dumetorum* to 268 cm in the branch-hook angle climber *Uncaria guianensis* (**Figure 3**). About half of all species showed maximal reaches of up to a metre and the remaining half between approximately 1 m to more than two and a half metres. The analysis of variance (ANOVA) on a subsample of 181 shoots belonging to 22 species represented by at least 3 shoots per species showed significant differences between species (*p*-Value = 1.62e-81) with 91% of the variation being attributed to species identity. Tendril-climbers and root-climbers (the latter represented by only *Hedera helix)* spanned the shortest range of distances from 14 to 91 cm. Twining species showed the widest range of distances from 10 cm to 225 cm. Branch-hook angle climbers species showed the longest distances ranging from 72 to 268 cm.

Reach and Morphology

Basal diameter varied by more than an order of magnitude from 0.59 mm (the stem twiner *Fallopia dumetorum*) to 13.74 mm (the branch-hook angle climber *Uncaria guianensis*) (**Figure 4A**). Overall, maximal reach increased with increasing basal shoot diameter indicating that in general wider stems develop longer reaches ($R^2 = 0.738$; *p*-value = 1.5e-56) (**Figure 4A**). There was a strong tendency for twiners to have smaller diameters than tendril climbers for a given reach, particularly for short and medium reaches. Branch-hook angle climbers tended to have the broadest basal stem and the longest reach (**Figure 4A**).

Total shoot fresh mass varied from 0.062 g in the stem twiner *Fallopia dumetorum* to 534.5 g in the branch-hook angle climber *Uncaria guianensis* (**Figure 4B**). Overall total shoot fresh mass also increased with reach ($R^2 = 0.783$; *p*-value = 2.5e-64) (**Figure 4B**). In general, longer searchers are also necessarily heavier than shorter ones. For a given reach, twiners are again distinguished by showing less fresh mass for a given reach compared with other groups. However, the longer and more weakly twining species, *Pereskia aculeata* and *Aegiphila laevis* did not follow this trend. Each showed a rather divergent habit with succulent stems (*Pereskia*) and expanded leaves (*Aegiphila*) possibly explaining their higher searcher fresh mass. Overall, the longest reaching species in the study were the heaviest.

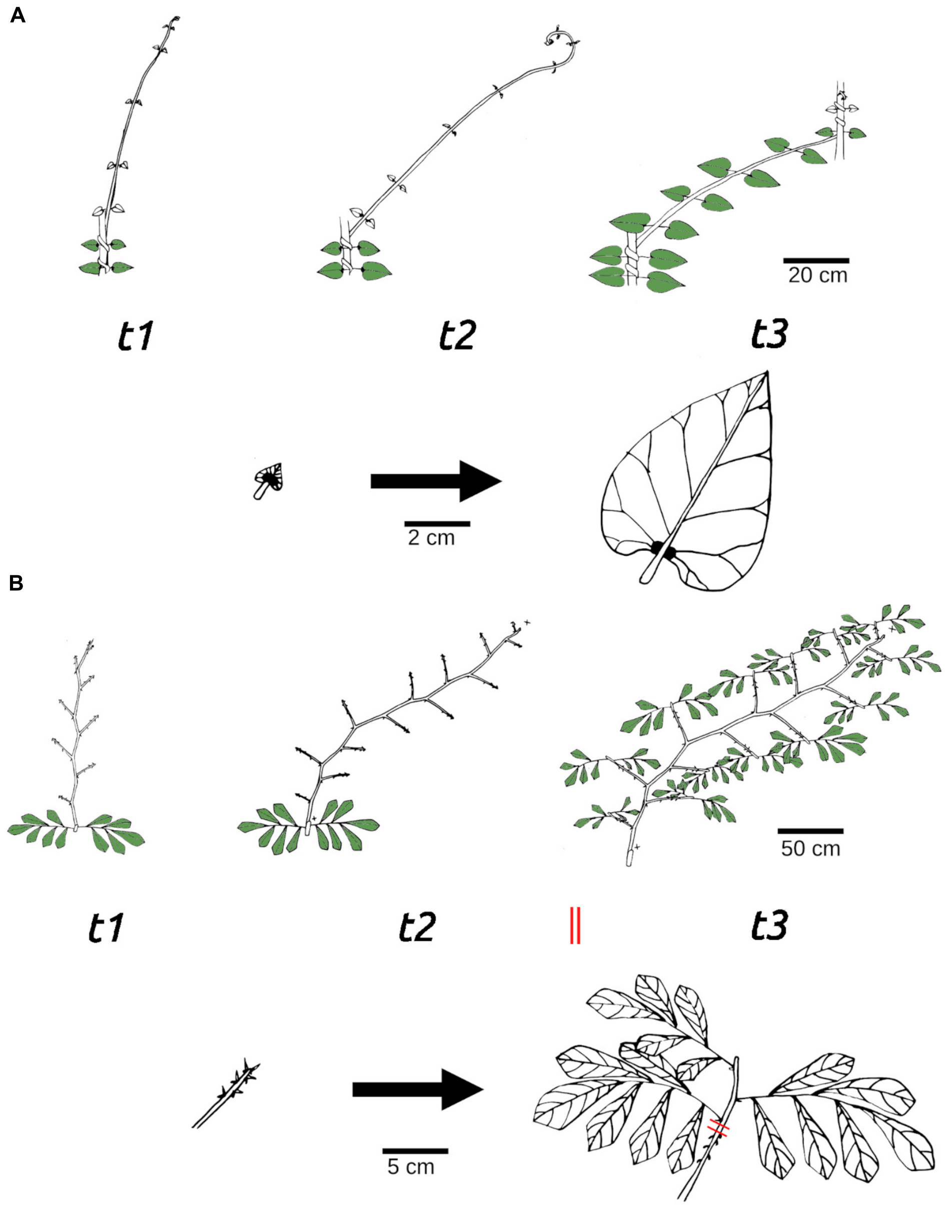

FIGURE 2 | Leaf display patterns on searcher shoots: **(A)** Delayed leaf development in the stem twiner *Stigmaphyllon sinuatum* (Malpighiaceae). The searcher maintains leaves at a young stage of development, apart from at the very base during the entire self-supporting phase (t1). Leaves develop and fully expand only when a support is attached (t2) or if the searcher does not find a support and becomes pendulous (t3). **(B)** Continuous leaf development in *Machaerium quinata* (Fabaceae) a branch-hook angle climber. The searcher shoot remains self-supporting during multiple growth episodes. Leaves are developed initially at the searcher base and are fully expanded (t1). While still self-supporting, further axial branches are developed (t2) and leaf development continues with fully expanded leaves developing along the searcher from lateral branches (t3).

Among searchers bearing leaves, leaf lamina area varied by more than two orders of magnitude from 0.18 cm^2 (*Fallopia dumetorum*) to 13455.43 cm^2 (the branch-hook angle climber *Uncaria guianensis*). Not all species presented leaf primordia or expanded leaves on the searcher stem (e.g., *Dioscorea sagittata; Odontadenia perotteti, Smilax aspera*) (R^2 = 0.449; *p*-Value = 1.81e-19) (**Figure 4C**). Leaf lamina area increased with reach length, but lamina area was highly variable across species and functional groups especially in the middle part of the reach range (**Figure 4B**). Interestingly, some medium and high reach species developed no leaf laminae. Only three twining stem species and one tendril climber produced strictly no leaves on the searcher stem. Leaf fresh mass, dry mass and lamina area generally increased with reach length across all species bearing leaf lamina at varying stages of expansion (**Supplementary Figure 3**). Twining stems with lower reaches stand out from other climbing types in showing less leaf development.

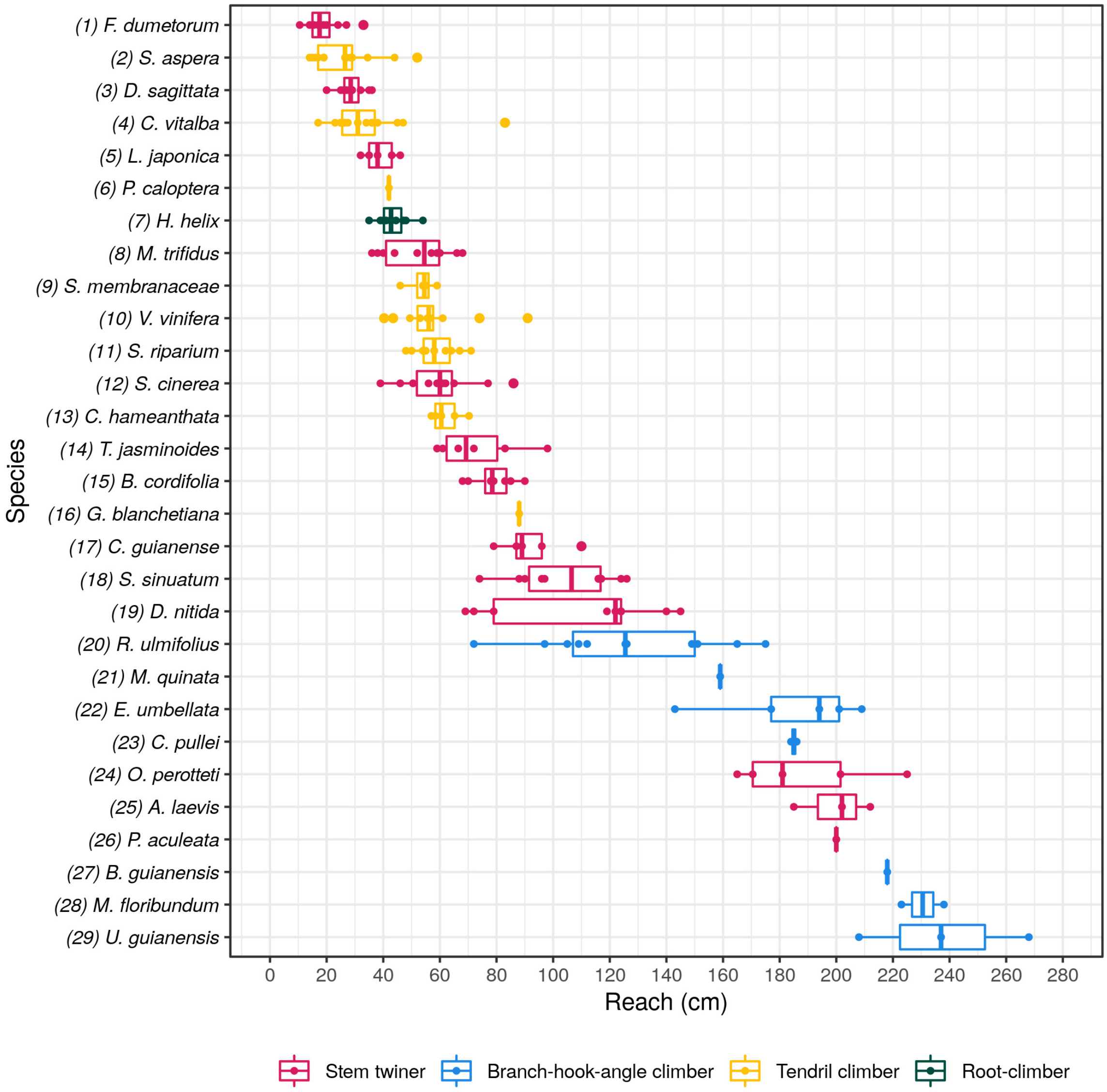

FIGURE 3 | Boxplots showing the maximal reach per species. Species are ordered by mean maximal reach capacity from the top and as four functional groups based broadly on attachment type including: stem twiners (red), tendril climbers (yellow), root climbers (green), branch-hook-angle climbers (blue). (box plots: line = median, box = 1st and 3rd quartiles).

Overall stem water content varied from c. 50 to 90% apart from the predominantly woody searchers of the angle climber *Uncaria guianensis* c. 20–30%. Overall, these values decreased with searcher reach ($R^2 = 0.189$; *p*-Value = 3.87e-10) (**Figure 4D**). Longer reaching branch-hook angle climbers showed noticeably lower water content whereas, stem twiners and tendril climbers tended to show higher water content.

Mechanical Properties

Flexural rigidity (*EI*) at the base of searcher shoots increased with increasing reach ($R^2 = 0.827$; *p*-Value = 6.49e-71) (**Figure 5A**) varying by 7 orders of magnitude across all species, from 3.20 $N.mm^2$ (*Fallopia dumetorum*) to 2.34×10^7 $N.mm^2$ (*Uncaria guianensis*). Stem twiners tended to show a lower flexural rigidity for a given reach for all reach distances compared with other groups.

A similar overall pattern was seen in terms of second moment of area of the basal searcher shoot stem segment (*I*) increased with reach ($R^2 = 0.711$; *p*-Value = 1.12e-50) (**Figure 5B**) varying by more than 5 orders of magnitude: from 6.05×10^{-3} mm^4 (*Fallopia dumetorum*) to 1517.048 mm^4 (*Uncaria guianensis*) (**Figure 5B**). Stem twiners tended to have smaller second moments than most other functional groups even among medium to longer reaching species.

Overall, structural Young's modulus (stem stiffness) (E_{str}) increased with reach ($R^2 = 0.453$; *p*-Value = 1.62e-25) (**Figure 5C**) and varied by two orders of magnitude, from 212.95 $MN.m^{-2}$ in the monocotyledonous spine and tendril-climbing *Smilax*

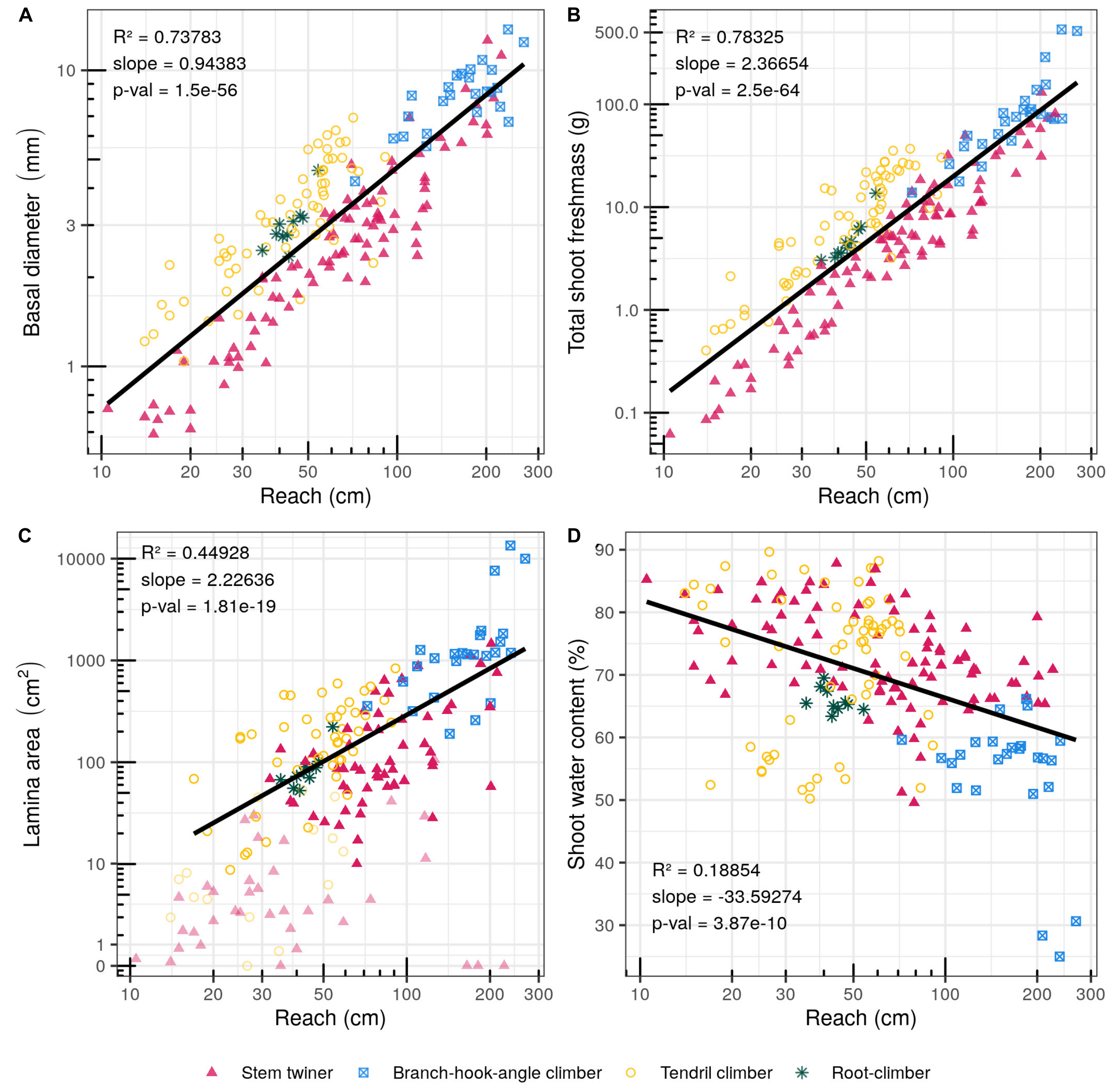

FIGURE 4 | Bivariate plots (log scale) of searcher reach (cm) and morphological traits. **(A)** Basal diameter (mm). **(B)** Total shoot fresh mass (g). **(C)** Lamina area (cm^2) (For searchers not producing leaves and for searchers bearing only leaf primordia or non-green leaves, the values were not included in the slope calculations and symbols are depicted as lighter shades). **(D)** Shoot water content (%) (fresh mass).

aspera to 15479.08 MN.m^{-2} in the branch angle climber *Uncaria guianensis*.

When stiffness was plotted against second moment of area, a much lower prediction value was found compared with stem rigidity (R^2 = 0.142; p-Value = 1.46e-07) (**Figure 5D**). Visual inspection of the data suggested that stem stiffness is not closely correlated with basal stem size across all species of searcher. In other words, for a given searcher basal size, there is a very wide range of structural Young's modulus values. This implies a large range of organisational and structural anatomical patterns. Among smaller diameter stems, twining stems tended to develop relatively higher stiffness for a given reach and for a given basal stem size. Larger diameter stems representing the longest reaching angle climbers represented by *Uncaria guianensis* and *Machaerium floribundum* showed the highest stiffness. The data also pointed to the fact at least among the searchers studied, that searchers or all kinds require a structural Young's modulus of c. 3000 MNm^{-2} to maintain a reach of over c. 80 cm (**Figure 5C**).

Tests were carried out on how mechanical parameters were scaled (slope) and constrained (R^2) from short to long reach capacities (**Figure 5** and **Table 3**). Flexural rigidity (*EI*) was expected to show a 10^4 relationship with reach capacity and did not differ significantly from the observed slope (slope = 4.089). This means that *EI* tends to remain proportional to the increase

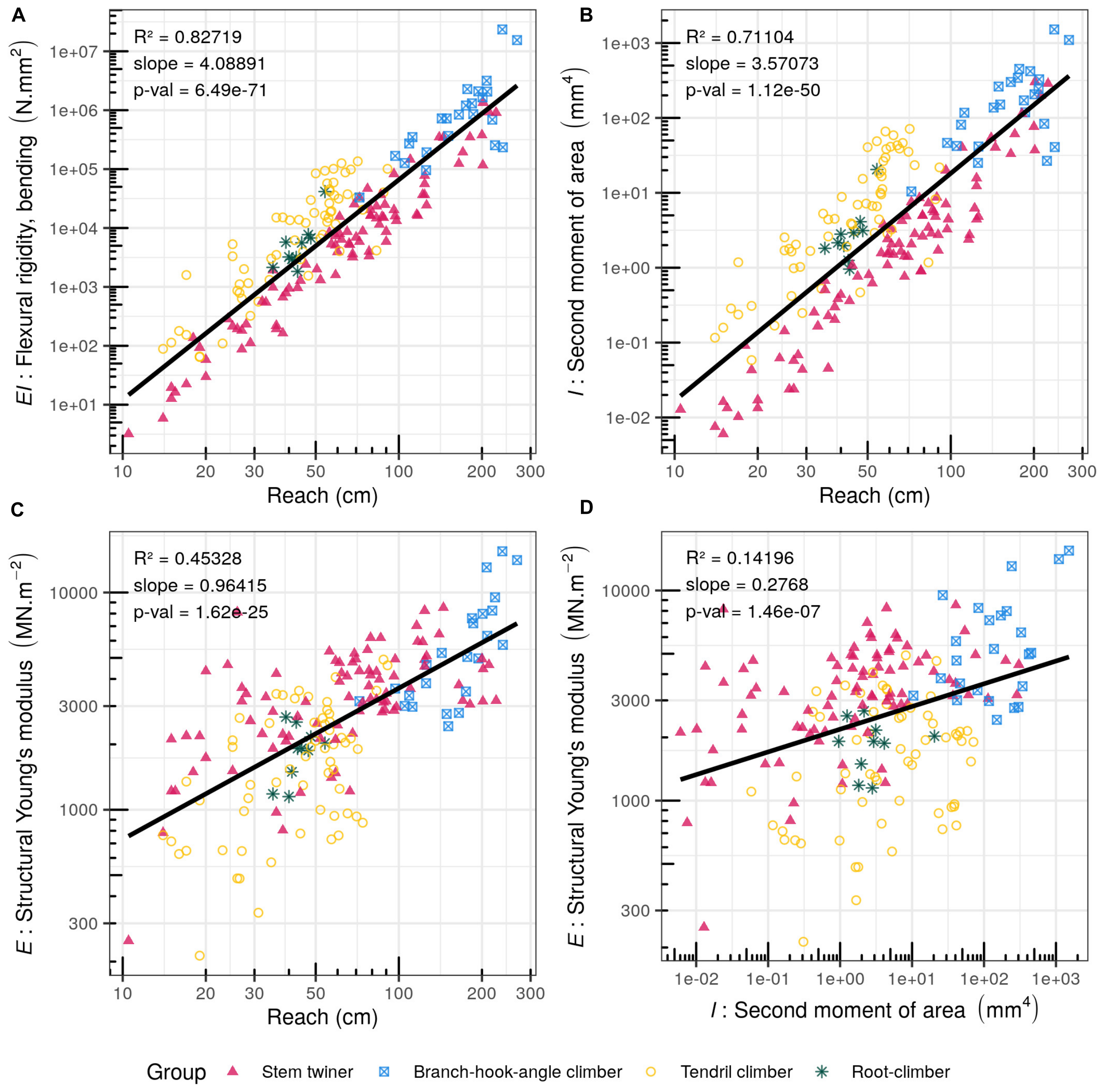

FIGURE 5 | Bivariate plots (log scale) of searcher reach (cm) and mechanical traits. **(A)** Flexural rigidity, *EI*, (N.mm^2). **(B)** Structural Young's modulus E_{str} (MN.m^{-2}). **(C)** Second moment of area, *I* (mm^4). **(D)** Bivariate plot of Structural Young's modulus E_{str} (MN.m^{-2}) against stem second moment of area *I* (mm^4).

in reach. Second moment of area (*I*) was also expected to show a 10^4 function with reach, but the estimated slope was significantly lower (slope = 3.571). This means that second moment of area (*I*) tended to be proportionally lower with increasing reach distance. The slope of stem stiffness (E_{str}) against reach was expected to show a 10^0 relationship was observed to be significantly higher than the expected one (slope = 0.964). This means that basal stiffness tended to be proportionally higher with increasing reach.

Anatomical Organisation

Anatomical organisations of the basal segments of searcher stems are remarkably diverse (**Figure 6**). They vary from short reaching, small cross-sections with relatively high proportions of primary tissues to longer reaching, larger sections with noticeably higher proportions of secondary tissues (**Figure 7A**). Stem twiners and tendril climbers are mostly represented by smaller cross-sections with large proportions of primary tissue although stem twiners are also present as medium and long reaching larger stem sections with well-developed wood cylinders (**Figures 6**, **7A**). Branch-hook angle climbers mostly include well-developed wood cylinders among larger, longer reaching searchers.

Overall, outlines of searcher bases were mostly circular to ellipsoidal and close to radially symmetrical, with the possible exception of *Paullinia caloptera,* a tendril climber (**Figure 6**(6)). Some of the smaller reach stems developed lobed outer stem outlines, often containing mechanical tissue packed into the distal extremities of the lobes (**Figures 6**(1,4,10)). Stem geometries of longer reach species were nearly all ellipsoid to rounded. This suggests that secondary growth has a "rounding" effect on stem geometry when wood and periderm replace outer primary tissues (**Figures 6**(16-29)). Searchers of the tendril climber *Cissus haematantha* showed a distinctly square external outline, with pointed wing-like extensions packed with collenchyma cells.

Cross-sectional area ranged from 0.30 mm^2 in the small twiner *Fallopia dumetorum* to 149.9 mm^2 in the large, long reaching branch-hook angle climber *Uncaria guianensis* (**Supplementary Table 1**).

Cross-sectional areas of mechanical tissues (xylem, cortical fibres and collenchyma) varied from 0.15 mm^2 (*Fallopia dumetorum*) to 103.6 mm^2 (*Uncaria guianensis*) and from 18% (*Hedera helix*) to 84% (*Bauhinia guianensis*). Second moment of area of all mechanical tissues combined varied from 0.0048 mm^4 (*Fallopia dumetorum*) to 1182.73 mm^4 (*Uncaria guianensis*) (**Supplementary Table 1**). The relative contribution of all mechanical tissues combined to the second moment of area (I) varied from 28.4% (*Smilax aspera*) to 80.8% (*Stigmaphyllon sinuatum*) (**Figure 7A**).

Cross sectional area of pith (medullary parenchyma and fibres combined) varied from 0.06 mm^2 (*Fallopia dumetorum*) to 33.8 mm^2 (*Rubus ulmifolius*) (**Figures 7A**, **8A**). Relative proportions varied from 2.97% (*Elaeagnus umbellata*) to 59% (*Rubus ulmifolius*) of the cross-sectional area and were not observed to vary significantly with the reach. Absolute values of pith area increased with reach (R^2 = 0.54; *p*-value = 1.5e-33) indicating that the pith is a potentially key trait linked to searcher length. Absolute second moment of area of pith varied from 0.00028 mm^4 (*Fallopia dumetorum*) to 93.74 mm^4 (*Rubus ulmifolius*). Pith contribution to second moment of area varied from 0.098% (*Elaeagnus umbellata*) to 43.6% (*Smilax aspera*) (**Figure 7B**). Some searcher stems containing a relatively large pith showed evidence of tissue voiding and the development of a pith cavity. Pith voids were not included in the calculations of the cross-sectional area but directly influenced values of second moment of area of the remaining pith and other tissues (**Figures 6**(5,11)).

Xylem cross-sectional area (cross-sectional area of primary xylem bundles for monocots and cross-sectional area of primary and secondary xylem for dicots) varied from 0.028 mm^2 (*Fallopia dumetorum*) to 103.59 mm^2 (*Uncaria guianensis*). Xylem relative proportion of cross-sectional area ranged from 6.46% (*Fallopia dumetorum*) to 81.2% (*Bauhinia guianensis*) of the cross-sectional area. Absolute second moment of area of xylem varied from 0.00033 mm^4 (*Fallopia dumetorum*) to 1182.73 mm^4 (*Uncaria guianensis*). Xylem relative contribution to the second moment of area varied from 3.02% (*Fallopia dumetorum)* to 71.9% (*Croton pullei*) (**Figure 8B**). Xylem relative contribution to the second moment of area (I) was significantly and positively correlated with the reach (R^2 = 0.635; *p*-Value = 5.3e-43).

Cross-sectional areas of bark supportive tissues (cortical fibers and collenchyma) were not observed in *Gouania blanchetiana*, *Elaeagnus umbellata*, *Davilla nitida*, *Croton pullei*, *Bauhinia guianensis*, *Aegiphila laevis* and *Uncaria guianensis*. But when present, it varied from 0.026 mm^2 (*Sabicea cinerea*) to 5.026 mm^2 (*Rubus ulmifolius*). In such case, stiff bark relative proportion of cross-sectional area ranged from 1.29% (*Sabicea cinerea*) to 42.86% (*Fallopia dumetorum*) of the cross-section area. Second moment of area of bark supportive tissues varied from 0.0045 mm^4 (*Fallopia dumetorum*) to 43.3054 mm^4 (*Rubus ulmifolius*). Contribution of bark supportive tissues to the second moment of area varied from 2.09% (*Sabicea cinerea*) to 64.17% (*Fallopia dumetorum*) (**Figure 8B**). Their relative contribution to the second moment of area (I) was significantly and negatively correlated with the reach (R^2 = 0.389; *p*-Value = 2.64e-19).

Overall, smaller reach species developed relatively less wood and notably produced higher proportions of peripheral extraxylary mechanical tissues (**Figure 7A**), especially cortical fibres and hypodermal collenchyma (**Supplementary Figures 1A–L**). Analyses of second moment of area indicate that for a number of small reach species including stem twiners and tendril climbers the peripheral placement of mechanical tissue occurs outside relatively large areas of cortical tissue. A variety of thickened fibre tissue was observed across species including lignified cells which represented either longitudinally elongated fibres (**Supplementary Figure 2B**) or longitudinally

TABLE 3 | Standardised major axis regression results.

Y	*X*	Log-transformation	*P*-values	R^2	Estimated slope	Expected slope	CI95
EI	R	**"xy"**	**6.49e-71**	0.827	4.089	4	3.837–4.357
E_{str}	R	**"xy"**	**1.62e-25**	0.453	0.964	0	0.852–1.091
I	R	**"xy"**	**1.12e-50**	0.711	3.571	4	3.286–3.881
E_{str}	I	**"xy"**	**1.46e-07**	0.142	0.277	0	0.236–0.325
D	R	**"xy"**	**1.50e-56**	0.738	0.944	1	0.875–1.018
$\text{Shoot}_{\text{freshmass}}$	R	**"xy"**	**2.50e-64**	0.783	2.367	1	2.202–2.543
A_{lamina}	R	**"xy"**	**1.81e-19**	0.449	2.226	2	1.963–2.525
SWC	R	**"x"**	**3.87e-10**	0.189	–33.593	0	(–38.618) – (–29.221)
A_{pith}	R	**"xy"**	**1.50e-33**	0.54	1.754	2	1.582–1.945
$I\%_{xylem}$	R	**"x"**	**5.30e-43**	0.635	56.514	0	51.92–61.515
$I\%_{bark}$	R	**"x"**	**2.64e-19**	0.389	–56.045	0	(–63.562) – (–49.417)
$\text{Fresh}_{\text{lamina}}$	R	**"xy"**	**1.86e-20**	0.467	2.281	2	2.02–2.576
$\text{Dry}_{\text{lamina}}$	R	**"xy"**	**2.47e-23**	0.516	2.466	2	2.182–2.788

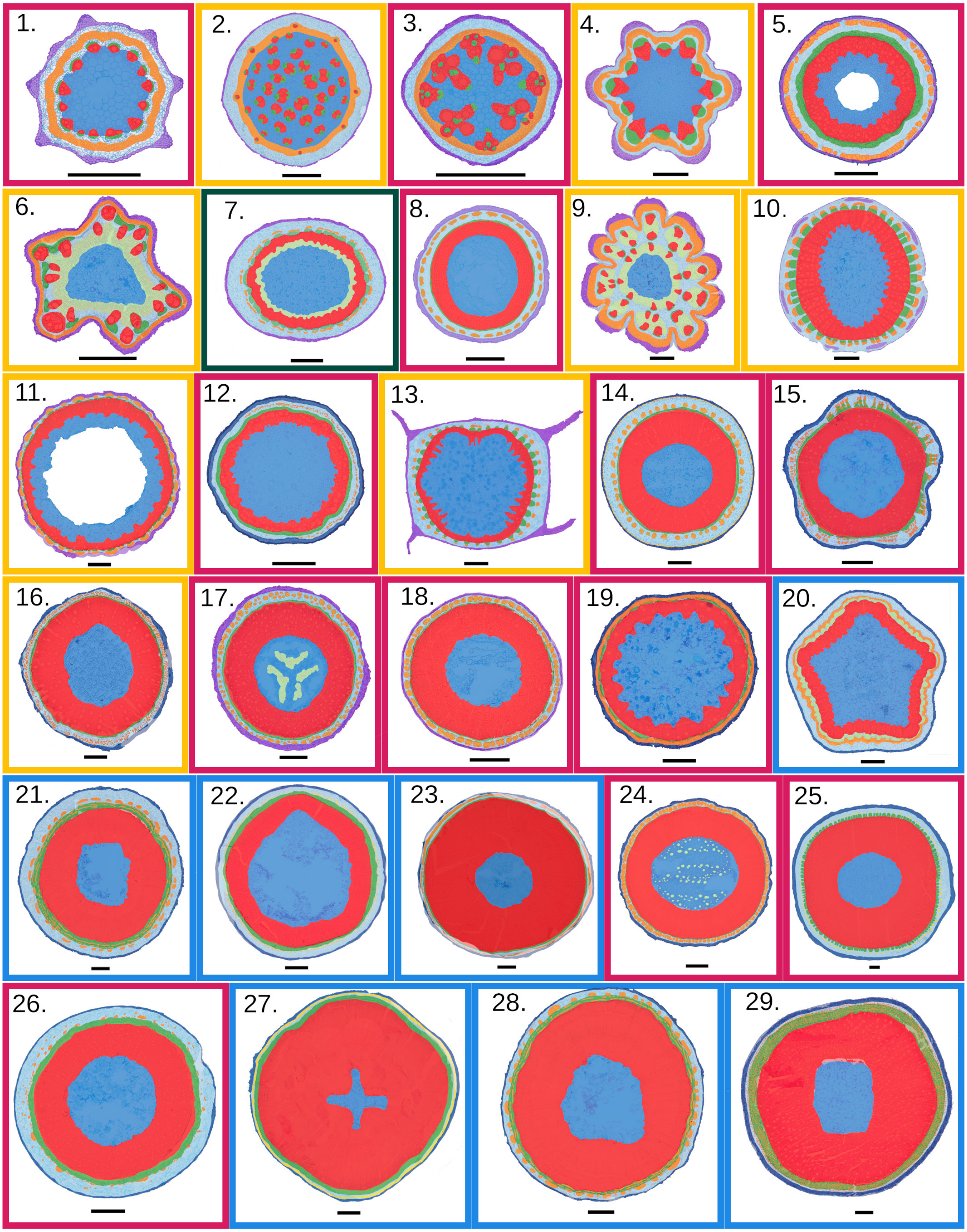

FIGURE 6 | Diversity of anatomical organisations organised by increasing mean reach per species (scale bar = 500 µm for all specimens). Colours distinguishing different tissues are the same than choose for **Figure 3**. **(1)** *Fallopia dumetorum*; **(2)** *Smilax aspera*; **(3)** *Dioscorea sagittata*; **(4)** *Clematis vitalba*; **(5)** *Lonicera japonica*; **(6)** *Paullinia caloptera*; **(7)** *Hedera helix*; **(8)** *Mesechites trifidus*; **(9)** *Serjania membranaceae*; **(10)** *V. Vitifera*; **(11)** *Styzophyllum riparium*; **(12)** *Sabicea cinerea*; **(13)** *Cissus haematantha*; **(14)** *T. jasminoïdes*; **(15)** *Byttneria cordifoli;* **(16)** *Gouania blanchatiana*; **(17)** *Condylocarpon guianense*; **(18)** *Stigmaphyllon sinuatum*; **(19)** *Davilla nitida*; **(20)** *Rubus ulmifolius*; **(21)** *Machaerium quinata*; **(22)** *Elaeagnus umbellata*; **(23)** *Croton pullei*; **(24)** *Odontadenia perotteti*; **(25)** *Aegiphila laevis*; **(26)** *Pereskia aculeata*; **(27)** *Bauhinia guianensis;* **(28)** *Machaerium floribundum*; **(29)** *Uncaria guianensis.* Functional groups are indicated by different coloured frames: stem twiners (red), tendril climbers (yellow), root climbers (green), branch-hook-angle climbers (blue).

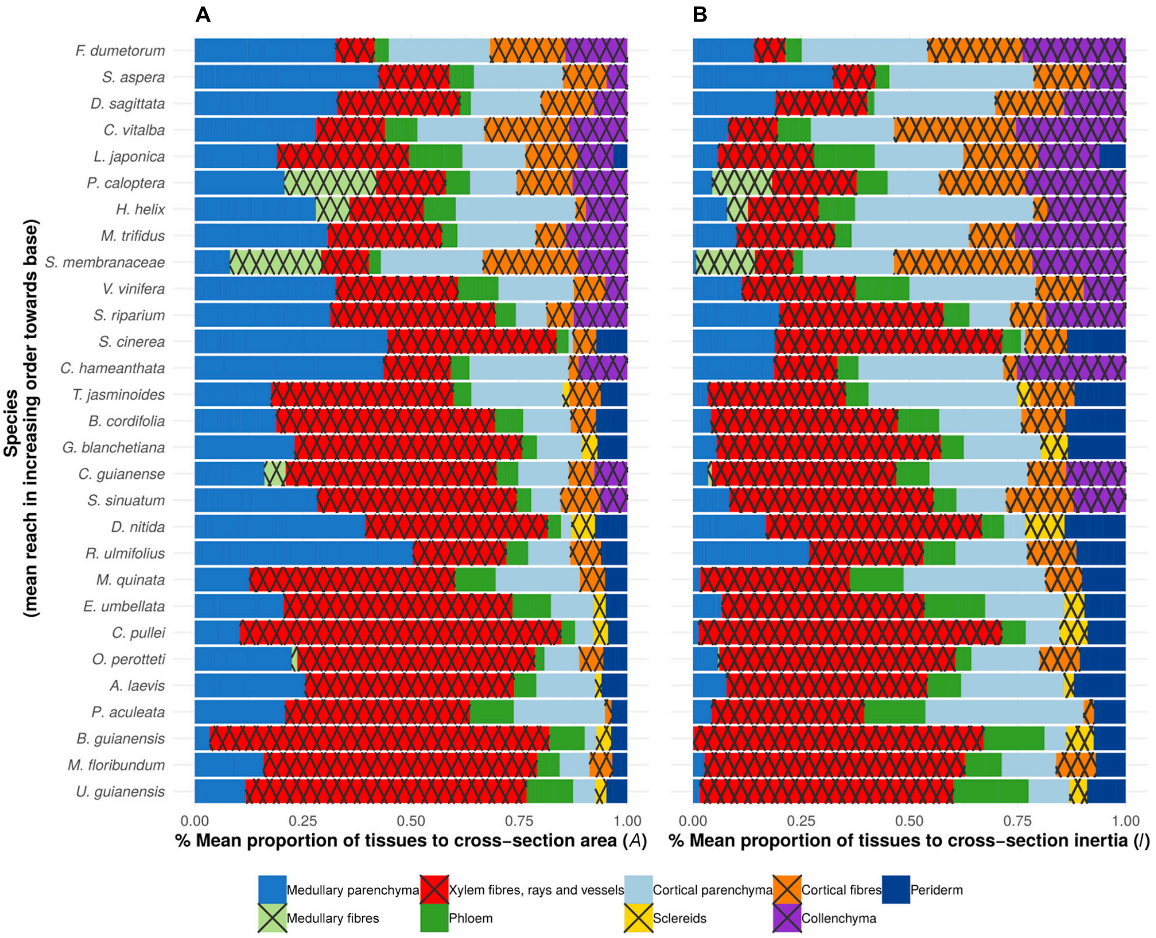

FIGURE 7 | Proportions of main tissues at base of searcher shoot **(A)** mean proportion of tissues to cross-sectional area ($A_{\%}$) **(B)** mean% contribution of tissues to second moment of area ($I_{\%}$).

foreshortened sclereids (**Supplementary Figure 2A**). Primary fibre organisations included entire rings of interconnected fibres (**Supplementary Figure 2F**), separated perivascular bundles (**Supplementary Figure 2E**), and also, notably in twining species of Apocynaceae and Malpighiaceae islets of cortical fibres with g-layer walls (**Supplementary Figures 2G–I**). Basal organisations of longer reach searchers overall showed a decreasing amount of primary fibre tissue in terms of both cross-sectional area and second moment of area concomitant with increasing amounts of vascular tissue (**Figures 7A,B** and **Supplementary Figures 2U–X**).

DISCUSSION

Morphological Diversity

This study compared the attachment and reach characteristics of 29 species of climber from tropical and temperate environments. The sampling included most of the well-known kinds of attachment strategies that characterise climbing plants, including stem twiners, tendril climbers, and branch-hook angle climbers. Our sample only included one root climbing species from temperate environments and this category is perhaps underrepresented. Despite this, the sampling overall reflects climbing mechanisms among many woody vines and lianas (Gallagher and Leishman, 2012).

One of the aims of this analysis was to find out how different reach capabilities might be linked to different attachment modes, climbing strategies, and stem structure and mechanics (Putz, 1984; Rowe et al., 2006; Wyka et al., 2013; Gianoli, 2015). Our field observations underlined the difficulty of attributing a single kind of attachment strategy or attachment mode. Instead, many temperate and tropical climbers rely on combinations of attachment mode during searching and climbing. For example, *Smilax aspera* has epicuticular structures modified into prickles as well as stipules modified into tendrils. Both of these are observed to anchor the plant to host plants in different ways and on different kinds of supports. Both *Dioscorea sagittata* and *Byttneria cordifolia* twine around supports via the main searcher axis but these plants also relied on relatively stiff and angled or reflexed-petioles that act as hooks to attach to host branches. These multi-attaching mechanisms underline the

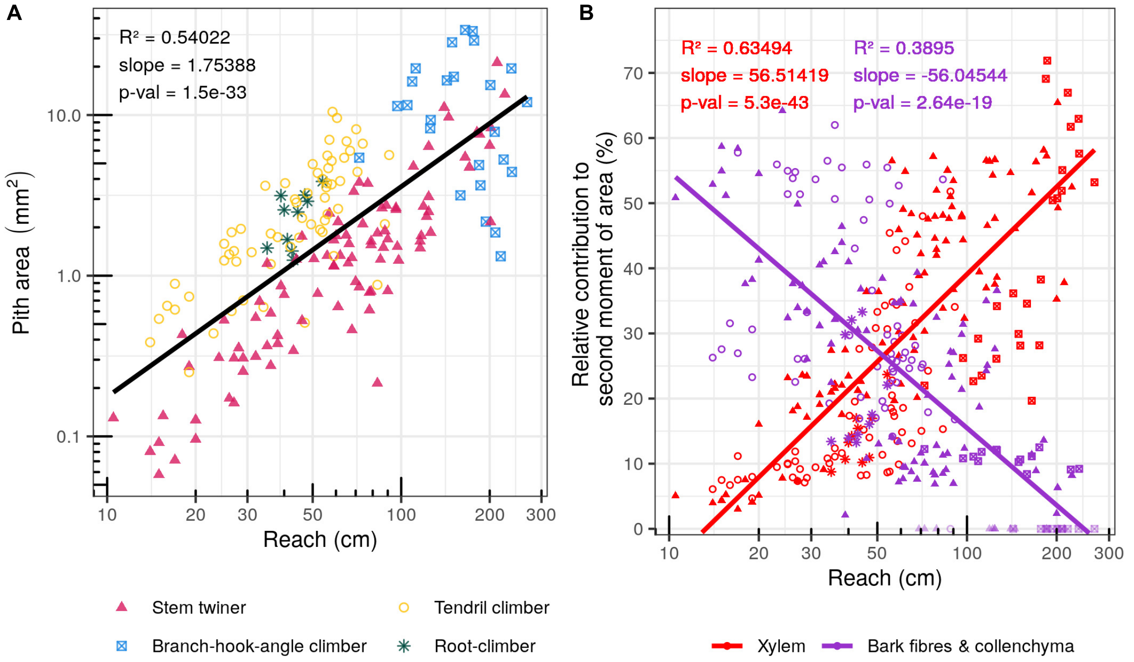

FIGURE 8 | Bivariate scatter plots of reach (cm) against main tissue types. **(A)** Plot of Reach (cm) against pith area (mm^2). **(B)** Plot of Reach (cm) against% contribution of xylem and bark to second moment of are of the stem (Values for searchers not encounting for cortical fibers and collenchyma in their stem anatomy were not included in the slope calculations and symbols are depicted as lighter shades).

difficulty of attributing species to a functional group based on attachment. It is clear that many species possess a combination of attachment and climbing methods (e.g., Cabanillas and Hurrell, 2012; Soffiatti and Rowe, 2020) that can operate at different scales and attachment forces (Steinbrecher et al., 2010). This likely influences the range of habitats and kinds of three-dimensional space they can exploit. The notion of "complex attachments" (Caballé, 1986), also supports the idea that attachment strategies cannot always be categorised in regard of a single organ. Studies attempting to integrate attachment mechanisms and ecological patterns possibly require more detailed methods of comparing complex combinations of growth and attachment mechanisms.

Reach Variation

Maximal reach varied markedly between species and was not strictly linked to mode of attachment. This was particularly the case in stem twining species where both short and long reach species are represented. Our measurements seeking to identify the maximal reaches for a given plant individual in the field also suggested that maximal reach can vary in amplitude among longer reach species. The implication is that some longer reach species might be able to exploit smaller gaps as self-supporting shoots foraging for supports, however a more detailed sampling including maximum and minimum reach would be necessary to explore this further.

Our study showed a highest reach limit of approximately 2.5 m, this is less than previous measurements of reach in tropical climbers (Putz, 1984), with lengths reported up to 3 m. However, sampling here focussed on searcher stems derived mostly from branches of mature individuals rather than young individuals in a juvenile self-supporting phase of growth (Caballé, 1998; Speck and Rowe, 1999). Some tropical climbing species can reach heights of well over 2.5 m as young self-supporting individuals, as can be regularly seen with species of *Strychnos* (Loganiaceae) as well as *Croton* and *Manihot* (Euphorbiaceae) (Gallenmüller et al., 2004; Rowe et al., 2006; Ménard et al., 2013). These can develop self-supporting statures comparable with treelets. Furthermore, our survey did not include some of the larger bodied monocot climbers, the rattans (Calamoideae) and genus *Desmoncus* (Arecaceae) (Isnard and Rowe, 2008). These non-woody palms can produce self-supporting attachment organs (cirri) that can also have reaches longer than 2.5 m. Clearly, the reach capabilities between different species and different life histories can also depend on the state of development as young "treelet"-sized individuals or as branches developing on individuals that are already attached and climbing. There are probably functional differences as well as risk differences between attachment strategies of juvenile plants and searcher branches of adults. For example, the collapse of searchers on adult branches is potentially an advantage representing a shift to alternative functions such as light capture. However, a young individual that collapse to the ground in the dark understory possibly faces a setback to the plants' development.

Mechanical Properties and Reach

Reach capacity is strongly linked to flexural rigidity at the base of the searcher shoot. Longer searchers have higher stem rigidity at their bases than shorter ones. Values of Young's modulus showed a huge range of values for a given reach and also for a given basal stem second moment of area. This suggests that different species have evolved many different ways of developing mechanical properties to enable a given rigidity and reach. This is consistent with the anatomical observations indicating a wide array of anatomical architectures.

The scaling relationships suggested that none of the searcher shoots were mechanically "over-designed." Instead, we found that they were just as rigid as necessary to sustain their total shoot fresh mass and traverse the gap distances consistent that they are putatively adapted for. This is consistent with the long-held belief that vines and lianas have diverse habitat preferences (Gentry, 1991), such as transitions from disturbed to stable environments (Laurance et al., 2014; Ledo and Schnitzer, 2014; Campbell et al., 2018); attachment to large- to small-diameter supports (Putz, 1984; Hegarty, 1991; Goriely and Neukirch, 2006; Carrasco-Urra and Gianoli, 2009) and establishment in early to late successional settings (Letcher and Chazdon, 2012; Letcher, 2015). We suggest that habitat preference also involves selection in terms of reach implying that different climbing plants are adapted for different three-dimensional habitats in terms of interspacing of supports.

The scaling relationship also indicated that longest reaching stems had proportionally smaller stem cross-sections with proportionally smaller second moments of area for their long reach. These longest reaching stems also developed the stiffest mechanical properties in terms of structural Young's modulus (E_{str}). The result is interesting because it suggests that even the longest reaching, broadest searcher stems remain proportionally narrow compared to short-reaching searchers.

Development of a wood cylinder with a significant contribution to rigidity is eventually necessary for sustaining a searcher shoot beyond a certain reach. The study suggests that searcher shoots of vines and lianas (at least those included in this study) do not cross a potential allometric divide separating them from trees. The study suggests that climbers do not grow like trees with indeterminate secondary growth of the stiff early growth-phase wood of the juvenile phase.

The mechanical data indicated that stem twiners potentially develop a different mechanical architecture compared with other tested groups. Overall, twiners developed less rigid, smaller cross-sections but apparently compensated for a small diameter by developing a relatively high Young's modulus (high stiffness of the tissues comprising the stem). For a given reach, stem twiners were also lighter than other climbing categories and at the same time also tended to have a higher shoot water content. We suspect that this reflects the need for turgor driven movements and circumnutation needed to deploy attachment and twining. Oscillatory movements are controlled by active water transport in cells, generating elongation on one side of the stem that is actively regulated by signals emitted on the compression side (Millet et al., 1988; Care et al., 1998; Rivière et al., 2017). Searcher organisation reflects the developmental compromise between being stiff and rigid enough at the base to mechanically support and orientate the searcher but at the same time retain flexibility and mobility nearer the apex. The presence of stem twining across such a large range of reaches is a striking result of this study. It contrasts with the narrower ranges of reach seen among tendril climbers and branch-angle climbers. Twiners seem able to do all of the reaches.

The Structural Diversity of Searchers

Overall, narrow searchers of short-reach species develop small cross-sectional areas and second moments of area of wood. Instead, they rely on peripheral primary tissues for stem stiffness. Long-reach searchers almost all have well-developed wood cylinders with large wood cross-sections and second moments of area.

The data also indicate that there is a threshold of maximum reach, which is limited by stem stiffness. Searchers generally develop a relatively high stiffness with a structural Youngs modulus of at least 3000 MNm^{-2} in order to cross spans of more than *c.* 80 cm. In other words, whatever the interplay of stem second moment of area (I) and stem stiffness (E) across all species, it appears that searchers must have tissues with high stiffness contributing to the rigidity in order to traverse gaps longer than 80 cm. It appears, at least among those tested, that climbing plants do not produce long reaches with wide diameters (high second moments of area) and with tissues that are low in stiffness (compliant). Short-reach searchers limit development of stiff wood whereas most long-reach species develop significant amounts of wood. However long reach searchers must develop stiff tissues to exceed gaps of 80 cm.

The study emphasised that pith size is a key developmental feature behind searcher stem diameter and rigidity. Measurements of second moment of area indicate that the pith can act as a geometrical spacer around which stiff tissues can be placed and provide relatively high rigidity for relatively little material (Mahley et al., 2018; Olson et al., 2018; Pittermann and Olson, 2018; Levionnois et al., 2020, 2021). A large pith occurred across different reach lengths and also between different attachment strategies. Short-reach twiners, in particular, developed a large pith with stiff primary fibre tissues positioned to the outside of the stem cross-section thus raising their second moment of area and contribution to rigidity. The principal is not just seen in short-reach twiners but is also well known in species of *Rubus*, a branch-hook climber and medium to long reach searcher. Stems produced a very large pith but with relatively little wood in the cross-sectional area producing a long reach and high rigidity. The pith acting as a central spacer is well known for fern and vascular plant petioles (Mahley et al., 2018; Levionnois et al., 2020) and self-supporting stems of plants in general (Borchert and Pockman, 2005; Rosell and Olson, 2014; Plavcová and Jansen, 2015). In the vines and lianas studied here, most short-reach species bear significant proportions of parenchyma tissues but this was also observed in a long-reach species (i.e., *Pereskia acuelata*). Abundant parenchyma cells may be linked to other functions. (i) fast growing systems that require tissues with a high volume:weight ratio to produce relatively high moments of inertia (e.g., the case of many short-reach species, vine-like and fast-growing lianas). (ii) searchers with active searching movements may require water capacitance to sustain growth in environments with high evapotranspiration (Borchert and Pockman, 2005).

G-fibres have been viewed as playing a role in attachment mechanisms via thigmomorphogenetic development (Meloche et al., 2006; Bowling and Vaughn, 2009). Extraxylary fibres with gelatinous wall layers are present in the bark tissues of many searcher shoots and these have been recently linked to stem development in the climbing habit (Chery et al., 2020). The presence of G-fibres was identified in *Stigmaphyllon sinuatum* and four species within the Apocynaceae. They were present as bundles of thick-walled gelatinous fibres in the outer part of the cross-stem section. These were mostly observed in twining species in which the searcher shoot needs to extend across gaps but also attach to supports via movement and twining. We suspect that G-fibres possibly facilitate small changes in motor tissue properties in some searchers to generate rapid postural responses. In contrast searcher shoots adapted for crossing large gaps between supports, such as some of the branch-hook angle climbers and tendril climbers may maximise second moment of area and stem stiffness but possibly at the risk of limiting stem mobility and active movements for finding and attaching actively to supports.

Leaf Development on Searcher Stems

To our knowledge, leaf development on searcher shoots has not been studied in any detail across different functional groups of climbers and in relation to searching, attaching, and climbing. Our survey showed a highly variable leaf development pattern. Previous observers have noted that leaf expansion during twining and attachment would hinder circumnutatory movements and connection with host supports (Raciborski, 1900; French, 1977). To some extent, this is borne out by our observations where stem twining species deploying long, curved, circumnutatory shoots are leafless or bear only leaf primordia or undeveloped leaves.

Some of the tendril climbers, especially *Clematis vitalba*, develop many leaves during searcher deployment representing a large proportion of the fresh mass that the searcher base must support. We suspect that in some searcher deployment mechanisms, early deployment of fully developed leaves would mean that searcher shoots would become elastically unstable. In *Clematis*, we have observed that this results in the collapse of the leafy searcher on top of host branches with leaves fully expanded thus ensuring that the climbers' leaves lie on top of the host leaves. The outcome would be similar to other species which accomplish a "leaves on top" strategy via a leaf ratcheting mechanism of micro hooks on the leaf surfaces (Bauer et al., 2011).

Elastic instability and flopping of searchers that do not reach a support are generally widespread in climbing plants. Some climbing life histories might take advantage of elastic instability for deploying leaf-ready stems that can cover host leaves before attachment. This kind of mechanism might be especially relevant among long range branch-hook angle climbers that deploy leaves early during the searcher self-supporting phase. Elastic instability and early leaf expansion might also be consistent with tendril and hook climbing mechanisms that attach to narrow branches on contact. It is perhaps less consistent with circumnutatory movements and twining attachment. In summary, some of the leaf deployment strategies are consistent with the idea that reach and leaf deployment on top of host leafy shoots might be coordinated.

Overall, most searcher shoots developed leaves to some extent but the development and positioning of leaves vary a lot between individual species and functional groups. Our observations of leafy searchers suggest that leaf development probably varies according to different searcher attachment mechanisms.

In the long reaching stem twiner *Odontadenia* leaf expansion occurs close to the basal attachment point of the searcher but leaf primordia along the rest of the searcher do not continue development if the searcher remains in an open self-supporting state. Among twiners, it appears that searchers can grow autonomously without leaves up to around 1 m in length but after this most species need to develop leaves to maintain growth. The longest reaching species *Uncaria guianensis* developed an order of magnitude more of leaf area than other species. This is consistent with its high rigidity and an attachment mode that does not rely on rapid movements and circumnutation. The example highlights the fact that some species can sacrifice active searching and circumnutatory movements for long reach with high rigidity, high leaf surface area (autonomy), and passive attachment mechanism via open hook-like organs.

Reach, Trade-Offs, and Approaches

Our survey of liana searchers and their reach has highlighted some important principles on how climbing plants cross gaps to attach to supports. First, at the risk of generalisation numerous studies have highlighted the huge diversity of cambial variants across many liana groups and its functional convergence to promote flexibility and toughness. We suggest that the diversity and convergence of the self-supporting and attaching phases of the life history are no less important for understanding the climbing growth habit, but have perhaps not been as fully studied. Our findings highlighted the fact that the reach of searchers is integrated with other essential functional traits. A key finding is that long reach requires sufficient rigidity in the basal part of the searcher. However, long-reach and high rigidity might limit active circumnutational and nutational searching movements to more distal parts of the searcher. We suspect that this basic underlying requirement and limit on searching movement is a key feature of liana growth strategies, from short range highly mobile searcher behaviours to long range less mobile searching and foraging behaviours. Our study suggests that this trade-off between reach length and searching behaviour also influences the strength and reliability of attachment. Most long-range searchers attach by branch-hook-angle mechanisms, which only need passive or swaying movements of the searcher to engage. Most shorter-range searching mechanisms rely on less rigid mechanical organisations and could depend on stem twining and tendril climbing. Long range branch-hook-angle attachments require that the searcher stays in tension to remain engaged whereas short range twining and tendril mechanisms can form irreversible attachments to the appropriate supports.

Our study only analysed the maximal reach of searcher shoots, in other words, the longest reaches a given species can span. It would be interesting for further studies to see, in particular, whether woody, long-reaching, branch-hook-angle climbers can attach and exploit short range supports in cluttered 3-D spaces or whether they are more restricted to spanning longer distances. The whole question of the ability of a given species to effectively reach and attach across short or long distances is an important ecological consideration.

This study is an unashamedly detailed exploration of reach, stem mechanics, tissue distributions, and attachment mechanisms in climbing plant searchers. Broad-based comparisons of many species at an ecological scale would probably require a shorter task list of nevertheless informative traits providing information on vine and liana dynamics. What are the key traits among the traits? We think that the shift from "stiff" to "flexible" is central to vine and liana biology and a major axis of the developmental spectrum that can potentially explain many patterns of functional diversity at an ecological level. The relationship between stem rigidity (*EI*), stem stiffness (*E*) and stem second moment of area (*I*) pioneered for climbing plants by Speck (1991) is a powerful approach and can also be relatively easily carried out in the field with minimal logistics. Conserving stem segments measured in basic storage media (alcohol) can enable further measurements of density, tissue development as well as chemical and ultrastructural traits at a later date if desired. Of course, without necessarily going into the same level of tissue mapping detail that we demonstrate in this paper. However, the opportunity to identify tissue patterns in relation to mechanical properties and measures of performance such as reach offer higher levels of interpretation than for example measurements restricted to stem or wood density.

From Climbing Plants to New Technologies

Our study on searcher biology highlighted the interest of observing and measuring liana searchers in field conditions, where functional traits can be measured in the context of the demands and constraints acting on them in the environment. These not only generate information on the functional biology and potential ecological implications of complex functional traits but can at the same time generate new information for bioinspired technologies. Plant stems have been of interest over recent years as potential models for new technological innovations (Milwich et al., 2006). Climbing plants have come under increasing scrutiny as biological role models for new technological applications, particularly in soft robotics (Fiorello et al., 2020). The light structured organisation of searcher shoots—the use of a light central pith as a mechanical spacer; externally placed rings, columns, ribs and struts of stiff, light, geometrically optimised tissues are all present in the limited sample we studied. All are of potential interest as transferable blueprints for new kinds of technical artefacts. Searcher-like artefacts for difficult-to-reach applications in cluttered, cramped, and unpredictable 3-D spaces have been developed from climbing plants (Walker, 2015; Wooten and Walker, 2018; Wooten et al., 2018). Other studies have explored climbing plant searchers for technical innovations in terms of new bio-inspired actuating mechanisms based on changes in stem orientation, stem shape, and swellability of their hydrogel-like tissues (Soffiatti and Rowe, 2020; Bastola et al., 2021a,b).

At the beginning of this paper, we mentioned that the presence of multi-attachment systems seemed "complex" and "difficult to suitably classify or group." This attachment organ dilemma highlights the difficulty and usefulness of trying to "group" climbing plant life histories or functional groups via a single "key syndrome." The issue is probably widespread in functional biology and ecology. In fact, detailed *in situ-field* observations indicate that multi-attachment systems are common and can show a meaningful and consistent overall functionality when observed with respect to the plant development (in time) and the spatial and three-dimensional contingencies in the environment (in space). Notions such as two-step attachment mechanisms in the spines and root-climbing attachment of a climbing cactus (Soffiatti and Rowe, 2020) and active, coordinated, multi-step attachment processes in the humble English ivy (Melzer et al., 2010) are the kinds of dynamic trait combination that when understood and measured in the field and lab can potentially resolve (i) the problem of "attempting to group climbing plant life histories by attachment type, (ii) demonstrate and resolve a detailed functionality and (iii) provide novel concepts for bioinspired technologies based on trait behaviours under real-world situations.

DATA AVAILABILITY STATEMENT

Data are available at https://zenodo.org/record/6347468.

AUTHOR CONTRIBUTIONS

NR, PH, and TH conceived and designed the study and performed the data analysis. TH, LP-B, PH, and NR collected the field samples and measured the morphological and biomechanical traits. TH, LP-B, and CH performed the anatomical sections. TH, PH, NR, and CH performed image interpretation and analysis. TH and NR wrote the manuscript with contribution of PH. All authors discussed the results and contributed valuable comments on the manuscript.

FUNDING

This project has received funding from the European Union's Horizon 2020 research and innovation program under Grant Agreement No. 824074 (GrowBot) and an "Investissement d'Avenir" grant from the Agence Nationale de la Recherche (CEBA: ANR-10-LABX-0025; ARBRE, ANR-11-LABX-0002-01). TH was supported by a doctoral fellowship from the CEBA.

ACKNOWLEDGMENTS

We thank Chantal Geniez (IRD, UMR AMAP) and Maryline Harroué (INRAE, UMR SILVA) for performing a significant part of the anatomical sections. We also thank

Quentin Le Blaye and Stéphane Fourtier (INRAe, UMR AMAP) for their contribution to the technical development of the study as well as Tancrède Alméras (CNRS, UMR LMGC) for sharing a script for analysis of second moment of area. We thank many colleagues of UMR ECOFOG: Geraldine Derroire and Laetitia Plaisance (CIRAD) for facilities on field work. In particular, we also thank Jacques Beauchêne (CIRAD) for hosting us at the wood lab of Pariacabo and the loan of equipment. We also thank Clément Stahl (INRAe) and Sabrina Coste (French Guiana University), from the ecophysiology lab (INRAe) for technical assistance. We would also like to thank SILVATECH (Silvatech, INRAE, 2018; Structural and functional analysis of tree and wood Facility, doi: 10.15454/1.5572400113627854E12) from UMR 1434 SILVA, 1136 IAM, 1138 BEF, and 4370 EA LERMAB from the research center INRAE Grand-Est Nancy for its contribution to stem cross-section production. SILVATECH facility was supported by the French National Research Agency through the Laboratory of Excellence ARBRE (ANR-11-LABX-0002-01).

SUPPLEMENTARY MATERIAL

The Supplementary Material for this article can be found online at: https://www.frontiersin.org/articles/10.3389/ffgc.2022.836247/full#supplementary-material

REFERENCES

Baillaud, L. (1962). "Les mouvements d'exploration et d'enroulement des plantes volubiles," in *Physiology of Movements / Physiologie der Bewegungen*, eds L. Aletsee, L. Anker, L. Baillaud, G. H. Banbury, L. Brauner, W. M. L. Crombie, et al. (Berlin: Springer Berlin Heidelberg), 635–715. doi: 10.1007/978-3-642-94852-7_18

Baret, S., Nicolini, E., Le Bourgeois, T., and Strasberg, D. (2003). Developmental patterns of the invasive bramble (*Rubus alceifolius* Poiret, Rosaceae) in Réunion Island: an architectural and morphometric analysis. *Ann. Bot.* 91, 39–48. doi: 10.1093/aob/mcg006

Bartumeus, F., and Catalan, J. (2009). Optimal search behavior and classic foraging theory. *J. Phys. Math. Theor.* 42:434002. doi: 10.1088/1751-8113/42/43/434002

Bastola, A. K., Rodriguez, N., Behl, M., Soffiatti, P., Rowe, N. P., and Lendlein, A. (2021a). Cactus-inspired design principles for soft robotics based on 3D printed hydrogel-elastomer systems. *Mater. Des.* 202:109515. doi: 10.1016/j.matdes.2021.109515

Bastola, A. K., Soffiatti, P., Behl, M., Lendlein, A., and Rowe, N. P. (2021b). Structural performance of a climbing cactus: making the most of softness. *J. R. Soc. Interface* 18:20210040. doi: 10.1098/rsif.2021.0040

Bauer, G., Klein, M.-C., Gorb, S. N., Speck, T., Voigt, D., and Gallenmüller, F. (2011). Always on the bright side: the climbing mechanism of *Galium aparine*. *Proc. R. Soc. B Biol. Sci.* 278, 2233–2239. doi: 10.1098/rspb.2010.2038

Borchert, R., and Pockman, W. T. (2005). Water storage capacitance and xylem tension in isolated branches of temperate and tropical trees. *Tree Physiol.* 25, 457–466. doi: 10.1093/treephys/25.4.457

Bowling, A. J., and Vaughn, K. C. (2009). Gelatinous fibers are widespread in coiling tendrils and twining vines. *Am. J. Bot.* 96, 719–727. doi: 10.3732/ajb.0800373

Caballé, G. (1986). *Sur la biologie des lianes ligneuses en forêt gabonaise*. Ph. D. thesis. Montpellier: Université des Sciences et Techniques du Languedoc.

Caballé, G. (1998). Le port autoportant des lianes tropicales : une synthèse des stratégies de croissance. *Can. J. Bot.* 76, 1703–1716.

Cabanillas, P. A., and Hurrell, J. A. (2012). Plantas trepadoras: tipo biologico y clasificacion. *Cienc. Morfol.* 14:95.

Cai, Z.-Q., Poorter, L., Han, Q., and Bongers, F. (2008). Effects of light and nutrients on seedlings of tropical Bauhinia lianas and trees. *Tree Physiol.* 28, 1277–1285. doi: 10.1093/treephys/28.8.1277

Campbell, M. J., Edwards, W., Magrach, A., Alamgir, M., Porolak, G., Mohandass, D., et al. (2018). Edge disturbance drives liana abundance increase and alteration of liana–host tree interactions in tropical forest fragments. *Ecol. Evol.* 8, 4237–4251. doi: 10.1002/ece3.3959

Care, A.-F., Nefed'ev, L., Bonnet, B., Millet, B., and Badot, P.-M. (1998). Cell elongation and revolving movement in *Phaseolus vulgaris* L. twining shoots. *Plant Cell Physiol.* 39, 914–921. doi: 10.1093/oxfordjournals.pcp.a029454

Carrasco-Urra, F., and Gianoli, E. (2009). Abundance of climbing plants in a southern temperate rain forest: host tree characteristics or light availability? *J. Veg. Sci.* 20, 1155–1162. doi: 10.1111/j.1654-1103.2009.01115.x

Chabbert, B., Monties, B., Rowe, N. P., and Speck, T. (1997). "Variability of lignin composition and lignification pattern in the lianescent and self-supporting growth phase of the liana *Condylocarponn guianense*," in *Plant Biomechanics: Conference Proceedings*, Vol. 1, eds G. J. Jeronimidis and J. F. V. Vincent (Reading: Centre for Biomimetics, The University of Reading), 73–78.

Charnov, E. L. (1976). Optimal foraging, the marginal value theorem. *Theor. Popul. Biol.* 9, 129–136. doi: 10.1016/0040-5809(76)90040-X

Chery, J. G., Glos, R. A. E., and Anderson, C. T. (2020). Do woody vines use gelatinous fibers to climb? *New Phytol.* 2020:17576. doi: 10.1111/nph.17576

Clair, B., Ghislain, B., Prunier, J., Lehnebach, R., Beauchêne, J., and Alméras, T. (2019). Mechanical contribution of secondary phloem to postural control in trees: the bark side of the force. *New Phytol.* 221, 209–217. doi: 10.1111/nph.15375

Coudurier, T. (1992). *Sur la place des lianes dans la forêt guyanaise : une approche qui utilise l'architecture végétale*. Ph. D. thesis. Montpellier: Université des Sciences et Techniques du Languedoc.

Darwin, C. (1875). *The Movements and Habits of Climbing Plants*. London: John Murray.

Ennos, R. (2011). *Solid Biomechanics*. Princeton: Princeton University Press, doi: 10.1515/9781400840649

Evert, R. F. (2006). *Esau's Plant Anatomy: Meristems, Cells, and Tissues of the Plant Body: Their Structure, Function, and Development*. Hoboken, NJ: John Wiley & Sons.

Ewers, F. W., Fisher, J. B., and Fichtner, K. (1991). "Water flux and xylem structure in vines," in *The Biology of Vines*, eds F. E. Putz and H. A. Mooney (Cambridge: Cambridge University Press), 127–160.

Fiorello, I., Del Dottore, E., Tramacere, F., and Mazzolai, B. (2020). Taking inspiration from climbing plants: methodologies and benchmarks—a review. *Bioinspir. Biomim.* 15:031001. doi: 10.1088/1748-3190/ab7416

French, J. C. (1977). Growth relationships of leaves and internodes in viny angiosperms with different modes of attachment. *Am. J. Bot.* 64, 292–304. doi: 10.1002/j.1537-2197.1977.tb15730.x

Gallagher, R. V., and Leishman, M. R. (2012). A global analysis of trait variation and evolution in climbing plants. *J. Biogeogr.* 39, 1757–1771. doi: 10.1111/j.1365-2699.2012.02773.x

Gallenmüller, F., Bauer, G., Kubinski, K.-R., Voigt, D., Gorb, S., and Speck, T. (2009). Plant leaves as attachment devices: an experimental approach. *Sixth Plant Biomech. Conf. Novemb. 16th 21st Cayenne Fr. Guyana Fr.* 2009:194.

Gallenmüller, F., Rowe, N. P., and Speck, T. (2004). Development and growth form of the neotropical liana *Croton nuntians*: the effect of light and mode of attachment on the biomechanics of the stem. *J. Plant Growth Regul.* 23, 83–97. doi: 10.1007/s00344-004-0045-z

Gartner, B. L. (1991). Is the climbing habit of poison oak ecotypic? *Funct. Ecol.* 5, 696–704. doi: 10.2307/2389490

Gentry, A. G. (1991). "The distribution and evolution of climbing plants," in *The Biology of Vines*, eds F. E. Putz and H. A. Mooney (Cambridge: Cambridge University Press), 3–42.

Gerbode, S. J., Puzey, J. R., McCormick, A. G., and Mahadevan, L. (2012). How the cucumber tendril coils and overwinds. *Science* 337, 1087–1091. doi: 10.1126/science.1223304

Gianoli, E. (2003). Phenotypic responses of the twining vine *Ipomoea purpurea* (Convolvulaceae) to physical support availability in sun and shade. *Plant Ecol.* 165, 21–26. doi: 10.1023/A:1021412030897

Gianoli, E. (2015). The behavioural ecology of climbing plants. *AoB Plants* 7:lv013. doi: 10.1093/aobpla/plv013

Givnish, T. J. (1995). "Plant Stems: biomechanical adaptation for energy capture and influence on species distributions," in *Plant Stems: Physiology and Functional Morphology* Physiological Ecology, ed. B. L. Gartner (San Diego: Academic Press), 3–49. doi: 10.1016/B978-012276460-8/50003-5

Goriely, A., and Neukirch, S. (2006). Mechanics of climbing and attachment in twining plants. *Phys. Rev. Lett.* 97:184302. doi: 10.1103/PhysRevLett.97.184302

Guerra, S., Peressotti, A., Peressotti, F., Bulgheroni, M., Baccinelli, W., D'Amico, E., et al. (2019). Flexible control of movement in plants. *Sci. Rep.* 9:16570. doi: 10.1038/s41598-019-53118-0

Hegarty, E. E. (1991). "Vine-host interactions," in *The Biology of Vines*, eds F. E. Putz and H. A. Mooney (Cambridge: Cambridge University Press), 357–375.

Hoffmann, B., Chabbert, B., Monties, B., and Speck, T. (2003). Mechanical, chemical and X-ray analysis of wood in the two tropical lianas *Bauhinia guianensis* and *Condylocarpon guianense*: variations during ontogeny. *Planta* 217, 32–40. doi: 10.1007/s00425-002-0967-2

Isnard, S., and Rowe, N. P. (2008). Mechanical role of the leaf sheath in rattans. *New Phytol.* 177, 643–652. doi: 10.1111/j.1469-8137.2007.02308.x

Isnard, S., Speck, T., and Rowe, N. P. (2003). Mechanical architecture and development in Clematis: implications for canalised evolution of growth forms. *New Phytol.* 158, 543–559. doi: 10.1046/j.1469-8137.2003.00771.x

Isnard, S., Speck, T., and Rowe, N. P. (2005). Biomechanics and development of the climbing habit in two species of the South American palm genus *Desmoncus* (Arecaceae). *Am. J. Bot.* 92, 1444–1456. doi: 10.3732/ajb.92.9.1444

Katabuchi, M. (2015). LeafArea: an R package for rapid digital image analysis of leaf area. *Ecol. Res.* 30, 1073–1077. doi: 10.1007/s11284-015-1307-x

Lahaye, R., Civeyrel, L., Speck, T., and Rowe, N. P. (2005). Evolution of shrub-like growth forms in the lianoid subfamily Secamonoideae (Apocynaceae s.l.) of Madagascar: phylogeny, biomechanics, and development. *Am. J. Bot.* 92, 1381–1396. doi: 10.3732/ajb.92.8.1381

Laurance, W. F., Andrade, A. S., Magrach, A., Camargo, J. L. C., Valsko, J. J., Campbell, M., et al. (2014). Long-term changes in liana abundance and forest dynamics in undisturbed Amazonian forests. *Ecology* 95, 1604–1611. doi: 10.1890/13-1571.1

Lauri, P. -É (1988). *Le mouvement morphogénétique : approche morphométrique et restitution graphique. L'exemple de quelques plantes tropicales*. Ph. D. thesis. Montpellier: Université de Montpellier, 565.

Lauri, P. -É, and Kelner, J.-J. (2001). Shoot type demography and dry matter partitioning: a morphometric approach in apple (*Malus* × *domestica*). *Can. J. Bot.* 79, 1270–1273. doi: 10.1139/b01-113

Ledo, A., and Schnitzer, S. A. (2014). Disturbance and clonal reproduction determine liana distribution and maintain liana diversity in a tropical forest. *Ecology* 95, 2169–2178. doi: 10.1890/13-1775.1

Lehnebach, R., Alméras, T., and Clair, B. (2020). How does bark contribution to postural control change during tree ontogeny? A study of six Amazonian tree species. *J. Exp. Bot.* 71, 2641–2649. doi: 10.1093/jxb/eraa070

Leroux, O. (2012). Collenchyma: a versatile mechanical tissue with dynamic cell walls. *Ann. Bot.* 110, 1083–1098. doi: 10.1093/aob/mcs186

Letcher, S. G. (2015). Patterns of liana succession in tropical forests. *Ecol. Lianas* 2015, 116–130. doi: 10.1002/9781118392409.ch10

Letcher, S. G., and Chazdon, R. L. (2012). Life history traits of lianas during tropical forest succession. *Biotropica* 44, 720–727. doi: 10.1111/j.1744-7429.2012.00865.x

Levionnois, S., Coste, S., Nicolini, E., Stahl, C., Morel, H., and Heuret, P. (2020). Scaling of petiole anatomies, mechanics and vasculatures with leaf size in the widespread Neotropical pioneer tree species *Cecropia obtusa* Trécul (Urticaceae). *Tree Physiol.* 40, 245–258. doi: 10.1093/treephys/tpz136

Levionnois, S., Salmon, C., Alméras, T., Clair, B., Ziegler, C., Coste, S., et al. (2021). Anatomies, vascular architectures, and mechanics underlying the leaf size-stem size spectrum in 42 Neotropical tree species. *J. Exp. Bot.* 72, 7957–7969. doi: 10.1093/jxb/erab379

Mahley, J. N., Pittermann, J., Rowe, N. P., Baer, A., Watkins, J. E., Schuettpelz, E., et al. (2018). Geometry, allometry and biomechanics of fern leaf petioles: their significance for the evolution of functional and ecological diversity within the pteridaceae. *Front. Plant Sci.* 9:197. doi: 10.3389/fpls.2018.00197

Meloche, C. G., Knox, J. P., and Vaughn, K. C. (2006). A cortical band of gelatinous fibers causes the coiling of redvine tendrils: a model based upon cytochemical and immunocytochemical studies. *Planta* 225, 485–498. doi: 10.1007/s00425-006-0363-4

Melzer, B., Steinbrecher, T., Seidel, R., Kraft, O., Schwaiger, R., and Speck, T. (2010). The attachment strategy of English ivy: a complex mechanism acting on several hierarchical levels. *J. R. Soc. Interface* 7, 1383–1389. doi: 10.1098/rsif.2010.0140

Ménard, L., McKey, D., and Rowe, N. P. (2009). Developmental plasticity and biomechanics of treelets and lianas in *Manihot* aff. *quinquepartita* (Euphorbiaceae): a branch-angle climber of French Guiana. *Ann. Bot.* 103, 1249–1259. doi: 10.1093/aob/mcp078

Ménard, L., McKey, D., Mühlen, G. S., Clair, B., and Rowe, N. P. (2013). The evolutionary fate of phenotypic plasticity and functional traits under domestication in manioc: changes in stem biomechanics and the appearance of stem brittleness. *PLoS One* 8:e74727. doi: 10.1371/journal.pone.0074727

Menninger, E. A. (1970). *Flowering vines of the world: an encyclopedia of climbing plants*. Downers Grove, IL: Hearthside Press.

Millet, B., Melin, D., and Badot, P.-M. (1988). Circumnutation in *Phaseolus vulgaris*. I. Growth, osmotic potential and cell ultrastructure in the free-moving part of the shoot. *Physiol. Plant.* 72, 133–138. doi: 10.1111/j.1399-3054.1988.tb06634.x

Milwich, M., Speck, T., Speck, O., Stegmaier, T., and Planck, H. (2006). Biomimetics and technical textiles: solving engineering problems with the help of nature's wisdom. *Am. J. Bot.* 93, 1455–1465. doi: 10.3732/ajb.93.10.1455

Mori, H., Ueno, S., Matsumoto, A., Kamijo, T., Tsumura, Y., and Masaki, T. (2018). Large contribution of clonal reproduction to the distribution of deciduous liana species (*Wisteria floribunda*) in an old-growth cool temperate forest: evidence from genetic analysis. *Ann. Bot.* 121, 359–365. doi: 10.1093/aob/mcx153

Moulia, B., Coutand, C., and Lenne, C. (2006). Posture control and skeletal mechanical acclimation in terrestrial plants: implications for mechanical modeling of plant architecture. *Am. J. Bot.* 93, 1477–1489. doi: 10.3732/ajb.93.10.1477

Nabe-Nielsen, J., and Hall, P. (2002). Environmentally induced clonal reproduction and life history traits of the liana *Machaerium cuspidatum* in an Amazonian rain forest, Ecuador. *Plant Ecol.* 12, 215–226.

Niklas, K. J. (1999b). "The mechanical stability of vertical stems," in *The evolution of plant architecture*, eds M. H. Kurmann and A. R. Hemsley (Kew: Royal Botanic Gardens), 377–397.

Niklas, K. J. (1999a). The mechanical role of bark. *Am. J. Bot.* 86, 465–469. doi: 10.2307/2656806

Niklas, K. J., and Spatz, H.-C. (2012). *Plant physics*. Chicago: University of Chicago Press.

Olson, M. E., Rosell, J. A., Muñoz, S. Z., and Castorena, M. (2018). Carbon limitation, stem growth rate and the biomechanical cause of Corner's rules. *Ann. Bot.* 122, 583–592. doi: 10.1093/aob/mcy089

Peñalosa, J. (1982). Morphological specialization and attachment success in two twining lianas. *Am. J. Bot.* 69, 1043–1045. doi: 10.1002/j.1537-2197.1982.tb13348.x

Peñalosa, J. (1984). Basal branching and vegetative spread in two tropical rain forest lianas. *Biotropica* 16:1. doi: 10.2307/2387886

Pittermann, J., and Olson, M. E. (2018). Transport efficiency and cavitation resistance in developing shoots: a risk worth taking. *Tree Physiol.* 38, 1085–1087. doi: 10.1093/treephys/tpy094

Plavcová, L., and Jansen, S. (2015). "The role of xylem parenchyma in the storage and utilization of nonstructural carbohydrates," in *Functional and Ecological Xylem Anatomy*, ed. U. Hacke (Cham: Springer International Publishing), 209–234. doi: 10.1007/978-3-319-15783-2_8

Putz, F. E. (1984). The natural history of lianas on Barro Colorado Island, Panama. *Ecology* 65, 1713–1724. doi: 10.2307/1937767

Putz, F. E., and Holbrook, N. M. (1991). "Biomechanical studies of vines," in *The Biology of Vines*, eds F. E. Putz and H. A. Mooney (Cambridge: Cambridge University Press), 73–97.

Pyke, G. H. (1984). Optimal foraging theory: a critical review. *Annu. Rev. Ecol. Syst.* 15, 523–575. doi: 10.1146/annurev.es.15.110184.002515

Raciborski, M. (1900). Über die Vorläuferspitze. *Flora* 87, 1–25.

Read, J., and Stokes, A. (2006). Plant biomechanics in an ecological context. *Am. J. Bot.* 93, 1546–1565. doi: 10.3732/ajb.93.10.1546

Rivière, M., Derr, J., and Douady, S. (2017). Motions of leaves and stems, from growth to potential use. *Phys. Biol.* 14:051001. doi: 10.1088/1478-3975/aa5945

Rosell, J. A., and Olson, M. E. (2014). The evolution of bark mechanics and storage across habitats in a clade of tropical trees. *Am. J. Bot.* 101, 764–777. doi: 10.3732/ajb.1400109

Rowe, N. P., and Speck, T. (1996). Biomechanical characteristics of the ontogeny and growth habit of the tropical liana *Condylocarpon guianense* (Apocynaceae). *Int. J. Plant Sci.* 157, 406–417. doi: 10.1086/297357

Rowe, N. P., Isnard, S., and Speck, T. (2006). "Diversity of mechanical architectures in climbing plants: an ecological perspective," in *Ecology and biomechanics: a mechanical approach to the ecology of animals and plants*, eds A. Herrel, T. Speck, and N. P. Rowe (Boca Raton, FL: CRC Press), 35–59. doi: 10.1111/j.1469-8137.2004.01309.x

Rowe, N., Isnard, S., and Speck, T. (2004). Diversity of mechanical architectures in climbing plants: an evolutionary perspective. *J. Plant Growth Regul.* 23, 108–128. doi: 10.1007/s00344-004-0044-0

Schenck, H. (1892). *Beiträge zur Biologie und Anatomie der Lianen im besonderen der in Brasilien einheimischen Arten*. Frankfurt am Main: G. Fischer.

Simonetti, V., Bulgheroni, M., Guerra, S., Peressotti, A., Peressotti, F., Baccinelli, W., et al. (2021). Can plants move like animals? A three-dimensional stereovision analysis of movement in plants. *Animals* 11:1854. doi: 10.3390/ani11071854

Soffiatti, P., and Rowe, N. P. (2020). Mechanical innovations of a climbing cactus: functional insights for a new generation of growing robots. *Front. Robot. AI* 7:64. doi: 10.3389/frobt.2020.00064

Sousa-Baena, M. S., Hernandes-Lopes, J., and Van Sluys, M.-A. (2021). Reaching the top through a tortuous path: helical growth in climbing plants. *Curr. Opin. Plant Biol.* 59:101982. doi: 10.1016/j.pbi.2020.101982

Sousa-Baena, M. S., Sinha, N. R., Hernandes-Lopes, J., and Lohmann, L. G. (2018). Convergent evolution and the diverse ontogenetic origins of tendrils in angiosperms. *Front. Plant Sci.* 9:403. doi: 10.3389/fpls.2018.00403

Speck, T. (1991). "Changes of the bending mechanics of lianas and self-supporting taxa during ontogeny", in: Natural structures. principles, Strategies and models in Architecture and Nature, Proceedings of the II International Symposium Sonderforschungsbereich 230, part I. *Mitteilungen des SFB 230 Heft* 6, 89–95.

Speck, T., and Rowe, N. P. (1999). "A quantitative approach for analytically defining size, growth form and habit in living and fossil plants," in *The evolution of plant architecture*, eds M. H. Kurmann and A. R. Hemsley (Kew: Royal Botanic Gardens), 447–479.

Steinbrecher, T., Danninger, E., Harder, D., Speck, T., Kraft, O., and Schwaiger, R. (2010). Quantifying the attachment strength of climbing plants: A new approach. *Acta Biomater.* 6, 1497–1504. doi: 10.1016/j.actbio.2009.10.003

Stolarz, M. (2009). Circumnutation as a visible plant action and reaction: physiological, cellular and molecular basis for circumnutations. *Plant Signal. Behav.* 4, 380–387. doi: 10.4161/psb.4.5.8293

Walker, I. D. (2015). Biologically inspired vine-like and tendril-like robots. *SAI* 2015, 714–720. doi: 10.1109/SAI.2015.7237221

Warton, D. I., Duursma, R. A., Falster, D. S., and Taskinen, S. (2012). smatr 3– an R package for estimation and inference about allometric lines. *Methods Ecol. Evol.* 3, 257–259. doi: 10.1111/j.2041-210X.2011.00153.x

Wooten, M., and Walker, I. (2018). Vine-inspired continuum tendril robots and circumnutations. *Robotics* 7:58. doi: 10.3390/robotics7030058

Wooten, M., Frazelle, C., Walker, I. D., Kapadia, A., and Lee, J. H. (2018). Exploration and inspection with vine-inspired continuum robots. *ICRA* 2018, 5526–5533. doi: 10.1109/ICRA.2018.8461132

Wyka, T. P., Oleksyn, J., Karolewski, P., and Schnitzer, S. A. (2013). Phenotypic correlates of the lianescent growth form: a review. *Ann. Bot.* 112, 1667–1681. doi: 10.1093/aob/mct236

Conflict of Interest: The authors declare that the research was conducted in the absence of any commercial or financial relationships that could be construed as a potential conflict of interest.

frontiers | Frontiers in Forests and Global Change

ORIGINAL RESEARCH
published: 12 April 2022
doi: 10.3389/ffgc.2022.834891

Lianas and Trees From a Seasonally Dry and a Wet Tropical Forest Did Not Differ in Embolism Resistance but Did Differ in Xylem Anatomical Traits in the Dry Forest

Chris M. Smith-Martin[1,2]*, Steven Jansen[3], Timothy J. Brodribb[4], José A. Medina-Vega[2,5,6], Christopher Lucani[4], Andrea Huppenberger[3] and Jennifer S. Powers[7]

[1] Department of Ecology, Evolution, and Evolutionary Biology, Columbia University, New York, NY, United States, [2] Smithsonian Tropical Research Institute, Balboa, Panama, [3] Institute of Systematic Botany and Ecology, Ulm University, Ulm, Germany, [4] School of Biological Sciences, University of Tasmania, Hobart, TAS, Australia, [5] Forest Ecology and Forest Management Group, Wageningen University and Research Centre, Wageningen, Netherlands, [6] Forest Global Earth Observatory, Smithsonian Tropical Research Institute, Washington, DC, United States, [7] Department of Ecology, Evolution, and Behavior, University of Minnesota, St. Paul, MN, United States

OPEN ACCESS

Edited by:
Geertje M. F. Van Der Heijden,
University of Nottingham,
United Kingdom

Reviewed by:
Hannes De Deurwaerder,
Princeton University, United States
Leonor Álvarez Cansino,
Seville University, Spain

***Correspondence:**
Chris M. Smith-Martin
chrismsmithmartin@gmail.com

Specialty section:
This article was submitted to
Tropical Forests,
a section of the journal
Frontiers in Forests and Global
Change

Received: 13 December 2021
Accepted: 16 February 2022
Published: 12 April 2022

Citation:
Smith-Martin CM, Jansen S, Brodribb TJ, Medina-Vega JA, Lucani C, Huppenberger A and Powers JS (2022) Lianas and Trees From a Seasonally Dry and a Wet Tropical Forest Did Not Differ in Embolism Resistance but Did Differ in Xylem Anatomical Traits in the Dry Forest.
Front. For. Glob. Change 5:834891.
doi: 10.3389/ffgc.2022.834891

One of the most prominent changes in neotropical forests has been the increase in abundance and size of lianas. Studies suggest that lianas have more acquisitive strategies than trees, which could allow them to take advantage of water more effectively when it is available in water-limited forests, but few studies compared across growth form (i.e., lianas vs. trees) and forest type (i.e., wet vs. seasonally dry). We measured hydraulic and anatomical traits of co-occurring lianas and trees that convey drought resistance (xylem embolism resistance and intervessel pit membranes) and water transport capacity (xylem vessel diameter and density) in a seasonally dry and a wet evergreen tropical forest to address: (1) Are there differences between vulnerability to embolisms (P_{50}—water potential at 50% loss of hydraulic conductivity) and hydraulic safety margins (HSM) across growth form and forest type? (2) How do vessel diameter and density vary across growth form and forest type? (3) Are there differences in xylem intervessel pit membrane thickness across growth form and forest type and does it predict xylem embolism vulnerability in trees and lianas? We examined hydraulic and xylem anatomical traits of 32 species—eight lianas and eight trees in each forest type. We found no difference in P_{50} and HSMs between lianas and trees and between the wetter and drier forest. Dry forest lianas had 81% greater maximum vessel diameter and 125% greater range in vessel diameter sizes than dry forest trees but, there was no significant difference between life forms in the wet forest. Dry forest species had 50% greater vessel density and 30% greater maximum pit membrane thickness than wet forest ones. Maximum pit membrane thickness was correlated to P_{50} and HSMs. The main difference between lianas and trees occurred in the dry forest, where lianas had larger maximum xylem vessel size than trees, implying that they have proportionally greater hydraulic conductive capacity than the trees in seasonal forests.

Keywords: canopy crane, Isthmus of Panama, plant functional traits, plant hydraulic strategies, P_{50} optical vulnerability technique, rainfall gradient, woody plant growth forms, xylem intervessel pit membranes

INTRODUCTION

Anthropogenic climate change has been causing shifts in rainfall patterns that are altering ecosystems worldwide and severe drought events have led to widespread forest mortality across many ecosystems, including tropical forests (Anderegg et al., 2012; Allen et al., 2015; Aleixo et al., 2019; Powers et al., 2020). Tropical ecosystems store the largest quantity of terrestrial aboveground biomass (Bonan, 2008; Pan et al., 2011) and rising tropical forest mortality could lead to large carbon losses to the atmosphere, turning these forests from a carbon sink to a source, and exacerbating climate change (Gatti et al., 2014). Because natural drought events are anticipated to become more severe and last longer (Duffy et al., 2015; Chadwick et al., 2016), high rates of forest mortality are likely to persist and even rise (Brodribb et al., 2020b). Increases in tree mortality and growth declines have been associated with severe drought across several neotropical forests (Chazdon et al., 2005; Uriarte et al., 2016; Leitold et al., 2018; Powers et al., 2020). Drought impacts, however, differ among species, and rates of mortality and declines in growth depend on a suite of species' non-independent functional traits, including hydraulic traits. Groups of species with the same growth form may also share traits leading them to perform similarly when water is limited, and this may result in, for example, lianas being less impacted from seasonality and drought compared to trees (Schnitzer, 2005; Schnitzer and Bongers, 2011; Schnitzer and van der Heijden, 2019; Smith-Martin et al., 2019). Yet, growth form-level responses to drought are still poorly understood (Smith-Martin et al., 2020). Accurately predicting how tropical forests respond to drought, including more frequent and severe drought events, requires a deeper understanding of not only species-level but also growth form-level responses to water deficit.

Lianas are one of the most abundant life forms, second only to trees, in many tropical forests (Gentry, 1991, 1995) representing up to 35% of woody species (Schnitzer et al., 2012) and up to 40% of woody stems (Schnitzer and Bongers, 2011). Contrary to most vascular plant groups which are more abundant in wetter tropical forests compared to drier ones, lianas are particularly dominant in forests that experience seasonal drought (Gentry, 1995; Schnitzer, 2005; DeWalt et al., 2015; Schnitzer, 2018). One of the most notable changes in neotropical forests over the past several decades has been the increase in abundance and size of lianas (Phillips et al., 2002; Wright et al., 2004; Schnitzer and Bongers, 2011; Yorke et al., 2013). The leading explanation for this increase in lianas is the seasonal growth advantage hypothesis, which states that plant species that grow well during seasonal drought obtain a growth advantage in forests with increasing seasonality relative to co-occurring species that grow poorly during seasonal drought (Schnitzer, 2005, 2018; Schnitzer and van der Heijden, 2019). Many lines of evidence support the seasonal growth advantage hypothesis; trees seem to suffer more from lack of water during seasonal drought than lianas and lianas may maintain better whole-plant water status (Smith-Martin et al., 2019) and grow more than trees during drought (Schnitzer and van der Heijden, 2019). Moreover, some studies have shown that lianas have more acquisitive strategies than trees (Asner and Martin, 2012; Werden et al., 2017; Smith-Martin et al., 2019; Medina-Vega et al., 2021a), which could allow them to take advantage of water more effectively when it is available in water-limited forests. However, liana resource acquisition strategies may differ depending on rainfall regimes. For example, lianas have been found to have "cheaper" and more efficient leaves in a drier forest compared to trees, whereas this difference did not exist in a wet forest (Medina-Vega et al., 2021a). Despite some evidence that differences between lianas and trees may be more pronounced in drier forests (Medina-Vega et al., 2021a), few studies have explored the physiological and anatomical traits that underly the differences in water use of lianas and trees in wetter and drier forests.

Functional traits related to water movement and drought resistance can shed light on performance under different water availability regimes. One of the mechanisms involved in drought-induced plant mortality is the catastrophic failure of the plant hydraulic system caused by embolisms in xylem conduits that restrict the movement of water to the leaves (Sperry et al., 1988, 2002; Sperry and Saliendra, 1994; Barigah et al., 2013; Hochberg et al., 2017; Johnson et al., 2018; Rodriguez-Dominguez et al., 2018; Powers et al., 2020; Brodribb et al., 2021; Johnson et al., 2022). Vascular plants transport water under negative pressure from the roots to the leaves through xylem conduits (Dixon and Joly, 1895; Pockman et al., 1995; Angeles et al., 2004). The continuous column of water in the plant vascular system exists in a metastable state because of the negative pressure of the water column (Dixon and Joly, 1895; Pockman et al., 1995; Angeles et al., 2004). During drought, this pressure becomes more negative, increasing the probability of embolisms being formed and propagating through "air-seeding" from a gas-filled conduits to neighboring, sap-filled ones via bordered pits with mesoporous pit membranes that have pore sizes between 5 and 50 nm (Zimmermann, 1983; Lewis, 1988; Sperry and Tyree, 1988; Tyree and Sperry, 1989; Sperry and Saliendra, 1994; Jansen et al., 2018; Kaack et al., 2019). This results in the blockage of xylem conduits by gas emboli (Zimmermann, 1983; Lewis, 1988; Sperry and Tyree, 1988; Tyree and Sperry, 1989; Sperry and Saliendra, 1994; Jansen et al., 2018; Kaack et al., 2019) and can ultimately lead to hydraulic failure (Brodribb and Cochard, 2009; Brodribb et al., 2010, 2020b; Barigah et al., 2013; Cochard and Delzon, 2013).

Xylem anatomical characteristics may vary depending on water availability (e.g., rainfall regimes) and on the resource use strategy of a plant. First, xylem vessel diameter is a key factor in water transport efficiency. The hydraulic conductance of a xylem conduit is theoretically equal to the fourth power of the diameter (Zimmermann, 1983; Tyree and Ewers, 1991), meaning that larger vessels have much higher potential conductivity than ones with smaller diameters. However, high water transport efficiency, and thus, high photosynthetic capacity is often thought to come at the cost of increased vulnerability to xylem embolism (Hargrave et al., 1994; Brodribb and Feild, 2000; Hubbard et al., 2001; Martínez-Vilalta et al., 2002; Hacke et al., 2006; Lens et al., 2011; Markesteijn et al., 2011). Vessels with larger diameters are expected to be more vulnerable to embolism than narrower vessels (Carlquist, 1988; Hargrave et al., 1994; Hacke et al., 2017; Jacobsen et al., 2019) although there are also papers suggesting that conduit diameter does not affect embolism resistance (Ryu et al., 2016; Guan et al., 2022). Larger vessels are thought to be at greater risk of implosion due to their larger lumen diameter (Hacke et al., 2001), and these vessels are speculated to be more prone to air-seeding because of their larger pitted wall areas (Hargrave et al., 1994; Jarbeau et al., 1995; Wheeler et al., 2005; Christman et al., 2009, 2012). Lianas have been shown to have large vessel diameter distributions within the same individual (Ewers et al., 1990; Angyalossy et al., 2012, 2015; Rosell and Olson, 2014; Meunier et al., 2020), but comparative data on vessel diameter distributions from co-occurring liana and tree species are lacking. Second, vessel density may also vary depending on the rainfall regime, as the density of xylem vessels is negatively related to groundwater availability (Schume et al., 2004). A third anatomical trait that may vary depending on water availability and hydraulic strategy are pit membranes in bordered pits. For water to move between two adjacent vessels it must pass through pit membranes (i.e., a mesh of cellulose microfibrils) in bordered pits that play an important role in restricting the spread of embolisms between conduits, while contributing to the hydraulic resistance of water transport (Choat et al., 2008; Kaack et al., 2019). It has long been suggested that pit membrane thickness is a key characteristic in determining embolism resistance (Jansen et al., 2009; Lens et al., 2011, 2013; Li et al., 2016; Dória et al., 2018; Kaack et al., 2021) and some previous studies have found an association between pit membrane thickness and embolism resistance (Dória et al., 2018; Jansen et al., 2018; Trueba et al., 2019; Levionnois et al., 2020a; Kaack et al., 2021), although pit membrane thickness in lianas was not examined in these studies.

In summary, the distribution patterns of lianas relative to trees across rainfall gradients are typically explained by the hypothesis that lianas have different, "more acquisitive" trait values compared to trees in drier forests, but these differences are less pronounced in wetter or less seasonal forests. However, the physiological and anatomical traits that underlie these patterns remain unclear. To elucidate the underlying mechanisms that lead to lianas outperforming trees in drier but not wetter forests we used targeted hydraulic and anatomical trait measurements of co-occurring lianas and trees in two tropical forests with different levels of rainfall to address the following questions: (1) Are there differences between vulnerability to embolisms (P_{50}—water potential at which a plant has lost 50% hydraulic conductivity) and risk of hydraulic failure (HSM—hydraulic safety margins) across growth form and forest type? (2) How do vessel diameter and density vary across growth form and forest type? (3) Are there differences in xylem inter-vessel pit membrane thickness across growth form and forest type and does it predict xylem embolism vulnerability in trees and lianas? We expected that within each forest lianas will have more acquisitive traits associated with greater hydraulic conductive capacity than trees at the expense of hydraulic safety—e.g., thinner pit membranes, larger xylem vessels, greater vulnerability to embolism, and narrower hydraulic safety margins.

MATERIALS AND METHODS

Study Sites

We conducted this study in two lowland forests with distinct rainfall that were located on opposite sides of the Isthmus of Panama: Parque Natural Metropolitano (PNM) a seasonally dry tropical forest referred to as drier forest (**Figure 1A**) and Parque Nacional San Lorenzo (PNSL) a wet evergreen tropical forest referred to as wetter forest (**Figure 1B**). At each location, the Smithsonian Tropical Research Institute has a tower crane that is used to access the forest canopy. PNM (8°59′41.55″ N, 79°32′35.22″ W) is a secondary forest located on the Pacific side of the Isthmus and is 30 m above sea level. At PNM, the mean temperature is 26°C and annual rainfall is 1,911 mm with a distinct dry season from January to April with over 90% of the rainfall occurring between May and December (Parolari et al., 2020). While we were conducting the study at PNM, the canopy crane was being repaired so we had to collect all the samples from the ground with a pruner attached to extension poles at PNM and nearby Parque Nacional Soberania near El Charco (PNS; 9°05′06.1″ N, 79°39′57.9″ W), which has a similar seasonal rainfall pattern compared to PNM with a slightly higher mean annual rainfall of 2,132 mm (Parolari et al., 2020) and also shares many of the same plant species with PNM. We collected exclusively sun-exposed samples using a heavy-duty pruner head (Jameson, Clover, SC, United States) mounted on three or four (depending on sample height) 6-feet (1.83 m) fiberglass poles allowing us to sample at heights over 5 m. Due to the seasonally dry tropical forest having a more open canopy this facilitated the collection of sun-exposed branches. PNSL (9°16′51.71″ N, 79°58′28.27″ W) is an old-growth forest on the Caribbean side of the Isthmus of Panama and is 130 m above sea level. The mean temperature at PNSL is 25.3°C with a mean annual rainfall of 3,236 mm with a period of reduced rainfall from January to March (Parolari et al., 2020). The canopy crane at PNSL is 52 m tall and has a jib of 54 m (Slot and Winter, 2017). While we recognize that there could be sampling error due to the samples at PNM and PNS being collected from the ground and the ones from PNSL being collected from the canopy crane, we

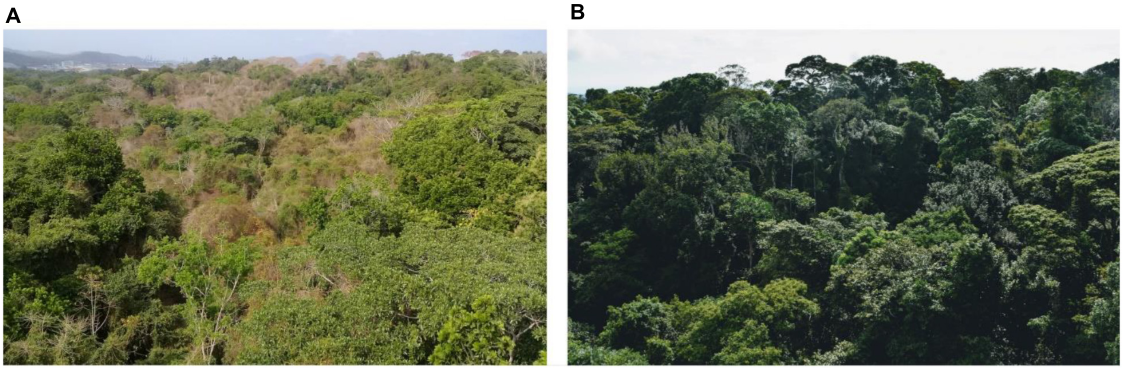

FIGURE 1 | Photo of the two study sites taken during the dry season. **(A)** Parque Natural Metropolitano a seasonally dry tropical forest and **(B)** Parque Nacional San Lorenzo a wet evergreen tropical forest. Photo **(A)** was taken by Brett T. Wolfe.

minimized this error as much as possible by exclusively sampling sun-exposed branches at all locations.

Species and Sample Collection

At each study site, we selected eight species of lianas and eight species of trees, for which we could access at least two individuals from the canopy cranes or from the ground with a pole pruner, for a total of 32 species from 24 plant families (**Table 1**). For the optical vulnerability curves, we collected sun-exposed branches that were >1.5 m long, immediately sealed the branches in large plastic bags with wet paper towels, and took them back to the Smithsonian Tropical Research Institute Gamboa Lab. For the transmission electron microscopy (TEM) imaging, we collected one ∼10 cm long and ∼1 cm in diameter branch section for each species (32 samples in total). As we collected each sample, we immediately wrapped them in moist paper towels and sealed them in Ziploc bags. All TEM samples were collected over a 48-h period and shipped fresh with 3-day shipping service to Ulm University, Germany.

Leaf and Stem Optical Vulnerability Curves

We used the optical vulnerability technique to measure xylem embolism accumulation in leaves and stems as described by Brodribb et al. (2016, 2017). We chose to use this technique as it has been validated in many studies on many species (Brodribb et al., 2016, 2017, 2020a; Skelton et al., 2018; Gauthey et al., 2020; Johnson et al., 2020; Pereira et al., 2020; Guan et al., 2021) with strong agreement in all but one case (Venturas et al., 2019). Briefly, for each branch, we secured a leaf and a small distal stem (∼3–6 mm in diameter depending on the species) inside a custom-built 3D-printed clamp (OpenSourceOV—OSOV) fitted with a small 8-megapixel Raspberry Pi camera and six bright light-emitting diodes operated by a Raspberry Pi microcomputer. Details of materials and instructions for construction, image capturing, and post-image processing using OSOV clamps are explained in detail at http://www.opensourceov.org. For the stems, we carefully removed a small area of bark (∼2 cm^2) from the small distal branch with healthy foliage to expose the xylem. Then we applied adhesive hydrogel (Tensive, Fairfield, NJ, United States) to the exposed xylem to reduce surface reflection and aid light penetration into the xylem, then we covered the area with a round glass coverslip, and secured the branch in the OSOV clamp. Once the leaf and stem were secured in the clamps, we set them to take a picture every 2 min until no embolism events were recorded for at least 12 h (∼72–96 h depending on the species) in a laboratory with controlled temperature that was maintained at around 23^{o}C. As the branches dried, we used a Pressure Chamber Instrument (PMS Instrument Company, Albany, OR, United States) to measure leaf water potential (Ψ) of excised leaves from the same branch. We used ImageJ software to analyze the pictures of leaf and stem embolisms following Brodribb et al. (2016, 2017) and as described in great detail at http://www.opensourceov.org. Briefly, we stacked all the images and converted the images to 8-bit grayscale with pixel values ranging from black (0) to white (255). Each image was subtracted from the next image in the sequence to reveal embolisms that appear as changes in light intensity (differences in pixel values). We removed manually differences in pixels due to noise or artifacts (e.g., sample movements or shrinkage) using the remove outlier function in ImageJ. Embolism accumulation in each stem was quantified as a cumulative total of embolized pixels in each image divided by the total number of embolized pixels in the fully dried sample (cumulative percentage xylem embolism). To determine the water potential at the time of image capture (Ψ_x), we fit a linear regression to the water potential measurements over time and extracted the values at 50% of the cumulative embolisms that had occurred (P_{50}). Full details of the procedure, including an overview of the technique, image processing, as well as ImageJ scripts, are available at http://www.opensourceov.org.

Vessel and Pit Membrane Thickness Imaging and Measuring

The samples were prepared following standard TEM techniques (Jansen et al., 2009, 2011; Scholz et al., 2013; Li et al., 2016). Briefly, stem sections were debarked and small sections were cut from the outermost sapwood. To avoid dehydration, the sections were kept wet and the initial steps of sample preparation were

TABLE 1 | List of 32 species, their families, the type of forest they occur in (drier Parque Natural Metropolitano or wetter Parque Nacional San Lorenzo), their growth form (liana or tree), and their leaf phenology (deciduous or evergreen) at our study sites based on Medina-Vega et al. (2021a,b).

Species	Family	Forest type	Growth form	Phenology
Amphilophium crucigerum	Bignoniaceae	Drier	Liana	Deciduous
Anacardium excelsum	Anacardiaceae	Drier	Tree	Evergreen
Annona spraguei	Annonaceae	Drier	Tree	Deciduous
Apeiba glabra	Tiliaceae	Wetter	Tree	Deciduous
Astronium graveolens	Anacardiaceae	Drier	Tree	Deciduous
Bonamia trichantha	Convolvulaceae	Drier	Liana	Evergreen
Callichlamys latifolia	Bignoniaceae	Drier	Liana	Deciduous
Cinnamomum triplinerve	Lauraceae	Drier	Tree	Evergreen
Coccoloba excelsa	Polygonaceae	Wetter	Liana	Evergreen
Cordia alliodora	Boraginaceae	Drier	Tree	Deciduous
Doliocarpus multiflorus	Dilleniaceae	Wetter	Liana	Evergreen
Guatteria dumetorum	Annonaceae	Wetter	Tree	Evergreen
Guazuma ulmifolia	Sterculiaceae	Drier	Tree	Evergreen
Heisteria scandens	Olacaceae	Wetter	Liana	Evergreen
Luehea seemannii	Tiliaceae	Drier	Tree	Evergreen
Maripa panamensis	Convolvulaceae	Wetter	Liana	Evergreen
Miconia minutiflora	Melastomataceae	Wetter	Tree	Evergreen
Omphalea diandra	Euphorbiaceae	Wetter	Liana	Deciduous
Pittoniotis trichantha	Rubiaceae	Drier	Tree	Deciduous
Pleonotoma variabilis	Bignoniaceae	Wetter	Liana	Deciduous
Salacia multiflora	Celastraceae	Wetter	Liana	Evergreen
Serjania mexicana	Sapindaceae	Drier	Liana	Evergreen
Stigmaphyllon hypagyreum	Malpighiaceae	Drier	Liana	Deciduous
Stizophyllum riparium	Bignoniaceae	Drier	Liana	Deciduous
Tachigali versicolor	Fabaceae	Wetter	Tree	Evergreen
Terminalia amazonia	Combretaceae	Wetter	Tree	Deciduous
Tocoyena pittieri	Rubiaceae	Wetter	Tree	Evergreen
Tontelea passiflora	Hippocrateaceae	Wetter	Liana	Evergreen
Trichostigma octandrum	Phytolaccaceae	Drier	Liana	Deciduous
Virola multiflora	Myristicaceae	Wetter	Tree	Evergreen
Vitis tiliifolia	Vitaceae	Drier	Liana	Deciduous
Vochysia ferruginea	Vochysiaceae	Wetter	Tree	Evergreen

conducted within 5-day sample collection. The sections were then cut into c.1 mm^3 blocks and fixed in a standard fixative (2.5% glutaraldehyde, 0.1 mol phosphate, 1% saccharose, pH 7.3). Then, samples were washed in a 0.05–0.2 M phosphate buffer and post-fixed with 1 or 2% buffered osmium tetroxide for 2–4 h at room temperature. The samples were then washed with a buffer solution, and dehydrated with a gradual ethanol series (30, 50, 70, 90, and 100%). Samples were embedded using Epon resin (Sigma-Aldrich, Steinheim, Germany) at 60°C. Transverse, semi-thin (c. 500 nm thick) sections were cut from the embedded samples with a glass knife, stained with 0.5% toluidine blue in 0.1 M phosphate buffer, and mounted on slides with Eukitt or DPX (Agar Scientific, Stansted, United Kingdom) and were imaged with a camera (Axiocam 305 color, Zeiss, Germany) mounted on a microscope (Axio Scope A1, Zeiss). These images were later used to measure vessel diameter and density. A diamond knife was used to cut ultrathin (60–90 nm) transverse sections, which were dried on 300 mesh copper grids or Formvar grids (Agar Scientific, Stansted, United Kingdom). Several grids were prepared for each TEM sample. Observations were conducted with a JEOL 1400 TEM (JEOL, Tokyo, Japan). TEM images of a minimum of 20 bordered intervessel pits per species were taken with a digital camera. We measured the thickness of each pit membrane at five different locations including at the thinnest and at the thickest point using ImageJ software (National Institutes of Health, Bethesda, MD, United States). Using the images of the semi-thin sections, we measured vessel diameter and vessel density. We strived to measure at least 20 xylem vessels per species although for four species we measured fewer. The number of vessels measured per species ranged from 14–173 vessels.

Data Analysis

Of the 32 species that we measured, we obtained optical vulnerability curves (OVC) for between 1 and 4 individuals for 28 of the species (**Supplementary Table 1**). We obtained leaf OVCs for 27 of the species and stems OVCs for 21 species (**Supplementary Table 1**). For the additional samples we measured we were unable to detect embolisms in the image stacks, thus we were unable to construct OVCs for these samples and had to discard these measurements. We successfully measured vessel diameter, vessel density, and pit membrane thickness on 31 of the 32 target species—for one species (*Stizophyllum riparium*) we were unable to prepare semi-thin wood sections for the wood anatomy measurements because the wood sections kept disintegrating (**Supplementary Table 1**). Among our focal species, eight (*Coccoloba excelsa*, *Miconia minutiflora*, *Pittoniotis trichantha*, *Stigmaphyllon hypagyreum*, *Tachigali versicolor*, *Terminalia amazonia*, *Tocoyena pittieri*, and *Vochysia ferruginea*) had vestured pits (protuberances of lignified cell wall on the borders of the pits) and the other 23 species did not. Because Levionnois et al. (2020a) found that species with vestured pits had thinner pit membranes than species without vestured pits, we conducted Welch's t-tests to determine if there was a significant difference between the pit membrane thickness of vestured-pit species (eight species) and non-vestured-pit species (23 species). We found no difference between vestured and non-vestured species [median pit membrane thickness $t_{(10)} = 0.59$, $p = 0.569$; minimum pit membrane thickness $t_{(10)} = 0.40$, $p = 0.694$; maximum pit membrane thickness $t_{(10)} = 0.88$, $p = 0.400$], thus we omitted this variable (vestured pits or not) from all further analyses. For each species, we calculated minimum, median, maximum pit membrane thickness—these values were obtained by averaging, for each species, the minimum, median, and maximum pit membrane thickness values obtained from each of the individually measured pit membranes (at least 20 measured pits per wood sample and one sample per species). We calculated hydraulic safety margins as the difference between leaf turgor loss point (Ψ_{tlp}), which has been shown to be a good proxy for stomatal closure (Brodribb et al., 2003; Rodriguez-Dominguez et al., 2016; Martin-StPaul et al., 2017), and the water potential at which 50% of total embolisms had occurred:

$$HSM = \Psi_{\text{tlp}} - P_{50}$$

For these calculations, we used previously collected Ψ_{tlp} that had been measured on the same species at the same two study sites (Medina-Vega et al., 2021a,b). For all analyses with P_{50} and HSM, we used species-level means for leaves and for stems or if there was only one measurement for a particular species then we used that value. We used two-way ANOVAs with forest type, growth form, and the interaction between these two variables as predictors and the response variables used were median, minimum, and maximum xylem pit membrane thickness, maximum vessel diameter, range in vessel diameter, mean vessel diameter, minimum vessel diameter, mean vessel density, leaf P_{50}, stem P_{50}, leaf HSM, and stem HSM. All ANOVAs were fit with the Anova function from the R/car package. When necessary, to be able to interpret significant differences, *post-hoc* Tukey's HSD tests were conducted with R/EMMEANS package. To link anatomical characteristics to metrics of vulnerability to drought, we used linear regressions. We evaluated the association between median, minimum, and maximum pit membrane thickness and the drought resistance traits: leaf P_{50}, stem P_{50}, leaf HSM, stem HSM. We also fit linear regressions between leaf P_{50} and stem P_{50} and the xylem vessel anatomical measurements: mean, minimum, maximum, and range in vessel diameter and mean vessel density. All analyses were conducted in R (Version 4.0.5).

RESULTS

P_{50} and Hydraulic Safety Margins

Interestingly, we found no significant difference in P_{50} and HSM between lianas and trees within each forest nor across the two forest types (**Figures 2A,B**, **Supplementary Figures 1A,B**, and **Supplementary Table 2**). Overall, species fell along a gradient of P_{50} (**Supplementary Figure 2A**) and HSM values (**Supplementary Figure 2B**). P_{50} values in the dry forest ranged from −1.98 to −4.47 MPa for lianas and from −2.42 to −4.01 MPa for trees, and similarly in the wet forest the range for lianas was −1.82 to −5.18 MPa and for trees was −1.67 to −4.62 MPa. The range in HSMs was also similar in both forests, with dry forest lianas ranging from 0.51 to 2.57 MPa, dry forest trees ranging from −0.13 to 2.41 MPa, wet forest lianas from −0.88 to 3.00 MPa, and wet forest trees from −0.19 to 2.63 MPa.

Vessel Diameter and Density

Dry forest lianas had 81% greater mean maximum vessel diameter across species than co-occurring dry forest trees and 68% wider maximum vessel diameters than the wet forest trees (**Figure 3A** and **Supplementary Table 2**). There was no difference in maximum vessel diameters between wet forest lianas and the trees from both the wet and dry forest (**Figure 3A** and **Supplementary Table 2**). The range in xylem vessel diameter followed a similar pattern with dry forest lianas having between 110–125% greater range in size of vessel diameters than trees independent of forest type, and again the wetter forest lianas fell in between the dry forest lianas and all the trees (**Figure 3B** and **Supplementary Table 2**). We found no significant difference between liana and tree mean and minimum vessel diameters within each forest type and across the two forests (**Supplementary Figures 3A,B**). Lianas and trees from the drier forest had over a 50% greater vessel density than species from the wetter forest (**Figure 3C** and **Supplementary Table 2**). There was no significant association between leaf and stem P50 with xylem vessel diameter or vessel density (**Supplementary Figures 4A–E**).

Pit Membrane Thickness

Overall, drier forest species consistently had on average 30% greater maximum pit membrane thickness than wetter forest species, with similar results for median and minimum pit membrane thickness (**Supplementary Table 2** and **Figure 4**). Within each forest type, there was no difference between lianas and trees (**Supplementary Table 2**). When comparing pit membrane thickness among growth form and forest type, lianas and trees from the drier forest had significantly thicker pit membranes than the trees in the wet forest but not greater than the wet forest lianas (**Figures 5A–C** and **Supplementary Table 2**). Species with thicker pit membranes were less vulnerable to embolism and less at risk of hydraulic failure. Species with more negative leaf and stem P_{50} values also tended to have thicker pit membranes (**Figure 6A** and **Supplementary Table 3**). Species with thicker pit membranes also tended to have wider hydraulic safety margins (**Figure 6B** and **Supplementary Table 3**).

DISCUSSION

We examined hydraulic and xylem anatomical traits of 32 woody plant species—eight species of lianas and eight species of trees growing in a drier and more seasonal tropical forest on the dry end of the rainfall gradient across the Isthmus of Panama and eight liana and eight tree species from the wettest end of the rainfall gradient. We found no difference in embolism resistance and hydraulic safety between lianas and trees. The main difference between lianas and trees was in vessel diameter and not P_{50}, HSM, and pit membrane thickness. Lianas tended to have larger maximum vessel diameter and a greater range in vessel diameter sizes than trees in the seasonally dry forest but not in the wet forest, suggesting that lianas are able to make larger vessels in the dry forest without an increase in the risk of embolism formation. Dry forest species in general had a higher vessel density than the wet forest species. We found thicker pit membranes among lianas and trees from the drier forest compared to trees in the wetter forest; however, there was no difference between lianas from the drier and wetter forest, nor between lianas and trees within each forest. Our results show an association between thicker pit membranes and greater resistance to embolisms (P_{50}) and hydraulic failure (HSM); but despite this association, species fell along a gradient of P_{50} and HSMs with no significant difference between the wetter and drier forest species nor between lianas and trees. Overall, the main difference between lianas and trees occurred in the drier forest where lianas have larger maximum xylem vessel size and a greater range in vessel sizes than the trees, implying that they have greater hydraulic conductive capacity than the trees. Being able to move larger quantities of water when it is available in seasonally dry tropical forests without an apparent increase in vulnerability to embolisms could be contributing to lianas outperforming

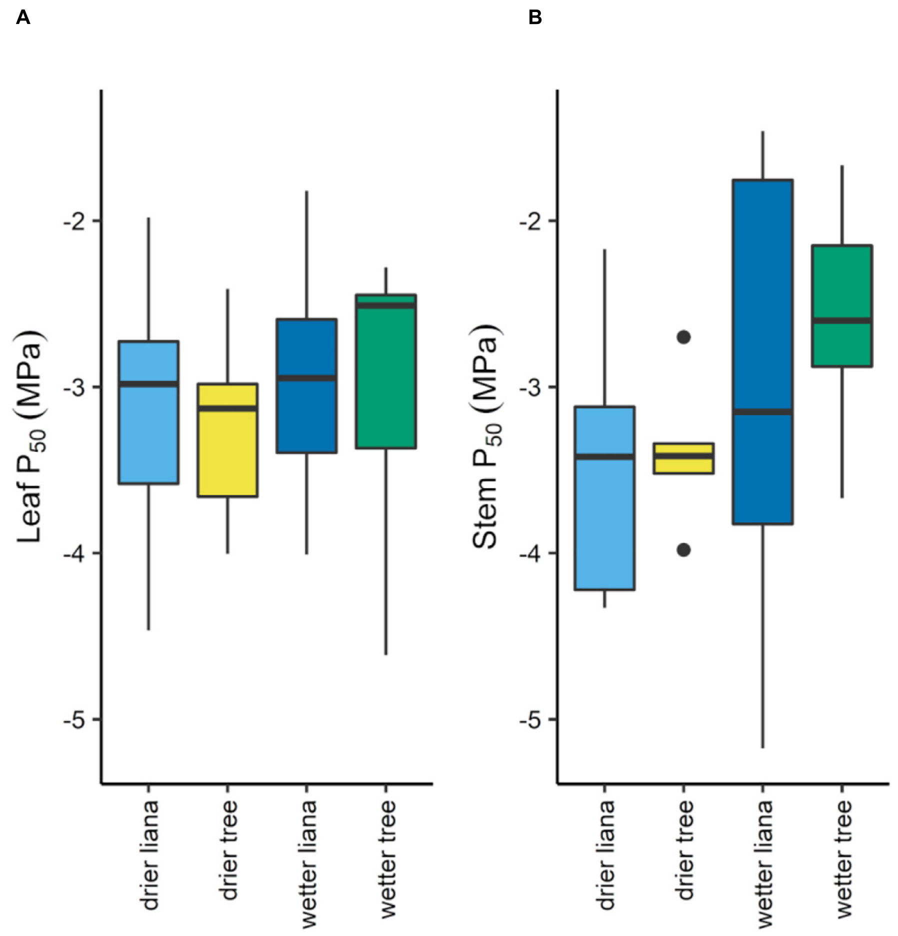

FIGURE 2 | Leaf **(A)** and stem **(B)** by growth form and forest type. Box plot midlines show medians, box edges, first and third quartiles, whiskers, minima and maxima, and points, outliers.

trees and contributing to the increase in lianas that has been documented in many Neotropical forests.

Gradient in Resistance to Embolisms and Hydraulic Failure Among the Wetter and Drier Forests

Lianas and trees from the two forest sites fell along a gradient of P_{50} and hydraulic safety margins. Despite the finding that dry forest species tended to have thicker pit membranes and that there was an association between greater pit membrane thickness and greater embolism resistance, this did not translate into significant differences in P_{50} and HSMs between species from the two forests. Consistent with our findings, several studies have observed a wide range in P_{50} and HSM values within tropical forest communities elsewhere (Santiago et al., 2018; Barros et al., 2019; Oliveira et al., 2019, 2021; van der Sande et al., 2019; Ziegler et al., 2019; Fontes et al., 2020; Powers et al., 2020; Vargas et al., 2021). The wide range in HSMs indicates that not all the species within our two studied forests function at the edge of their hydraulic capacity. This is at odds with the expectation that species should operate with narrow HSMs to sustain CO_2 assimilation for as long as possible before closing their stomata as water becomes more limited (Tyree and Sperry, 1988; Choat et al., 2012; Barros et al., 2019; Fontes et al., 2020). A growing number of studies show that there is a lot more variation in terms of hydraulic safety within forests, even at locations where water is not limited (Santiago et al., 2018; Barros et al., 2019; Oliveira et al., 2019, 2021; van der Sande et al., 2019; Ziegler et al., 2019; Fontes et al., 2020; Powers et al., 2020; Vargas et al., 2021), suggesting that within-community variation in embolism resistance and hydraulic safety is more widespread than previously thought. This is important also because Anderegg et al. (2016) showed that communities with greater hydraulic diversity are more resilient to drought.

Differences in Xylem Vessel Size Between Lianas and Trees

The most striking anatomical difference that we found between lianas and trees was in the vessel diameter distributions: dry forest lianas had much greater maximum vessel diameters and a greater range in vessel diameter size than the trees in both forests. The

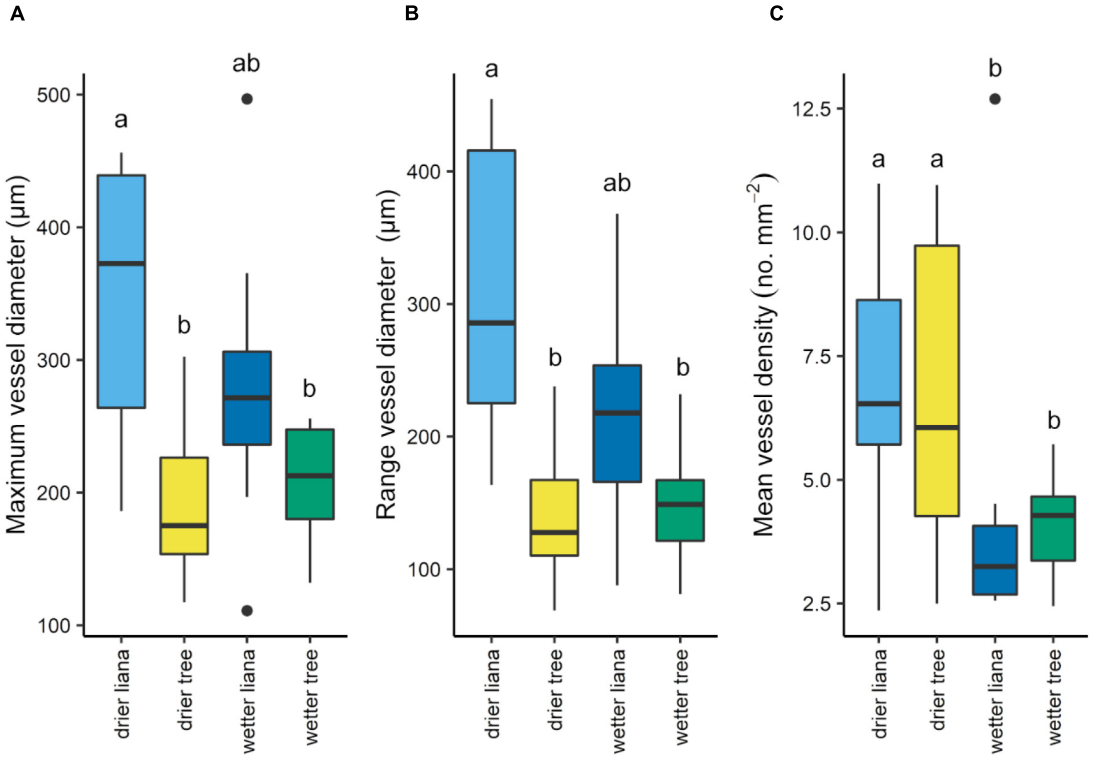

FIGURE 3 | Maximum xylem vessel diameter **(A)**, range in vessel diameter **(B)**, and vessel density **(C)** by growth form and forest type. Letters indicate significant ($P < 0.05$) differences among groups based on Tukey's HSD tests. Box plot midlines show medians, box edges, first and third quartiles, whiskers, minima and maxima, and points, outliers.

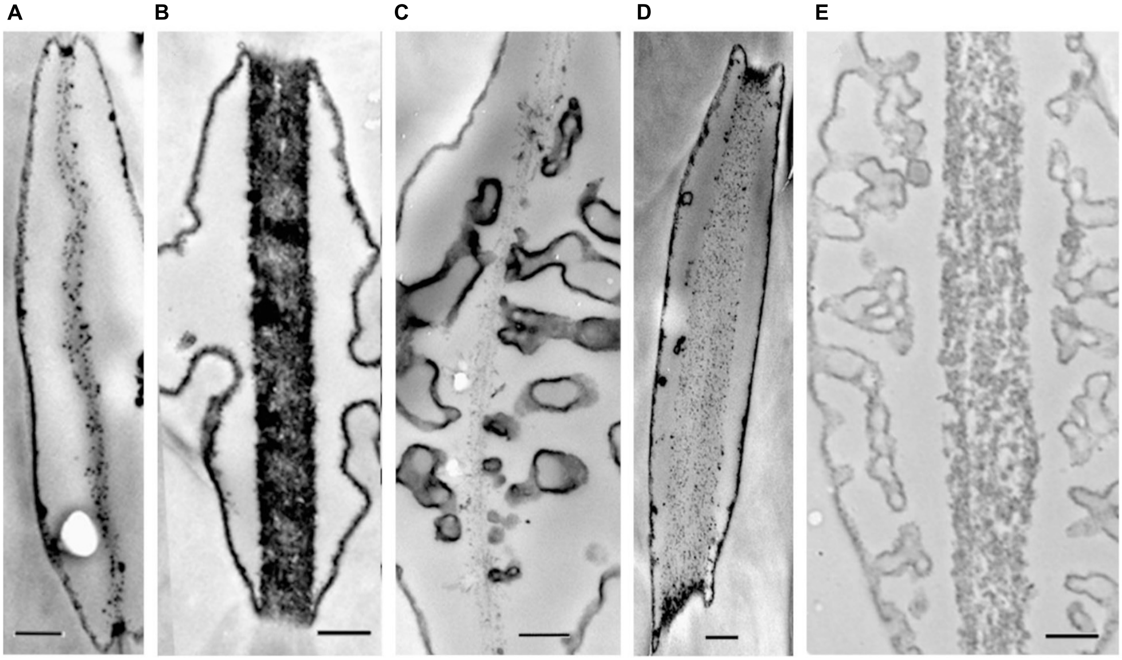

FIGURE 4 | Transmission electron microscopy images of transverse sections of intervessel pit membranes of five of our focal species **(A)** *Guatteria dumetorum* (tree), **(B)** *Pleonotoma variabilis* (liana), **(C)** *Tachigali versicolor* (tree), **(D)** *Cordia alliodora* (tree), **(E)** *Stigmaphyllon hypagyreum* (liana). Vestured pits occur in **(B,C,E)**. Scale bar is 200 nm.

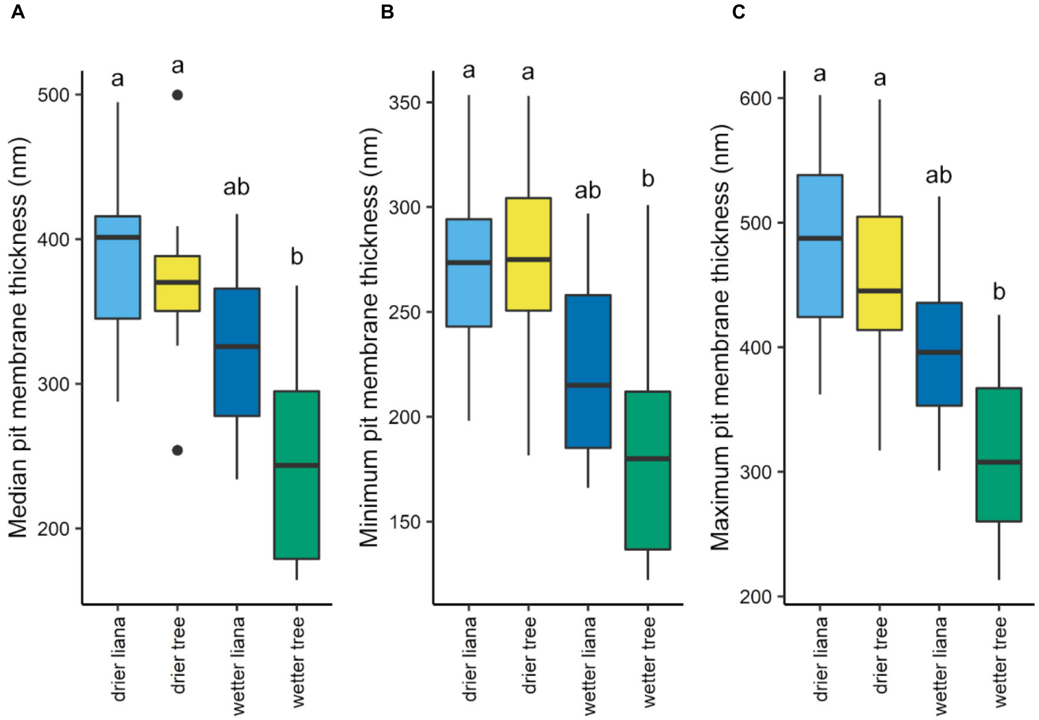

FIGURE 5 | Median **(A)**, minimum **(B)**, and maximum **(C)** pit membrane thickness by growth form and forest type. Letters indicate significant ($P < 0.05$) differences among groups based on Tukey's HSD tests. Box plot midlines show medians, box edges, first and third quartiles, whiskers, minima and maxima, and points, outliers.

dry forest lianas had 81% greater maximum vessel diameter than co-occurring dry forest trees, 68% higher than wet forest trees, and 125 and 110% respectively greater vessel diameter range than the dry forest and wet forest trees. Because lianas are structural parasites (Stevens, 1987) they tend to have high canopy to stem ratios compared to trees (Putz, 1983; Ewers and Fisher, 1991; Ewers et al., 1992; Schnitzer and Bongers, 2002). A previous study conducted at the same location and with the same species as our study found that lianas in the dry forest had a lower Huber Value (HV, branch-cross section/leaf area) than the co-occurring trees and the lowest values overall across both the dry and wet forest, whereas lianas and trees in the wet forest did not differ in their HV (Medina-Vega et al., 2021a). The larger vessel diameters we found in the dry forest lianas could explain why they also have the lowest HV because smaller stems diameters could potentially supply water to a greater leaf canopy. Other previous studies have also shown that smaller liana stems support propositionally larger canopies, for example, Ewers and Fisher (1991) showed that within the genus *Bauhinia*, species with liana growth form had smaller stems proportional to the distal leaf area than trees of the same genus. Similar to our speculations, other authors have also suggested that the proportionally larger canopies of lianas are thought to be made possible due to lianas having, at least a proportion of, longer and wider xylem vessels (Ewers and Fisher, 1991; Angyalossy et al., 2015).

We found no difference in mean nor minimum vessel diameter between lianas and trees. Similarly, Werden et al. (2017), also found no difference in mean vessel diameter between dry forest lianas and trees, and in an extensive study of 424 species conducted on Mexico, Rosell and Olson (2014) also found no difference in mean vessel diameter of climbing plants compared to self-supporting ones. Consistent with our findings, Meunier et al. (2020) showed a large range in vessel sizes in French Guiana rainforest liana species, however, this study did not examine the vessel size of co-occurring trees. Rosell and Olson (2014) also found that the climbing plants in their study had, on average, a small number of wider vessels and narrower vessels than those found in self-supporting plants. Taken together these findings imply that the big difference between co-occurring lianas and trees may be attributed to the observation that lianas have some proportion of vessels that are much larger than the largest tree vessels and that the spread or range of vessel diameters from small to large is much greater in lianas than in co-occurring trees; differences that may be particularly accentuated in seasonally dry forests.

In theory, the largest vessels in lianas lead to higher hydraulic conductive capacity than co-occurring trees. Because flow rates increase with the fourth power of vessel diameter (Zimmermann, 1978), larger vessels can theoretically move exponentially more water than smaller ones, meaning that the population of larger vessels found in liana stems would make lianas much more effective at moving water than the co-occurring trees. Putz (1983) found that most of the xylem vessels in (sub)tropical liana stems are functional, whereas in trees, xylem vessels are only functional for a few years (sapwood) and then transition into non-conductive wood that provides structural support; by contrast,

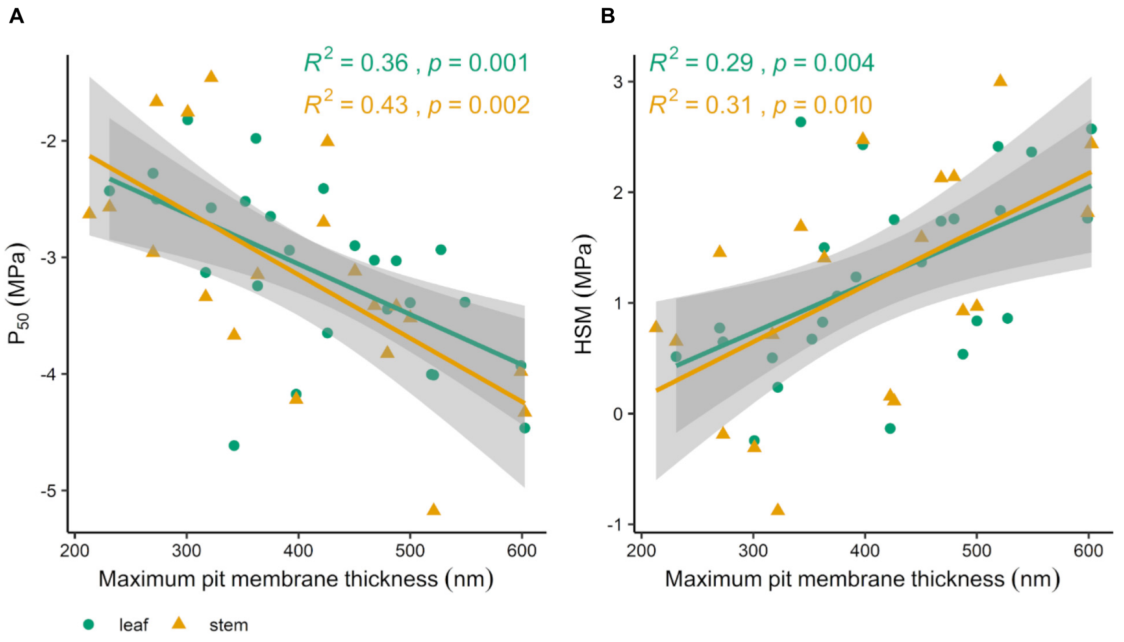

FIGURE 6 | Associations between maximum pit membrane thickness and P_{50} **(A)** and hydraulic safety margins [HSM; **(B)**]. Colors indicate whether P_{50} and HSM were measured on leaves (green circles) or stems (orange triangles). Lines depict linear regressions and shaded areas represent 95% confidence intervals.

the structural needs of lianas are much lower as they rely on trees for support potentially allowing their vessels to be active for longer. Because lianas have some large vessels and most vessels are conductive, each increment in a liana's stem diameter can, in theory, supply water and nutrients to proportionally more leaves than an equivalent stem increment in a tree (Putz, 1983). Indeed, previous studies have found that lianas have greater stomatal conductance than trees growing under the same environmental conditions (Johnson et al., 2013; Smith-Martin et al., 2019) and higher stem hydraulic conductance (De Guzman et al., 2016). This proportionally greater hydraulic capacity of lianas than trees may be contributing to their competitive advantage in seasonal forests allowing them to take advantage of water when it is available, which is consistent with a more resource-acquisitive strategy. However, a recent study with grapevine (*Vitis vinifera*) using reconstructed xylem vessel network from X-ray micro-computed tomography and *in vivo* magnetic resonance velocity flow imaging found that the heterogeneity of the vessel network leads to sap flowing from wide to narrow vessels, such that the wide vessels only accounted for 15% of the total sap flow (Bouda et al., 2019).

Dry Tropical Forest Species Had Thicker Pit Membranes Than the Wet Forest

Overall dry forest species had on average 30% thicker pit membranes than wet forest species. We found that when growth form was taken into account, lianas and trees from the dry forest had thicker pit membranes than wet forest trees, but the wet forest lianas fell in between the co-occurring wet forest trees and dry forest lianas and trees. Our findings suggest that the trees from the dry forest may have thicker pit membranes as an adaptation to growing in drier environments that experience greater water deficits compared to wet forest trees. Interestingly, lianas do not seem to employ this strategy of thick pit membranes to prevent embolism as there was no difference between dry forest and wet forest lianas, despite the overall 30% higher values. While we did not find a significant difference between the pit membrane thickness of species that had vestured pits compared to the ones that did not, vestured pits is a common occurrence among tropical species (eight out of 31 of or species had them) and is an anatomical feature that could also be contributing to embolism resistance (Jansen et al., 2003; Medeiros et al., 2019). The pit membrane thicknesses that we found for the dry forest species fell on the low end of the values found by Levionnois et al. (2020a) in a wet forest in French Guiana with similar mean annual rainfall (3,102 mm) as our wet forest site (3,236 mm). Levionnois et al. (2020a) found maximum pit membrane thicknesses that ranged from 400 nm to over 1,000 nm, whereas the values that we record for our dry forest species fell in between 300 and 600 nm and our wet forest species have overall lower values than what was found in French Guiana. Pit membrane thickness seems to be site-specific with some wetter forest species tending to have thicker pit membranes than species from other forests with similar rainfall. Similar to Levionnois et al. (2020a) we found that pit membrane thickness is species-specific with some species in the wet forest having thicker pit membranes than species in the seasonally dry forest. However, independent of species-specific and site-specific differences, our findings do show that when comparing within relatively smaller geographic ranges (across the isthmus of Panama) there is an overall increase in pit membrane thickness with a decrease in rainfall.

Species with thicker pit membranes tended to be more resistant to drought-induced xylem embolisms, as measured by P_{50} and HSM. Our findings reinforce the expected importance of pit membrane thickness for preventing air-seeding in tropical forest species both in wetter and drier forests. Our findings align with the findings from two previous studies, which also found an association between pit membrane thickness and resistance to embolisms (Trueba et al., 2019; Levionnois et al., 2020a). Studying species in the wet forest of French Guiana, Levionnois et al. (2020a) found a high association between P_{50} and maximum pit membrane thickness ($R^2 = 0.53$) for 15 species with non-vestured pits as they had found that species with vestured pit had significantly thinner pit membranes. The association we found between maximum pit membrane thickness and P_{50} values for leaves ($R^2 = 0.36$) and stems ($R^2 = 0.43$) was lower but still notable for our 31 species, although, because we found no significant difference between vestured and non-vestured species we did not remove vestured species. The range in P_{50} values was also greater among the French Guiana species, with species with P_{50} values as low as −8 MPa meaning that this forest has some highly drought-resistant species (Levionnois et al., 2020a,b), whereas only one of our focal species had a P_{50} of −5 MPa and most of our studied species had higher values. Thus, the thinner pit membranes that we found among our focal species align with the recorded higher P_{50} values, and the thicker pit membranes among the French Guiana species align with the more negative P_{50} values found for those species (Levionnois et al., 2020a,b). One other study also examined the association between pit membrane thickness and P_{50} in vessel-less and vessel-bearing species from rainforests in New Caledonia (Trueba et al., 2019). In this study, Trueba et al. (2019) found a similar overall association between pit membrane thickness and P_{50} ($R^2 = 0.34$), although this association was much higher for the seven vessel-bearing species ($R^2 = 0.95$). Overall, pit membrane thickness seems to play an important role in preventing embolisms in tropical species as had also been shown for temperate species (Dória et al., 2018; Jansen et al., 2018; Kaack et al., 2021).

CONCLUSION

We conclude that: (1) there was no significant difference of P_{50} and HSMs among forests and life forms, with species from both forests falling along a gradient of levels of resistance to embolisms and hydraulic failure. However, (2), lianas in the drier forest did have greater maximum vessel diameter and greater range in vessel diameter, which could allow them to be more efficient at moving water with their larger vessel. (3) Having thicker pit membranes is a potential adaptation of species in drier forests for withstanding greater levels of water deficit, which species in wetter forests would not experience. (4) Lianas did not have thinner pit membranes than trees within each forest, contrary to what we expected due to their predicted higher conductive capacity. (5) Thicker pit membranes are related to greater resistance to embolisms (P_{50}) and hydraulic failure (HSM), underscoring the role of this trait in resistance to embolisms and hydraulic failure. The overlapping hydraulic traits between forests and among life forms suggests a range of responses of woody plant species to changing rainfall conditions, which ultimately may feedback to alter community composition.

DATA AVAILABILITY STATEMENT

The raw data supporting the conclusions of this article will be made available by the authors, without undue reservation.

AUTHOR CONTRIBUTIONS

CS-M, SJ, TB, CL, and JP designed the research. CS-M and JM-V collected data in the field. CS-M, SJ, and AH performed TEM sample preparation, imaging, and processing. CS-M analyzed data and wrote a draft of the manuscript with substantial input from SJ, JM-V, TB, CL, and JP. All authors contributed to the article and approved the submitted version.

FUNDING

CS-M received a National Science Foundation Doctoral Dissertation Improvement Grant (DDIG 1700855), Big Ten Academic Alliance Smithsonian Fellowship from the Smithsonian Institution, and a University of Minnesota Natural History Award from the Dayton Bell Museum Fund. JP thanks DOE grant DE-SC0020344.

ACKNOWLEDGMENTS

The electron microscopy section at Ulm University is acknowledged for TEM sample preparation and sectioning. We thank S. Joseph Wright and Helene C. Muller-Landau for support and advice during fieldwork at the Smithsonian Tropical Research Institute in Panama.

SUPPLEMENTARY MATERIAL

The Supplementary Material for this article can be found online at: https://www.frontiersin.org/articles/10.3389/ffgc.2022.834891/full#supplementary-material

REFERENCES

Aleixo, I., Norris, D., Hemerik, L., Barbosa, A., Prata, E., Costa, F., et al. (2019). Amazonian rainforest tree mortality driven by climate and functional traits. *Nat. Clim. Change* 9, 384–388.

Allen, C. D., Breshears, D. D., and Mcdowell, N. G. (2015). On underestimation of global vulnerability to tree mortality and forest die-off from hotter drought in the Anthropocene. *Ecosphere* 6:art129.

Anderegg, W. R. L., Berry, J. A., Smith, D. D., Sperry, J. S., Anderegg, L. D. L., and Field, C. B. (2012). The roles of hydraulic and carbon stress in a widespread climate-induced forest die-off. *Proc. Natl. Acad. Sci. U.S.A.* 109, 233–237. doi: 10.1073/pnas.1107891109

Anderegg, W. R. L., Klein, T., Bartlett, M., Sack, L., Pellegrini, A. F. A., Choat, B., et al. (2016). Meta-analysis reveals that hydraulic traits explain cross-species patterns of drought-induced tree mortality across the globe. *Proc. Natl. Acad. Sci. U.S.A.* 113, 5024–5029. doi: 10.1073/pnas.1525678113

Angeles, G., Bond, B., Boyer, J. S., Brodribb, T., Brooks, J. R., Burns, M. J., et al. (2004). The cohesion-tension theory. *New Phytol.* 163, 451–452.

Angyalossy, V., Angeles, G., Pace, M. R., Lima, A. C., Dias-Leme, C. L., Lohmann, L. G., et al. (2012). An overview of the anatomy, development and evolution of the vascular system of lianas. *Plant Ecol. Divers.* 5, 167–182.

Angyalossy, V., Pace, M. R., and Lima, A. C. (2015). "Liana anatomy: a broad perspective on structural evolution of the vascular system," in *Ecology of Lianas*, eds S. A. Schnitzer, F. Bongers, R. J. Burnham, and F. E. Putz (London: John Wiley Blackwell), 251–287.

Asner, G. P., and Martin, R. E. (2012). Contrasting leaf chemical traits in tropical lianas and trees: implications for future forest composition. *Ecol. Lett.* 15, 1001–1007. doi: 10.1111/j.1461-0248.2012.01821.x

Barigah, T. S., Charrier, O., Douris, M., Bonhomme, M., Herbette, S., Améglio, T., et al. (2013). Water stress-induced xylem hydraulic failure is a causal factor of tree mortality in beech and poplar. *Ann. Bot.* 112, 1431–1437. doi: 10.1093/aob/mct204

Barros, F. D. V., Bittencourt, P. R. L., Brum, M., Restrepo-Coupe, N., Pereira, L., Teodoro, G. S., et al. (2019). Hydraulic traits explain differential responses of Amazonian forests to the 2015 El Niño-induced drought. *New Phytol.* 223, 1253–1266. doi: 10.1111/nph.15909

Bonan, G. B. (2008). Forests and climate change: forcings, feedbacks, and the climate benefits of forests. *Science* 320, 1444–1449. doi: 10.1126/science.1155121

Bouda, M., Windt, C. W., Mcelrone, A. J., and Brodersen, C. R. (2019). In vivo pressure gradient heterogeneity increases flow contribution of small diameter vessels in grapevine. *Nat. Commun.* 10:5645. doi: 10.1038/s41467-019-13673-6

Brodribb, T., Brodersen, C. R., Carriqui, M., Tonet, V., Rodriguez Dominguez, C., and Mcadam, S. (2021). Linking xylem network failure with leaf tissue death. *New Phytol.* 232, 68–79. doi: 10.1111/nph.17577

Brodribb, T. J., Bowman, D. J. M. S., Nichols, S., Delzon, S., and Burlett, R. (2010). Xylem function and growth rate interact to determine recovery rates after exposure to extreme water deficit. *New Phytol.* 188, 533–542. doi: 10.1111/j.1469-8137.2010.03393.x

Brodribb, T. J., Carriqui, M., Delzon, S., and Lucani, C. (2017). Optical measurement of stem xylem vulnerability. *Plant Physiol.* 174, 2054–2061. doi: 10.1104/pp.17.00552

Brodribb, T. J., Powers, J., Cochard, H., and Choat, B. (2020b). Hanging by a thread? Forests and drought. *Science* 368, 261–266. doi: 10.1126/science.aat7631

Brodribb, T. J., Carriquí, M., Delzon, S., Mcadam, S. A. M., and Holbrook, N. M. (2020a). Advanced vascular function discovered in a widespread moss. *Nat. Plants* 6, 273–279. doi: 10.1038/s41477-020-0602-x

Brodribb, T. J., and Cochard, H. (2009). Hydraulic failure defines the recovery and point of death in water-stressed conifers. *Plant Physiol.* 149, 575–584. doi: 10.1104/pp.108.129783

Brodribb, T. J., and Feild, T. S. (2000). Stem hydraulic supply is linked to leaf photosynthetic capacity: evidence from New Caledonian and Tasmanian rainforests. *Plant Cell Environ.* 23, 1381–1388.

Brodribb, T. J., Holbrook, N. M., Edwards, E. J., and Gutiérrez, M. V. (2003). Relations between stomatal closure, leaf turgor and xylem vulnerability in eight tropical dry forest trees. *Plant Cell Environ.* 26, 443–450.

Brodribb, T. J., Skelton, R. P., Mcadam, S. A. M., Bienaimé, D., Lucani, C. J., and Marmottant, P. (2016). Visual quantification of embolism reveals leaf vulnerability to hydraulic failure. *New Phytol.* 209, 1403–1409. doi: 10.1111/nph.13846

Carlquist, S. J. (1988). *Comparative Wood Anatomy: Systematic, Ecological, and Evolutionary Aspects of Dicotyledon Wood*. Berlin: Springer-Verlag.

Chadwick, R., Good, P., Martin, G., and Rowell, D. P. (2016). Large rainfall changes consistently projected over substantial areas of tropical land. *Nat. Clim. Change* 6, 177–181. doi: 10.1038/nclimate2805

Chazdon, R. L., Brenes, A. R., and Alvarado, B. V. (2005). Effects of climate and stand age on annual tree dynamics in tropical second-growth rain forests. *Ecology* 86, 1808–1815.

Choat, B., Cobb, A. R., and Jansen, S. (2008). Structure and function of bordered pits: new discoveries and impacts on whole-plant hydraulic function. *New Phytol.* 177, 608–626. doi: 10.1111/j.1469-8137.2007.02317.x

Choat, B., Jansen, S., Brodribb, T. J., Cochard, H., Delzon, S., Bhaskar, R., et al. (2012). Global convergence in the vulnerability of forests to drought. *Nature* 491, 752–755. doi: 10.1038/nature11688

Christman, M. A., Sperry, J. S., and Adler, F. R. (2009). Testing the 'rare pit' hypothesis for xylem cavitation resistance in three species of Acer. *New Phytol.* 182, 664–674. doi: 10.1111/j.1469-8137.2009.02776.x

Christman, M. A., Sperry, J. S., and Smith, D. D. (2012). Rare pits, large vessels and extreme vulnerability to cavitation in a ring-porous tree species. *New Phytol.* 193, 713–720. doi: 10.1111/j.1469-8137.2011.03984.x

Cochard, H., and Delzon, S. (2013). Hydraulic failure and repair are not routine in trees. *Ann. For. Sci.* 70, 659–661. doi: 10.1007/s13595-013-0317-5

De Guzman, M. E., Santiago, L. S., Schnitzer, S. A., and Álvarez-Cansino, L. (2016). Trade-offs between water transport capacity and drought resistance in neotropical canopy liana and tree species. *Tree Physiol.* 37, 1404–1414. doi: 10.1093/treephys/tpw086

DeWalt, S. J., Schnitzer, S. A., Alves, L. F., Bongers, F., Burnham, R. J., Cai, Z., et al. (2015). "Biogeographical patterns of liana abundance and diversity," in *Ecology of Lianas*, eds S. A. Schnitzer, F. Bongers, R. J. Burnham, and F. E. Putz (West Sussex: John Wiley & Sons, Ltd), 131–146. doi: 10.1111/brv.12508

Dixon, H. H., and Joly, J. (1895). On the ascent of sap. *Philos. Trans. R. Soc. Lond. B Biol. Sci.* 186, 563–576.

Dória, L. C., Podadera, D. S., Del Arco, M., Chauvin, T., Smets, E., Delzon, S., et al. (2018). Insular woody daisies (*Argyranthemum*, Asteraceae) are more resistant to drought-induced hydraulic failure than their herbaceous relatives. *Funct. Ecol.* 32, 1467–1478. doi: 10.1111/1365-2435.13085

Duffy, P. B., Brando, P., Asner, G. P., and Field, C. B. (2015). Projections of future meteorological drought and wet periods in the Amazon. *Proc. Natl. Acad. Sci. U.S.A.* 112, 13172–13177. doi: 10.1073/pnas.1421010112

Ewers, F., and Fisher, J. (1991). Why vines have narrow stems: histological trends in Bauhinia (Fabaceae). *Oecologia* 88, 233–237. doi: 10.1007/BF00320816

Ewers, F., Fisher, J., and Chiu, S. (1990). A survey of vessel dimensions in stems of tropical lianas and other growth forms. *Oecologia* 84, 544–552. doi: 10.1007/BF00328172

Ewers, F. W., Fisher, J. B., and Fichtner, K. (1992). "Water flux and xylem structure in vines," in *The Biology of Vines*, eds F. E. Putz and H. A. Mooney (Cambridge: Cambridge University Press), 127–160. doi: 10.1093/jxb/erh137

Fontes, C. G., Fine, P. V. A., Wittmann, F., Bittencourt, P. R. L., Piedade, M. T. F., Higuchi, N., et al. (2020). Convergent evolution of tree hydraulic traits in Amazonian habitats: implications for community assemblage and vulnerability to drought. *New Phytol.* 228, 106–120. doi: 10.1111/nph.16675

Gatti, L. V., Gloor, M., Miller, J. B., Doughty, C. E., Malhi, Y., Domingues, L. G., et al. (2014). Drought sensitivity of Amazonian carbon balance revealed by atmospheric measurements. *Nature* 506, 76–80. doi: 10.1038/nature12957

Gauthey, A., Peters, J. M. R., Carins-Murphy, M. R., Rodriguez-Dominguez, C. M., Li, X., Delzon, S., et al. (2020). Visual and hydraulic techniques produce similar estimates of cavitation resistance in woody species. *New Phytol.* 228, 884–897. doi: 10.1111/nph.16746

Gentry, A. H. (1991). "The distribution and evolution of climbing plants," in *The Biology of Vines*, eds F. E. Putz and H. A. Mooney (Cambridge: Cambridge University Press), 3–50.

Gentry, A. H. (1995). "Diversity and floristic composition of Neotropical dry forests," in *Seasonally Dry Tropical Forests*, eds S. H. Bullock, H. A. Mooney, and E. Medina (Cambridge: Cambridge University Press), 146–194.

Guan, X., Pereira, L., Mcadam, S. A. M., Cao, K. F., and Jansen, S. (2021). No gas source, no problem: proximity to pre-existing embolism and segmentation affect embolism spreading in angiosperm xylem by gas diffusion. *Plant Cell Environ.* 44, 1329–1345. doi: 10.1111/pce.14016

Guan, X., Werner, J., Cao, K. F., Pereira, L., Kaack, L., McAdam, S. A. M., et al. (2022). Stem and leaf xylem of angiosperm tress experiences minimal embolism in temperate forests during two consecutive summers with moderate drought. *Plant Biol.* [Online ahead of print]. doi: 10.1111/plb.13384

Hacke, U. G., Sperry, J. S., Pockman, W. T., Davis, S. D., and Mcculloh, K. A. (2001). Trends in wood density and structure are linked to prevention of xylem implosion by negative pressure. *Oecologia* 126, 457–461. doi: 10.1007/s004420100628

Hacke, U. G., Sperry, J. S., Wheeler, J. K., and Castro, L. (2006). Scaling of angiosperm xylem structure with safety and efficiency. *Tree Physiol.* 26, 689–701. doi: 10.1093/treephys/26.6.689

Hacke, U. G., Spicer, R., Schreiber, S. G., and Plavcová, L. (2017). An ecophysiological and developmental perspective on variation in vessel diameter. *Plant Cell Environ.* 40, 831–845. doi: 10.1111/pce.12777

Hargrave, K. R., Kolb, K. J., Ewers, F. W., and Davis, S. D. (1994). Conduit diameter and drought-induced embolism in *Salvia mellifera* Greene (Labiatae). *New Phytol.* 126, 695–705.

Hochberg, U., Windt, C. W., Ponomarenko, A., Zhang, Y.-J., Gersony, J., Rockwell, F. E., et al. (2017). Stomatal closure, basal leaf embolism and shedding protect the hydraulic integrity of grape stems. *Plant Physiol.* 174, 764–775. doi: 10.1104/pp.16.01816

Hubbard, R. M., Ryan, M. G., Stiller, V., and Sperry, J. S. (2001). Stomatal conductance and photosynthesis vary linearly with plant hydraulic conductance in ponderosa pine. *Plant Cell Environ.* 24, 113–121.

Jacobsen, A. L., Brandon Pratt, R., Venturas, M. D., Hacke, U. G., and Lens, F. (2019). Large volume vessels are vulnerable to water-stress-induced embolism in stems of poplar. *IAWA J.* 40, 4–S4.

Jansen, S., Baas, P., Gasson, P., and Smets, E. (2003). Vestured pits: do they promote safer water transport? *Int. J. Plant Sci.* 164, 405–413.

Jansen, S., Choat, B., and Pletsers, A. (2009). Morphological variation of intervessel pit membranes and implications to xylem function in angiosperms. *Am. J. Bot.* 96, 409–419. doi: 10.3732/ajb.0800248

Jansen, S., Gortan, E., Lens, F., Gullo, M. A. L., Salleo, S., Scholz, A., et al. (2011). Do quantitative vessel and pit characters account for ion-mediated changes in the hydraulic conductance of angiosperm xylem? *New Phytol.* 189, 218–228. doi: 10.1111/j.1469-8137.2010.03448.x

Jansen, S., Klepsch, M., Li, S., Kotowska, M. M., Schiele, S., Zhang, Y., et al. (2018). *Challenges in Understanding Air-Seeding in Angiosperm Xylem*. Leuven: International Society for Horticultural Science (ISHS), 13–20.

Jarbeau, J. A., Ewers, F. W., and Davis, S. D. (1995). The mechanism of water-stress-induced embolism in two species of chaparral shrubs. *Plant Cell Environ.* 18, 189–196. doi: 10.1111/j.1365-3040.1995.tb00352.x

Johnson, D. M., Domec, J. C., Woodruff, D. R., Mcculloh, K. A., and Meinzer, F. C. (2013). Contrasting hydraulic strategies in two tropical lianas and their host trees. *Am. J. Bot.* 100, 374–383. doi: 10.3732/ajb.1200590

Johnson, K. M., Brodersen, C., Carins-Murphy, M. R., Choat, B., and Brodribb, T. J. (2020). Xylem embolism spreads by single-conduit events in three dry forest angiosperm stems. *Plant Physiol.* 184, 212–222. doi: 10.1104/pp.20.00464

Johnson, K. M., Jordan, G. J., and Brodribb, T. J. (2018). Wheat leaves embolized by water stress do not recover function upon rewatering. *Plant Cell Environ.* 41, 2704–2714. doi: 10.1111/pce.13397

Johnson, K. M., Lucani, C., and Brodribb, T. J. (2022). In vivo monitoring of drought-induced embolism in Callitris rhomboidea trees reveals wide variation in branchlet vulnerability and high resistance to tissue death. *New Phytol.* 233, 207–218. doi: 10.1111/nph.17786

Kaack, L., Altaner, C. M., Carmesin, C., Diaz, A., Holler, M., Kranz, C., et al. (2019). Function and three-dimensional structure of intervessel pit membranes in angiosperms: a review. *IAWA J.* 40, 673–702. doi: 10.3390/plants9020231

Kaack, L., Weber, M., Isasa, E., Karimi, Z., Li, S., Pereira, L., et al. (2021). Pore constrictions in intervessel pit membranes provide a mechanistic explanation for xylem embolism resistance in angiosperms. *New Phytol.* 230, 1829–1843. doi: 10.1111/nph.17282

Leitold, V., Morton, D. C., Longo, M., Dos-Santos, M. N., Keller, M., and Scaranello, M. (2018). El Niño drought increased canopy turnover in Amazon forests. *New Phytol.* 219, 959–971.

Lens, F., Sperry, J. S., Christman, M. A., Choat, B., Rabaey, D., and Jansen, S. (2011). Testing hypotheses that link wood anatomy to cavitation resistance and hydraulic conductivity in the genus Acer. *New Phytol.* 190, 709–723. doi: 10.1111/j.1469-8137.2010.03518.x

Lens, F., Tixier, A., Cochard, H., Sperry, J. S., Jansen, S., and Herbette, S. (2013). Embolism resistance as a key mechanism to understand adaptive plant strategies. *Curr. Opin. Plant Biol.* 16, 287–292. doi: 10.1016/j.pbi.2013.02.005

Levionnois, S., Jansen, S., Wandji, R. T., Beauchêne, J., Ziegler, C., Coste, S., et al. (2020a). Linking drought-induced xylem embolism resistance to wood anatomical traits in Neotropical trees. *New Phytol.* 229, 1453–1466. doi: 10.1111/nph.16942

Levionnois, S., Ziegler, C., Jansen, S., Calvet, E., Coste, S., Stahl, C., et al. (2020b). Vulnerability and hydraulic segmentations at the stem–leaf transition: coordination across Neotropical trees. *New Phytol.* 228, 512–524. doi: 10.1111/nph.16723

Lewis, A. M. (1988). A test of the air-seeding hypothesis using sphagnum hyalocysts. *Plant Physiol.* 87, 577–582. doi: 10.1104/pp.87.3.577

Li, S., Lens, F., Espino, S., Karimi, Z., Klepsch, M., Schenk, H. J., et al. (2016). Intervessel pit membrane thickness as a key determinant of embolism resistance in angiosperm xylem. *IAWA J.* 37, 152–171. doi: 10.1093/aob/mcy233

Markesteijn, L., Poorte, L., Paz, H., Sack, L., and Bongers, F. (2011). Ecological differentiation in xylem cavitation resistance is associated with stem and leaf structural traits. *Plant Cell Environ.* 34, 137–148. doi: 10.1111/j.1365-3040.2010.02231.x

Martínez-Vilalta, J., Prat, E., Oliveras, I., and Piñol, J. (2002). Xylem hydraulic properties of roots and stems of nine Mediterranean woody species. *Oecologia* 133, 19–29. doi: 10.1007/s00442-002-1009-2

Martin-StPaul, N., Delzon, S., and Cochard, H. (2017). Plant resistance to drought depends on timely stomatal closure. *Ecol. Lett.* 20, 1437–1447. doi: 10.1111/ele.12851

Medeiros, J. S., Lens, F., Maherali, H., and Jansen, S. (2019). Vestured pits and scalariform perforation plate morphology modify the relationships between angiosperm vessel diameter, climate and maximum plant height. *New Phytol.* 221, 1802–1813. doi: 10.1111/nph.15536

Medina-Vega, J. A., Bongers, F., Poorter, L., Schnitzer, S. A., and Sterck, F. J. (2021a). Lianas have more acquisitive traits than trees in a dry but not in a wet forest. *J. Ecol.* 109, 2367–2384.

Medina-Vega, J. A., Bongers, F., Schnitzer, S. A., and Sterck, F. J. (2021b). Lianas explore the forest canopy more effectively than trees under drier conditions. *Funct. Ecol.* 35, 318–329.

Meunier, F., Krishna Moorthy, S. M., De Deurwaerder, H. P. T., Kreus, R., Van Den Bulcke, J., Lehnebach, R., et al. (2020). Within-site variability of liana wood anatomical traits: a case study in Laussat, French Guiana. *Forests* 11:523.

Oliveira, R. S., Costa, F. R. C., Baalen, E. V., Jonge, A. D., Bittencourt, P. R., Almanza, Y., et al. (2019). Embolism resistance drives the distribution of Amazonian rainforest tree species along hydro-topographic gradients. *New Phytol.* 221, 1457–1465. doi: 10.1111/nph.15463

Oliveira, R. S., Eller, C. B., Barros, F. D. V., Hirota, M., Brum, M., and Bittencourt, P. (2021). Linking plant hydraulics and the fast–slow continuum to understand resilience to drought in tropical ecosystems. *New Phytol.* 230, 904–923. doi: 10.1111/nph.17266

Pan, Y., Birdsey, R. A., Fang, J., Houghton, R., Kauppi, P., Kurz, W., et al. (2011). A large and persistent carbon sink in the world's forests. *Science* 333, 988–993. doi: 10.1126/science.1201609

Parolari, A. J., Paul, K., Griffing, A., Condit, R., Perez, R., Aguilar, S., et al. (2020). Liana abundance and diversity increase with rainfall seasonality along a precipitation gradient in Panama. *Ecography* 43, 25–33.

Pereira, L., Bittencourt, P. R. L., Pacheco, V. S., Miranda, M. T., Zhang, Y., Oliveira, R. S., et al. (2020). The Pneumatron: an automated pneumatic apparatus for estimating xylem vulnerability to embolism at high temporal resolution. *Plant Cell Environ.* 43, 131–142. doi: 10.1111/pce.13647

Phillips, O. L., Martinez, R. V., Arroyo, L., Baker, T. R., Killeen, T., Lewis, S. L., et al. (2002). Increasing dominance of large lianas in Amazonian forests. *Nature* 418, 770–774. doi: 10.1038/nature00926

Pockman, W. T., Sperry, J. S., and O'leary, J. W. (1995). Sustained and significant negative water pressure in xylem. *Nature* 378, 715–716. doi: 10.1093/jxb/erm281

Powers, J. S., Vargas, G. G., Brodribb, T. J., Schwartz, N. B., Pérez-Aviles, D., Smith-Martin, C. M., et al. (2020). A catastrophic tropical drought kills hydraulically vulnerable tree species. *Glob. Change Biol.* 26, 3122–3133. doi: 10.1111/gcb.15037

Putz, F. E. (1983). Liana biomass and leaf area of a "Tierra Firme" forest in the Rio Negro Basin, Venezuela. *Biotropica* 15, 185–189.

Rodriguez-Dominguez, C. M., Carins-Murphy, M. R., Lucani, C., and Brodribb, T. J. (2018). Mapping xylem failure in disparate organs of whole plants reveals extreme resistance in olive roots. *New Phytol.* 218, 1025–1035. doi: 10.1111/nph.15079

Rodriguez-Dominguez, C. M., Buckley, T. N., Egea, G., Cires, A. D., Hernandez-Santana, V., Martorell, S., et al. (2016). Most stomatal closure in woody species under moderate drought can be explained by stomatal responses to leaf turgor. *Plant Cell Environ.* 39, 2014–2026. doi: 10.1111/pce.12774

Rosell, J. A., and Olson, M. E. (2014). Do lianas really have wide vessels? Vessel diameter–stem length scaling in non-self-supporting plants. *Perspect. Plant Ecol. Evol. Syst.* 16, 288–295.

Ryu, J., Hwang, B. G., Kim, Y. X., and Lee, S. J. (2016). Direct observation of local xylem embolisms induced by soil drying in intact *Zea mays* leaves. *J. Exp. Bot.* 67, 2617–2626. doi: 10.1093/jxb/erw087

Santiago, L. S., De Guzman, M. E., Baraloto, C., Vogenberg, J. E., Brodie, M., Hérault, B., et al. (2018). Coordination and trade-offs among hydraulic safety, efficiency and drought avoidance traits in Amazonian rainforest canopy tree species. *New Phytol.* 218, 1015–1024. doi: 10.1111/nph.15058

Schnitzer, S. A. (2005). A mechanistic explanation for global patterns of liana abundance and distribution. *Am. Nat.* 166, 262–276. doi: 10.1086/431250

Schnitzer, S. A. (2018). Testing ecological theory with lianas. *New Phytol.* 220, 366–380. doi: 10.1111/nph.15431

Schnitzer, S. A., and Bongers, F. (2002). The ecology of lianas and their role in forests. *Trends Ecol. Evol.* 17, 223–230. doi: 10.1016/s0169-5347(02)02491-6

Schnitzer, S. A., and Bongers, F. (2011). Increasing liana abundance and biomass in tropical forests: emerging patterns and putative mechanisms. *Ecol. Lett.* 14, 397–406. doi: 10.1111/j.1461-0248.2011.01590.x

Schnitzer, S. A., Mangan, S. A., Dalling, J. W., Baldeck, C. A., Hubbell, S. P., Ledo, A., et al. (2012). Liana abundance, diversity, and distribution on Barro Colorado Island, Panama. *PLoS One* 7:e52114. doi: 10.1371/journal.pone.0052114

Schnitzer, S. A., and van der Heijden, G. M. F. (2019). Lianas have a seasonal growth advantage over co-occurring trees. *Ecology* 100:e02655. doi: 10.1002/ecy.2655

Scholz, A., Rabaey, D., Stein, A., Cochard, H., Smets, E., and Jansen, S. (2013). The evolution and function of vessel and pit characters with respect to cavitation resistance across 10 *Prunus* species. *Tree Physiol.* 33, 684–694. doi: 10.1093/treephys/tpt050

Schume, H., Grabner, M., and Eckmullner, O. (2004). The influence of an altered groundwater regime on vessel properties of hybrid poplar. *Trees* 18, 184–194.

Skelton, R. P., Dawson, T. E., Thompson, S. E., Shen, Y., Weitz, A. P., and Ackerly, D. (2018). Low vulnerability to xylem embolism in leaves and stems of North American oaks. *Plant Physiol.* 177, 1066–1077. doi: 10.1104/pp.18.00103

Slot, M., and Winter, K. (2017). *In situ* temperature response of photosynthesis of 42 tree and liana species in the canopy of two Panamanian lowland tropical forests with contrasting rainfall regimes. *New Phytol.* 214, 1103–1117. doi: 10.1111/nph.14469

Smith-Martin, C. M., Bastos, C. L., Lopez, O. R., Powers, J. S., and Schnitzer, S. A. (2019). Effects of dry-season irrigation on leaf physiology and biomass allocation in tropical lianas and trees. *Ecology* 100:e02827. doi: 10.1002/ecy.2827

Smith-Martin, C. M., Xu, X., Medvigy, D., Schnitzer, S. A., and Powers, J. S. (2020). Allometric scaling laws linking biomass and rooting depth vary across ontogeny and functional groups in tropical dry forest lianas and trees. *New Phytol.* 226, 714–726. doi: 10.1111/nph.16275

Sperry, J. S., Donnelly, J. R., and Tyree, M. T. (1988). A method for measuring hydraulic conductivity and embolism in xylem. *Plant Cell Environ.* 11, 35–40. doi: 10.1111/j.1365-3040.1988.tb01774.x

Sperry, J. S., Hacke, U. G., Oren, R., and Comstock, J. P. (2002). Water deficits and hydraulic limits to leaf water supply. *Plant Cell Environ.* 25, 251–263. doi: 10.1046/j.0016-8025.2001.00799.x

Sperry, J. S., and Saliendra, N. Z. (1994). Intra- and inter-plant variation in xylem cavitation in *Betula occidentalis*. *Plant Cell Environ.* 17, 1233–1241. doi: 10.1111/j.1365-3040.1994.tb02021.x

Sperry, J. S., and Tyree, M. T. (1988). Mechanism of water stress-induced xylem embolism. *Plant Physiol.* 88, 581–587. doi: 10.1104/pp.88.3.581

Stevens, G. C. (1987). Lianas as structural parasites: the bursera simaruba example. *Ecology* 68, 77–81.

Trueba, S., Delzon, S., Isnard, S., and Lens, F. (2019). Similar hydraulic efficiency and safety across vesselless angiosperms and vessel-bearing species with scalariform perforation plates. *J. Exp. Bot.* 70, 3227–3240.

Tyree, M. T., and Ewers, F. W. (1991). The hydraulic architecture of trees and other woody plants. *New Phytol.* 119, 345–360. doi: 10.1111/j.1469-8137.1991.tb00035.x

Tyree, M. T., and Sperry, J. S. (1988). Do woody plants operate near the point of catastrophic xylem dysfunction caused by dynamic water stress?: answers from a model. *Plant Physiol.* 88, 574–580. doi: 10.1104/pp.88.3.574

Tyree, M. T., and Sperry, J. S. (1989). Vulnerability of xylem to cavitation and embolism. *Annu. Rev. Plant Physiol. Plant Mol. Biol.* 40, 19–36. doi: 10.1146/annurev.pp.40.060189.000315

Uriarte, M., Lasky, J. R., Boukili, V. K., and Chazdon, R. L. (2016). A trait-mediated, neighbourhood approach to quantify climate impacts on successional dynamics of tropical rainforests. *Funct. Ecol.* 30, 157–167.

van der Sande, M. T., Poorter, L., Schnitzer, S. A., Engelbrecht, B. M. J., and Markesteijn, L. (2019). The hydraulic efficiency–safety trade-off differs between lianas and trees. *Ecology* 100:e02666. doi: 10.1002/ecy.2666

Vargas, G. G., Brodribb, T. J., Dupuy, J. M., González-M, R., Hulshof, C. M., Medvigy, D., et al. (2021). Beyond leaf habit: generalities in plant function across 97 tropical dry forest tree species. *New Phytol.* 232, 148–161. doi: 10.1111/nph.17584

Venturas, M. D., Pratt, R. B., Jacobsen, A. L., Castro, V., Fickle, J. C., and Hacke, U. G. (2019). Direct comparison of four methods to construct xylem vulnerability curves: differences among techniques are linked to vessel network characteristics. *Plant Cell Environ.* 42, 2422–2436. doi: 10.1111/pce.13565

Werden, L. K., Waring, B. G., Smith-Martin, C. M., and Powers, J. S. (2017). Tropical dry forest trees and lianas differ in leaf economic spectrum traits but have overlapping water-use strategies. *Tree Physiol.* 38, 517–530. doi: 10.1093/treephys/tpx135

Wheeler, J. K., Sperry, J. S., Hacke, U. G., and Hoang, N. (2005). Inter- vessel pitting and cavitation in woody Rosaceae and other vesselled plants: a basis for a safety versus efficiency trade- off in xylem transport. *Plant Cell Environ.* 28, 800–812.

Wright, S. J., Calderon, O., Hernandez, A., and Paton, S. (2004). Are lianas increasing in importance in tropical forests? A 17-year record from Panama. *Ecology* 85, 484–489. doi: 10.1890/02-0757

Yorke, S. R., Schnitzer, S. A., Mascaro, J., Letcher, S. G., and Carson, W. P. (2013). Increasing liana abundance and basal area in a tropical forest: the contribution of long-distance clonal colonization. *Biotropica* 45, 317–324. doi: 10.1111/btp.12015

Ziegler, C., Coste, S., Stahl, C., Delzon, S., Levionnois, S., Cazal, J., et al. (2019). Large hydraulic safety margins protect Neotropical canopy rainforest tree species against hydraulic failure during drought. *Ann. For. Sci.* 76:115.

Zimmermann, M. H. (1978). Hydraulic architecture of some diffuse-porous trees. *Can. J. Bot.* 56, 2286–2295.

Zimmermann, M. H. (1983). *Xylem Structure and the Ascent of Sap*. Berlin: Springer.

Conflict of Interest: The authors declare that the research was conducted in the absence of any commercial or financial relationships that could be construed as a potential conflict of interest.

frontiers | Frontiers in Forests and Global Change

ORIGINAL RESEARCH
published: 15 April 2022
doi: 10.3389/ffgc.2022.809904

Hydro-Edaphic Gradient and Phylogenetic History Explain the Landscape Distribution of a Highly Diverse Clade of Lianas in the Brazilian Amazon

Caian Souza Gerolamo[1], Flavia R. C. Costa[2], Alexandre R. Zuntini[3], Alberto Vicentini[2], Lúcia G. Lohmann[1], Juliana Schietti[2,4], Elisangela X. Rocha[2,5], Veronica Angyalossy[1] and Anselmo Nogueira[6]**

[1] Departamento de Botânica, Instituto de Biociências, Universidade de São Paulo, São Paulo, Brazil, [2] Instituto Nacional de Pesquisas da Amazônia, Manaus, Brazil, [3] Royal Botanic Gardens, Kew, Kew Green, Richmond, United Kingdom, [4] Departamento de Biologia, Universidade Federal do Amazonas, Manaus, Brazil, [5] Instituto de Pesquisa Ambiental da Amazônia, Canarana, Brazil, [6] Centro de Ciências Naturais e Humanas, Universidade Federal do ABC, São Bernardo do Campo, Brazil

Edited by:
Stefan A. Schnitzer,
Marquette University, United States

Reviewed by:
Sergio Estrada Villegas,
Yale University, United States
Julia Sfair,
Federal University of Ceará, Brazil

***Correspondence:**
Caian Souza Gerolamo
caian.gerolamo@usp.br
Anselmo Nogueira
a.nogueira@ufabc.edu.br

Specialty section:
This article was submitted to Tropical Forests, a section of the journal Frontiers in Forests and Global Change

Received: *05 November 2021*
Accepted: *23 March 2022*
Published: *15 April 2022*

Citation:
Gerolamo CS, Costa FRC, Zuntini AR, Vicentini A, Lohmann LG, Schietti J, Rocha EX, Angyalossy V and Nogueira A (2022) Hydro-Edaphic Gradient and Phylogenetic History Explain the Landscape Distribution of a Highly Diverse Clade of Lianas in the Brazilian Amazon. Front. For. Glob. Change 5:809904. doi: 10.3389/ffgc.2022.809904

Plant distribution patterns may indicate habitat specialization either by closely related species with conserved traits or by phylogenetically distant species with converging traits. Lianas represent a large proportion of the overall tropical species diversity and abundance. Despite their importance, little is known about the relationship between habitat specialization and the phylogenetic structure of lianas, especially at the landscape scale where forest disturbances and hydro-edaphic gradients are crucial. To explore this knowledge gap, we used one of the most diverse lineages of Neotropical lianas to test whether (i) landscape environmental gradients explain liana species diversity and composition, (ii) habitat specialization is phylogenetically conserved along ecological gradients, and (iii) closely related liana species have more similar distribution patterns. We hypothesized that hydro-edaphic and forest disturbance gradients determine the compartmentalization of a subset of closely related species in different portions of the ecological gradients. To test our hypothesis, we examined the distribution of the tribe Bignonieae on 34 1-ha permanent plots systematically distributed over a 42 km^2 forested landscape area in Central Amazon. We used proxies for the hydro-edaphic, forest disturbance, and soil nutrient gradients. Liana diversity increased along the hydro-edaphic gradient (i.e., toward dry plateaus), but slightly decreased along the forest disturbance gradient. Further, we found evidence of habitat specialization along the hydro-edaphic gradient on plateaus with deeper water tables, where liana assemblages are subsets of closely related species, exhibiting phylogenetic clustering. The opposite pattern was found on valleys, where liana assemblages were phylogenetically overdispersed. Our results support the role of phylogenetic niche conservatism on plateaus and a stronger environmental filter within the hydrologically dynamic valleys, associated with a functional convergence of more distantly related species. The selection of more distantly related species on hydrologically dynamic areas is a general pattern among trees, palms and now lianas. We conclude that ecological filters and phylogenetic history have played fundamental roles in structuring liana assemblages unevenly at the landscape scale. Fine-scale hydrology determines several aspects of plant community organization, whose mechanisms need to be experimentally investigated in the Amazon basin.

Keywords: gradient analyses, habitat specialization, liana diversity, phylogenetic community structure, *terra firme* forest, vines

INTRODUCTION

Patterns of species distribution and richness along environmental gradients have intrigued ecologists and evolutionary biologists for a long time (Darwin, 1859; Hawkins, 2001; Hawkins and Diniz-Filho, 2004; Ricklefs, 2005). During the past decades, several studies have described plant species distribution patterns at different spatial scales in tropical forests (Soares-Filho et al., 2006; Laurance et al., 2011; Bullock et al., 2020). On a regional scale, the Amazon basin includes a variety of forest types, such as *terra firme* forests, floodplain/inundated forests, and white-sand areas. The broad environmental heterogeneity between these vegetation types contributes to high basin-wide species richness and high turnover in plant species composition (Gentry, 1988; Fine et al., 2005). Within vegetation types, topographic and soil heterogeneity drives species richness and species turnover due to specific abiotic conditions and habitat-specific biotic interactions favoring the survival, growth, and reproduction of species subsets (Pitman et al., 2001; Schietti et al., 2014; Tuomisto et al., 2017). Overall, the environmental heterogeneity of tropical forests can promote ecologically mediated speciation and habitat specialization (Fine et al., 2005; Fine and Kembel, 2011). However, habitat specialization can also be shuffled by stochastic events, such as blowdowns (Bordon et al., 2019), and constrained by the evolutionary history of plant lineages (Webb and Peart, 1999; Webb et al., 2002; Graham and Fine, 2008), determining the current diversity patterns found in tropical forests.

From an eco-evolutionary perspective, a major challenge to be investigated is whether habitats filter species subsets by their traits because of their common recent history. It has long been held that the most closely related species should have greater ecological similarity due to the common ancestry (Darwin, 1859; Ricklefs and Schluter, 1993; Webb, 2000; Wiens and Graham, 2005). Therefore, if shared traits enhance fitness in particular environments, then environmental filters could generate local communities composed of closely related species, creating a pattern of phylogenetic clustering. On the other hand, interspecific competition and character displacement, or convergent evolution mediated by extreme environmental conditions, could lead to an assemblage structure made up of local groupings of distantly related species, thereby creating a pattern of phylogenetic overdispersion (Webb et al., 2002; Wiens and Donoghue, 2004; Cavender-Bares et al., 2009).

Phylogenetic patterns of habitat specialization have often been described for tree and palm assemblages in tropical forests (Fine and Kembel, 2011; Eiserhardt et al., 2013; Freitas et al., 2014). However, the prevalence of phylogenetic clustering or overdispersion cannot be generalized. For example, Amazonian tree and palm assemblages were shown to be formed by more closely related species than expected by chance within *terra-firme*, floodplain, and pre-montane forests (Fine and Kembel, 2011; Eiserhardt et al., 2013; Muscarella et al., 2019), indicating a pattern of phylogenetic clustering (synonym of phylogenetic niche conservatism here; Webb et al., 2002). This pattern has been explained by environmental filtering under hydro-edaphic conditions of each habitat and limited seed dispersal across habitats (Fine and Kembel, 2011; Eiserhardt et al., 2013; Muscarella et al., 2019). On the other hand, Amazonian tree and palm assemblages on more stressful restinga and white-sand vegetation are composed of more distantly related species (Fine and Kembel, 2011; Eiserhardt et al., 2013; Muscarella et al., 2019). Moreover, palm assemblages of *terra firme* forests shift their phylogenetic structure from overdispersion in the white-sand valleys to a phylogenetically random structure toward upland plateaus (Freitas et al., 2014). Plant assemblages composed of more distantly related species have been associated with the action of environmental filters, convergent plant evolution, and, less likely, by competitive exclusion between ecologically similar close relatives (Eiserhardt et al., 2013; Freitas et al., 2014). Therefore, while some habitats are composed of more closely related plant species, others are composed of more distantly related species. Notably, both patterns are shared by trees and palms throughout the Amazon Forest landscape (**Supplementary Table 1**).

Few studies have focused on the diversity patterns and drivers of assemblage structure of neglected plant habits, such as lianas, even though these plants represent a large proportion of the overall tropical species diversity and abundance (Putz and Mooney, 1991; Schnitzer and Bongers, 2002; Burnham, 2004; Schnitzer, 2018). While studies of trees and palms have shown that environmental filtering generates edaphic specialization patterns (Fine et al., 2005; Fine and Kembel, 2011; Zuquim et al., 2012; Oliveira et al., 2014), it remains unclear whether lianas also show specialization to portions of gradients driven by forest disturbance, soil nutrients, and water availability. Moreover, we do not know if such specialization in lianas is due to the filtering of functional traits, allowing plant survival and reproduction in habitats with extreme environmental conditions (resulting in phylogenetic overdispersion), or from a historical legacy owing to trait conservatism within each environment (resulting in phylogenetic clustering). To address these unknowns, we investigated the relationship between habitat specialization and the phylogenetic structure of liana assemblages on 34 1-ha plots distributed over the landscape scale (~42 km^2) of Reserva Ducke in Central Amazon, where forest disturbances and hydro-edaphic gradients are crucial to species distribution (Toledo et al., 2012; Schietti et al., 2014). We used one of the most diverse lineages of Neotropical lianas (Bignonieae tribe, Bignoniaceae), a clade that shows species composition patterns that are congruent with those documented for other plant and animal groups (Landeiro et al., 2012; Schietti et al., 2014) and the whole liana assemblage in Central Amazonia (Rocha et al., 2021). We tested whether (i) landscape environmental gradients, such as soil water condition, forest disturbance, and soil fertility, explain the patterns of liana species diversity and composition; (ii) habitat specialization is associated with a pattern of phylogenetically clustering along these ecological gradients, and (iii) closely related liana species have more similar distribution patterns than expected by chance. We hypothesized that the three independent factors–soil water condition, forest disturbance, and soil nutrients gradients–determine the compartmentalization of subsets of more closely related species within different portions of ecological gradients. Although specialization and phylogenetic structure within habitats do not allow straightforward generalizations, the clustering pattern has been the more frequently reported for other Amazonian plant assemblages (e.g., Fine and Kembel, 2011; Eiserhardt et al., 2013; Muscarella et al., 2019) under a large set of explanatory processes (Webb, 2000; Cavender-Bares et al., 2009; Vamosi et al., 2009). Under this scenario, the most likely explanation would be phylogenetic clustering linked to environmental filtering as a basis for habitat specialization.

MATERIALS AND METHODS

Study Area and Liana Sampling Design

This study was conducted at Ducke Reserve managed by the National Institute of Amazonian Research (INPA), located 26 km northwest of Manaus (02°55′S, 59°59′W at reserve headquarters) in the state of Amazonas, Brazil. The Reserve houses 10,000 ha of lowland tropical *terra firme* rainforest. The vegetation is characterized by a closed canopy 30–37 m tall, but with emergent trees up to 45 m high and generally low light levels in the understory (Guillaumet and Kahn, 1982; Ribeiro et al., 1999; Oliveira et al., 2008). The soils represent a continuum from clayey latosols in the highest flat plateaus to increasing sand content on the slopes and turning into pure sand on valley bottoms (Chauvel et al., 1987; Mertens, 2004). The mean annual temperature is around 26°C, and the mean annual precipitation is 2,300 mm. The rainy season occurs from October to June and the dry season from July to September when rainfall is generally < 100 mm.month^{-1} (Marques Filho et al., 1981).

The Reserve has a 64 km^2 grid of trails established by the LTER-Brazil Program (Long-term Ecological Research) and PPBio (the Brazilian Biodiversity Research Program). Our liana inventory was conducted in 34 plots systematically distributed over the landscape of 42 km^2 with plots at least 1 km distant from each other. Each permanent plot was 250 m long and 40 m wide (1 ha), following the altitudinal contour (see Costa et al., 2005 and Costa and Magnusson, 2010, for further sampling design details). This sampling design aimed to reduce internal variation in the hydro-edaphic features of each plot (Costa and Magnusson, 2010). From August 2004 to October 2005, every individual liana stem rooted inside the plot with >1 cm in diameter at 130 cm from the rooting point was tagged and then counted and identified. We measured the stem diameter according to Gerwing et al. (2006). For lianas with non-cylindrical stems, we measured the minimum section ($S_{\min}$) and maximum section ($S_{\max}$) and applied the equation $D = \sqrt{Smin \times Smax}$ to obtain a corrected estimate of stem diameter. Lianas of the tribe Bignonieae (from now on called Bignonieae lianas) were identified at the species level in the study area by A. Nogueira, L. G. Lohmann and A. R. Zuntini. Bignonieae lianas represent ∼25% of Ducke's lianas species and are the most diverse lineage of lianas at Ducke reserve (Ribeiro et al., 1999; Costa et al., 2008). All lianas with a diameter (D) $\geq$ 5 cm were sampled in 1 ha (40 × 250 m), and lianas with 1 cm $\leq$ D $\leq$ 4.9 cm were subsampled in 0.25 ha (10 × 250 m) (Nogueira et al., 2011). The botanical nomenclature of all Bignonieae liana species follows Lohmann et al. (2020). For each species, liana density was expressed as the number of stems per hectare. Liana plots inventory is available in the data repository at ppbio.inpa.gov.br/en/DataBank and ForestPlots.net.

Hydro-Edaphic Gradient, Tree Turnover, and Soil Phosphorus

Several organisms, including different plant groups, have a concordant pattern of species turnover along the edaphic and topographic gradients in Central Amazonia (Landeiro et al., 2012). Variation of height above the nearest drainage (HAND) appears to be the most robust available metric describing a hydro-edaphic gradient at Ducke Reserve (Schietti et al., 2014). Therefore, we used HAND to represent one of the environmental gradients at Ducke Reserve. HAND describes the vertical height to the nearest drainage of each plot, which is an indirect estimate of the distance to the water table derived from a Shuttle Radar Topography Mission (SRTM) digital elevation model (DEM; Rennó et al., 2008; Schietti et al., 2014). Plots with high HAND values are vertically far from the water table and have clayey soils (plateaus) at Ducke Reserve, while plots with low HAND values are in lowland areas closer to the water table and have sandy soils (valleys). The HAND gradient varied from 1.4 to 52.5 m across the sampled plots. At the Ducke Reserve, HAND describes both soil texture and hydrological aspects associated with the topography, generating a strong local hydro-edaphic gradient, given the convergence of water toward the lower sandy grounds predominantly through groundwater flow (Fan et al., 2013; Schietti et al., 2014).

At Ducke Reserve, the HAND gradient is also positively correlated with the concentration of exchangeable bases (sum of bases–sodium, magnesium, potassium, and calcium) and nitrogen, but not with soil phosphorus (P; mg.kg^{-1}) concentration, commonly scarce and nutritional restrictive for plants in the Amazon basin (Dalling et al., 2016). The soil phosphorus is a macronutrient essential for energy storage and metabolic reactions in plants (Jennifer et al., 2013; Malhotra et al., 2018). Therefore, we used the phosphorus concentration (data from Castilho et al., 2006) as another environmental gradient at

Ducke Reserve. In each plot, six superficial soil samples (0–5 cm deep) were collected at 50-m intervals, mixed into a composite sample, dried at 105°C, sieved (2 mm mesh size), and analyzed at the INPA Soil Laboratory (Castilho et al., 2006). The soil phosphorus gradient varied from 0.77 to 6.71 mg.kg^{-1} across the sampled plots.

Additionally, lianas use trees as supports to reach the canopy; therefore, changes in the dynamics of trees can correspondingly affect the dynamics of lianas (Schnitzer and Bongers, 2002). Thus, estimates of tree turnover per plot (average of annual mortality and recruitment rates) were calculated using the data from Castilho et al. (2010), considering the total number of dead and recruited trees with diameter at breast height (DBH) $>$ 1 cm for 2 years. We used tree censuses undertaken between 2001/2003 and 2003/2005 to calculate the average of annualized rates of tree mortality and recruitment (Phillips and Gentry, 1994). These data were collected in the same 34 permanent plots where we sampled Bignonieae lianas. Plot width sampled for trees varied according to size class. More specifically, trees with DBH $\geq$ 30 cm were sampled at 40 × 250 m (1 ha). Trees with DBH $\geq$ 10 cm were sub-sampled in 20 × 250 m plots (0.5 ha), and trees with DBH $\geq$ 1 cm were sampled in 4 × 250 m plots (0.1 ha). Tree turnover rate calculations were standardized for the 1 ha area (Castilho et al., 2006), the same area used for the liana plots. We used the tree turnover rate, varying from 0.30 to 1.38 across the sampled plots, as the third environmental gradient at Ducke Reserve.

Phylogeny of the Tribe Bignonieae

We estimated the phylogeny of the tribe Bignonieae (Bignoniaceae) based on DNA sequences (i.e., *ndh*F and *Pep*C genes) from 133 liana species. Sequences from 118 species were obtained from Lohmann (2006), while 15 Bignonieae liana species were newly sequenced for this study (**Supplementary Table 2**). The complete list of accessions used can be found in **Supplementary Table 3**. The new sequences were obtained from DNA extractions from fresh leaves collected at Ducke Reserve. The details of DNA extraction, PCR amplification, cloning (*Pep*C gene), and sequencing are presented in Zuntini et al. (2013). Of the 133 liana species of the tribe Bignonieae included in the phylogeny, 38 were also sampled in the assembled community dataset.

We aligned each marker using Muscle (Edgar, 2004), followed by visual inspection and manual corrections when needed. A Bayesian phylogenetic tree was inferred using BEAST 1.8 (Drummond et al., 2012) using the substitution models selected by the JModelTest 2 (Darriba et al., 2012). Seven substitution schemes were used, including Bayesian information criteria. The best-fit models were TVM+G and HKY+G for the *ndh*F and *pep*C markers, respectively. The analyses were conducted using the Yule speciation model and uncorrelated lognormal clocks for each marker. Two independent runs, each with 10,000,000 generations, were performed, sampling trees every 1,000 generations. To confirm stationarity and effective sampling of parameter distribution, the logs were analyzed in Tracer 1.6 (Rambaut et al., 2014). After discarding 10% of the initial trees and combining the results from runs, we obtained the species tree in TreeAnnotator using maximum clade credibility. Posterior probabilities (pp) were used to evaluate the support of each node. Phylogeny reconstruction was run in CIPRES.

Liana Species Diversity and Composition

To characterize the species diversity and composition of the liana assemblages of the tribe Bignonieae, we used Fisher's alpha, Faith's phylogenetic diversity index and a single Non-Metric Multidimensional Scaling (NMDS) dimension describing the species composition of each of the 34 forest plots sampled.

The Fisher's alpha diversity index (α) was calculated as

$$S = \alpha \ln (1 + N/\alpha),$$

where S and N are the total number of Bignonieae liana species and individuals in the sample, respectively (Fisher et al., 1943; Magurran, 1988). Faith's phylogenetic diversity index was calculated by the sum of the lengths of the phylogenetic branches joining the basal node to the tips of all the species in the forest plots (Faith, 1992).

Liana species composition of the tribe Bignonieae distributed on the 34 plots was reduced to a single dimension using the Non-Metric Multidimensional Scaling (NMDS) ordination method, based on a dissimilarity matrix constructed with the Bray-Curtis index. The NMDS is a flexible and robust ordination technique that accommodates many distance measures with a unique assumption that the recovered dissimilarity among objects has a monotonic relationship with original distances (Minchin, 1987). The NMDS ordination performs better than other multivariate methods in recovering known structures, describing well especially ecological gradients (Minchin, 1987; Clarke, 1993). We choose the Bray-Curtis index, which is also pointed as one of the best to recover compositional similarity when applied over site-standardized data (Clarke, 1993; Legendre and Legendre, 1998; Ricotta and Podani, 2017). This standardization (species abundance transformed to relative abundance in each plot) avoids the caveats indicated by Jost et al. (2011) and was adopted here. In the NMDS, the number of dimensions in which distances among objects will be recovered is chosen before analysis. To evaluate the quality of the NMDS ordination and decide the number of axes to be used, we initially checked if the stress value was equal or less than 0.20 in the NMDS ordination with one, two, and three dimensions (Clarke, 1993). As the single NMDS dimension was within the acceptable stress limit, we present the single-dimension ordination analysis, facilitating biological interpretation in further hypothesis testing. Finally, we constructed the Shepard stress plot (**Supplementary Figure 1**) showing the relationship between the observed dissimilarities between plots and the ordination distances and estimated the linear and non-linear fit coefficient of determination to evaluate the NMDS goodness-of-fit (Clarke, 1993; Legendre and Legendre, 1998).

Phylogenetic Community Structure

To describe the phylogenetic structure of Bignonieae liana assemblages, we used four indexes of community phylogenetic structure applied to each plot (local communities): Net Relatedness Index (NRI), Nearest Taxon Index (NTI), Phylogenetic Species Variability (PSV), and Phylogenetic Species Clustering (PSC) (Webb et al., 2002; Pearse et al., 2014).

Net Relatedness Index and Nearest Taxon Index measure differences between the observed local and random communities generated by a null model of the independent swap algorithm proposed by Gotelli and Entsminger (2003). This null model randomizes the observed community matrix, keeping fixed the number of species and the frequency of occurrence in each plot (constrained null model). This null model is recommended to detect niche-based community assembly and is preferable to other null models (Webb et al., 2008; Kembel, 2009). The Net Relatedness Index (NRI) compares the phylogenetic distance among all community members, while the Nearest Taxon Index (NTI) examines only distances among nearest relatives. We calculated the NRI and NTI as

$$\mathrm{NRI} = -1 \times (\mathrm{MPD}_{\mathrm{observed}} - \mathrm{MPD}_{\mathrm{randomized}}) / sd\ (\mathrm{MPD}_{\mathrm{randomized}}) \text{ and}$$

$$\mathrm{NTI} = -1 \times (\mathrm{MNTD}_{\mathrm{observed}} - \mathrm{MNTD}_{\mathrm{randomized}}) / sd\ (\mathrm{MNTD}_{\mathrm{randomized}}),$$

where MPD and MNTD represent the Mean Pairwise Distance and the Mean Nearest Taxon Distance among co-occurring species in the plot, respectively. $\mathrm{MPD}_{\mathrm{observed}}$ and $\mathrm{MNTD}_{\mathrm{observed}}$ refer to values for the observed local community in the plot, whereas $\mathrm{MPD}_{\mathrm{randomized}}$ and $\mathrm{MNTD}_{\mathrm{randomized}}$ are the mean MPD/MNTD of the randomized assemblages ($n = 10{,}000$), and *sd* is the standard deviation of the $\mathrm{MPD}_{\mathrm{randomized}}/\mathrm{MNTD}_{\mathrm{randomized}}$. Zero values are expected for the NRI and NTI in plots without any phylogenetic structure, while positive values indicate phylogenetic clustering and negative values indicate phylogenetic overdispersion.

We calculated Phylogenetic Species Variability (PSV), which measures whether the distribution of species across the phylogeny differs from the expectation under a Brownian null model. PSV equals one when all species in the community are less closely related than expected by chance and approaches zero when species are more closely related. Phylogenetic Species Clustering (PSC) is the same as PSV, but modified to reveal how species in an assembly are clustered toward the tip of the phylogeny. PSC approaches one when species are less related to each other at the tips (Helmus et al., 2007). PSV and PSC are analogous to NRI and NTI, respectively (Miller et al., 2017).

The species pool considered was composed of 38 liana species of the tribe Bignonieae distributed across the 34 sampled plots. Alternatively, we considered a species pool consisting of 50 liana species of the tribe as described in the flora of the Ducke Reserve (Oliveira et al., 2008) and other local surveys. However, the results using this larger species pool did not differ from the species pool used initially (data not shown).

Similarity in the Distribution Curves of Liana Species

We modeled the distribution of each Bignonieae liana species along the HAND gradient, applying the kernel density curve on the occurrence data of each species across the 34 plots. We initially replaced species occurrence by the respective HAND value of the plot where the species occurred. Therefore, the HAND values recovered for each species were modeled with the kernel density function, a non-parametric method that calculates population density distributions in the niche or functional trait space (Mouillot et al., 2005; Mason et al., 2011). This method attributes a bell-shaped density distribution to each datum, in our case to each HAND value, using the following kernel function:

$$\mathrm{D}_{\mathrm{xX_i}} = e^{-\left((x-X_i)/h\right)^2} / 2\sqrt{2\pi n h},$$

where $\mathrm{D}_{\mathrm{xXi}}$ is the density (ordinal height of the bell-shaped curve) at functional trait value x = HAND for datum Xi, n is the number of data points (measurements), and h is the bandwidth that controls the smoothness of the estimator and defines the default value as $1.06\sigma n - 1/5$ with σ being the standard deviation of the trait values (Stine and Heyse, 2001). Species probability density at the HAND value is calculated as the sum of kernel density functions for each data point. Once the density distribution of each species was generated, the niche overlap between each pair of species ($\mathrm{O_{ij}}$) was calculated as the area of overlapping (%) between two probability density functions using the equation:

$$\mathrm{O_{ij}} = \int \min\left(f_{it}(x)\,,\ f_{it}(x)\right) dx,$$

where $\mathrm{f_{it}}$ and $\mathrm{f_{jt}}$ are kernel-generated probability density functions for species i and j, respectively, and x is the HAND gradient. See **Supplementary Figure 2** to visually observe the area of overlap between pairs of species (shaded area). In addition, we extracted the HAND value associated with the peak of the kernel density curve (niche optimum *sensu* Carscadden et al., 2020) for each species (see **Supplementary Figure 2**) and calculated the distance between the peaks of the curves of each species pair. We used the distance (in HAND units) as a measure of dissimilarity between niche optimums.

Statistical Analyses

To assess if hydro-edaphic (i.e., HAND), tree turnover rate, and soil phosphorus concentration gradients explain liana species diversity and composition, we used generalized linear multiple models (GLMs) with the Gaussian probabilistic distribution. We used Fisher's alpha index, Faith's phylogenetic diversity index and species composition summarized by the first and unique NMDS dimension as response variables, while the three ecological gradients were used as continuous fixed factors.

To investigate whether the phylogenetic structure of the liana assembly was related to the ecological gradients at Ducke Reserve, we used generalized linear multiple models (GLMs) with Gaussian probabilistic distribution. We used the four indexes of community phylogenetic structure (NRI, NTI, PSV, and PSC) as the response variables and the same three ecological gradients as fixed continuous factors.

Lastly, to test if closely related Bignonieae liana species have more similar distribution patterns than expected by chance, we applied matrix correlation tests (Mantel tests). In this case, the metrics for similarity of species distribution curves for each species pair were (i) the overlapping distribution area (%) and (ii) the distance between niche optimums. We used patristic phylogenetic distance among species. Similarity and distance matrices were constructed for the Mantel tests, and the significance level was determined with 10,000 permutations. Although the Mantel test is not the most suitable analytical method for testing phylogenetic signals, it is the only option when data are only expressed in pairwise distances among taxa, as suggested by Harmon and Glor (2010). This situation is the case with our measure of species overlap. To maintain the consistency of our analyses, we also applied the Mantel test to the species' niche optimum. We only considered Bignonieae liana species in the Mantel tests that occurred in at least four plots (24 species).

All statistical analyses were performed in the R environment (v. 3.2.1; R Foundation for Statistical Computing, Vienna, Austria). Fisher's alpha index and NMDS were calculated using the Vegan package (Oksanen et al., 2019). Faith's Phylogenetic Diversity, MPD, MNTD, PSV, and PSC indexes were calculated using the Picante package (Helmus et al., 2007; Kembel et al., 2010). Normality and homoscedasticity of the residuals were checked in all models using plot inspection. Multicollinearity among independent variables was always checked, evaluating each model's Variance Inflation Factor (VIF). We considered VIF of less than 2.5 as low levels of multicollinearity (Zuur et al., 2009; Adeboye et al., 2014), which was true for all our cases. We also calculated the partial determination coefficients for each predictor in the models describing the variance partition using the rsq.partial function of the R rsq package. We calculated the Gaussian kernel density curves for each Bignonieae liana species along the HAND gradient using the density function of the R stats package.

RESULTS

The Bignonieae liana assemblage was composed of 1,861 stems of 38 species in the 34 plots. On average, we found 54.7 (±37.6) stems.ha^{-1} and about 9 (±4.0) species.ha^{-1} of Bignonieae at Ducke Reserve. Most species were members of three main clades: (i) *Adenocalymma* Clade, composed of species of *Adenocalymma* exclusively (10 species); (ii) the *Fridericia*-and-Allies Clade, composed primarily of species of *Fridericia* (8), *Cuspidaria* (3), *Tanaecium* (2), and *Tynanthus* (2); and (iii) the Multiples-of-Four Clade, composed primarily of species of *Bignonia* (4), *Amphilophium* (4), and *Anemopaegma* (2). Apart from those clades, we also sampled species of *Pachyptera* (2), *Callichlamys* (1), and *Pleonotoma* (4). *Adenocalymma validum*, *Anemopaegma robustum*, *Pachyptera aromatica*, *Adenocalymma longilineum*, and *Adenocalymma adenophorum* had the highest stem density per hectare (>10 stems.ha^{-1}, **Figure 1**). *Adenocalymma longilineum*, *Pachyptera aromatica*, and *Fridericia triplinervia* occur in more than 50% of the sampled plots (**Figure 1**).

Phylogeny of Bignonieae Lianas

The Bignonieae species tree obtained using a Bayesian algorithm was broadly congruent with previous topologies reconstructed for tribe Bignonieae (Lohmann, 2006; Pace et al., 2016), with *Perianthomega vellozoi* appearing as sister to all remaining Bignonieae and the *Adenocalymma* clade appearing as sister to the core Bignonieae. Within the latter, basal relationships are poorly resolved, although two well-supported clades emerged: the Multiples-of-Four Clade, formed by *Anemopaegma*, *Bignonia*, *Mansoa*, and *Pyrostegia*, and the *Fridericia*-and-Allies Clade formed by *Cuspidaria*, *Fridericia*, *Lundia*, *Tanaecium*, *Tynanthus*, and *Xylophragma*. All 15 new accessions fall into their expected genera.

Habitat Specialization of Lianas Along Environmental Gradients

The relative importance of environmental gradients in explaining taxonomic and phylogenetic diversity was tested for the complete liana assemblage of the tribe Bignonieae. We found that Fisher's alpha diversity index was positively related to the HAND gradient (β_{st} = 0.91, df = 25, $r^2_{partial}$ = 0.21, p = 0.01; **Figure 2A**), but it was not associated with tree turnover (**Figure 2B**) nor with soil phosphorus concentration (**Figure 2C**). Faith's phylogenetic diversity index was positively related to HAND (β_{st} = 0.02, df = 25, $r^2_{partial}$ = 0.52, $p < 0.01$; **Figure 2D**) and negatively related to tree turnover (β_{st} = −0.009, df = 25, $r^2_{partial}$ = 0.18, p = 0.02; **Figure 2E**), but not associated with soil phosphorus concentration (**Figure 2F**). Therefore, both taxonomic and phylogenetic diversity of Bignonieae lianas increased along the HAND gradient. At the same time, phylogenetic diversity decreased in areas with higher tree turnover. The partial determination coefficient showed the HAND gradient as the most important predictor of liana taxonomic and phylogenetic diversity, accounting for 21 and 52% of the variance explained by the linear models, respectively. Analytical details of the models in **Figures 2**, **3** are available in **Supplementary Table 4**.

Species composition of the Bignonieae liana assemblage was represented in a single NMDS dimension with a satisfactory ordination goodness-of-fit (Stress = 0.20; linear r^2 = 0.89, non-linear r^2 = 0.96; see also the Shepard stress plot for visual inspection in the **Supplementary Figure 1**). The NMDS axis was correlated negatively with the HAND gradient (β_{st} = −0.34, df = 25, $p < 0.01$; **Figure 3A**), but it was not associated with tree turnover (**Figure 3B**) nor with soil phosphorus concentration (**Figure 3C**). A partition of the relative importance of predictors showed the HAND gradient as the most important predictor of liana assemblage composition ($r^2_{partial}$ = 0.47), accounting for 47% of the variance explained by the model.

Relative species abundance distributions along the HAND gradient showed that few Bignonieae liana species were consistently restricted to areas with lower HAND values (<13 m), i.e., those close to the valleys (*Pachyptera kerere*, *Anemopaegma robustum*, *Amphilophium magnolipholium*, and *Amphilophium elongatum*; **Figure 3D**). Toward plateau areas, a higher number of Bignonieae liana species co-occurred in areas with the highest HAND values (*Pleonotoma longiflora*, *Adenocalymma adenophorum*, *Adenocalymma tanaeciicarpum*, and *Adenocalymma validum*; **Figure 3D**). Overall, a gradual turnover of liana species composition along the HAND gradient was observed with some Bignonieae restricted to the gradient

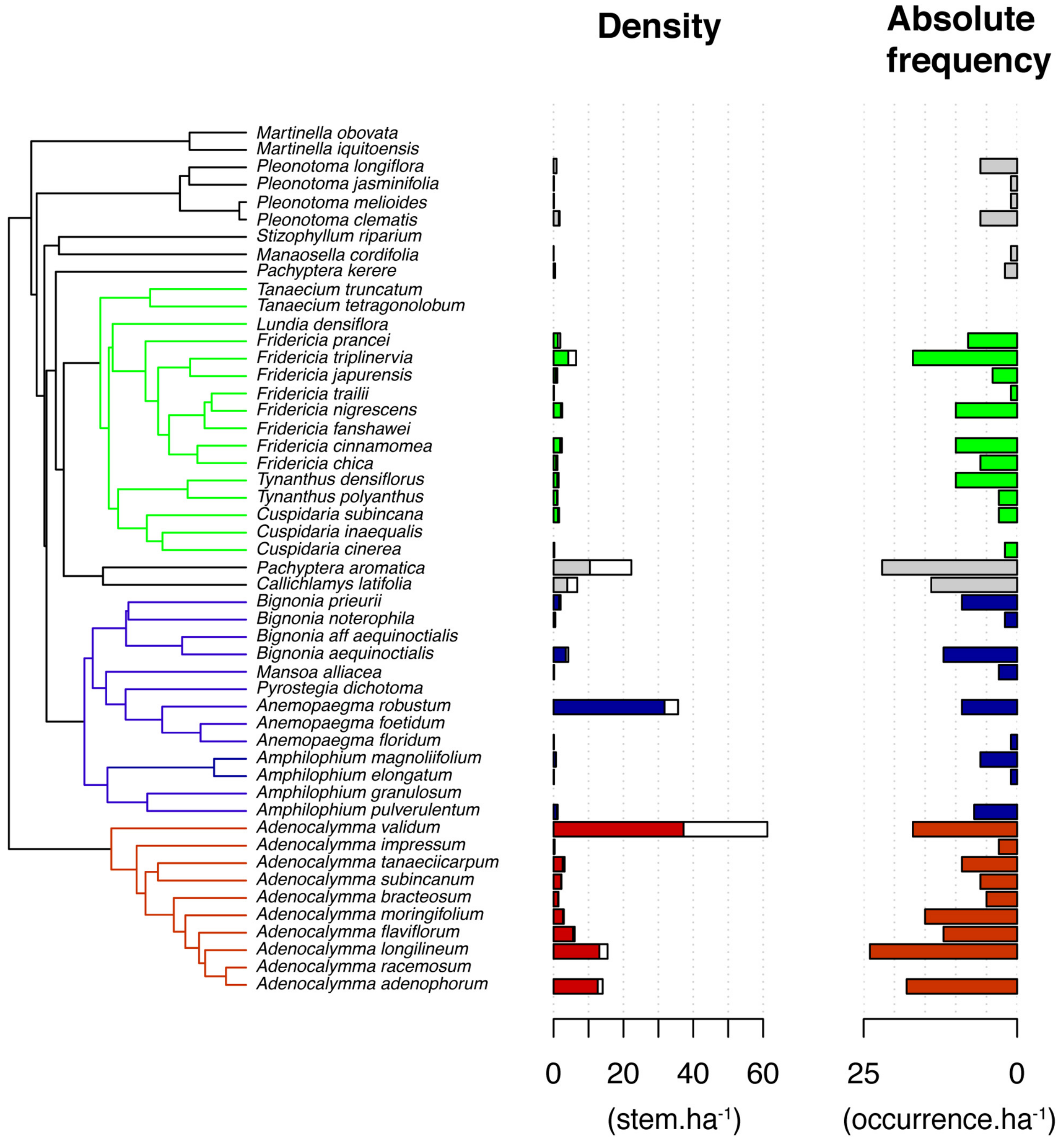

FIGURE 1 | Phylogenetic relationships among the 38 liana species of the tribe Bignonieae (Bignoniaceae) and their stem density (genets in filled bar and ramets in the hollow bar) and absolute frequency in plots sampled at Ducke Reserve (Central Amazon, Brazil). Red, blue, and green highlight the three main clades of the tribe Bignonieae: *Adenocalymma*, Multiples-of-Four, and Fridericia-and-Allies, respectively.

extremes, indicating habitat specialization along the hydro-edaphic gradient.

Different Phylogenetic Structures of Liana Assemblages Along the Hydro-Edaphic Gradient

We found that indices of species relatedness within plots (NTI) were positively related to the HAND gradient (β_{st} = 0.41, *df* = 25, $r^2_{partial}$ = 0.16, p = 0.01; **Figure 4A**), but not associated with tree turnover (**Figure 4B**) nor with soil phosphorus concentration (**Figure 4C**). Similarly, we found that PSC was negatively related to the HAND gradient (β_{st} = −0.11, *df* = 25, $r^2_{partial}$ = 0.57, p < 0.0001; **Figure 4D**), but not associated with tree turnover (**Figure 4E**) nor with soil phosphorus concentration (**Figure 4F**). In addition, PSV was negatively related to tree turnover gradient (β_{st} = −0.011, *df* = 25, $r^2_{partial}$ = 0.14, p = 0.047; **Figure 4H**), but not associated with HAND (**Figure 4G**) nor with

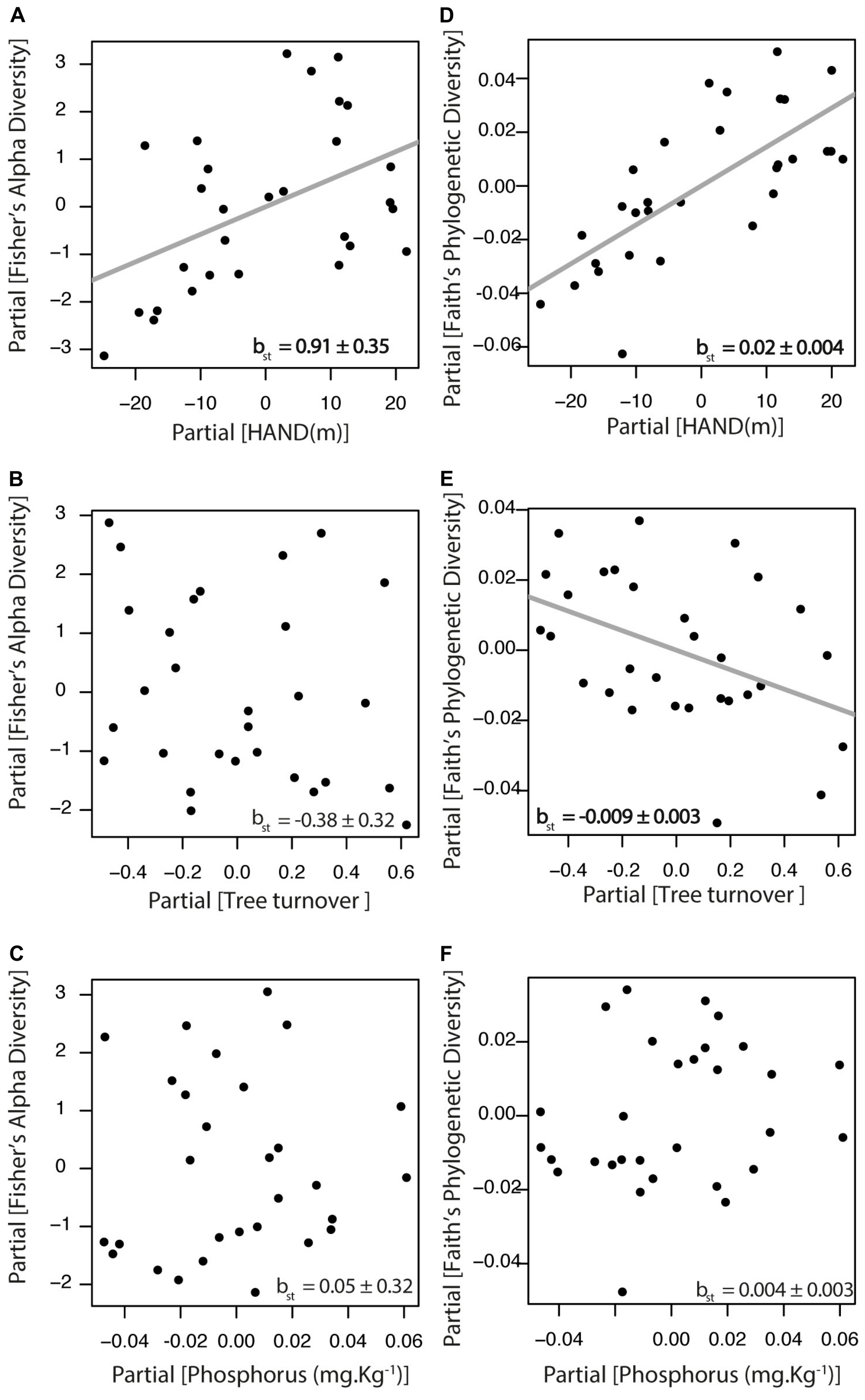

FIGURE 2 | Relationship between liana species diversity and the three environmental gradients at Ducke Reserve (Central Amazon, Brazil). All relationships are partial regressions from models, including HAND (height above the nearest drainage), tree turnover and soil P content as predictive variables. **(A–C)** Fisher's alpha diversity index; **(D–F)** Faith's phylogenetic diversity. Gray lines represent significant relationships ($p < 0.05$), and standardized multiple linear regression coefficients (β_{st} ± SE) are shown in the graphs.

soil phosphorus concentration (**Figure 4I**). In general, valleys (<13 m of HAND) had liana assemblages composed of less phylogenetically related Bignonieae species, switching to a more phylogenetically clustered liana assemblage in the plateaus with higher HAND values. NRI was unrelated to any of the three environmental gradients [$F_{(3,25)} = 0.81$, $r^2 = 0.08$, $p = 0.50$, **Supplementary Figure 3**]. Analytical details of the models in **Figure 4** are available in **Supplementary Table 5**.

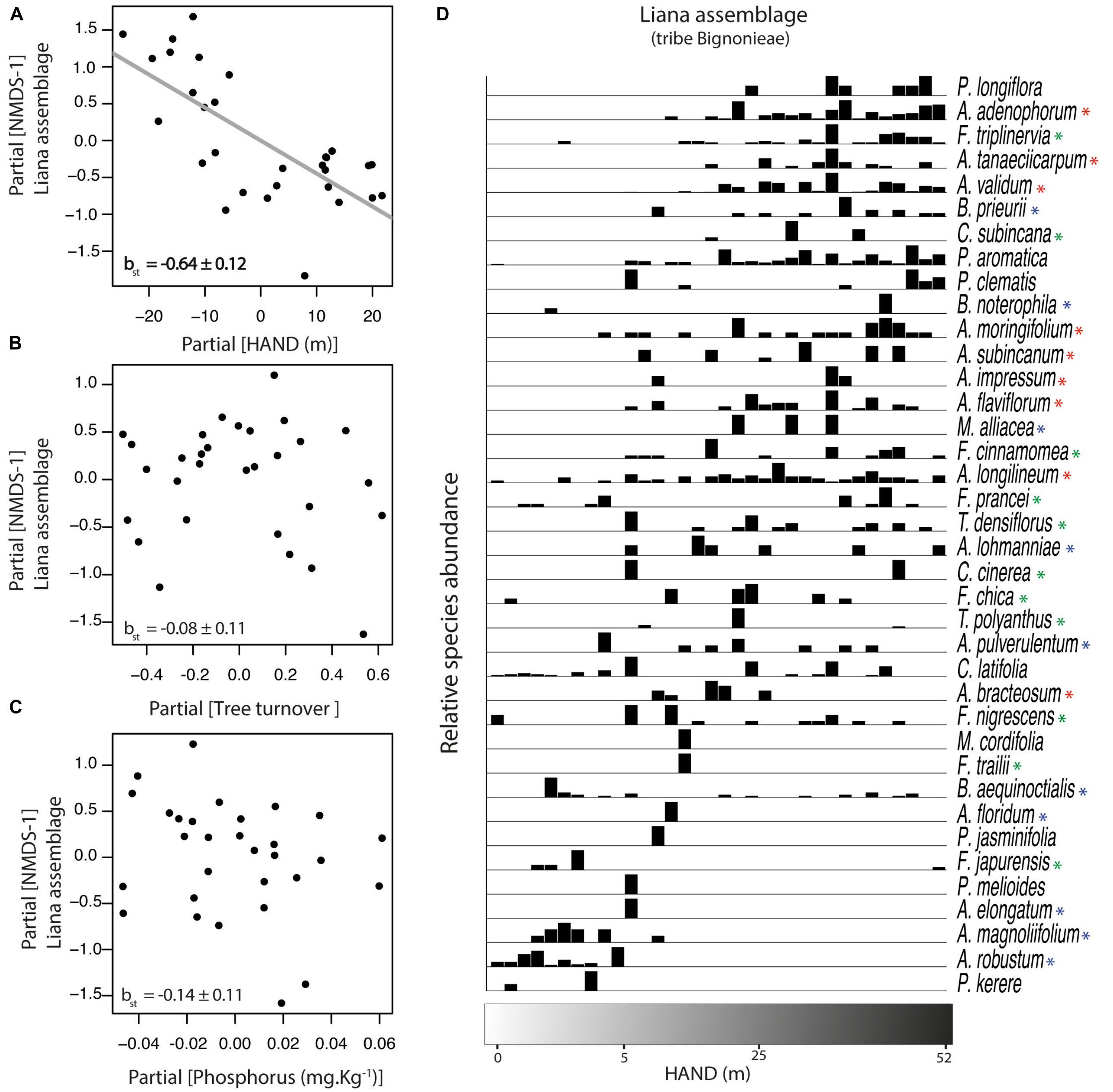

FIGURE 3 | Relationship between liana species composition (NMDS-1) and the three environmental gradients at Ducke Reserve (Central Amazon, Brazil). Relationships **(A–C)** are partial regressions from models, including HAND (height above the nearest drainage), tree turnover and soil P concentration as predictive variables. The gray line represents a significant relationship ($p < 0.05$). Standardized multiple linear regression coefficients (β_{st} ± SE) are shown in the graphs. **(D)** Species abundance distribution on the 34 plots is based on direct ordination along the HAND gradient. See **Figure 1** for abbreviations of scientific terms. Red, blue, and green asterisks highlight the three main clades of the tribe Bignonieae: *Adenocalymma*, Multiples-of-Four, and Fridericia-and-Allies, respectively.

Modeling the distribution of each Bignonieae liana species along the hydro-edaphic gradient using the kernel density curve showed that liana species of the *Adenocalymma* Clade are more abundant in areas with higher HAND values. Similarly, closely related species in this clade are more abundant in more elevated portions of the HAND gradient with rare exceptions (**Figure 5A**). On the other hand, liana species of the Multiple-of-Four Clade were more often distributed in areas with lower HAND values with more exceptions in species distribution (**Figure 5A**). Species of the *Fridericia*-and-Allies Clade were more evenly distributed across the HAND gradient, although often associated with higher HAND values. In that case, closely related species often occupied higher portions of the HAND gradient (**Figure 5A**), although we found exceptions to this pattern. All other Bignonieae liana species outside these three major clades included closely related

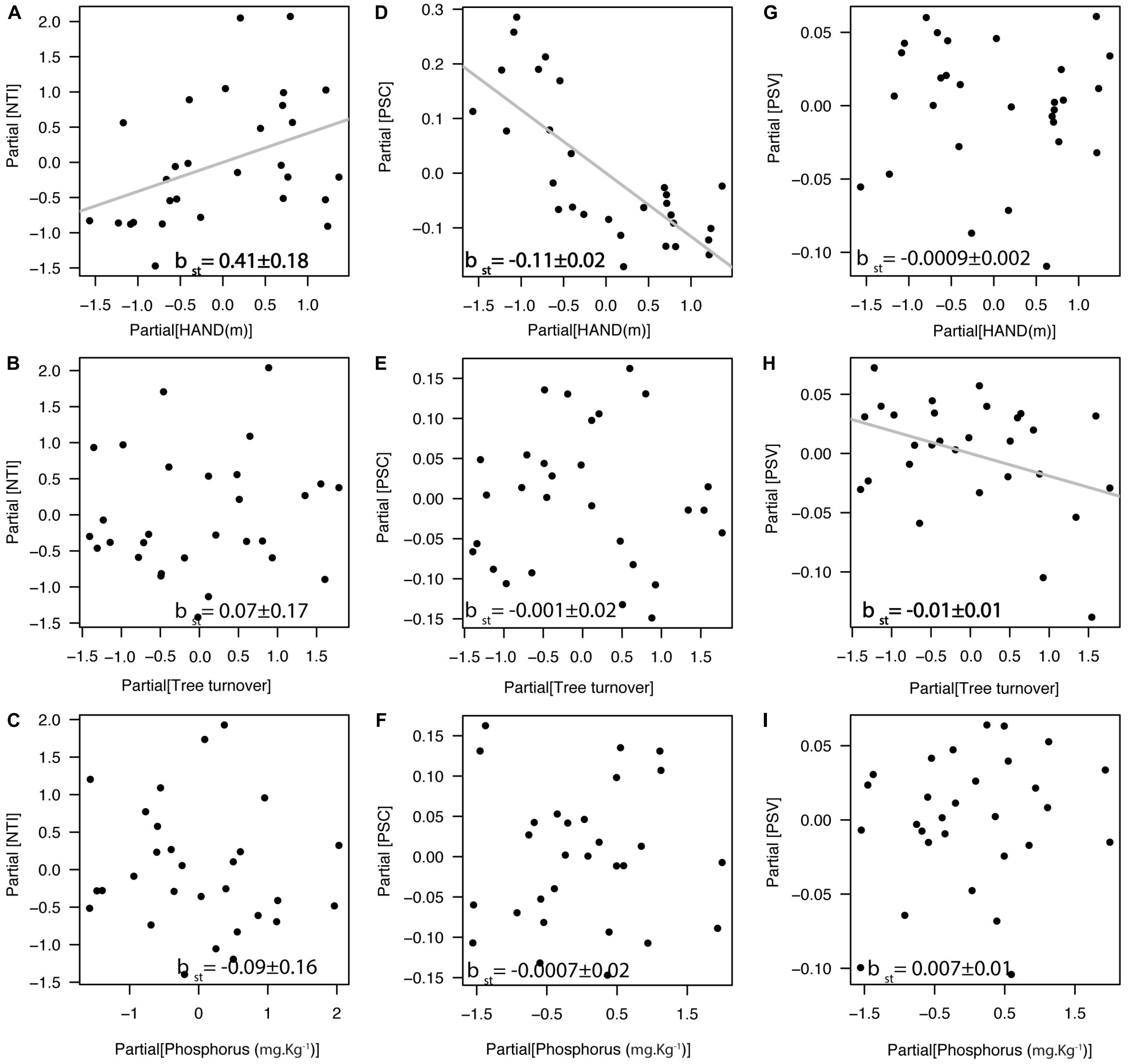

FIGURE 4 | Relationship between the phylogenetic structure of the liana assemblage and the three environmental gradients at Ducke Reserve (Central Amazon, Brazil). All relationships are partial regressions from models, including HAND (height above the nearest drainage), tree turnover and soil P content as predictive variables. **(A–C)** Nearest taxon index (NTI); **(D–F)** Phylogenetic species clustering (PSC); **(G–I)** Phylogenetic species variability (PSV). Gray lines and bold values represent significant relationships ($p < 0.05$), and standardized multiple linear regression coefficients (β_{st} ± SE) are shown in the graphs. Higher NTI values and lower PSC or PSV values indicate phylogenetic clustering, and lower NTI values and higher PSC or PSV values indicate phylogenetic overdispersion, relative to a null model of random shuffling of taxa labels across the tips of the phylogenetic tree including all taxa.

species that occupied contrasting portions of the HAND gradient (**Supplementary Figure 4**).

The Mantel test detected a negative relationship between the overlap of the species distribution curve along the HAND gradient and phylogenetic distance ($r = -0.12$, $p = 0.02$, **Figure 5B**). The Mantel test also detected a positive relationship between the pairwise distance of niche optimum in the HAND gradient and phylogenetic distance ($r = 0.15$, $p = 0.02$, **Figure 5C**). Therefore, closely related liana species of the tribe Bignonieae had a greater overlap in their distribution and smaller distance of niche optimum in the HAND gradient.

DISCUSSION

Variation in forest disturbance, soil nutrients, and soil hydrology constitute gradients affecting the assemblage of different plant groups at the landscape scale. However, the diversity and

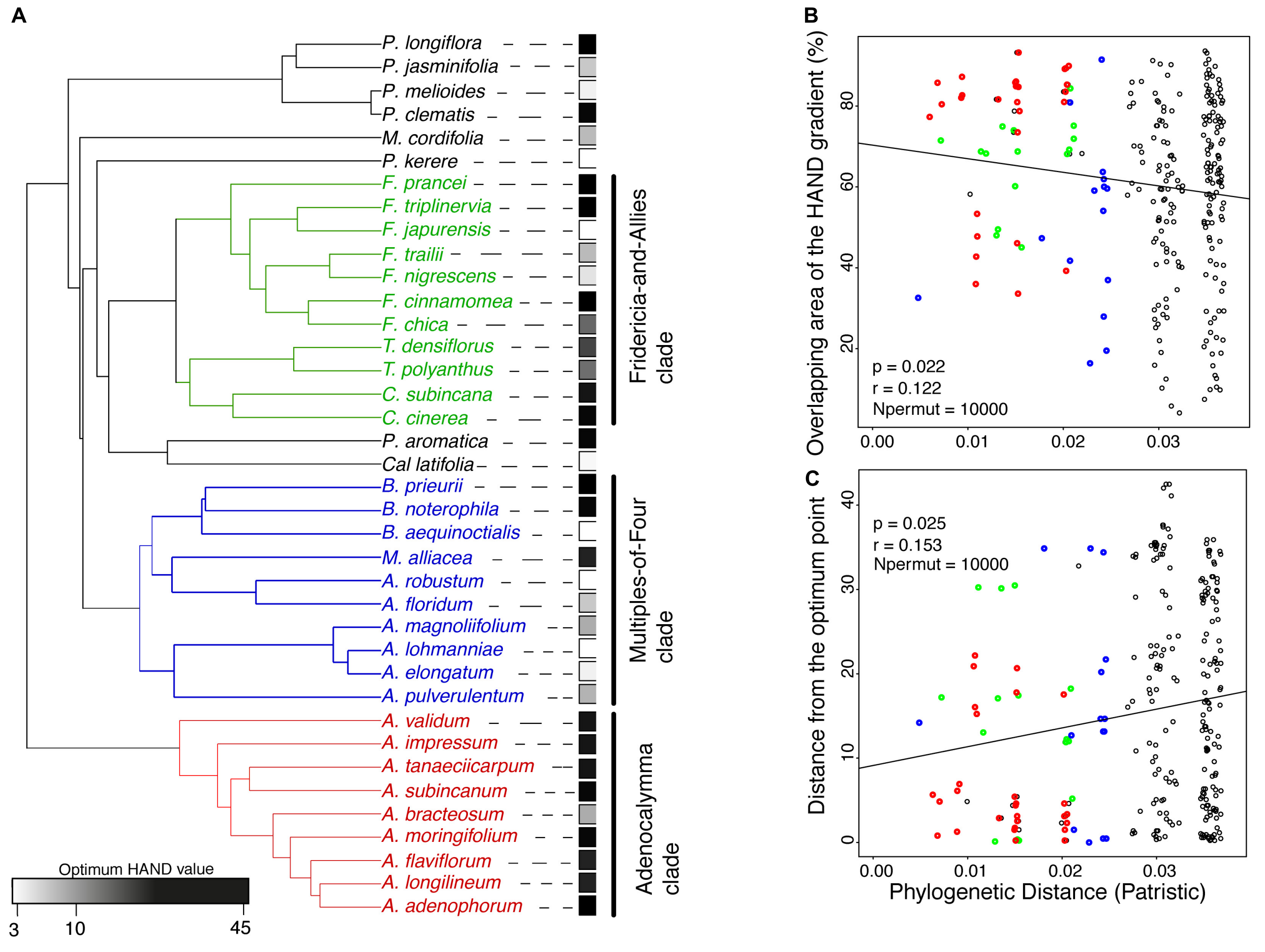

FIGURE 5 | Relationship between phylogenetic pattern and liana species distribution of the tribe Bignonieae in the HAND gradient. **(A)** Phylogenetic relationship of the tribe Bignonieae with the optimum value of each species in the HAND gradient. **(B)** Negative relationship between the overlapping area of the HAND gradient and the Phylogenetic Distance (Patristic). **(C)** Positive relationship between the distance from the optimum value of each species in the HAND gradient and the phylogenetic distance (Patristic). See **Figure 1** for abbreviations of scientific terms. Red, blue, and green highlight the three main clades of the tribe Bignonieae: *Adenocalymma*, Multiples-of-Four, and Fridericia-and-Allies, respectively. Black points represent other species of the tribe Bignonieae.

composition of lianas in our study site were explained almost exclusively by the hydro-edaphic gradient, as defined by the height above the nearest drainage (HAND). We found that (1) liana species composition of the tribe Bignonieae changes along the hydro-edaphic gradient, partially owing to habitat specialization, with wet valleys holding a lower taxonomic diversity of phylogenetically dispersed species, while well-drained plateaus concentrated higher diversity of closely related taxa, and (2) in general, closely related liana species had a larger distribution overlap and smaller distances among hydro-edaphic niche optimum values. These findings indicate habitat filtering by different mechanisms depending on specific environmental conditions along the hydro-topographic gradient.

To understand the divergent patterns of habitat filtering in this forest, we need to understand the physicochemical conditions created by topography and how they affect forest structure. Topography generates a strong local hydro-edaphic gradient, given the convergence of water toward the lower grounds, predominantly through groundwater flow (Fan et al., 2013; Schietti et al., 2014; Costa et al., 2022). Where the water table is close to the surface, in sandy valley soils, water availability is more extensive through the year, although this condition also generates waterlogging at least seasonally (Hodnett et al., 1997). Waterlogging comes with anoxia and reduced nitrogen availability (Ponnamperuma, 1972; Luizão et al., 2004), both limiting conditions for plant development (Parent et al., 2008; Kreuzwieser and Gessler, 2010). Waterlogging also leads to a loose, less cohesive aggregation among soil particles which is summed to the sandy soil type and the shallow rooting imposed by shallow water tables (Fan et al., 2017), decreasing the soil capacity to anchor roots firmly (Fraser, 1962; Ennos, 2000). As we move away from valleys toward the top of hills, water table depth increases, and the soil becomes progressively clayey (Chauvel et al., 1987; Luizão et al., 2004). Clayey plateau soils hold more nutrients, such as nitrogen and exchangeable bases (Luizão et al., 2004; Costa et al., 2005), have lower permeability and higher water-holding capacity than sandy valley soils (Sanchez, 2019). However, during the dry season, these portions of the hydro-edaphic gradient have lower water availability for plants, especially in extreme drought years (Costa et al., 2020). The clayey soils on the plateaus are deep and well-structured, providing a good root anchoring (Quesada et al., 2009). Thus, the topography, hydrology, and edaphic factors comprise a complex scenario that creates distinct habitats for plants along the hydro-edaphic gradient of Ducke Reserve.

The habitats formed along the hydro-edaphic gradient, in turn, affect forest structure, determining potential support for lianas in the lower strata of the forest. Valleys are associated with a lower density of trees and a high density of palms (Kahn and Castro, 1985; Nogueira et al., 2011) that typically offer poor support for the canopy rise of lianas (Putz, 1984b; Nogueira et al., 2011). Compared to valleys, clayey plateaus on the opposite side of the hydro-edaphic gradient have a higher density of trees, including trees of different sizes and fewer canopy palms (Castilho et al., 2006; Nogueira et al., 2011). This forest structure in the plateaus creates favorable conditions with the greatest potential to support liana climbing during development and its maintenance after reaching the forest canopy (Nogueira et al., 2011). This set of favorable and unfavorable environmental conditions below and above-ground across the hydro-edaphic gradient constitute differential filters of the lianas species assemblage, affecting the diversity and distribution of plants, as discussed below.

Assembly Along the Hydro-Edaphic Gradient

The more restrictive conditions in valleys, as noted above, result in strong environmental filtering of a small set of species. Decreased plant species diversity is expected in more restrictive environments (Givnish, 1999), such as flooded forests with hypoxic to anoxic soils, limiting the growth, survival, and reproduction of non-edaphic specialists (Parolin, 2009; Parolin and Wittmann, 2010). Although wind-dispersed seeds of Bignonieae liana species may often arrive in valleys, our data highlight that only a few liana species can grow in these restrictive conditions. A lower diversity in wetlands and flooded forests compared to that in uplands was also found for liana and tree assemblages in other regions of the Amazon basin (Burnham, 2002; Muscarella et al., 2019). Functional traits required to be successful in these conditions may include the ability to germinate, establish and propagate in anoxic waterlogged soils (Parent et al., 2008; Parolin, 2009). The high rates of vegetative propagation of the few Bignonieae liana species that grow in valleys may contribute to maintaining individuals of these species locally (Rocha et al., 2020). In those species, such as the most abundant liana species of valleys *Anemopaegma robustum*, it is common the production of a high number of adventitious roots with denser lenticels (CG personal observations) which can improve root oxygenation during waterlogging. Also, other undocumented traits for lianas could be crucial under such conditions. For example, alternative energy production routes, such as fermentation, and as plants grow, the existence of aerenchyma (Parent et al., 2008; Parolin, 2009).

Non-exclusive mechanisms can explain the habitat specialization associated with a phylogenetically overdispersed pattern in valleys–evolutionary convergence in functional traits and biotic interactions. Repeated colonization through time by multiple species from different clades bearing particular and similar functional traits appropriate for this more restrictive environment, i.e., evolutionary convergence, may create an overdispersed phylogenetic pattern. Evolutionary convergence agrees well with the distribution of functional traits of lianas described along the hydro-edaphic gradient (Rocha et al., 2021). Liana species in valleys share similar traits, including Bignonieae lianas, such as lower wood density and specific leaf area, larger stomata size and self-supporting xylem area (Rocha et al., 2021), despite the large phylogenetic distance among those liana species. Low wood density species with cheaper stem construction tend to grow more rapidly in short but more favorable periods of the year (King et al., 2006; Larjavaara and Muller-Landau, 2010; Rüger et al., 2012), which may be advantageous in the seasonally waterlogged valleys, where the short dry season provide the most favorable mesic soil conditions for growth. In addition, the larger self-supporting xylem area in the stems allow lianas to behave as freestanding woody plants in the understory during unfavorable periods along development.

Biotic interactions may also be invoked to explain the overdispersion pattern in more restrictive habitats, although these are so far more speculative arguments. For example, interspecific competition and facilitation could both generate or reinforce an overdispersion pattern. Past competition could lead to local extinction of ecologically similar and closely related species if strong competitive interactions dominate (Webb et al., 2002; Cavender-Bares et al., 2004, 2009). However, under stressful conditions, positive interactions among plant species as facilitation are more likely than competition (Bertness and Callaway, 1994). Although the facilitation process is a speculative explanation here, a particular attachment structure found in Bignonieae liana associated with valleys–the adhesive tendrils (e.g., *Amphilophium magnoliifolium* and *Bignonia aequinoctiales*) allows this possibility. Adhesive tendrils enable lianas to attach and climb to vertical supports independently of their overall size and shape (Sousa-Baena et al., 2018; Sperotto et al., 2020), potentially overcoming the limitations of inadequate supports such as palms. After establishing themselves, these liana species can act as adequate support for other younger liana species with different attachment structures to climb, i.e., they facilitate their climbing process. If the facilitation process is more recurrent within valley liana species than in plateaus species, the presence of a first canopy Bignonieae liana established in inadequate support could contribute to the local establishment of newly arriving younger lianas of more distantly related species (e.g., Verdú et al., 2009; Valiente-Banuet and Verdú, 2013).

As we move away from the valleys toward the top of the hills, we detect an increase in liana species diversity that is composed of a different set of Bignonieae liana species. The greater soil fertility, higher density of adequate support, and the more stable and less restrictive conditions of plateaus allow the co-occurrence of a higher number of liana species (Rocha et al., 2021), including lianas of the tribe Bignonieae, despite the lower water availability than valleys. Soil water restriction in the dry season probably does not limit lianas at Ducke Reserve, as species associated with plateaus show higher embolism resistance than those of valleys (Gerolamo et al., 2018 unpublished data; Oliveira et al., 2019). Lianas under such conditions may also rely on deep roots, hydraulic redistribution associated with multifocal growing strategies, or higher water storage capacity (de Azevedo Amorim et al., 2018).

On plateaus, habitat specialization is associated with a high diversity of more closely related liana species of the tribe Bignonieae. This phylogenetically clustered pattern may have emerged from the weak interspecific competition and a predominance of environmental filtering of conserved traits (Webb et al., 2002; Cavender-Bares et al., 2004, 2009; Hubbell, 2005). Supporting this, we noticed similar functional traits (e.g., higher wood density) in the liana species co-occurring in the higher portions of the hydro-edaphic gradient (Rocha et al., 2021). The higher wood density is associated with the high hydraulic resistance (Hacke and Sperry, 2001; Jacobsen et al., 2005) probably required for liana maintenance in the plateaus. This pattern supports trait conservatism across Bignonieae liana species on the plateau.

Therefore, hydro-edaphic habitat specialization associated with different patterns of phylogenetic structure of lianas of the tribe Bignonieae is mediated by specific functional traits at Ducke Reserve, probably generated by a strong species filtering in the valleys and a distinct and soft species filtering in plateaus. This differential filtering pattern of liana species of the tribe Bignonieae associated to hydro-edaphic conditions here described is similar to the patterns of other plant groups found at the same site (Drucker et al., 2008; Landeiro et al., 2012; Freitas et al., 2014; Schietti et al., 2014; Cosme et al., 2017; Oliveira et al., 2019; Costa et al., 2020) and elsewhere (Fine et al., 2005; Eiserhardt et al., 2013; Muscarella et al., 2019; **Supplementary Table 1**). In addition, the overdispersed phylogenetic pattern observed for the Bignonieae lianas in the valleys of Ducke Reserve was also found for palm assemblages at the same site (Freitas et al., 2014). Overdispersion under such conditions appears to be shared among sites beyond Central Amazonia, e.g., trees and shrubs in flooded forest or white-sand habitats with periodic flooding (Fine et al., 2005; Fine and Kembel, 2011; Eiserhardt et al., 2013; Oliveira et al., 2014; Araújo and Santos, 2019), pointing to generality in these Amazonian systems (but see Baraloto et al., 2021 for a discussion at higher taxonomic levels). Under such conditions, we highlight that the convergence of functional traits to deal with more stressful environments and less likely facilitation among plant species could explain the phylogenetic structure of all plant groups beyond lianas.

Phylogenetic diversity of Bignonieae lianas was negatively related to tree turnover rate. Higher tree turnover rates occur in areas with a higher frequency of tree fall (canopy gaps) with a consequent increase in light availability (Canham et al., 1990). Light availability increases the recruitment of lianas and, thus, liana stem densities (Schnitzer et al., 2000; Dalling et al., 2012; Gerolamo et al., 2018; Schnitzer, 2018), but not liana diversity, as a few more opportunistic species quickly occupy patches with high light availability (Putz, 1984a). Bignonieae liana diversity and species composition were unrelated to soil phosphorus concentration, similar to other reports (e.g., Dalling et al., 2012). This pattern may simply be a consequence of the short extent of the phosphorus gradient in the landscape (Pansonato et al., 2013), which is valid for our study site (mean concentration of available soil phosphorus 3.2 ± SD2.3 mg.kg^{-1}, Costa et al., 2005). The soil diversity in the Amazon basin is mainly related to differences in geology manifesting mostly at the regional rather than local to meso scales (Quesada et al., 2011). Liana species diversity and composition have been shown to respond to soil phosphorus in other sites (e.g., the Montane subtropical forest) (Malizia et al., 2010), but this effect has remained elusive in the Amazon forest.

CONCLUSION

We identified a general pattern of phylogenetic clustering among lianas of the tribe Bignonieae at Ducke Reserve. This pattern emerges from the fact that most liana species occur in the higher portions of the HAND gradient, where the phylogenetic structure of the liana assemblage is clustered. Thus, niche conservatism emerges as the most general pattern for this clade of lianas in this central Amazon forest, where more closely related species co-occur in higher portions of the hydro-edaphic gradient. However, valleys diverge from this pattern by having phylogenetically overdispersed assemblages.

We conclude that ecological filters and phylogenetic history have played fundamental roles in structuring liana assemblies at the landscape scale. In sum, the pattern of hydro-edaphic habitat specialization results from different ecological processes that have contributed to the assembly of local communities from valleys to plateaus, with the strength of environmental filters varying along this gradient. These findings highlight the need for future experimental studies to understand the causes behind the diversity of liana assemblies across habitats. For example, studies investigating how different liana strategies varying in leaf, stem, and root functional traits are responsible for the good performance of liana species along the hydro-edaphic gradient. Data of this nature will, in turn, help clarify the role of fine-scale soil hydrology in the evolutionary history of Amazonian flora.

DATA AVAILABILITY STATEMENT

The raw data supporting the conclusions of this article will be made available by the authors, without undue reservation.

AUTHOR CONTRIBUTIONS

AN, AV, and FC conceived the ideas and designed the experiments. AN and AZ collected the data. AN, LL, and AZ identified the plant species. CG, AZ, and AN analyzed the data and led the writing of the manuscript. All authors contributed to the manuscript writing and revision and approved the final version.

FUNDING

This study was supported by the Coordenação de Aperfeiçoamento de Pessoal de Nível Superior - Brasil (CAPES) Finance code 88882.333016/2019-01, São Paulo Research Foundation (FAPESP 2018/06917-7, 2018/23899-2), and Conselho Nacional de Desenvolvimento Científico e Tecnológico (CNPq Grants 441282/2016-4, 403764/2012-2, and 558244/2009-2) that funded the Central Amazon Long-term Ecological Project, the plots of which were used for this study. Additional funds were provided to LL by CNPq through a Pq-1B grant (310871/2017-4) and to AN by CNPq through a Postdoctoral Fellowship (CNPq Grant 234000/2014-7) and Research Grant (434692/2018-2), and by the FAPESP through a Young Investigators Grant (FAPESP 2019/19544-7).

ACKNOWLEDGMENTS

We thank Paulo Inacio for the valuable discussion on data analyses in the first ideas of this work. We also thank all staff at the Department of Reserves (DSER) of the National Institute for Amazonian Research (INPA) for logistical support, as well as everyone involved in fieldwork, especially João Batista da Silva, Raimunda Nazaré Oliveira de Araújo, and Sebastião Salvino de Souza.

SUPPLEMENTARY MATERIAL

The Supplementary Material for this article can be found online at: https://www.frontiersin.org/articles/10.3389/ffgc.2022.809904/full#supplementary-material

REFERENCES

Adeboye, N. O., Fagoyinbo, I. S., and Olatayo, T. (2014). Estimation of the Effect of Multicollinearity on the Standard Error for Regression Coefficients. *IOSR J. Math.* 10, 16–20. doi: 10.9790/5728-10411620

Araújo, F. D. C., and Santos, R. M. (2019). Different degrees of water-related stress affect evolutionary diversity in a seasonally dry biome. *Oecologia* 189, 795–802. doi: 10.1007/s00442-019-04358-4

Baraloto, C., Vleminckx, J., Engel, J., Petronelli, P., Dávila, N., RÍos, M., et al. (2021). Biogeographic history and habitat specialization shape floristic and phylogenetic composition across Amazonian forests. *Ecol. Monogr*. 91:e01473. doi: 10.1002/ecm.1473.

Bertness, M. D., and Callaway, R. (1994). Positive interactions in communities. *Trends Ecol. Evol.* 9, 191–193. doi: 10.1201/9780203738559

Bordon, N. G., Nogueira, A., Leal Filho, N., and Higuchi, N. (2019). Blowdown disturbance effect on the density, richness and species composition of the seed bank in Central Amazonia. *For. Ecol. Manage.* 453:117633. doi: 10.1016/j.foreco.2019.117633

Bullock, E. L., Woodcock, C. E., Souza, C., and Olofsson, P. (2020). Satellite-based estimates reveal widespread forest degradation in the Amazon. *Glob. Chang. Biol.* 26, 2956–2969. doi: 10.1111/gcb.15029

Burnham, R. J. (2002). Dominance, diversity and distribution of lianas in Yasuní, Ecuador: Who is on top? *J. Trop. Ecol.* 18, 845–864. doi: 10.1017/S0266467402002559

Burnham, R. J. (2004). Alpha and beta diversity of Lianas in Yasuní, Ecuador. *For. Ecol. Manage.* 190, 43–55. doi: 10.1016/j.foreco.2003.10.005

Canham, C. D., Denslow, J. S., Platt, W. J., Runkle, J. R., Spies, T. A., and White, P. S. (1990). Light regimes beneath closed canopies and tree-fall gaps in temperate and tropical forests. *Can. J. For. Res.* 20, 620–631.

Carscadden, K. A., Emery, N. C., Arnillas, C. A., and Cadotte, M. W. (2020). Niche breadth: Causes and consequences for ecology, evolution, and conservation. *Q. Rev. Biol.* 953, 179–214.

Castilho, C. V., Magnusson, W. E., De Araújo, R. N. O., and Luizão, F. J. (2010). Short-term temporal changes in tree live biomass in a central amazonian forest, Brazil. *Biotropica* 42, 95–103. doi: 10.1111/j.1744-7429.2009.00543.x

Castilho, C. V., Magnusson, W. E., de Araújo, R. N. O., Luizão, R. C. C., Luizão, F. J., Lima, A. P., et al. (2006). Variation in aboveground tree live biomass in a central Amazonian Forest: Effects of soil and topography. *For. Ecol. Manage.* 234, 85–96. doi: 10.1016/j.foreco.2006.06.024

Cavender-Bares, J., Kitajima, K., and Bazzaz, F. A. (2004). Multiple trait associations in relation to habitat differentiation among 17 Floridian oak species. *Ecol. Monogr.* 74, 635–662. doi: 10.1890/03-4007

Cavender-Bares, J., Kozak, K. H., Fine, P. V. A., and Kembel, S. W. (2009). The merging of community ecology and phylogenetic biology. *Ecol. Lett.* 12, 693–715. doi: 10.1111/j.1461-0248.2009.01314.x

Chauvel, A., Lucas, Y., and Boulet, R. (1987). On the genesis of the soil mantle of the region of Manaus. *Experientia* 43, 234–241.

Clarke, K. R. (1993). Non-parametric multivariate analyses of changes in community structure. *Aust. J. Ecol.* 18, 117–143.

Cosme, L. H. M., Schietti, J., Costa, F. R. C., and Oliveira, R. S. (2017). The importance of hydraulic architecture to the distribution patterns of trees in a central Amazonian forest. *New Phytol.* 215, 113–125. doi: 10.1111/nph.14508

Costa, F. R. C., Castilho, C., Drucker, D. P., Kinupp, V., Nogueira, A., and Spironello, W. (2008). "Flora," in *Reserva Ducke: A biodiversidade Amazônica Através de Uma Grade*, eds M. L. de Oliveira, F. B. Baccaro, R. Braga-Neto, and W. E. Magnusson (Manaus, Brazil: Áttema Design Editoria), 23–30.

Costa, F. R. C., and Magnusson, W. E. (2010). The need for large-scale, integrated studies of biodiversity - the experience of the program for biodiversity research in Brazilian Amazonia. *Nat. Conserv.* 8, 3–12. doi: 10.4322/natcon.00801001

Costa, F. R. C., Magnusson, W. E., and Luizao, R. C. (2005). Mesoscale distribution patterns of Amazonian understorey herbs in relation to topography, soil and watersheds. *J. Ecol.* 93, 863–878. doi: 10.1111/j.1365-2745.2005.01020.x

Costa, F. R. C., Zuanon, J. A. S., Baccaro, F. B., de Almeida, J. S., Menger, J. da S., Souza, J. L. P., et al. (2020). Effects of climate change on central amazonian forests: A two decades synthesis of monitoring tropical biodiversity. *Oecologia Aust.* 24, 317–335. doi: 10.4257/oeco.2020.2402.07

Costa, F. R., Schietti, J., Stark, S. C., and Smith, M. N. (2022). The other side of tropical forest drought: Do shallow water table regions of Amazonia act as large-scale hydrological refugia from drought? *New Phytol.* 3–29. doi: 10.1111/nph.17914

Dalling, J. W., Heineman, K., Lopez, O. R., Wright, S. J., and Turner, B. L. (2016). "Nutrient Availability in Tropical Rain Forests: The Paradigm of Phosphorus Limitation," in *Tropical Tree Physiology*, eds. G. Goldstein and L. Santiago (New York: Springer), 261–273. doi: 10.1038/248302c0.

Dalling, J. W., Schnitzer, S. A., Baldeck, C., Harms, K. E., John, R., Mangan, S. A., et al. (2012). Resource-based habitat associations in a neotropical liana community. *J. Ecol.* 100, 1174–1182. doi: 10.1111/j.1365-2745.2012.01989.x

Darriba, D., Taboada, G. L., Doallo, R., and Posada, D. (2012). JModelTest 2: More models, new heuristics and parallel computing. *Nat. Methods* 9:772. doi: 10.1038/nmeth.2109

Darwin, C. (1859). *On the Origin of Species*. London: Murray, J.

de Azevedo Amorim, T., Nunes-Freitas, A. F., and Rosado, B. H. P. (2018). Revisiting the hypothesis for increasing liana abundance in seasonal forests: a theoretical review. *Plant Soil* 430, 1–6. doi: 10.1007/s11104-018-3730-6.

Drucker, D. P., Costa, F. R. C., and Magnusson, W. E. (2008). How wide is the riparian zone of small streams in tropical forests? A test with terrestrial herbs. *J. Trop. Ecol.* 24, 65–74. doi: 10.1017/S0266467407004701

Drummond, A. J., Suchard, M. A., Xie, D., and Rambaut, A. (2012). Bayesian phylogenetics with BEAUti and the BEAST 1.7. *Mol. Biol. Evol.* 29, 1969–1973. doi: 10.1093/molbev/mss075

Edgar, R. C. (2004). MUSCLE: Multiple sequence alignment with high accuracy and high throughput. *Nucleic Acids Res.* 32, 1792–1797. doi: 10.1093/nar/gkh340

Eiserhardt, W. L., Svenning, J. C., Borchsenius, F., Kristiansen, T., and Balslev, H. (2013). Separating environmental and geographical determinants of phylogenetic community structure in Amazonian palms (Arecaceae). *Bot. J. Linn. Soc.* 171, 244–259. doi: 10.1111/j.1095-8339.2012.01276.x

Ennos, A. R. (2000). The mechanics of root anchorage. *Adv. Bot. Res.* 33, 133–157. doi: 10.1016/s0065-2296(00)33042-7

Faith, D. P. (1992). Conservation evaluation and phylogenetic diversity. *Biol. Conserv.* 61, 1–10. doi: 10.1016/0006-3207(92)91201-3

Fan, Y., Li, H., and Miguez-Macho, G. (2013). Global patterns of groundwater table depth. *Science* 339, 940–943. doi: 10.1126/science.1229881

Fan, Y., Miguez-Macho, G., Jobbágy, E. G., Jackson, R. B., and Otero-Casal, C. (2017). Hydrologic regulation of plant rooting depth. *Proc. Natl. Acad. Sci. U. S. A.* 114, 10572–10577. doi: 10.1073/pnas.1712381114

Fine, P. V. A., Daly, D. C., Muñoz, G. V., Mesones, I., and Cameron, K. M. (2005). The Contribution of Edaphic Heterogeneity To the Evolution and Diversity of Burseraceae Trees in the Western Amazon. *Evolution* 59, 1464. doi: 10.1554/04-745

Fine, P. V. A., and Kembel, S. W. (2011). Phylogenetic community structure and phylogenetic turnover across space and edaphic gradients in western Amazonian tree communities. *Ecography (Cop.).* 34, 552–565. doi: 10.1111/j.1600-0587.2010.06548.x

Fisher, R. A., Corbet, A. S., and Williams, C. B. (1943). The Relation Between the Number of Species and the Number of Individuals in a Random Sample of an Animal Population. *J. Anim. Ecol.* 12, 42. doi: 10.2307/1411

Fraser, A. I. (1962). The soil and roots as factors in tree stability. *Forestry* 34, 117–127. doi: 10.1093/forestry/34.2.117

Freitas, C. G., de Sales Dambros, C., Eiserhardt, W. L., Costa, F. R. C., Svenning, J. C., and Balslev, H. (2014). Phylogenetic structure of a palm community in the central Amazon: changes along a hydro-edaphic gradient. *Plant Ecol.* 215, 1173–1185. doi: 10.1007/s11258-014-0376-1

Gentry, A. (1988). Changes in Plant Community Diversity and Floristic Composition on Environmental and Geographical Gradients. *Ann. Missouri Bot. Gard.* 75, 1–34.

Gerolamo, C. S., Nogueira, A., Costa, F. R. C., de Castilho, C. V., and Angyalossy, V. (2018). Local dynamic variation of lianas along topography maintains unchanging abundance at the landscape scale in central Amazonia. *J. Veg. Sci.* 29, 651-661. doi: 10.1111/jvs.12644.

Gerwing, J. J., Schnitzer, S. A., Burnham, R. J., Bongers, F., Chave, J., DeWalt, S. J., et al. (2006). A Standard Protocol for Liana Censuses. *Ecology* 38, 256–261.

Givnish, T. J. (1999). On the causes of gradients in tropical tree diversity. *J. Ecol.* 87, 193–210. doi: 10.1046/j.1365-2745.1999.00333.x

Gotelli, N. J., and Entsminger, G. L. (2003). Swap Algorithms in Null Model Analysis. *Ecology* 84, 532–535.

Graham, C. H., and Fine, P. V. A. (2008). Phylogenetic beta diversity: Linking ecological and evolutionary processes across space in time. *Ecol. Lett.* 11, 1265–1277. doi: 10.1111/j.1461-0248.2008.01256.x

Guillaumet, J.-L., and Kahn, F. (1982). Structure et dynamisme de la forêt. *Acta Amaz.* 12, 61–77. doi: 10.1590/1809-43921982123s061

Hacke, U. G., and Sperry, J. S. (2001). Functional and ecological xylem anatomy. *Funct. Ecol. xylem Anat.* 4/2, 97–115.

Harmon, L. J., and Glor, R. E. (2010). Poor statistical performance of the mantel test in phylogenetic comparative analyses. *Evolution* 64, 2173–2178. doi: 10.1111/j.1558-5646.2010.00973.x

Hawkins, B. A. (2001). Ecology's oldest pattern ? *rends Ecol. Evol.* 16:470.

Hawkins, B. A., and Diniz-Filho, J. A. F. (2004). "Latitude" and Geographic Patterns in Species Richness. *Ecography* 27, 268–272.

Helmus, M. R., Bland, T. J., Williams, C. K., and Ives, A. R. (2007). Phylogenetic measures of biodiversity. *Am. Nat*. 169, E68-83. doi: 10.1086/511334.

Hodnett, M. G., Vendrame, I., De O. Marques Filho, A., Oyama, M. D., and Tomasella, J et al. (1997). Soil water storage and groundwater behaviour in a catenary sequence beneath forest in central Amazonia: I. Comparisons between plateau, slope and valley floor. *Hydrol. Earth Syst. Sci.* 1, 265–277. doi: 10.5194/hess-1-265-1997

Hubbell, S. P. (2005). Neutral theory in community ecology and the hypothesis of functional equivalence. *Funct. Ecol.* 19, 166–172. doi: 10.1111/j.0269-8463.2005.00965.x

Jacobsen, A. L., Ewers, F. W., Pratt, R. B., Paddock, W. A., and Davis, S. D. (2005). Do xylem fibers affect vessel cavitation resistance? *Plant Physiol.* 139, 546–556. doi: 10.1104/pp.104.058404

Jennifer, Morgan, B., and Connolly, E. L. (2013). Plant-Soil Interactions : Nutrient Uptake. *Nat. Educ. Knowl.* 4, 2–7.

Jost, L., Chao, A., and Chazdon, R. L. (2011). "Compositional similarity and β (beta) diversity," in *Biological Diversity: Frontiers in Measurement and Assessment*, eds B. A. Maurer and B. J. McGill. (Oxford: Oxford University Press), 66–84.

Kahn, F., and Castro, A. (1985). The Palm Community in a Forest of Central Amazonia, Brazil. *Biotropica* 17, 210–216.

Kembel, S. W. (2009). Disentangling niche and neutral influences on community assembly: Assessing the performance of community phylogenetic structure tests. *Ecol. Lett.* 12, 949–960. doi: 10.1111/j.1461-0248.2009.01354.x

Kembel, S. W., Cowan, P. D., Helmus, M. R., Cornwell, W. K., Morlon, H., Ackerly, D. D., et al. (2010). Picante: R tools for integrating phylogenies and ecology. *Bioinformatics* 26, 1463–1464. doi: 10.1093/bioinformatics/btq166

King, D. A., Davies, S. J., Tan, S., and Noor, N. S. M. (2006). The role of wood density and stem support costs in the growth and mortality of tropical trees. *J. Ecol.* 94, 670–680. doi: 10.1111/j.1365-2745.2006.01112.x

Kreuzwieser, J., and Gessler, A. (2010). Global climate change and tree nutrition: Influence of water availability. *Tree Physiol.* 30, 1221–1234. doi: 10.1093/treephys/tpq055

Landeiro, V. L., Bini, L. M., Costa, F. R. C., Franklin, E., Nogueira, A., De Souza, J. L. P., et al. (2012). How far can we go in simplifying biomonitoring assessments? An integrated analysis of taxonomic surrogacy, taxonomic sufficiency and numerical resolution in a megadiverse region. *Ecol. Indic.* 23, 366–373. doi: 10.1016/j.ecolind.2012.04.023

Larjavaara, M., and Muller-Landau, H. C. (2010). Rethinking the value of high wood density. *Funct. Ecol.* 24, 701–705. doi: 10.1111/j.1365-2435.2010.01698.x

Laurance, W. F., Camargo, J. L. C., Luizão, R. C. C., Laurance, S. G., Pimm, S. L., Bruna, E. M., et al. (2011). The fate of Amazonian forest fragments: A 32-year investigation. *Biol. Conserv*. 144, 56–67. doi: 10.1016/j.biocon.2010.09.021

Legendre, P., and Legendre, L. (1998). *Numerical Ecology*. second edi. Amsterdam: Elsevier Scince B.V. doi: 10.1007/978-94-017-9484-8.

Lohmann, L. (2006). Untangling the phylogeny of neotropical lianas (Bignonieae, Bignoniaceae). *Am. J. Bot*. 93, 304–318.

Lohmann, L. G., Kaehler, M., Fonseca, L.H.M., Farias-Singer, R., Firetti, F., Silva-Castro, M. M et al. (2020). *Bignoniaceae in Flora do Brasil 2020*. Jard: Botânico do Rio Janeiro.

Luizão, R. C. C., Luizao, F. J., Paiva, R. Q., Monteiro, T. F., Sousa, L. S., and Kruijt, B. (2004). Variation of carbon and nitrogen cycling processes along a topographic gradient in a central Amazonian forest. *Glob. Chang. Biol.* 10, 592–600. doi: 10.1111/j.1529-8817.2003.00757.x

Magurran, A. E. (1988). *Ecological Diversity and Its Measurement*. Princeton: Princeton university press doi: 10.1007/978-94-015-7358-0.

Malhotra, H., Vandana, Sharma, S., and Pandey, R. (2018). "Phosphorus Nutrition: Plant Growth in Response to Deficiency and Excess," in *Plant Nutrients and Abiotic Stress Tolerance*, eds M. Hasanuzzaman, M. Fujita, H. Oku, K. Nahar, and B. Hawrylak-Nowak (New York: Springer Nature Singapore Pte Ltd.), 1–590. doi: 10.1007/978-981-10-9044-8.

Malizia, A., Grau, H. R., and Lichstein, J. W. (2010). Soil phosphorus and disturbance influence liana communities in a subtropical montane forest. *J. Veg. Sci.* 21, 551–560. doi: 10.1111/j.1654-1103.2009.01162.x

Marques Filho, A. de O., Ribeiro, M. de N. G., Santos, H. M. Santos, J. M et al. (1981). Estudos climatológicos da Reserva Florestal Ducke - Manaus-AM. IV. Precipitação. *Acta Amaz.* 11, 759–768. doi: 10.1590/1809-43921981114759

Mason, N. W. H., De Bello, F., Doležal, J., and Lepš, J. (2011). Niche overlap reveals the effects of competition, disturbance and contrasting assembly processes in experimental grassland communities. *J. Ecol.* 99, 788–796. doi: 10.1111/j.1365-2745.2011.01801.x

Mertens, J. (2004). *The Characterization of Selected Physical and Chemical Soil Properties of the Surface Soil Layer in the "'Reserva Ducke"', Manaus, Brazil, with Emphasis on Their Special Distribution.*[P.h.D.thesis]. Berlin: Humboldht University

Miller, E. T., Farine, D. R., and Trisos, C. H. (2017). Phylogenetic community structure metrics and null models: a review with new methods and software. *Ecography* 40, 461–477. doi: 10.1111/ecog.02070

Minchin, P. R. (1987). "An evaluation of the relative robustness of techniques for ecological ordination," in *Theory and Models in Vegetation Science*, ed. E. Van

Der Maareu (Dordrecht, The Netherlands: Springer), 89–107. doi: 10.1007/978-94-009-4061-1.

Mouillot, D., Stubbs, W., Faure, M., Dumay, O., Tomasini, J. A., Wilson, J. B., et al. (2005). Niche overlap estimates based on quantitative functional traits: A new family of non-parametric indices. *Oecologia* 145, 345–353. doi: 10.1007/s00442-005-0151-z

Muscarella, R., Bacon, C. D., Faurby, S., Antonelli, A., Kristiansen, S. M., Svenning, J. C., et al. (2019). Soil fertility and flood regime are correlated with phylogenetic structure of Amazonian palm communities. *Ann. Bot.* 123, 641–655. doi: 10.1093/aob/mcy196

Nogueira, A., Costa, F. R. C., and Castilho, C. V. (2011). Liana Abundance Patterns: The Role of Ecological Filters during Development. *Biotropica* 43, 442–449. doi: 10.1111/j.1744-7429.2010.00722.x

Oksanen, A. J., Blanchet, F. G., Friendly, M., Kindt, R., Legendre, P., Mcglinn, D., et al. (2019). Vegan. *Encycl. Food Agric. Ethics*, 2395–2396. doi: 10.1007/978-94-024-1179-9_301576.

Oliveira, A. A., Vicentini, A., Chave, J., Castanho, C. D. T., Davies, S. J., Martini, A. M. Z., et al. (2014). Habitat specialization and phylogenetic structure of tree species in a coastal Brazilian white-sand forest. *J. Plant Ecol.* 7, 134–144. doi: 10.1093/jpe/rtt073

Oliveira, M. L., Baccaro, F. B., Braga-Neto, R., and Magnusson, W. E. (2008). *Reserva Ducke: a biodiversidade amazônica através de uma grade.* Manaus, Brazil: Átema Desing. doi: 10.1007/978-3-642-41714-6_190602.

Oliveira, R. S., Costa, F. R. C., van Baalen, E., de Jonge, A., Bittencourt, P. R., Almanza, Y., et al. (2019). Embolism resistance drives the distribution of Amazonian rainforest tree species along hydro-topographic gradients. *N. Phytol.* 221, 1457–1465. doi: 10.1111/nph.15463

Pace, M. R., Zuntini, A. R., Lohmann, L. G., and Angyalossy, V. (2016). Phylogenetic relationships of enigmatic Sphingiphila (Bignoniaceae) based on molecular and wood anatomical data. *Taxon* 65, 1050–1063. doi: 10.12705/655.7

Pansonato, M. P., Costa, F. R. C., de Castilho, C. V., Carvalho, F. A., and Zuquim, G. (2013). Spatial scale or amplitude of predictors as determinants of the relative importance of environmental factors to plant community structure. *Biotropica* 45, 299–307. doi: 10.1111/btp.12008

Parent, C., Capelli, N., Berger, A., Crèvecoeur, M., and Dat, J. (2008). An overview of plant responses to soil waterlogging. *Plant Stress* 2, 20–27.

Parolin, P. (2009). Submerged in darkness: Adaptations to prolonged submergence by woody species of the Amazonian floodplains. *Ann. Bot.* 103, 359–376. doi: 10.1093/aob/mcn216

Parolin, P., and Wittmann, F. (2010). Struggle in the flood: tree responses to flooding stress in four tropical floodplain systems. *AoB Plants* 2010, 1–19. doi: 10.1093/aobpla/plq003

Pearse, W. D., Purvis, A., Cavender-Bares, J., and Helmus, M. R. (2014). "Metrics and Models of Community Phylogenetics," in *Modern Phylogenetic Comparative Methods and their Application in Evolutionary Biology*, ed. L. Z. Garamszegi. Berlin: Springer-Verlag. doi: 10.1007/978-3-662-43550-2 1–552

Phillips, O. L., and Gentry, A. H. (1994). Increasing turnover through time in tropical. *Science* 263, 954–958. doi: 10.1126/science.263.5149.954.

Pitman, N. C. A., Terborgh, J. W., Silman, M. R., Núñez, P. V., Neill, D. A., Cerón, C. E., et al. (2001). Dominance and distribution of tree species in upper Amazonian terra firme forests. *Ecology* 82, 2101–2117. doi: 10.1890/0012-96582001082

Ponnamperuma, F. N. (1972). The Chemistry of Submerged Soils. *Adv. Agron.* 24, 29–96.

Putz, F. (1984a). The Natural History of Lianas on Barro Colorado Island, Panama. 65, 1713–1724.

Putz, F. E. (1984b). How Trees Avoid and Shed Lianas. *Biotropica* 16, 19–23.

Putz, F. E., and Mooney, H. A. (1991). *The Biology of Vines*. Cambridge: Cambridge University Press. doi: 10.5860/choice.30-0291.

Quesada, C. A., Lloyd, J., Anderson, L. O., Fyllas, N. M., Schwarz, M., and Czimczik, C. I. (2011). Soils of Amazonia with particular reference to the RAINFOR sites. *Biogeosciences* 8, 1415–1440. doi: 10.5194/bg-8-1415-2011

Quesada, C. A., Lloyd, J., Schwarz, M., Baker, T. R., Phillips, O. L., Patiño, S., et al. (2009). Regional and large-scale patterns in Amazon forest structure and function are mediated by variations in soil physical and chemical properties. *Biogeosciences Discuss.* 6, 3993–4057. doi: 10.5194/bgd-6-3993-2009

Rambaut, A., Suchard, M., and Drummond, A. (2014). TRACER v1.6. Available online at http://beast.bio.ed.ac.uk/software/tracer/ (accessed October, 2020).

Rennó, C. D., Nobre, A. D., Cuartas, L. A., Soares, J. V., Hodnett, M. G., Tomasella, J., et al. (2008). HAND, a new terrain descriptor using SRTM-DEM: Mapping terra-firme rainforest environments in Amazonia. *Remote Sens. Environ.* 112, 3469–3481. doi: 10.1016/j.rse.2008.03.018

Ribeiro, J. E. L. S., Hopkins, M. J. G., Vicentini, A., Sothers, C. A., Costa, M. A. S., Brito, J. M., et al. (1999). *Flora da Reserva Ducke*. Manaus, Brazil: Instituto Nacional de Pesquisas da Amazônia (INPA) & Department for International Development (DFID).

Ricklefs, R. E. (2005). Historical and ecological dimensions of global patterns in plant diversity. *Biol. Skr.* 55, 583–603.

Ricklefs, R. E., and Schluter, D. (1993). *Species Diversity in Ecological Communities*. Chicago, Illinois, USA: Chicago University Press.

Ricotta, C., and Podani, J. (2017). On some properties of the Bray-Curtis dissimilarity and their ecological meaning. *Ecol. Complex.* 31, 201–205. doi: 10.1016/j.ecocom.2017.07.003

Rocha, E. da X., Nogueira, A., Costa, F. R. C., Burnham, R., Gerolamo, C et al. (2021). Liana functional assembly along the hydrological gradient in Central Amazonia. *Res. Sq.* [preprint]. doi: 10.21203/rs.3.rs-1083529/v1.

Rocha, E. X., Schietti, J., Gerolamo, C. S., Burnham, R. J., and Nogueira, A. (2020). Higher rates of liana regeneration after canopy fall drives species abundance patterns in central Amazonia. *J. Ecol.* 108, 1311-1321. doi: 10.1111/1365-2745.13345.

Rüger, N., Wirth, C., Wright, S. J., and Condit, R. (2012). Functional traits explain light and size response of growth rates in tropical tree species. *Ecology* 93, 2626–2636. doi: 10.1890/12-0622.1

Sanchez, P. A. (2019). "Soil Physical Properties," in *Properties and Management of Soils in the Tropics* (Cambridge University Press: Cambridge, United Kingdom), 21–254. doi: 10.13031/2013.22670.

Schietti, J., Emilio, T., Rennó, C. D., Drucker, D. P., Costa, F. R., Nogueira, A., et al. (2014). Vertical distance from drainage drives floristic composition changes in an Amazonian rainforest. *Plant Ecol. Divers.* 7, 241–253. doi: 10.1080/17550874.2013.783642

Schnitzer, S. A. (2018). Testing ecological theory with lianas. *N. Phytol.* 220, 366–380. doi: 10.1111/nph.15431

Schnitzer, S. A., and Bongers, F. (2002). The ecology of lianas and their role in forests. *Trends Ecol. Evol.* 17, 223–230. doi: 10.1016/S0169-5347(02)02491-6

Schnitzer, S. A., Dalling, J. W., and Carson, W. P. (2000). The impact of lianas on tree regeneration in tropical forest canopy gaps: Evidence for an alternative pathway of gap-phase regeneration. *J. Ecol.* 88, 655–666. doi: 10.1046/j.1365-2745.2000.00489.x

Soares-Filho, B. S., Nepstad, D. C., Curran, L. M., Cerqueira, G. C., Garcia, R. A., Ramos, C. A., et al. (2006). Modelling conservation in the Amazon basin. *Nature* 440, 520–523. doi: 10.1038/nature04389

Sousa-Baena, M. S., Sinha, N. R., Hernandes-Lopes, J., and Lohmann, L. G. (2018). Convergent evolution and the diverse ontogenetic origins of tendrils in angiosperms. *Front. Plant Sci.* 9, 1–19. doi: 10.3389/fpls.2018.00403

Sperotto, P., Acevedo-Rodríguez, P., Vasconcelos, T. N. C., and Roque, N. (2020). Towards a Standardization of Terminology of the Climbing Habit in Plants. *Bot. Rev.* 86, 180–210. doi: 10.1007/s12229-020-09218-y.

Stine, R. A., and Heyse, J. F. (2001). Non-parametric estimates of overlap. *Stat. Med.* 20, 215–236. doi: 10.1002/1097-0258(20010130)20:2.

Toledo, J. J., Magnusson, W. E., Castilho, C. V., and Nascimento, H. E. M. (2012). Tree mode of death in Central Amazonia: Effects of soil and topography on tree mortality associated with storm disturbances. *For. Ecol. Manage.* 263, 253–261. doi: 10.1016/j.foreco.2011.09.017

Tuomisto, H., Ruokolainen, K., Vormisto, J., Duque, A., Sánchez, M., Paredes, V. V., et al. (2017). Effect of sampling grain on patterns of species richness and turnover in Amazonian forests. *Ecography* 40, 840–852. doi: 10.1111/ecog.02453.

Valiente-Banuet, A., and Verdú, M. (2013). Plant facilitation and phylogenetics. *Annu. Rev. Ecol. Evol. Syst.* 44, 347–366. doi: 10.1146/annurev-ecolsys-110512-135855

Vamosi, S. M., Heard, S. B., Vamosi, J. C., and Webb, C. O. (2009). Emerging patterns in the comparative analysis of phylogenetic community structure. *Mol. Ecol.* 18, 572–592. doi: 10.1111/j.1365-294X.2008.04001.x

Verdú, M., Rey, P. J., Alcántara, J. M., Siles, G., and Valiente-Banuet, A. (2009). Phylogenetic signatures of facilitation and competition in successional communities. *J. Ecol.* 97, 1171–1180. doi: 10.1111/j.1365-2745.2009.01565.x

Webb (2000). Exploring the Phylogenetic Structure of Ecological Communities: An Example for Rain Forest Trees. *Am. Nat.* 156:145. doi: 10.2307/3079215

Webb, C. O., Ackerly, D. D., and Kembel, S. W. (2008). Phylocom: Software for the analysis of phylogenetic community structure and trait evolution. *Bioinformatics* 24, 2098–2100. doi: 10.1093/bioinformatics/btn358

Webb, C. O., Ackerly, D. D., McPeek, M. A., and Donoghue, M. J. (2002). Phylogenies and community ecology. *Annu. Rev. Ecol. Syst.* 33, 475–505. doi: 10.1146/annurev.ecolsys.33.010802.150448

Webb, C. O., and Peart, D. R. (1999). Seedling Density Dependence Promotes Coexistence of Borean Rain Forest Trees. *Ecology* 80, 2006–2017.

Wiens, J. J., and Donoghue, M. J. (2004). Historical biogeography, ecology and species richness. *Trends Ecol. Evol.* 19, 639–644. doi: 10.1016/j.tree.2004.09.011

Wiens, J. J., and Graham, C. H. (2005). Niche conservatism: Integrating evolution, ecology, and conservation biology. *Annu. Rev. Ecol. Evol. Syst.* 36, 519–539. doi: 10.1146/annurev.ecolsys.36.102803.095431

Zuntini, A. R., Fonseca, L. H. M., and Lohmann, L. G. (2013). Primers for Phylogeny Reconstruction in Bignonieae (Bignoniaceae) Using Herbarium Samples. *Appl. Plant Sci.* 1:1300018. doi: 10.3732/apps.1300018

Zuquim, G., Tuomisto, H., Costa, F. R. C., Prado, J., Magnusson, W. E., Pimentel, T., et al. (2012). Broad Scale Distribution of Ferns and Lycophytes along Environmental Gradients in Central and Northern Amazonia, Brazil. *Biotropica* 44, 752–762. doi: 10.1111/j.1744-7429.2012.00880.x

Zuur, A. F., Ieno, E. N., Walker, N. J., Saveliev, A. A., and Smith, G. M. (2009). *Mixed Effects Models and Extensions in Ecology with R.* New York, NY: Springer.

Conflict of Interest: The authors declare that the research was conducted in the absence of any commercial or financial relationships that could be construed as a potential conflict of interest.

frontiers | Frontiers in Forests and Global Change

ORIGINAL RESEARCH
published: 18 April 2022
doi: 10.3389/ffgc.2022.838357

Increasing Liana Abundance and Associated Reductions in Tree Growth in Secondary Seasonally Dry Tropical Forest

Justin M. Becknell[1]*, German Vargas G.[2], Lacey A. Wright[1], Natalie-Francesca Woods[1], David Medvigy[3] and Jennifer S. Powers[4,5]

[1] Environmental Studies, Colby College, Waterville, ME, United States, [2] School of Biological Sciences, The University of Utah, Salt Lake City, UT, United States, [3] Department of Biological Sciences, University of Notre Dame, Notre Dame, IN, United States, [4] Department of Ecology, Evolution and Behavior, University of Minnesota, St. Paul, MN, United States, [5] Department of Plant and Microbial Biology, University of Minnesota, St. Paul, MN, United States

OPEN ACCESS

Edited by:
Geertje M. F. Van Der Heijden,
University of Nottingham,
United Kingdom

Reviewed by:
Francis Edward Putz,
University of Florida, United States
Romà Ogaya,
Centre for Ecological Research
and Forestry Applications (CREAF),
Spain

***Correspondence:**
Justin M. Becknell
justin.becknell@colby.edu

Specialty section:
This article was submitted to
Tropical Forests,
a section of the journal
Frontiers in Forests and Global
Change

Received: 17 December 2021
Accepted: 25 March 2022
Published: 18 April 2022

Citation:
Becknell JM, Vargas G G,
Wright LA, Woods NF, Medvigy D and
Powers JS (2022) Increasing Liana
Abundance and Associated
Reductions in Tree Growth
in Secondary Seasonally Dry Tropical
Forest.
Front. For. Glob. Change 5:838357.
doi: 10.3389/ffgc.2022.838357

Lianas are thought to be increasing and altering tree growth and ecosystem productivity in tropical forests, but less research has focused on secondary or seasonally dry tropical forest. We report on an 11-year study of tree growth and liana presence from Guanacaste, Costa Rica, where we measured the diameter growth and liana presence on more than 1,700 trees in regenerating forest of different ages. We find that the proportion of trees without lianas is decreasing and the number of trees with lianas occupying more than 10% of tree's crowns is increasing. We also find that lianas are affecting the diameter growth of trees. The 11-year average relative growth rates of trees with lianas in more than 10% of the tree's crown are lower than the relative growth of trees with no lianas or lianas in less than 10% of their crown. Year-to-year, tree relative growth rate is related to annual precipitation and tree diameter. However, trees that were heavily infested with lianas (i.e., with lianas in more than 50% of their crowns) had lower relative growth and a weaker precipitation-growth relationship. This work underscores the value of long-term longitudinal data in secondary forest and adds critical data on dry forest liana abundance change.

Keywords: liana abundance, seasonally dry tropical forest, tree growth, secondary forest, dendrometers

INTRODUCTION

Lianas (woody vines) are an important component in forest ecosystems around the planet that can provide habitat and foster biodiversity, all while parasitizing trees (Putz, 1984b, 1991; Gentry and Dodson, 1987; Clark and Clark, 1990). In recent decades, lianas appear to be increasing in tropical forests in abundance and biomass (Phillips et al., 2002; Yorke et al., 2013; Laurance et al., 2014). While reports of this increase are widespread, the cause for increasing liana abundance in particular and the general controls over liana distribution remain a matter of intense study (Muller-Landau and Pacala, 2020; Schnitzer et al., 2021). This increase likely has ecosystem consequences because lianas have long been known to affect the demographic rates their host trees (Clark and Clark, 1990; Putz, 1991). A decrease in growth and increase in mortality associated with increasin liana abundance has the potential to alter tropical forest carbon uptake and storage, although many aspects of these dynamics are unclear (van der Heijden et al., 2013).

A variety of intrinsic and extrinsic factors have been investigated to explain the increase in tropical forest liana abundance, though increasing evidence suggests that disturbances and the resulting post-disturbance forest structure may play an important role (Schnitzer et al., 2021). In general, lianas may be more resistant and resilient to common tropical disturbances than their host trees. The distinct physiology of lianas means that they can often capitalize on drought disturbances with typically high water-use efficiency and hydraulic conductivity relative to tree hosts and competitors (Cai et al., 2009; Chen et al., 2015; Smith-Martin et al., 2019; van der Sande et al., 2019). Marginal shifts in water availability due to increases in drought severity and frequency have been found to contribute to the rise in liana abundance particularly in the seasonal tropics where water can be more of a limiting factor than light (Schnitzer, 2005). Lianas are also poised to take advantage of gaps and or open patches created by anthropogenic disturbances, thus altering light availability and facilitating rapid and aggressive liana growth (Schnitzer and Bongers, 2011; Schnitzer et al., 2021). Lianas require trees for support and use small tree or other lianas as trellises to move toward the canopy, which could result in existing lianas facilitating further liana colonization (Putz, 1984b; Balfour and Bond, 1993; Campbell et al., 2018). Both climate and disturbance patterns (including anthropogenic and other disturbances) are changing in ways that promote environments that are more suited to thriving lianas.

There are different mechanisms through which lianas interact with host trees. Lianas are aggressive competitors that, in high numbers, can affect the growth, fecundity, and mortality patterns of trees (Putz, 1984a, 1990; Schnitzer and Bongers, 2002; Reis et al., 2020). For example, some lianas colonize canopy tree crowns and block large portions of light from reaching their host's leaves leading to lower growth rates (Clark and Clark, 1990; van der Heijden and Phillips, 2009). There is evidence of tree growth reductions associated with lianas (Putz, 1984b; Clark and Clark, 1990; Schnitzer and Bongers, 2002; Grauel and Putz, 2004) or increases in tree growth following liana removal (Estrada-Villegas and Schnitzer, 2018). Others have documented the complex causes of these reductions that may go beyond light interception and structural damage. For example, the below-ground resource acquisition of lianas can limit tree sapling growth even in environments with high light availability and in gaps lianas can slow or inhibit the growth of seedlings (Schnitzer and Carson, 2010; Pasquini et al., 2015).

Even though lianas appear to be more abundant in seasonally dry tropical forest (SDTF) compared to wet forest (Gentry, 1991; Schnitzer, 2005; DeWalt et al., 2015), we know less about SDTF liana dynamics compared to areas that receive more rainfall, particularly in secondary SDTF. On the one hand, SDTFs may have a climate and disturbance regime that is more hospitable to lianas relative to a seasonal wet forests (Schnitzer, 2005), and many liana species experience fewer growth reductions with seasonal drought compared to co-occurring trees (Smith-Martin et al., 2019). On the other hand, research on SDTF lianas has shown that they occupy a similar range of water use physiologies as host trees (Werden et al., 2018) and do not differ in hydraulic traits like hydraulic safety margin or water potential at 50% loss of hydraulic conductivity (Smith-Martin et al., 2022). Similarly, a recent large-scale liana removal experiment in a dry forest in Panama showed that many trees did not experience increased growth rates when lianas were cut, and some species even showed decreases in growth rates (Estrada-Villegas et al., 2021). These unusual results remain unexplained. But, Estrada-Villegas et al. (2021) suggest they may be the result of tree allocation of resources to roots, a lack of root competition between lianas and trees, an increase of solar radiation and soil drying after liana removal, or water limitation in dry forests outweighing the negative effects of liana presence. Resolving whether liana abundance is increasing in SDTF and whether this leads to decreased tree growth rates is a high priority as both changing disturbance and climatic regimes may favor trees over lianas in this biome.

In this 11-year study in Guanacaste, Costa Rica, we annually measured tree growth and recorded liana presence using a four-level ordinal scale in secondary seasonally dry tropical forest plots ranging from 5 to 60 years since agricultural abandonment (largely pasture with rare remnant trees). We used these longitudinal data to evaluate changes in liana presence and the potential for effects of lianas on tree growth and mortality. Specifically, we ask, (1) Do the number of trees with lianas change over time? (2) Does the degree liana crown presence change over time? (3) Does liana presence affect tree growth? (4) Does liana presence impact tree mortality?

MATERIALS AND METHODS

Site Description

Our study was conducted in seasonally dry tropical forests (SDTF) of Guanacaste Province, Costa Rica. In 2008, 18 permanent research plots (0.1 ha each) were established in Área de Conservación Guanacaste, Sector Santa Rosa (Santa Rosa National Park) and Área de Conservación Arenal Tempisque (Palo Verde National Park; Becknell et al., 2021). Both of these parks are a patchwork of forests in different successional stages recovering from agricultural abandonment at different times over the past century (Powers et al., 2009). The mean annual rainfall is 1,575 mm in Santa Rosa (1980–2020) and 1,445 mm in Palo Verde (1995–2018)[1,2]. The majority of precipitation at both sites occurs between May and late November leading to a ∼6-month dry season with little or no rainfall. Our 18 20 m × 50 m (0.1 ha) plots were established to document forest succession. At the start of the study plots spanned an age range from 5 to 60 years since agricultural abandonment. Six sites were in forests initially dominated by a single oak species, *Quercus oleoides* ("evergreen oak"). The other twelve sites represented the more common diverse and majority deciduous SDTF in the lowlands of Santa Rosa and Palo Verde. These same plots have been described

---

[1] www.acguanacaste.ac.cr

[2] tropicalstudies.org

in several other studies of succession, ecosystem function, and drought disturbance (Powers and Peréz-Aviles, 2013; Schilling et al., 2016; Becknell et al., 2021).

Field Measurements

Steel dendrometer bands were affixed to all trees within the plot with DBH >10 cm starting in 2008. We then added dendrometers to trees >7 cm DBH in 2013. Dendrometers were read each year at the start of the dry season (typically in late December or early January). When dendrometers were read each year, visual observations of lianas were also made on an ordinal scale. We coded each tree into one of four liana index categories: 0: no lianas, 1: lianas present on the tree's trunk and/or in <10% of the tree's crown, 2: lianas present in 10–50% of a tree's crown, and 3: lianas present in more than 50% of the tree's crown. Dendrometer measurements and liana observations were made separately for each stem of multi-stem trees which divided below 1.3 m. To keep observations and measurements consistent, the same field manager was present for all censuses and trained new field workers on dendrometer measurements and liana index observations.

Data Analysis

To examine changes in liana abundance, we calculated the number and proportion of trees in each liana category for each year. Then we used simple linear regression on the proportion of trees in each category as a function of time. To examine the growth effects of lianas, we took two approaches. First, we calculated the study-long mean relative growth rate for all trees with more than 4 years in our record and compared this across liana presence categories. Because the liana presence categories changed for many trees over the course of the study, we averaged the liana index and rounded it to the nearest value. We also omitted trees with less than 4 years of observed growth (1,408 trees remained). Next, we compared the distributions of mean relative growth rates across liana index categories with the non-parametric Kruskal–Wallis test. Then, to compare growth effects of lianas among years and include annual rainfall and tree size we used a linear mixed-effects model to evaluate the effects of liana index on relative growth rates each year while including tree size and annual precipitation as fixed effects and individual tree identifier and tree species as random effects to account for repeated measures, and the likely important but unbalanced effect of different tree species. Because tree species differences were not the focus of this analysis, we included species as a random effect, which meant that individual intercept values were calculated for each species, but fixed effects were determined using all species. We also included two interaction terms: one between the liana index and tree diameter and the other between liana index and annual rainfall. Before running this analysis, we removed data where relative growth rates were more than 4 standard deviations from the mean as has been done in similar analyses (Visser et al., 2018). We also included interactions between liana index and annual rainfall as well as an interaction term between annual rainfall and tree size. Our model is as follows.

$$ln(relative\ growth\ rate) \sim liana\ index + annual\ rainfall +$$

$$tree\ diameter + (liana\ index : annual\ rainfall) +$$

$$(annual\ rainfall : tree\ diameter) + (1|individual\ tree\ ID) +$$

$$(1|tree\ species)$$

To examine tree mortality, we calculated the annual mortality rate (λ) for each year for trees in each of the four liana categories using the method explained by Sheil et al. (1995):

$$\lambda = ln(N_0/N_t)/t$$

Where N_0 is number of live trees at the start of the census period, Nt is the number of surviving trees at the end of the census period, and t time in years between observations. Then we compared these mortality rates across liana categories using the non-parametric Kruskal–Wallis test.

We also attempted to determine if our data showed evidence of trees shedding lianas. To do this, we compared the liana index for each tree at the start and end of their record in our study looking for decreases in the liana index. For each tree, we took the mean liana index in the first and second halves of our record. We then tallied which of those trees with a mean liana index greater than 1 in the first half of the record had a liana index decline of more than 0.5 in the mean liana index by the second half of the study. We used only the trees for which we had 4 or more consecutive years of observations. All analyses were conducted using the R statistical computing language (R Core Team, 2021). All data were pooled over the 18 plots for this analysis.

RESULTS

Our data included annual growth measurements and liana observations on 1,745 unique stems with DBHs from 7 to 96 cm, representing 102 tree species from 86 genera. Of the 1,745 stems, 623 (35%) were observed in all 12 years. Another 493 were observed for 7 years due to the fact that in the first 5 years of the study we included only trees 10 cm DBH and above. In, 2013 we added dendrometers to trees between 7 and 10 cm DBH which were observed for the first time in 2014. Averaged across all years, 49% of trees in our study had no lianas, 16% of trees had lianas that occupied less than 10% of the tree's crown, 18% of trees had lianas which occupied 10–50% of the tree's crown, and 17% of trees had lianas which occupied more than 50% of a tree's crown.

Excluding trees >7 cm DBH that were added to the survey in 2014, the proportion of trees in each liana presence category changed over time (**Figure 1**). The number of trees with no lianas declined over time from 52% in 2010 to 45% in 2017. Linear regression fit to this proportion by year suggests that the proportion of trees with no lianas declines at a rate of 1.3% per

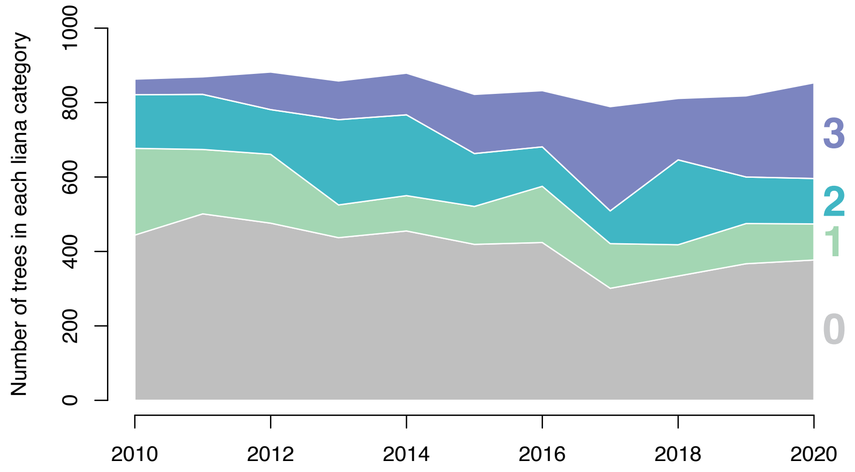

FIGURE 1 | The change in the number of trees per liana presence category by year. The overall number of trees in the study changes little among years. The number of trees in categories 2 and 3 increase while the number of trees in categories 0 and 1 decrease over time. This analysis omits trees under 10 cm DBH which were first observed in 2014.

year (p = 0.0066, R^2 = 0.53). The number of trees with a liana index of 2 or 3 (i.e., those with lianas occupying more than 10% of the tree's crown) increased over time from 21% in 2010 to 41% in 2020 increasing at a rate of 2.1% per year (p = 0.0023, R^2 = 0.62).

With respect to liana shedding, of the 490 stems with a mean liana index over 1 in the first half of the record (35% of stems with more than 4 years of observations), 13.7% (67) had a mean liana index that decreased by more than 0.5 in the second half of the study. We examined the liana index records of each of these 67 stems and found that the liana declines in 28 of these records could be explained by a likely mis-code in the liana index, i.e., a single high liana value toward the start of the record or a single low liana value toward the end of the record. Or, in several cases, a liana record that increased and decreased dramatically throughout the record, indicated a tree with a liana that was difficult to code. This analysis leaves 39 of 490 stems (8% of stems starting with high liana values) that show evidence of liana shedding over the length of our study. This suggests a liana shedding rate of 0.7% of trees shedding lianas per year. The 39 trees included four trees which died, but in all four cases, the death occurred two or more years after the liana index had gone to zero.

In our analysis of study-long average relative growth rates, we found that trees with liana index of 0 or 1 (no liana, or liana present in less than 10% of the tree's crown) had higher mean relative growth rates than trees with liana index of 2 or more (i.e., lianas present in more than 10% of the crown; **Figure 2**; Kruskal–Wallis p-value = $3.563 \cdot 10^{-08}$). The Bonferroni adjusted Dunn Q test showed that trees with liana index of 3 had significantly lower growth rates than trees with no lianas (p = 0.00042) and trees with liana index of 1 (p = 0.00074). Trees with liana index of 2 also had significantly lower relative growth rates compared to those without lianas (p = 0.000012) and trees with liana index of 1 (p = 0.000063). Relative growth rates did not differ between liana index of 0 and 1 nor did they differ between trees with liana index of 2 and 3. Median relative growth rates for trees with liana index of 0, 1, 2, and 3 were 0.0137, 0.0140, 0.00983, and 0.00735, respectively. Trees with lianas in more than 10% of trees' crowns had 34% lower median relative growth rates compared to trees with no lianas and lianas occupying less than 10% of trees' crowns.

Next, we used a linear mixed-effects model to evaluate the effects of liana index on relative growth rates each year while including tree size, annual precipitation, as fixed effects and individual tree identifier and tree species as random effects to account for repeated measures and the likely important but imbalanced effect of different tree species (**Table 1** and **Figure 3**). Relative growth was significantly higher for liana index of 1 and lower for liana index of 3. Both annual rainfall and tree diameter had significant effects on relative growth rate. There was an interaction between rainfall and liana index where the effect of rainfall on relative growth rate was lower for trees with a liana index of 3.

We calculated the annual mortality rate of trees in each liana category that died each year. While the trend is for trees with liana values of 3 to have higher mortality rates (**Figure 4**), there was no significant difference among categories (Kruskal–Wallis p-value = 0.5211).

DISCUSSION

Our 11-year study of lianas in Costa Rica provides evidence that lianas are increasing in abundance in a secondary seasonally dry tropical forest and that lianas negatively impact the growth of trees. This result represents one of a small number of studies on liana increase and growth effects in a seasonally dry forest. This result is also unique as it provides annually resolved records of the effects of liana index on growth in each year of our study. Many studies that census lianas and/or tree growth use less

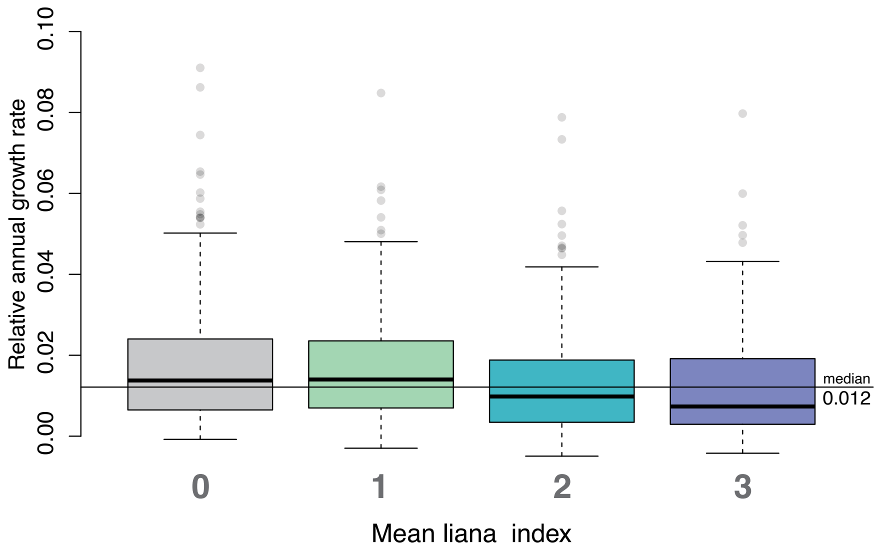

FIGURE 2 | Overall median relative growth rates for trees with different average liana index over all study years. Trees with liana index of 0 and 1 had significantly higher relative growth than trees with lianas present in more than 10% of the tree's crowns.

TABLE 1 | Results from linear mixed effects model relating tree growth to liana index, annual rainfall, and tree diameter.

Variable	Scaled coefficient	*P*-values
Intercept	$\mathbf{1.49 \times 10^{-02}}$	$\mathbf{<2 \times 10^{-16}}$
Liana index of 1	$\mathbf{1.14 \times 10^{-03}}$	**0.0252**
Liana index of 2	-6.81×10^{-04}	0.20122
Liana index of 3	$\mathbf{-1.65 \times 10^{-03}}$	**0.00426**
Annual rainfall	$\mathbf{4.49 \times 10^{-03}}$	$\mathbf{<2 \times 10^{-16}}$
Tree diameter	$\mathbf{-2.18 \times 10^{-03}}$	$\mathbf{5.03 \times 10^{-11}}$
Liana index of 1: annual rainfall	-7.67×10^{-04}	0.07789
Liana index of 2: annual rainfall	-6.98×10^{-04}	0.12043
Liana index of 3: annual rainfall	$\mathbf{-1.99 \times 10^{-03}}$	$\mathbf{2.99 \times 10^{-05}}$
Annual rainfall: tree diameter	-1.53×10^{-04}	0.3247

Liana index coefficients represent slope modifiers relative to a liana index value of 0. Other coefficients represent slope values. Bolded values represent those with p-values less than 0.05.

frequent intervals. One of our novel results was the interaction between liana presence index and annual rainfall; i.e., the liana-related reductions in annual growth rates were similar among liana presence classes in years with low rainfall, but varied more among liana presence classes during years of high rainfall. This liana-related suppression of growth over a decade of observations and the post-drought increase in lianas implies that lianas have a strong ongoing impact on ecosystem function and successional trajectories in these secondary SDTFs.

The number of trees with lianas increased over time in our study as did the number of trees in each liana index category, with more trees severely impacted by lianas by the end of the study. More than half of the trees in our study had lianas present which, on an annual basis increased, to 55% by the end of our study. This liana increase was evident in all 18 study plots, which included very early secondary successional sites (as young as 5 years at the start of the study) as well as plots with mid to late successional secondary forest (70 years by the end of the study). While some liana increase was evident early in the study, the liana index of trees increased markedly after the 2015 drought and its associated tree mortality (Powers et al., 2020). Whether these increases in lianas are a result of successional processes, drought and other gap-scale disturbances, or some other factor is difficult to determine.

Understanding the degree to which host trees can shed lianas is an important parameter for efforts to incorporate lianas into simulation models. Our data show some evidence of liana shedding among a small percentage of trees. Approximately 8% of trees starting with high liana values showed decreases in liana index over the course of our study which amounts to less than 1% of trees shedding lianas per year. This 8% represents a small number of trees and it is difficult to determine the degree to which lianas are actually "shed" using our data. Some tree species have been observed to be free of lianas while others are able to shed lianas (Putz, 1984a). It is not clear from our work whether this regularly occurs at our site or if particular species are common liana shedders. The most represented species in our list of trees that appear to shed lianas are the most common species in our dataset and the number of shedding trees we found was too low to allow further analysis of species.

Liana increases have been reported in many tropical forest regions over the past decades (Phillips et al., 2002; Wright et al., 2004; Schnitzer and Bongers, 2011), but the mechanism behind this increase remains a topic of research. Several important factors may be combining to facilitate liana expansion. These include past disturbances or ongoing minor disturbances and gap dynamics as well as extrinsic factors like CO_2 fertilization, climate warming, or nutrient status (Schnitzer et al., 2011, 2020, 2021). In disturbed, fragmenting, or regenerating forests, the factors leading to liana increases likely include the structure of these

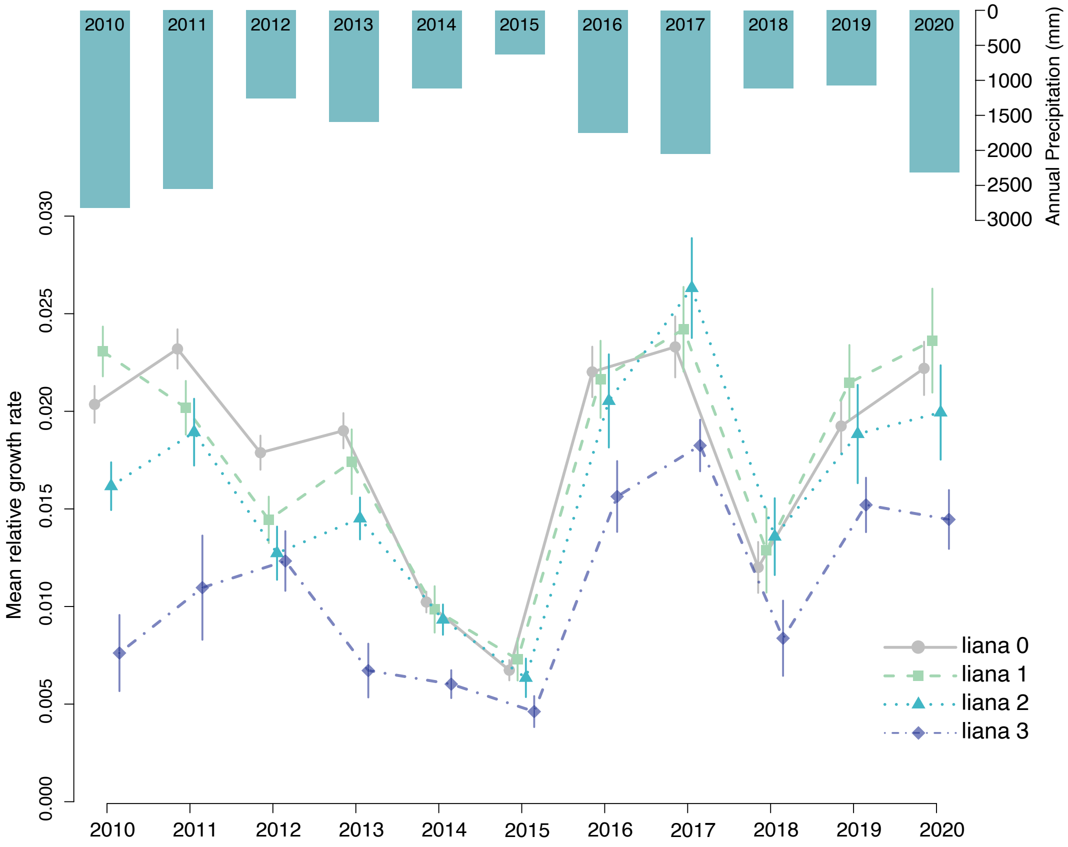

FIGURE 3 | Annual mean relative growth rate for all trees in each liana category. Error bars represent standard error. Bars at the top show annual precipitation, which is positively correlated with annual growth. While growth in all categories appears to rise and fall with precipitation, trees in category 3 show significantly lower relative growth rates and growth in these trees responded less to annual precipitation.

forests including small trees and lianas acting as trellises and facilitating further liana colonization and growth (Putz, 1984b; Balfour and Bond, 1993; Campbell et al., 2018). Declines in liana abundance with succession have also been observed (Dewalt et al., 2000). While succession and disturbance are likely important factors at our study site, we cannot eliminate other possible drivers of liana increase. All of our sites are recovering from agricultural abandonment to differing degrees. Further, halfway through our study was a major drought leading to unusually high tree mortality (Powers et al., 2020) and followed by a large uptick in liana abundance. A continuation of liana increase combined with more frequent droughts could severely impact the productivity, carbon uptake, and carbon storage of this region.

Liana increases have also been documented in other tropical dry forest regions. A decade-long survey of lianas in Indian tropical dry forests shows liana increases in some but not all study sites (Pandian and Parthasarathy, 2003). Moist seasonal forests of the Americas show liana increases in several studies (Ingwell et al., 2010; Schnitzer and Bongers, 2011), and there is a general pattern toward higher liana density with lower precipitation (Parolari et al., 2020). But whether or not there is widespread liana increase in dry forests has not been sufficiently studied. Further, if this liana increase is common in dry forests, it's not clear which mechanisms might be at play. But the likely explanation would seem to be the same successional and disturbance response patterns observed in liana increases in moist and wet forests (Schnitzer et al., 2021).

Our data firmly establish that tree growth rates are being negatively impacted by high liana crown presence at our study site. From our study-long average of growth rates, lianas slowed growth by 34% in trees with lianas present in more than 10% of the tree's crown. When considering years separately and including the effects of tree size and annual rainfall, only the trees with lianas in more than 50% of their crowns appear to have reduced growth. This difference in result between study-long average versus annual growth suggests that while high liana presence (lianas in >50% of crown) reduces growth in all years, liana index 2 (lianas in 10–50% of crown) only reduced growth in some years. This could be because liana index 2 is a category that includes much more variation in the degree to which the liana is affecting the tree. Or this pattern may represent a real but unnoticed ecological or physiological effects such as differences among liana species in crown presence or effects on tree growth. Trees with lianas in 20–50% of their crowns had higher growth rates in 2017 and 2018, 2 years following a major drought which led to higher than normal tree mortality. Perhaps this was driven

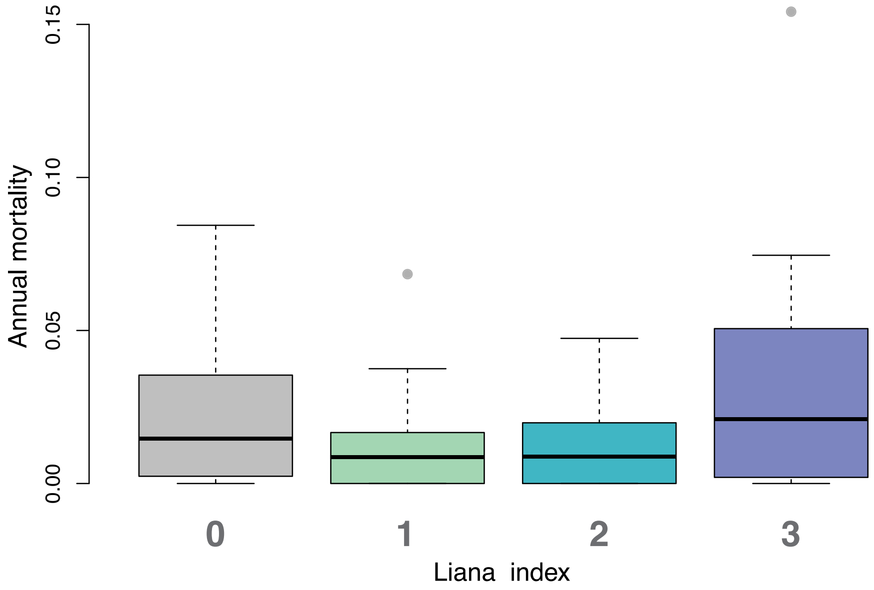

FIGURE 4 | Distributions of annual mortality rate for each liana index value. Each box and whisker plot represents 11 points, one from each year. The median annual mortality rate for liana level 3 (lianas present in more than 50% of the tree's crown) is highest. But non-parametric comparison of means test shows no significant differences among factors.

by trees whose growth was "released" by the death of adjacent liana-laden trees. These surviving neighbors may have been able to increase their growth as canopy gaps opened despite their moderate liana loads. Despite these differences in growth effects with analytical approach, it is clear that lianas are reducing growth in many trees in our study area. This reduced growth effect is persistent in wet and dry years and across our sites of varied age and tree species composition.

These growth effects are mirrored by the patterns we can observe in our mortality data. However, our small sample size limits our ability to show clear differences in mortality among liana categories. Despite this, the pattern we can observe in our data combined with evidence from other studies of liana-driven mortality leads us to conclude that lianas are impacting mortality here. Expanding our study to include more trees and continuing it for more years will likely make this pattern clearer.

Negative effects of lianas on tree growth have been documented in a variety of secondary and old growth forests, but early successional forests are less studied (Estrada-Villegas and Schnitzer, 2018). A recent secondary SDTF liana removal experiment showed no impact of lianas (Estrada-Villegas et al., 2021). In contrast, our results that lianas do indeed reduce growth directly contradict this work. Taken together, these results suggest a complicated picture of liana impacts on tree growth in secondary SDTF. Both sites had similar climate, similar land-use history, and both sites included historically low precipitation in 2015 (Estrada-Villegas et al., 2021). Estrada-Villegas et al. (2021) have more very early successional sites, suggesting that growth in mid-successional forests may be more affected by lianas. Other possible explanations for this difference in result include, species differences, past land-use history, disturbance history, or edaphic differences.

We acknowledge that a liana index resulting from a rapid visual assessment and can produce inconsistent data. We have minimized inconsistency by using the same field personnel throughout our study. That said, ground-based assessment of the amount of crown area taken up by lianas is difficult leading to both over and underestimates in liana index. Though, there is no evidence that these errors should be greater in the direction of over or under estimating lianas. This analysis excludes consideration of tree species or liana species both of which are likely important factors in explaining liana abundance changes and their impacts on tree growth. Tree species differentially respond to liana presence (Visser et al., 2018) and liana species have different effects on trees due to differences in morphology and life-history traits (Smith-Martin et al., 2020). We also acknowledge that assessing growth impacts of lianas using diameter growth alone leaves out important aspects of tree growth.

These findings have implications for understanding seasonally dry tropical forest function, restoration, and disturbance dynamics. More than half of trees had lianas and 35% of trees had levels of liana presence that reduced diameter growth. These trees were competitively disadvantaged and had reduced carbon uptake. Assuming these sites accurately represent liana levels across the landscape in this region, regional carbon uptake could be impacted by lianas.

Now that liana increases and tree growth impacts have been established in this landscape, further research is needed to fully understand this phenomenon's impact on regional ecology and ecosystem function. Surveys of liana biomass or liana removal experiments may help to understand their impact on ecosystem carbon cycling more accurately (Laurance et al., 2014; Estrada-Villegas and Schnitzer, 2018). Studies of liana morphology and physiology will help to unravel the mechanisms behind these phenomena (Smith-Martin et al., 2020; Meunier et al., 2021). Continued longitudinal studies that include more detailed liana data may help to illustrate the mechanisms behind the liana increase. Remote sensing and modeling work are needed to extend this work beyond what is possible in the field (di Porcia e Brugnera et al., 2019). Comparative work on different forest types, across soil gradients, elevation gradients, and rainfall gradients may help to discern where in the landscape liana expansion is occurring and where those lianas impact growth. Along with studies in other systems these extensions of liana research can help explain the ecological role of lianas secondary SDTFs.

In summary, this work provides two key results: (1) lianas are increasing in abundance in secondary SDTFs we studied, and (2) these lianas have clear, negative effects on the growth of trees. This work demonstrates liana increases in secondary SDTF and adds support to other findings that lianas negatively impact tree growth in this forest type. Our observed liana increases may be explained by a combination of successional patterns, forest structural patterns, and tree mortality disturbance relating to the drought in the middle of our study. However, more work is needed to confirm this hypothesis and uncover the mechanisms behind liana impacts on growth, and whether these relationships are tree and liana-species specific.

DATA AVAILABILITY STATEMENT

The raw data supporting the conclusions of this article will be made available by the authors, without undue reservation.

AUTHOR CONTRIBUTIONS

JB conceived of the study, conducted initial field work, analyzed the data, and wrote the manuscript. GV collected field data, advised on the analysis, and edited the manuscript. LW and N-FW entered data, analyzed the data, and helped to write the manuscript. DM advised on the study and edited the manuscript. JP conceived of the study, conducted field work, and edited the manuscript. All authors contributed to the article and approved the submitted version.

ACKNOWLEDGMENTS

We thank Department of Energy Terrestrial Ecosystem Science Program grants DE-SC0014363 and DE-SC0020344 and National Science Foundation Grant DEB-1053237 for funding. We also thank Daniel Pérez-Aviles, Erick Schilling, and Damaris Pereira for help in the field. We thank the staff of Area de Conservacioìn Guanacaste, the staff of Palo Verde, and the Palo Verde OTS research station for facilitating this work.

REFERENCES

Balfour, D. A., and Bond, W. J. (1993). Factors limiting climber distribution and abundance in a southern african. *Source: J. Ecol.* 81, 93–100. doi: 10.2307/2261227

Becknell, J. M., Vargas, G., Pérez-Aviles, D., Medvigy, D., and Powers, J. S. (2021). Above-ground net primary productivity in regenerating seasonally dry tropical forest: contributions of rainfall, forest age and soil. *J. Ecol.* 109, 3903–3915. doi: 10.1111/1365-2745.13767

Cai, Z. Q., Schnitzer, S. A., and Bongers, F. (2009). Seasonal differences in leaf-level physiology give lianas a competitive advantage over trees in a tropical seasonal forest. *Oecologia* 161, 25–33. doi: 10.1007/s00442-009-1355-4

Campbell, M. J., Edwards, W., Magrach, A., Alamgir, M., Porolak, G., Mohandass, D., et al. (2018). Edge disturbance drives liana abundance increase and alteration of liana-host tree interactions in tropical forest fragments. *Ecol. Evol.* 8, 4237–4251. doi: 10.1002/ECE3.3959

Chen, Y. J., Cao, K. F., Schnitzer, S. A., Fan, Z. X., Zhang, J. L., and Bongers, F. (2015). Water-use advantage for lianas over trees in tropical seasonal forests. *New Phytol.* 205, 128–136. doi: 10.1111/NPH.13036

Clark, D. B., and Clark, D. A. (1990). Distribution and effects on tree growth of lianas and woody hemiepiphytes in a Costa Rican tropical wet forest. *J. Tropical Ecol.* 6, 321–331. doi: 10.1017/S0266467400004570

DeWalt, S. J., Schnitzer, S. A., Alves, L. F., Bongers, F., Burnham, R. J., Cai, Z., et al. (2015). "Biogeographical patterns of liana abundance and diversity," in *Ecology of Lianas*, eds S. Schnitzer, F. Bongers, R. J. Burnham, and F. E. Putz (West Sussex, SXW: John Wiley & Sons), 131–146. doi: 10.1111/brv.12508

Dewalt, S. J., Schnitzer, S. A., and Denslow, J. S. (2000). Density and diversity of lianas along a chronosequence in a central Panamanian lowland forest. *J. Trop. Ecol.* 16, 1–19. doi: 10.1017/S0266467400001231

di Porcia e Brugnera, M., Meunier, F., Longo, M., Krishna Moorthy, S. M., de Deurwaerder, H., Schnitzer, S. A., et al. (2019). Modeling the impact of liana infestation on the demography and carbon cycle of tropical forests. *Global Change Biol.* 25, 3767–3780. doi: 10.1111/GCB.14769

Estrada-Villegas, S., and Schnitzer, S. A. (2018). A comprehensive synthesis of liana removal experiments in tropical forests. *Biotropica* 50, 729–739. doi: 10.1111/BTP.12571

Estrada-Villegas, S., Hall, J. S., van Breugel, M., and Schnitzer, S. A. (2021). Lianas do not reduce tree biomass accumulation in young successional tropical dry forests. *Oecologia* 195, 1019–1029. doi: 10.1007/s00442-021-04877-z

Gentry, A. H. (1991). "Chapter 1: The distribution and evolution of climbing plants" in *The Biology of Vines*, eds F. E. Putz and H. A. Mooney (Cambridge: Cambridge University Press), 3–50. doi: 10.1017/CBO9780511897658.003

Gentry, A. H., and Dodson, C. (1987). Contribution of nontrees to species richness of a tropical rain forest. *Biotropica* 19, 149–156. doi: 10.2307/2388737

Grauel, W. T., and Putz, F. E. (2004). Effects of lianas on growth and regeneration of *Prioria copaifera* in Darien, Panama. *Forest Ecol. Manag.* 190, 99–108. doi: 10.1016/J.FORECO.2003.10.009

Ingwell, L. L., Joseph Wright, S., Becklund, K. K., Hubbell, S. P., and Schnitzer, S. A. (2010). The impact of lianas on 10 years of tree growth and mortality on Barro Colorado Island, Panama. *J. Ecol.* 98, 879–887. doi: 10.1111/j.1365-2745.2010.01676.x

Laurance, W. F., Andrade, A. S., Magrach, A., Camargo, J. L. C., Valsko, J. J., Campbell, M., et al. (2014). Long-term changes in liana abundance and forest dynamics in undisturbed Amazonian forests. *Ecology* 95, 1604–1611. doi: 10.1890/13-1571.1

Meunier, F., Verbeeck, H., Cowdery, B., Schnitzer, S. A., Smith-Martin, C. M., Powers, J. S., et al. (2021). Unraveling the relative role of light and water competition between lianas and trees in tropical forests: a vegetation model analysis. *J. Ecol.* 109, 519–540. doi: 10.1111/1365-2745.13540

Muller-Landau, H. C., and Pacala, S. W. (2020). "What determines the abundance of lianas and vines?," in *Unsolved Problems in Ecology*, eds A. Dobson, D. Tilman, and R. D. Holt (Princeton, NJ: Princeton University Press).

Pandian, E., and Parthasarathy, N. (2003). Decadal (2003-2013) changes in liana diversity, abundance and aboveground biomass in four inland tropical dry evergreen forest sites of peninsular India. *J. Forestry Res.* 27, 133–146. doi: 10.1007/s11676-015-0146-145

Parolari, A. J., Paul, K., Griffing, A., Condit, R., Perez, R., Aguilar, S., et al. (2020). Liana abundance and diversity increase with rainfall seasonality along a precipitation gradient in Panama. *Ecography* 43, 25–33. doi: 10.1111/ECOG.04678

Pasquini, S. C., Wright, S. J., Santiago, L. S., and Uriarte, M. (2015). Lianas always outperform tree seedlings regardless of soil nutrients: results from a long-term fertilization experiment. *Ecology* 96, 1866–1876. doi: 10.1890/14-1660.1

Phillips, O. L., Vésquez Martínez, R., Arroyo, L., Baker, T. R., Killeen, T., Lewis, S. L., et al. (2002). Increasing dominance of large lianas in Amazonian forests. *Nature* 418, 770–774. doi: 10.1038/nature00926

Powers, J. S., and Peréz-Aviles, D. (2013). Edaphic factors are a more important control on surface fine roots than stand age in secondary tropical dry forests. *Biotropica* 45, 1–9. doi: 10.1111/J.1744-7429.2012.00881.X

Powers, J. S., Becknell, J. M., Irving, J., and Pèrez-Aviles, D. (2009). Diversity and structure of regenerating tropical dry forests in Costa Rica: geographic patterns and environmental drivers. *Forest Ecol. Manag.* 258, 959–970. doi: 10.1016/j.foreco.2008.10.036

Powers, J. S., Vargas, G., Brodribb, T. J., Schwartz, N. B., Pérez-Aviles, D., et al. (2020). A catastrophic tropical drought kills hydraulically vulnerable tree species. *Global Change Biol.* 26, 3122–3133. doi: 10.1111/GCB.15037

Putz, F. E. (1984a). How trees avoid and shed lianas. *Biotropica* 16:19. doi: 10.2307/2387889

Putz, F. E. (1984b). *The Natural History of Lianas on*. Panama: Barro Colorado Island.

Putz, F. E. (1990). Liana stem diameter growth and mortality rates on Barro Colorado Island. Panama. *Biotropica* 22:103. doi: 10.2307/2388725

Putz, F. E. (1991). "Silvicultural effects of lianas," in *Biology of vines*, eds F. E. Putz and H. A. Mooney (Cambridge: Cambridge University Press), 493–501. doi: 10.1017/cbo9780511897658.020

R Core Team (2021). *R: A Language and Environment for Statistical Computing*. Vienna: R Foundation for Statistical Computing.

Reis, S. M., Marimon, B. S., Morandi, P. S., Elias, F., Esquivel-Muelbert, A., Marimon Junior, B. H., et al. (2020). Causes and consequences of liana infestation in southern Amazonia. *J. Ecol.* 108, 2184–2197. doi: 10.1111/1365-2745.13470

Schilling, E. M., Waring, B. G., Schilling, J. S., and Powers, J. S. (2016). Forest composition modifies litter dynamics and decomposition in regenerating tropical dry forest. *Oecologia* 182, 287–297. doi: 10.1007/s00442-016-3662-x

Schnitzer, S. A. (2005). A mechanistic explanation for global patterns of liana abundance and distribution. *Ame. Natural.* 166, 262–276. doi: 10.1086/431250

Schnitzer, S. A., and Bongers, F. (2002). The ecology of lianas and their role in forests. *Trends Ecol. Evol.* 17, 223–230. doi: 10.1016/s0169-5347(02)02491-6

Schnitzer, S. A., and Bongers, F. (2011). Increasing liana abundance and biomass in tropical forests: emerging patterns and putative mechanisms. *Ecol. Lett.* 14, 397–406. doi: 10.1111/j.1461-0248.2011.01590.x

Schnitzer, S. A., and Carson, W. P. (2010). Lianas suppress tree regeneration and diversity in treefall gaps. *Ecol. Lett.* 13, 849–857. doi: 10.1111/J.1461-0248.2010.01480.X

Schnitzer, S. A., Bongers, F., and Wright, S. J. (2011). Community and ecosystem ramifications of increasing lianas in neotropical forests. *Plant Signal Behav.* 6, 598–600. doi: 10.4161/PSB.6.4.15373

Schnitzer, S. A., DeFilippis, D. M., Visser, M., Estrada-Villegas, S., Rivera-Camaña, R., Bernal, B., et al. (2021). Local canopy disturbance as an explanation for long-term increases in liana abundance. *Ecol. Lett.* 24, 2635–2647. doi: 10.1111/ele.13881

Schnitzer, S. A., Estrada-Villegas, S., and Wright, S. J. (2020). The response of lianas to 20 yr of nutrient addition in a Panamanian forest. *Ecology* 101:e03190. doi: 10.1002/ECY.3190

Sheil, D., Burslem, D. F. R. P., and Alder, D. (1995). The interpretation and misinterpretation of mortality rate measures. *J. Ecol.* 83, 331–333. doi: 10.2307/2261571

Smith-Martin, C. M., Bastos, C. L., Lopez, O. R., Powers, J. S., and Schnitzer, S. A. (2019). Effects of dry-season irrigation on leaf physiology and biomass allocation in tropical lianas and trees. *Ecology* 100:e02827. doi: 10.1002/ECY.2827

Smith-Martin, C. M., Jansen, S., Brodribb, T. J., Medina-Vega, J. A., Lucani, C., Huppenberger, A., et al. (2022). Lianas and trees from a seasonally dry and a wet tropical forest did not differ in embolism resistance but did differ in xylem anatomical traits in the dry forest. *Front. For. Glob. Change* 5:834891. doi: 10.3389/ffgc.2022.834891

Smith-Martin, C. M., Xu, X., Medvigy, D., Schnitzer, S. A., and Powers, J. S. (2020). Allometric scaling laws linking biomass and rooting depth vary across ontogeny and functional groups in tropical dry forest lianas and trees. *New Phytol.* 226, 714–726. doi: 10.1111/NPH.16275

van der Heijden, G. M. F., and Phillips, O. L. (2009). Liana infestation impacts tree growth in a lowland tropical moist Forest. *Biogeosciences* 6, 2217–2226. doi: 10.5194/BG-6-2217-2009

van der Heijden, G. M., Schnitzer, S. A., Powers, J. S., and Phillips, O. L. (2013). Liana impacts on carbon cycling, storage and sequestration in tropical forests. *Biotropica* 45, 682–692. doi: 10.1111/btp.12060

van der Sande, M. T., Poorter, L., Schnitzer, S. A., Engelbrecht, B. M. J., and Markesteijn, L. (2019). The hydraulic efficiency-safety trade-off differs between lianas and trees. *Ecology* 100:e02666. doi: 10.1002/ECY.2666

Visser, M. D., Schnitzer, S. A., Muller-Landau, H. C., Jongejans, E., de Kroon, H., Comita, L. S., et al. (2018). Tree species vary widely in their tolerance for liana infestation: a case study of differential host response to generalist parasites. *J. Ecol.* 106, 781–794. doi: 10.1111/1365-2745.12815

Werden, L. K., Waring, B. G., Smith-Martin, C. M., and Powers, J. S. (2018). Tropical dry forest trees and lianas differ in leaf economic spectrum traits but have overlapping water-use strategies. *Tree Physiol.* 38, 517–530. doi: 10.1093/treephys/tpx135

Wright, S. J., Calderón, O., Hernandéz, A., and Paton, S. (2004). Are lianas increasing in importance in tropical forests? A 17-year record from panama. *Ecology* 85, 484–489. doi: 10.1890/02-0757

Yorke, S. R., Schnitzer, S. A., Mascaro, J., Letcher, S. G., and Carson, W. P. (2013). Increasing liana abundance and basal area in a tropical forest: the contribution of long-distance clonal colonization. *Biotropica* 45, 317–324. doi: 10.1111/btp.12015

Conflict of Interest: The authors declare that the research was conducted in the absence of any commercial or financial relationships that could be construed as a potential conflict of interest.

frontiers | Frontiers in Forests and Global Change

ORIGINAL RESEARCH
published: 09 June 2022
doi: 10.3389/ffgc.2022.787950

Climate Change Affects Reproductive Phenology in Lianas of Australia's Wet Tropics

Nara O. Vogado[1]*, Jayden E. Engert[1], Tore L. Linde[2], Mason J. Campbell[1], William F. Laurance[1] and Michael J. Liddell[1]

[1] Centre for Tropical Environmental and Sustainability Science, College of Science and Engineering, James Cook University, Cairns, QLD, Australia, [2] Skyrail Rainforest Cableway, Cairns, QLD, Australia

Lianas are increasing in abundance in many tropical forests. This increase can alter forest structure and decrease both carbon storage and tree diversity *via* antagonistic relationships between lianas and their host trees. Climate change is postulated as an underlying driver of increasing liana abundances, *via* increases in dry-season length, forest-disturbance events, and atmospheric CO_2 concentrations; all factors thought to favour lianas. However, the impact of climate change on liana reproductive phenology, an underlying determinant of liana abundance, has been little studied, particularly outside of Neotropical forests. Over a 15-year period (2000–2014), we examined the phenological patterns of a liana community in intact rainforests of the Wet Tropics bioregion of Australia; a World Heritage Area and hotspot of floral diversity. Specifically, we assessed (1) flowering and fruiting patterns of liana species; (2) potential climate drivers of flowering and fruiting activity; and (3) the influence of El Niño-related climatic disturbances on liana phenology. We found that flowering and fruiting of the studied liana species increased over time. Liana reproduction, moreover, rose in apparent response to higher temperatures and reduced rainfall. Finally, we found flowering and fruiting of the liana species increased following El Niño events. These results suggest that liana reproduction and abundance are likely to increase under predicted future climate regimes, with potentially important impacts on the survival, growth, and reproduction of resident trees and thus the overall health of Australian tropical rainforests.

Keywords: flowering, fruiting, rainforest, ENSO (El Niño Southern Oscillation), forest disturbance, woody vines

Edited by:
Geertje M. F. Van Der Heijden,
University of Nottingham,
United Kingdom

Reviewed by:
Francis Edward Putz,
University of Florida, United States
Rachael Gallagher,
Western Sydney University, Australia

****Correspondence:***
Nara O. Vogado
vogado.nara@gmail.com

Specialty section:
This article was submitted to Tropical Forests, a section of the journal Frontiers in Forests and Global Change

Received: *01 October 2021*
Accepted: *25 March 2022*
Published: *09 June 2022*

Citation:
Vogado NO, Engert JE, Linde TL, Campbell MJ, Laurance WF and Liddell MJ (2022) Climate Change Affects Reproductive Phenology in Lianas of Australia's Wet Tropics. Front. For. Glob. Change 5:787950. doi: 10.3389/ffgc.2022.787950

INTRODUCTION

The combined pressures of global climate change and anthropogenic land modification are having profound impacts on the structure and function of tropical forests (Laurance et al., 2002; Phillips et al., 2002; Lewis et al., 2004). Losses of old-growth trees and the proliferation of pioneers and lianas have been documented in degraded and fragmented forests across the tropics (Laurance et al., 2014; Marshall et al., 2020). However, even fully intact forests may be subjected to changes in forest structure and composition resulting from large-scale drivers such as global climate change or rising atmospheric CO_2 levels, as has been observed in the Brazilian Amazon (Phillips et al., 2002; Laurance et al., 2014). Natural disturbances such as cyclones and droughts also shape tropical forest ecosystems by controlling their structure, species composition, and functional processes (Dale et al., 2001). Changes to the structure and composition of tropical forests will have important implications for biodiversity conservation and ecosystem services (Rice et al., 2004; Hector et al., 2011).

An important driver of forest structure and function is the change in timing and intensity of floral phenological activity due to variations in climate conditions (Gray and Ewers, 2021). Global and regional models of climate change project substantial change in temperature and rainfall patterns, as well as future increases in extreme climatic events, such as cyclones and ENSO, as well as natural disturbance events (IPCC, 2021). Plant phenology is primarily regulated by climate with current expectations suggesting a shift in the timing and intensity of flower and fruit production as a response to climate change (Menzel et al., 2006; Cleland et al., 2007; Richardson et al., 2013; Tang et al., 2016). Modification of rainfall patterns and increases in the frequency of El Niño events will result in more regular drought events in tropical forests (Cai et al., 2014) also impacting phenological patterns. Additionally, the stresses of higher ambient temperatures will result in more leaf-shedding events, higher tree mortality rates, and an increase in tropical forest fires (Cochrane and Laurance, 2008). Disruption to phenological patterns, as well as natural disturbances, may favour the proliferation of early successional tree species and other disturbance-adapted plant guilds such as lianas.

Previous studies have shown that liana abundance is increasing in intact tropical forests in response to large-scale drivers (Laurance et al., 2001a; Schnitzer and Bongers, 2002, 2011; Schnitzer, 2005; Campbell et al., 2015, 2018). Climate-related changes in the phenology and reproduction of lianas and trees could further influence their relative abundance in tropical forests. For example, increasing reproduction of liana species has been observed in Panama (Wright and Calderón, 2006, 2018; Chapman et al., 2018) and Mexico (Cortés-Flores et al., 2015), and may relate to rising levels of atmospheric CO_2 (Granados and Korner, 2002), dry-season intensity, or temperature (Marvin et al., 2015). Additionally, lianas have structural and physiological adaptations that make them resilient to, and allow them to benefit from, many types of disturbances (Oliveira et al., 1997; Laurance et al., 2006, 2011; Schnitzer and Carson, 2010; Paul and Yavitt, 2011; Ledo and Schnitzer, 2014). Schnitzer et al. (2021), for example, proposed that the ability of lianas to increase and capitalise on forest disturbance and the spiralling interaction between disturbance and climate change, could be behind increasing liana abundance in Neotropical forests. As such, predicted increases in the rates of disturbance and drier conditions pantropically will likely increase liana abundances relative to old-growth trees and other plant species adapted to undisturbed tropical forests.

Potential increases in liana abundance are important for forest management and conservation as the proliferation of lianas can have a detrimental impact on host trees (Schnitzer and Bongers, 2002). Lianas are a structural parasite of trees and compete for nutrients, water, and sunlight; severely impacting tree growth and survival (Putz, 1984; Laurance et al., 2001a). Increased liana loads have been found to negatively impact tree reproduction in Uganda (Babweteera et al., 2018), Brazil (Kainer et al., 2006), Panama (Wright, 2005; García León et al., 2018), and Malaysia (Wright et al., 2015). Evidence also indicates that lianas may have higher comparative pollination success when compared to trees (Boulter et al., 2009). Hence, a proliferation of lianas could lead to both higher mortality and reduced recruitment of tropical trees, with important implications for forest biodiversity and carbon storage.

Here we present a long-term phenological study of the liana community found across an elevational gradient (ca. 5–540 m elevation) in the Australian wet tropics, as well as an analysis of the relationship between climate drivers and liana phenology. Specifically, we examined: (1) flowering and fruiting patterns and seasonality of the liana community; (2) the potential climate drivers of these flowering and fruiting patterns; and (3) assessed how liana phenology was responding to observed changes in temperature and rainfall through time, with the aim of projecting future changes in phenological timing and duration for the liana species assemblage we studied.

MATERIALS AND METHODS

Study Area

Phenological observations of the canopy of a tropical rain forest were conducted for 15 years (2000–2014 inclusive) using the Skyrail Rainforest Cableway,[1] a 7.5 km scenic gondola cableway running above the Barron Gorge National Park (**Figure 1**). Barron Gorge National Park comprises part of the Wet Tropics World Heritage Area of Australia (16.84°S, 145.64°E), whose listing was partially due to its recognition as a hotspot of plant and animal biodiversity. The vegetation community of the park, part of the traditional lands of the Djabugandji people (traditional owners), is composed of a closed-canopy mesophyll/notophyll vine forest (Tracey, 1982).

The study region experiences climatic seasonality, with a drier season from June to November and a wetter season from December to May (**Figure 1**). The forests in the Wet tropics are frequently subjected to disturbances including cyclones and El Niño-related droughts and heat-waves; making them highly vulnerable to climate change impacts (Hughes, 2003; Turton, 2012). Climatic information for the study area was obtained through the Australian Bureau of Meteorology (BOM) for the Kuranda Railway Station weather station (BOM, n.d., station numbers 031036 and 031011) (**Figure 2**) located at the upper end of the cableway.

Phenological Observations

Flowering and fruiting activity along a 7.5 km transect of the Skyrail gondola were recorded weekly from January 2000 to December 2014 by the same observer. The observer scored phenology from above using a maintenance gondola with

---

[1] https://www.skyrail.com.au

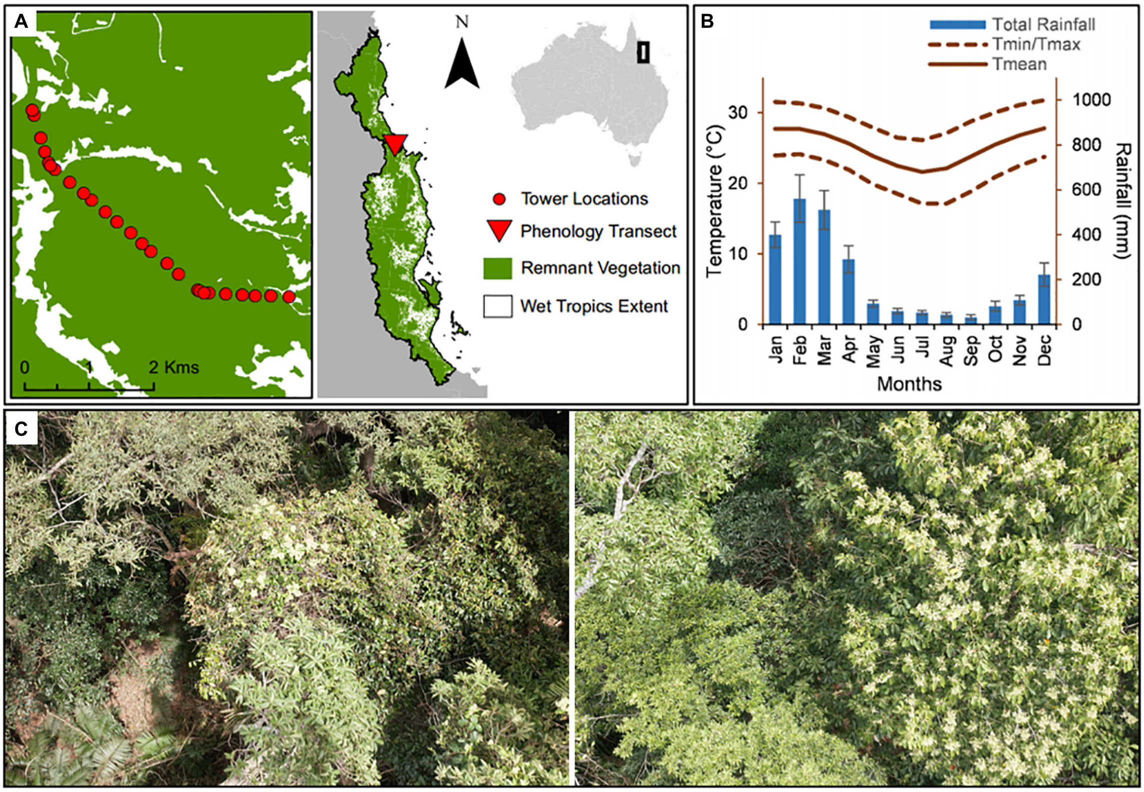

FIGURE 1 | Location and mean annual climate for the study region. **(A)** Wet Tropics World Heritage Area extent with phenology transect located in Barron Gorge National Park, Far North Queensland, Australia. **(B)** Monthly general meteorological patterns of rainfall (mm), maximum temperature (Tmax °C), minimum temperature (Tmin °C), and mean temperature (Tmean °C) from January 2000 to December 2014, and **(C)** View from the forest canopy as seen from the gondola.

unimpeded visual access to the canopy. To quantify observation records, the total area sampled was divided into 10 subplots of ∼100 m width and ∼25 m length, between each pair of towers, for a total of 320 subplots. The total area sampled using the 320 subplots was estimated to be approximately 0.75 km^2. We recorded presence or absence of flowering and fruiting activity within each subplot for the conspicuous liana community, composed of 17 species (**Supplementary Table 1**).

Visual identification of species from the gondola was cross-checked against plant ground samples (flowers, fruits, and leaves) that were identified using the Australian Rainforest Key (Zich et al., 2018), developed by the Australian Tropical Herbarium. The botanical observer was trained by professional botanists (Australian Tropical Herbarium, Cairns Regional Council) and independent verification of plant identification was carried out using plant samples collected on the ground. In addition high resolution digital photographs (Sony DSLR α-700P 12MP) were collected along the 7.5 km transect and these were then examined against the Australian Rainforest Key to further cross-check the ability of the observer to correctly identify liana activity to the species level from the gondola. We considered presence of phenological activity (flowers or fruits) in a single subplot as a single observation. We then calculated, for each week and month, the mean percentage of phenological activity for the transect. To calculate the percentage activity for the transect, we found, for each species, the maximum number of subplots (from a total of 320) presenting phenological activity at one time. We then summed these maximum values to estimate the potential maximum activity for the entire transect, and calculated the percentage activity by comparing the total activity at each time point to this maximum value (**Figure 2**). Percentage activity was calculated using the weekly observations of the original records, and aggregated to monthly values by taking the maximum percentage.

Species-specific phenological patterns were assessed for the eight most dominant species, which together accounted for 80% of the phenological records. We assessed the long-term weekly patterns for each species individually and the summed percent of weekly activity. The most dominant species were: *Austrosteenisia blackii* (F.Muell.), *Austrosteenisia stipularis* (C.T.White) Jessup, *Cissus penninervis* (F.Muell.) Planch, *Dichapetalum papuanum* (Becc.) Boerl, *Embelia caulialata* S.T.Reynolds, *Faradaya splendida* F.Muell., *Neosepicaea jucunda* (F.Muell.) Steenis, and *Parsonsia latifolia* (Benth.) S.T.Blake.

Statistical Analysis

To assess year-to-year phenological patterns and seasonality, we conducted circular statistical analyses using the monthly percentage of activity for flowering and fruiting. To calculate the circular statistical parameters, months were converted to

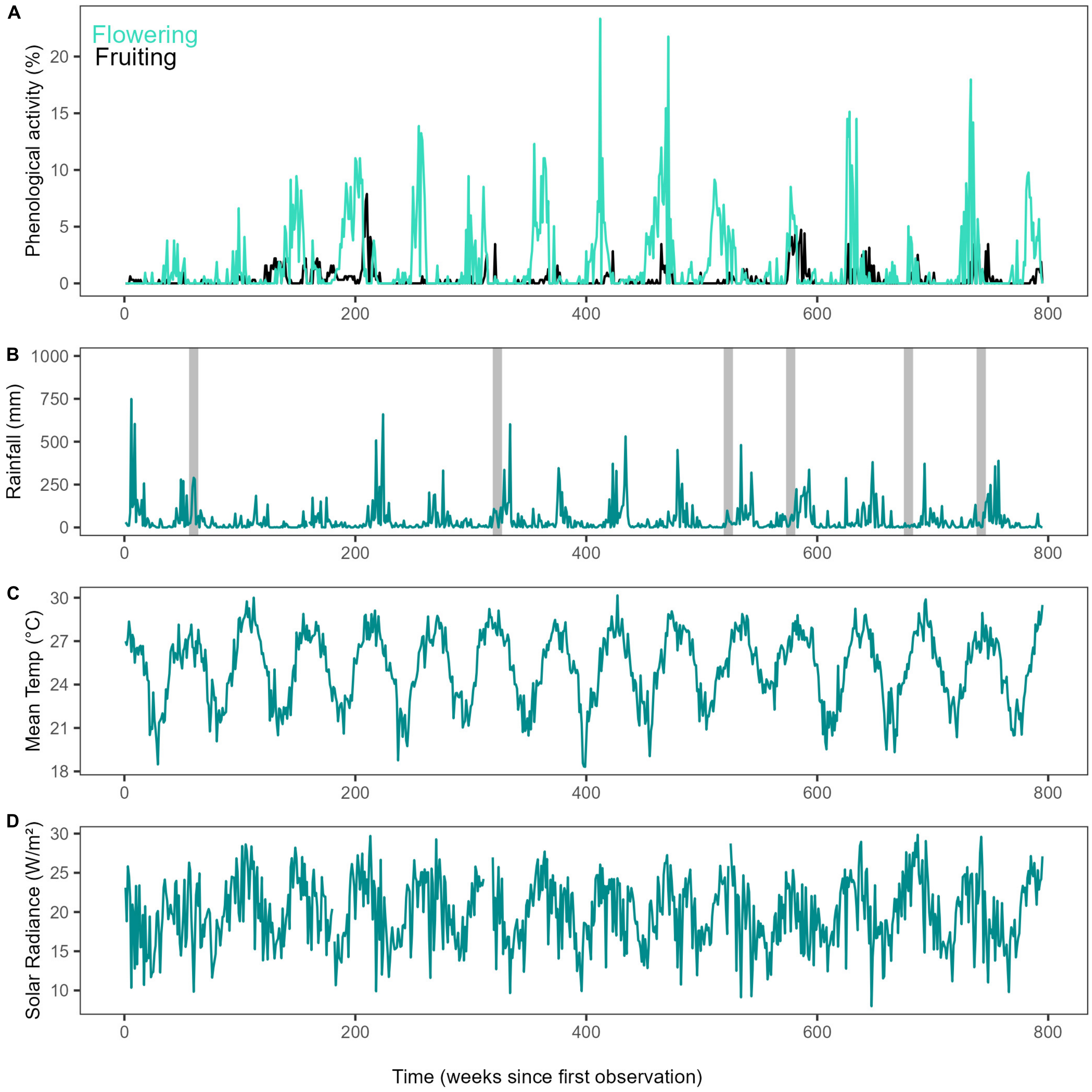

FIGURE 2 | Time series of long-term phenology and climate. **(A)** Weekly proportion of plots with flowering and fruiting activity for the studied period (2000–2014) in Barron Gorge National Park, Far North Queensland, Australia, **(B)** Time series for weekly rainfall (mm) and cyclones (grey bars), **(C)** Mean daily temperature (°C), and **(D)** Mean daily solar irradiance (W/m^2).

angles, where the first month, January, is transformed into angle 0° and subsequent months are added in intervals of 30° until December at 330° (Morellato et al., 2010). We then calculated the mean angle, circular standard deviation (SD), and vector length (r). Vector length (r) indicates the degree of seasonality, varying from 0 (aseasonal) to 1 (seasonal) (Zar, 1996), while the circular standard deviation can be an indicator of season length (Ting et al., 2008). To determine if phenological patterns were significantly seasonal, we used Rayleigh tests (Zar, 1999).

We assessed long-term patterns of flowering and fruiting using generalised additive models (GAMs) with monthly phenology (maximum weekly percentage of activity for the month) as the response variable and date, temperature, rainfall, and solar radiation as the explanatory variables. Phenological and climate time series were detrended in order to remove the intra-annual seasonal and random components using the R package "forecast" (Hyndman et al., 2021).

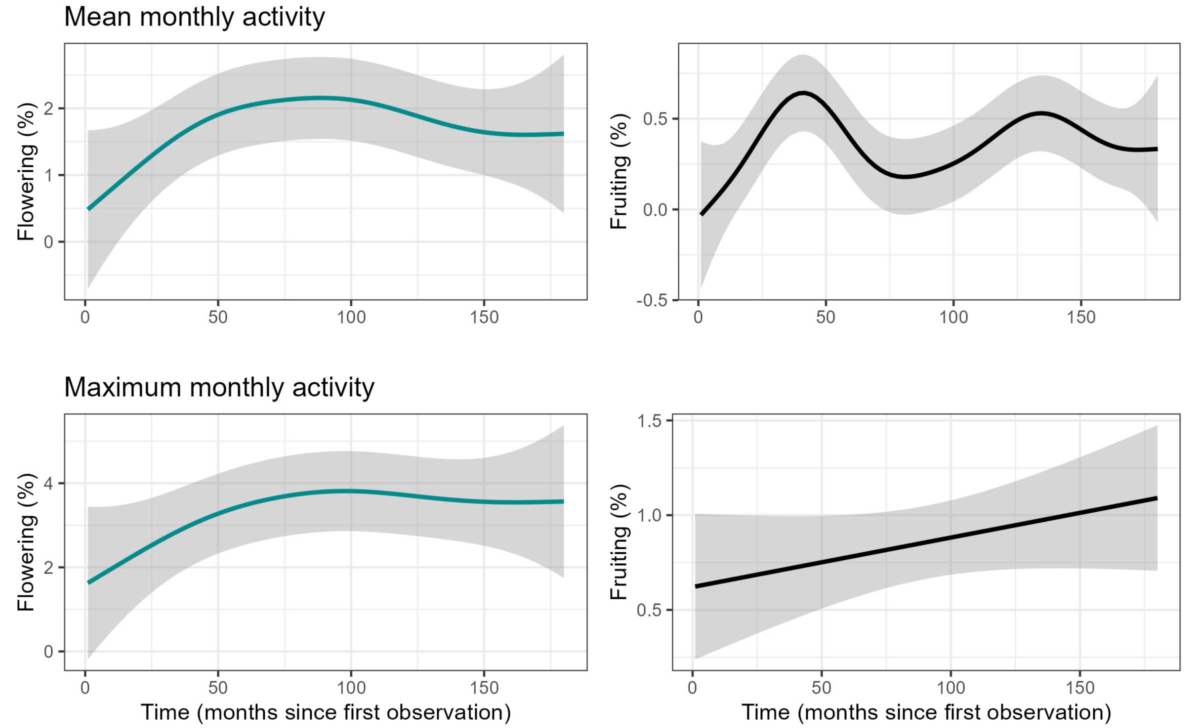

FIGURE 3 | Fitted GAM-smoother for long-term relationship between monthly mean and maximum phenological activity and time (months since first observation), for the liana community in Barron Gorge National Park, Far North Queensland, Australia.

We identified the potential climate drivers of liana phenology based on both seasonal patterns (prior to detrending) and long-term trends (post detrending). As relationships between phenological activity and drivers are often reported as being non-linear, we used Generalised Additive Models for Location, Scale and Shape (GAMLSS) to model relationships (Hudson et al., 2010). We used GAMLSS as they accommodate unconventional distributions and the temporal autocorrelation inherent to phenological series. Model distributions were chosen to maximise fit of each model. We assumed a Beta distribution, however, the model fit and residuals were substantially better when a Gaussian distribution was used for both flowering and fruiting (with a log link function). We developed the GAMLSS models using a cubic spline smoothing function, and included an auto-regressive AR(1) correlation structure for the response variable (term of 1 month). Collinearity between explanatory variables was assessed with concurvity, a generalisation of collinearity appropriate for GAMs. Proportion of individual subplots in flowering or fruiting activity were used as response variables, and monthly rainfall (mm), monthly mean temperature (°C), monthly mean photoperiod (h/day), and monthly mean solar radiation (W/m^2) were used as predictor variables. Optimal models were selected using the Aikaike Information Criteria (AIC).

To assess possible influence of climatic disturbance events, ENSO variation and cyclones, as well as inter-annual influence of climate variables on phenological activity, we conducted cross-correlation analyses against the phenological activity time series. We decomposed the phenological activity time series and removed the seasonal component prior to cross-correlation using the "stl" function in base R. Influence of ENSO was modelled using the multivariate ENSO index (MEI) and cyclones were treated as a discrete event with values of 1 for months when cyclones occurred and 0 when they did not occur. Time series analysis was conducted using the "timeSeries" R package (Wuertz, 2020). All analyses have been conducted in R studio (R Core Team, 2019).

RESULTS

We identified a long-term increase in flowering activity of the liana community in the study area and two supra-annual peaks in fruiting activity, in November 2004 and January 2011 (**Figure 2**). Overall visualisation of annual total rainfall and mean maximum temperature showed that although rainfall may be variable in the region, temperature has been increasing since 1950 (**Supplementary Figure 3**). The studied period was not anomalous to the general trends and patterns. Time in number of months since first observation was found to have a significant positive effect on both flowering and fruiting activity ($F = 31.74$, $P < 0.0001$ and $F = 38.54$, $P < 0.001$, respectively) as assessed using GAMs performed on seasonally detrended data (trend component of time series) of monthly maximum values. Long-term patterns of flowering noted a continuous increase through time, but fruiting increased, decreased and

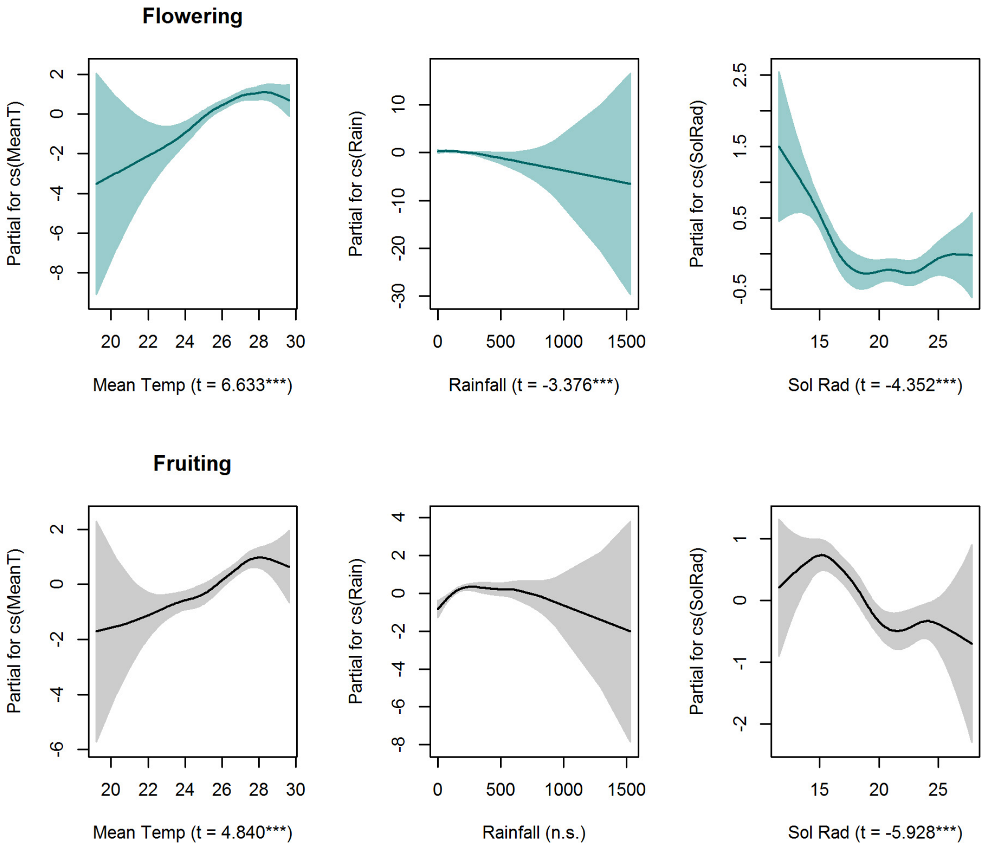

FIGURE 4 | Partial effects of GAMLSS explanatory variables on flowering and fruiting seasonal trends in a liana community (17 species) (Cox Snell R^2 0.48 and R^2 0.26, respectively), in Barron Gorge National Park, Far North Queensland, Australia. The shaded areas indicate the 95% confidence intervals. GAMLSS-smoother terms for total monthly rainfall (mm), mean monthly temperature (°C), and mean monthly solar radiation (MJ/m^2) were significant for flowering ($P < 0.05$) whereas mean temperature (°C) and mean monthly solar radiation (MJ/m^2) were significant for fruiting. *T*-values and significance (***$P < 0.001$) are presented within parenthesis in *x*-axis title.

increased again, forming two peaks (**Figure 3**) when assessing the data visually. Rainfall showed a linear decrease, while mean temperature showed a linear increase over time (**Supplementary Figure 4**). Additionally, mean temperature (flowering: $F = 5.62$, $P < 0.001$, and fruiting: $F = 3.58$, $P < 0.01$), rainfall (flowering: $F = 2.85$, $P < 0.01$ and fruiting: $F = 7.32$, $P < 0.0001$), solar irradiance (flowering: $F = 9.01$, $P < 0.0001$ and fruiting: $F = 5.61$, $P < 0.001$), and MEI (flowering: $F = 4.41$, $P < 0.01$ and fruiting: $F = 22.46$, $P < 0.0001$) all influenced long-term flowering and fruiting trends.

When analysing intra-annual patterns, GAMLSS smoothers for temperature, rainfall and solar radiation were significant ($P < 0.001$) for flowering activity (**Figure 4** and **Supplementary Table 3**). Conversely, smoothers for temperature and solar radiation were significant for fruiting activity (**Figure 4** and **Supplementary Table 3**). The seasonal peak of fruiting activity was significantly related to higher mean temperatures and low levels of solar radiation (**Figure 4**). Similarly, flowering activity increased with an increase in temperature, peaking when the temperature was between 28 and 30 degrees Celsius. Additionally, flowering activity was negatively correlated with rainfall (**Figure 4**). Fruiting presented a negative relationship with solar radiation, peaking at the minimum levels of solar radiation (**Figure 4**).

MEI (ENSO index) had a significant influence on both flowering and fruiting activity (as assessed using cross-correlation analyses), and a significant influence of cyclones on flowering. Flowering increased at a lag of 19 months following increased MEI values, indicating an El Niño event ($r = 0.20$), and fruiting activity was found to decrease 4 months after an El Niño event ($r = -0.18$), and then increased 9 months after an El Niño event ($r = 0.24$). As the relationship between phenological activity and MEI was related to increases in MEI, the results suggest the relationship was caused by El Niño events. In tropical Australia, El Niño events lead to dry, hot weather, and this relationship is supported by cross-correlation analyses between MEI and rainfall, temperature, and solar radiation (**Table 1A**). Moreover, these cross-correlation analyses between MEI and climate variables indicated that solar radiation increased 4 months before increase in MEI, with mean temperature increasing 4 months after increase in MEI. MEI and rainfall had concurrent changes, with lag of 0 being the significant one, indicating a significant decrease in rainfall (**Table 1A**). Flowering

TABLE 1 | Cross correlations among monthly values of flowering and fruiting activity (percentage of subplots showing phenological activity) on Barron Gorge National Park, Far North Queensland; **(A)** Between three indices of the El Niño Southern Oscillation and climate variables (rainfall, mean temperature, and solar irradiance) recorded the study area, and **(B)** Between climate variables, including El Niño Southern Oscillation index and cyclone, and phenological activity (flowering and fruiting).

(A)

	Temperature		Rainfall		Solar irradiance	
	r	**Lag[†] (months)**	**r**	**Lag[†] (months)**	**r**	**Lag[†] (months)**
MEI	0.25	−4	−0.23	0	0.18	4
ENSO122	*n.s.*		*n.s.*		*n.s.*	
ENSO342	0.3	−5	−0.22	−1	*n.s.*	

(B)

	Flowering		Fruiting	
	r	**Lag (months)**	**r**	**Lag (months)**
MEI	0.20	−19	−0.18	−4
ENSO122	*n.s.*		*n.s.*	
ENSO342	0.18	2	0.24	−12
Rainfall	0.22	5	0.32	3
Cyclone	−0.27	4	*n.s.*	
Mean Temperature	0.20	8	0.20	−3
Solar Radiation	*n.s.*		−0.18	0

[†] *Negative lags indicate that the variation in phenological activity occurred after variation in local climate or the El Niño Southern Oscillation Index. Results show the highest significant cross-correlation coefficient ($P < 0.05$).*

activity was also found to significantly decrease 4 months before a cyclone (*r* = -0.27), while fruiting was not significantly affected (**Table 1B**).

In general, the studied liana community presented intra-annual seasonality, with a peak of flowering activity at the end of the dry season (October) and a peak of fruiting activity in the middle of the wet season (January) (**Supplementary Figure 1**) when the weekly circular phenological data was analysed over the whole study period. Seasonal phenological patterns were consistent among species, and community patterns were not dependent on any dominant species (**Figure 5**). A general pattern of increase in flowering was found for the community with five out of the eight species presenting an increase. Further, the majority of species increased fruiting activity. Two clear exceptions were present, however, with *Parsonsia latifolia* presenting a decrease in fruiting activity and *Cissus penninervis*, displaying a decrease in activity of both phenophases over time. Flowering at community level was seasonal in all years, and fruiting was mostly seasonal years with the exception of 2000 and 2009 (Rayleigh test $P < 0.05$; **Supplementary Table 2**) as determined through assessing the weekly phenological data using circular statistics.

Although presenting clear seasonality in the flowering and fruiting activity for most years (**Supplementary Table 2**), the synchronicity of activity was low (below 20%). However, the percentage of flowering activity occurred in supra-annual peaks–activity above 15%, in October 2007 (23.3%), November 2008 (21.8%), November 2011 (15.1%), and November 2013 (18%). When comparing differences among years, fruiting showed increased activity in 2003 (2.04-fold) and in 2011 (1.6-fold).

We found a significant delay in timing of flowering for the years of 2001, 2010, 2011, and 2012 with delays of 18, 33, 25, and 25 days, respectively, when comparing mean dates from each year to the general mean date for the whole studied period. The years of 2010 and 2011 endured concurrent La Niña and cyclones events. Fruiting activity was highly variable, but mean dates were mainly found to occur between late November and January (**Supplementary Table 2**).

DISCUSSION

Reproductive Activity of Lianas Is Increasing Through Time

Reproductive activity (flowering and fruiting) of lianas in our study site in the Australian wet tropics showed an increase over the study period from 2000 to 2014. Species-specific patterns, although variable, suggest community patterns were not significantly influenced by any individual species. In fact, five of the eight dominant species showed an increase in flowering activity over the examined time. However, one species, *Cissus penninervis*, displayed a decrease in both flowering and fruiting activity. Moreover, the species *Parsonsia latifolia*, displayed an interesting sharp increase in flowering activity, but a decrease in fruiting. These finding suggest, that at least in part, some responses to climate and climate change may be species dependent, though whether the responses are due to physiological or ecological limitations (or a synergism of the two) requires further investigation. Overall, an increase in liana phenological activity over time, particularly flowering, has also been found in other tropical regions such as Panama

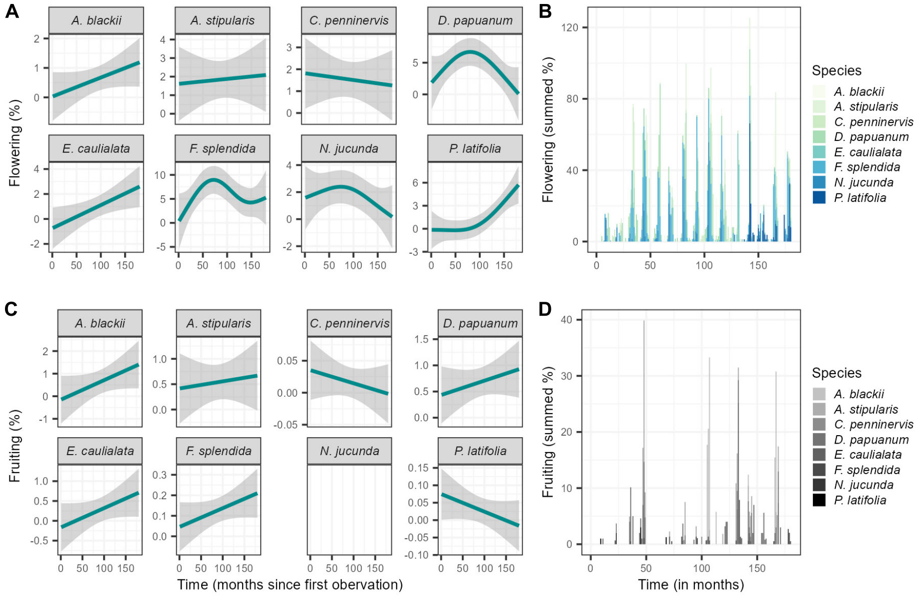

FIGURE 5 | (A) Fitted GAM-smoother for monthly mean percentage of overall flowering and fruiting trends for each of the dominant species and **(B)** Summed monthly mean activity of flowering and fruiting for the dominant species in Barron Gorge National Park, Far North Queensland, Australia.

(Wright and Calderón, 2006; Pau et al., 2018). This increase may be linked to an increase in temperature, seasonality, or higher fertilisation of plant species from rising atmospheric CO_2 levels (Granados and Korner, 2002; Körner, 2009), as suggested by Manzanedo et al. (2018) and Pau et al. (2018). Additionally, both fruiting and flowering activity in liana species increased with higher temperatures, both between and within years. This fertilisation response, coupled with rising mean temperatures due to apparent climate change (Australia has warmed by 1.44 ± 0.24°C since 1910; Commonwealth of Australia, 2020), may be triggering faster growth and reproduction of lianas in the Australian wet tropics.

Our findings also demonstrate that increased flowering activity of liana species was associated with lower rainfall, both between and within different years. In Ghana, Swaine and Grace (2007) found that liana richness was higher in drier forests, suggesting an adaptation of lianas to habitats with high evapotranspirative demand. Cai et al. (2009) and Medina-Vega et al. (2021) likewise found that physiological and trait differences give lianas an adaptive advantage over trees in more seasonal and drier forests. Australia's Wet tropics region is expected to see higher mean temperatures and an increase in rainfall seasonality, and hence altered dry-season length and drier conditions, under climate change (IPCC, 2021). These results suggest liana reproductive activity and abundance are likely to continue increasing in the Australian wet tropics (Syktus et al., 2020), and presumably elsewhere in the global tropics as well.

Phenological Activity Related to Cyclones and El Niño Disturbances

Supra-annual variations in liana reproduction, with fruit production increasing in specific years, suggests they may be responding to disturbance events such as El Niños and cyclones (Laurance and Curran, 2008). El Niños and cyclones both occur with some regularity in tropical Australia (Turton and Stork, 2009), making it difficult to untangle the influence of such events on plant phenology without multi-decadal studies. Despite this challenge, we were able to identify an increase in both liana fruiting and flowering following El Niño events—observations that align with findings in the Neotropics and African tropics (e.g., Panama: Wright and Calderón, 2006; Puerto Rico: Zimmerman et al., 2007; Uganda: Chapman et al., 2018).

Various studies have demonstrated that increasing forest disturbances, tree mortality, and forest turnover lead to an increase in liana abundance (Putz, 1984; Schnitzer and Bongers, 2011; Hogan et al., 2017; Umaña et al., 2019). As El Niño events often increase tree mortality and leaf shedding by drought-stressed trees, they can increase canopy openness and allow lianas to rapidly colonise forests (Laurance et al., 2001a) *via* their seeds, advance regeneration, or lateral growth. This facilitates large-scale recruitment of lianas in disturbed forests, which is then followed by fast vertical growth towards the canopy (Ingwell et al., 2010; Schnitzer and Bongers, 2011). There is also evidence that lianas are more physiologically capable than trees under drier conditions (Medina-Vega et al., 2021). Increasing liana reproduction related to disturbance events, coupled with their strong ability to colonise disturbed forests, is expected to increase liana abundance in tropical forests under climate change.

Increased Liana Reproduction and Changing Tropical Forests

The observed increase in liana reproduction may contribute to changes in forest composition and structure in the future. An increase in abundance of vines and lianas has already been observed in the Amazon (Laurance et al., 2014) and other Neotropical forests (Schnitzer et al., 2014) and in Southeast Asia (Wright et al., 2015). However, long-term studies on the competitive balance between trees and lianas in Australia are lacking. These results may provide preliminary evidence of increasing liana abundance in the tropical forests of Australia.

A greater abundance of lianas, and the associated increase in mortality of infested trees may result in important compositional and structural changes in tropical rainforests, including reduced tree diversity and forest-carbon storage (Laurance et al., 2001b). Moreover, an increase in liana abundance at the expense of climax tree species in Australian rain forests may have cascading impacts such as an increase in insect diversity (Odell et al., 2019) and a reduction in fruit resources for keystone species such as the southern cassowary – due to a proportionate increase in wind-dispersed seeds and decrease in per unit area fruit production (Zich et al., 2020). Liana species are often more adept than trees at responding to large-scale disturbance events, such as cyclones and El Niño droughts, and small-scale disturbances such as tree falls (Putz, 1984; Schnitzer and van der Heijden, 2019). The ability of lianas to grow faster and use water more efficiently than trees, particularly during the dry season (Schnitzer, 2005; Cai et al., 2009), facilitates their colonisation of treefall gaps after disturbance. Additionally, physiological adaptations such as higher hydraulic conductivity, maximum carbon-assimilation rate, increased water-use efficiency and decrease susceptibility to cavitation in the dry season (Zhu and Cao, 2010), could provide liana species further advantages under higher temperature and rainfall seasonality expected due to climate change.

Changes in Seasonality

The period 2010–2012 endured concurrent cyclones and La Niñas, and presented a significant delay in mean flowering date (33, 25, and 25 days, respectively). Contrastingly, years when El Niños occurred had an advance in the mean date of flowering when compared to the mean date for the study period. In regions where multiple extreme events can occur at the same time, as is the case for the Wet Tropics, it can be challenging to determine which event is the main influence. However, our results suggest that extreme events in the region may cause changes to the mean dates of flowering periods.

Changes to timing of flowering or fruiting may constitute a change to resource availability for pollinators and frugivores. Mismatches in activity can happen between flowering plants and their pollinators, which can decrease fruiting (Morellato et al., 2016), and resource availability for pollinators and nectivores. Hence, the delays in the timing of liana flowering observed in relation to extreme events might also have adverse impacts on forest communities.

Observed liana fruiting activity was generally low, a pattern previously observed in liana species in Africa (Ley and Claßen-Bockhoff, 2013) and Asia (Nakonechnaya et al., 2021). Interestingly, the supra-annual peaks we observed for flowering were not accompanied by a proportional increase in fruit availability. Previous work in tree and shrub species has shown that reduced fruit set in relation to flower production may be due to resource limitation or reduced pollinator activity (Rathcke, 2000; Cunningham et al., 2020). When combined with the observed overall increase in liana activity and potential changes to floristic composition and structure, these extreme events are also unlikely to provide any benefit to frugivore communities.

CONCLUSION

We found that liana reproductive activity has been increasing through time (2000–2014) in rainforests of the Australian wet tropics. The increased activity was associated with increases in temperatures, rainfall seasonality, and climatic disturbances such as El Niño events. The observed increase in liana fruiting was also coupled with a change in timing and contraction of fruiting-season duration. Such changes may mitigate any potential advantages for frugivore species associated with increased liana fecundity. These results suggest that liana reproduction, and hence abundance, is likely to increase in the Australian wet tropics region in response to future climate change, negatively impacting resident tree species and degrading forest structure.

DATA AVAILABILITY STATEMENT

The raw data supporting the conclusions of this article will be made available by the authors, without undue reservation.

AUTHOR CONTRIBUTIONS

NV conceived and wrote the manuscript with conceptual input from JE and ML, and editorial input from JE, MC, WL, and ML. TL collected the data. NV and JE prepared all figures. All authors contributed to the article and approved the submitted version.

ACKNOWLEDGMENTS

We acknowledge the traditional owners of the study region, and thank Skyrail Rainforest Cableway staff for their help and support with data collection.

SUPPLEMENTARY MATERIAL

The Supplementary Material for this article can be found online at: https://www.frontiersin.org/articles/10.3389/ffgc.2022.787950/full#supplementary-material

REFERENCES

Babweteera, F., Plumptre, A. J., Adamescu, G. S., Shoo, L. P., Beale, C. M., Reynolds, V., et al. (2018). The ecology of tree reproduction in an African medium altitude rain forest. *Biotropica.* 50, 405–417. doi: 10.1111/btp.12563

BOM (n.d.). *Climate Data Online: Kuranda Railway Station*. Available online at: http://www.bom.gov.au/jsp/ncc/cdio/weatherData/av?p_nccObsCode=139&p_display_type=dataFile&p_startYear=&p_c=&p_stn_num=031036 (accessed November 09, 2021).

Boulter, S. L., Kitching, R. L., Gross, C. L., Goodall, K. L., and Howlett, B. G. (2009). "Floral morphology, phenology and pollination in the Wet tropics," in *Living in a Dynamic Tropical Forest Landscape*, eds S. L. Turton and N. E. Stork (Oxford: Blackwell Publishing, Ltd), 224–239. doi: 10.1186/1999-3110-55-15

Cai, W., Borlace, S., Lengaigne, M., van Rensch, P., Collins, M., Vecchi, G., et al. (2014). Increasing frequency of extreme El Niño events due to greenhouse warming. *Nat. Clim. Chang.* 4, 111–116.

Cai, Z., Schnitzer, S. A., and Bongers, F. (2009). Seasonal differences in leaf-level physiology give lianas a competitive advantage over trees in a tropical seasonal forest. *Oecologia* 161, 25–33. doi: 10.1007/s00442-009-1355-4

Campbell, M., Magrach, A., and Laurance, W. F. (2015). "Liana diversity and the future of tropical forests," in *Biodiversity of Lianas*, ed. N. Parthasarathy (Cham: Springer International Publishing), 255–274. doi: 10.1007/978-3-319-14592-1_13

Campbell, M. J., Edwards, W., Magrach, A., Alamgir, M., Porolak, G., Mohandass, D., et al. (2018). Edge disturbance drives liana abundance increase and alteration of liana–host tree interactions in tropical forest fragments. *Ecol. Evol.* 8, 4237–4251. doi: 10.1002/ece3.3959

Chapman, C. A., Valenta, K., Bonnell, T. R., Brown, K. A., and Chapman, L. J. (2018). Solar radiation and ENSO predict fruiting phenology patterns in a 15-year record from Kibale National Park, Uganda. *Biotropica.* 50, 384–395. doi: 10.1111/btp.12559

Cleland, E. E., Chuine, I., Menzel, A., Mooney, H. A., and Schwartz, M. D. (2007). Shifting plant phenology in response to global change. *Trends Ecol. Evol.* 22, 357–365. doi: 10.1016/j.tree.2007.04.003

Cochrane, M. A., and Laurance, W. F. (2008). Synergisms among fire, land use, and climate change in the Amazon. *Ambio* 37, 522–527. doi: 10.1579/0044-7447-37.7.522

Commonwealth of Australia (2020). *State of the Climate 2020*. Canberra, ACT: CSIRO.

Cortés-Flores, J., Cornejo-Tenorio, G., and Ibarra-Manríquez, G. (2015). Flowering phenology and pollination syndromes in species with different growth forms in a neotropical temperate forest of Mexico. *Botany* 93, 361–367. doi: 10.1139/cjb-2014-0218

Cunningham, S. A., Evans, M. J., Neave, M., Armstrong, J., and Barton, P. S. (2020). Pollination and resource limitation as interacting constraints on almond fruit set. *Plant Biol.* 22, 112–113. doi: 10.1111/plb.13045

Dale, V. H., Joyce, L. A., McNulty, S., Neilson, R. P., Ayres, M. P., Flannigan, M. D., et al. (2001). Climate change and forest disturbances: climate change can affect forests by altering the frequency, intensity, duration, and timing of fire, drought, introduced species, insect and pathogen outbreaks, hurricanes, windstorms, ice storms, or landslides. *Bioscience* 51, 723–734.

García León, M. M., Izquierdo, L. M., Mello, F. N. A., Powers, J. S., and Schnitzer, S. A. (2018). Lianas reduce community-level canopy tree reproduction in a Panamanian forest. *J. Ecol.* 106, 737–745. doi: 10.1111/1365-2745.12807

Granados, J., and Korner, C. (2002). In deep shade, elevated CO_2 increases the vigor of tropical climbing plants. *Glob. Chang. Biol.* 8, 1109–1117. doi: 10.1046/j.1365-2486.2002.00533.x

Gray, R. E. J., and Ewers, R. M. (2021). Monitoring forest phenology in a changing world. *Forests* 12:297. doi: 10.3390/f12030297

Hector, A., Philipson, C., Saner, P., Chamagne, J., Dzulkifli, D., O'Brien, M., et al. (2011). The Sabah biodiversity experiment: a long-term test of the role of tree diversity in restoring tropical forest structure and functioning. *Phil. Trans. R. Soc. B.* 366, 3303–3315. doi: 10.1098/rstb.2011.0094

Hogan, J., Mayorquín, S., Rice, K., Thompson, J., Zimmerman, J., and Brokaw, N. (2017). Liana dynamics reflect land-use history and hurricane response in a Puerto Rican forest. *J. Trop. Ecol.* 33, 155–164. doi: 10.1017/s0266467417000049

Hudson, I. L., Kim, S. W., and Keatley, M. R. (2010). "Climatic influences on the flowering phenology of four eucalypts: a GAMLSS approach phenological research," in *Phenological Research*, eds I. L. Hudson and M. R. Keatley (Dordrecht: Springer Netherlands Link).

Hughes, L. (2003). Climate change and Australia: trends, projections and impacts. *Austral Ecol.* 28, 423–443. doi: 10.1046/j.1442-9993.2003.01300.x

Hyndman, R., Athanasopoulos, G., Bergmeir, C., Caceres, G., Chhay, L., O'Hara-Wild, M., et al. (2021). *Forecast: Forecasting Functions for Time Series and Linear Models. R Package Version 8.15*. Available online at: https://pkg.robjhyndman.com/forecast/ (accessed November 09, 2021).

Ingwell, L. L., Joseph Wright, S., Becklund, K. K., Hubbell, S. P., and Schnitzer, S. A. (2010). The impact of lianas on 10 years of tree growth and mortality on Barro Colorado Island, Panama. *J. Ecol.* 98, 879–887. doi: 10.1111/j.1365-2745.2010.01676.x

IPCC (2021). *Climate Change 2021: The Physical Science Basis. Contribution of Working Group I to the Sixth Assessment Report of the Intergovernmental Panel on Climate Change*, eds V. Masson-Delmotte, P. Zhai, A. Pirani, S. L. Connors, C. Péan, S. Berger, et al. (Cambridge: Cambridge University Press).

Kainer, K. A., Wadt, L. H. O., Gomes-Silva, D. A. P., and Capanu, M. (2006). Liana loads and their association with *Bertholletial excelsa* fruit and nut production, diameter growth and crown attributes. *J. Trop. Ecol.* 22, 147–154. doi: 10.1017/s0266467405002981

Körner, C. (2009). Responses of humid tropical trees to rising CO_2. *Annu. Rev. Ecol. Evol. Syst.* 40, 61–79. doi: 10.1073/pnas.1704811114

Laurance, W. F., Andrade, A. S., Magrach, A., Camargo, J. L. C., Valsko, J. J., Campbell, M., et al. (2014). Long-term changes in liana abundance and forest dynamics in undisturbed Amazonian forests. *Ecology* 95, 1604–1611. doi: 10.1890/13-1571.1

Laurance, W. F., Camargo, J. L. C., Luizao, R. C. C., Laurance, S. G., Pimm, S. L., Bruna, E. M., et al. (2011). The fate of Amazonian forest fragments: a 32-year investigation. *Biol. Conserv.* 144, 56–67. doi: 10.1016/j.biocon.2010.09.021

Laurance, W. F., and Curran, T. J. (2008). Impacts of wind disturbance on fragmented tropical forests: a review and synthesis. *Austral Ecol.* 33, 399–408. doi: 10.1111/j.1442-9993.2008.01895.x

Laurance, W. F., Lovejoy, T. E., Vasconcelos, H. L., Bruna, E. M., Didham, R. K., Stouffer, P. C., et al. (2002). Ecosystem decay of Amazonian Forest fragments: a 22-year investigation. *Conserv. Biol.* 16, 605–618. doi: 10.1046/j.1523-1739.2002.01025.x

Laurance, W. F., Nascimento, H. E. M., Laurance, S. G., Andrade, A. C., Fearnside, P. M., Ribeiro, J. E. L., et al. (2006). Rain forest fragmentation and the proliferation of successional trees. *Ecology* 87, 469–482. doi: 10.1890/05-0064

Laurance, W. F., Perez-Salicrup, D., Delamonica, P., Fearnside, P. M., D'Angelo, S., Jerozolinski, A., et al. (2001a). Rain forest fragmentation and the structure of Amazonian liana communities. *Ecology* 82, 105–116. doi: 10.1890/0012-9658(2001)082[0105:rffats]2.0.co;2

Laurance, W. F., Williamson, G. B., Delamonica, P., Oliveira, A., Lovejoy, T. E., Gascon, C., et al. (2001b). Effects of a strong drought on Amazonian forest fragments and edges. *J. Trop. Ecol.* 17, 771–785. doi: 10.1017/s0266467401001596

Ledo, A., and Schnitzer, S. A. (2014). Disturbance and clonal reproduction determine liana distribution and maintain liana diversity in a tropical forest. *Ecology* 95, 2169–2178. doi: 10.1890/13-1775.1

Lewis, S. L., Phillips, O. L., Baker, T. R., Lloyd, J., Malhi, Y., Almeida, S., et al. (2004). Concerted changes in tropical forest structure and dynamics: evidence from 50 South American long-term plots. *Philos. Trans. R. Soc. Lond. B Biol. Sci.* 359, 421–436. doi: 10.1098/rstb.2003.1431

Ley, A. C., and Claßen-Bockhoff, R. (2013). Breeding system and fruit set in African Marantaceae. *Flora Morphol. Distrib. Funct. Ecol. Plants* 208, 532–537. doi: 10.1016/j.flora.2013.07.011

Manzanedo, R. D., Ballesteros-Cánovas, J., Schenk, F., Stoffel, M., Fischer, M., and Allan, E. (2018). Increase in CO_2 concentration could alter the response of *Hedera helix* to climate change. *Ecol. Evol.* 8, 8598–8606. doi: 10.1002/ece3.4388

Marshall, A. R., Platts, P. J., Chazdon, R. L., Seki, H., Campbell, M. J., Phillips, O. L., et al. (2020). Conceptualising the global forest response to liana proliferation. *Front. For. Glob. Change.* 3:35.

Marvin, D. C., Winter, K., Burnham, R. J., and Schnitzer, S. A. (2015). No evidence that elevated CO_2 gives tropical lianas an advantage over tropical trees. *Glob. Chang. Biol.* 21, 2055–2069. doi: 10.1111/gcb.12820

Medina-Vega, J. A., Bongers, F., Poorter, L., Schnitzer, S. A., and Sterck, F. J. (2021). Lianas have more acquisitive traits than trees in a dry but not in a wet forest. *J Ecol.* 109, 2367–2384. doi: 10.1111/1365-2745.13644

Menzel, A., Sparks, T. H., Estrella, N., and Roy, D. B. (2006). Altered geographic and temporal variability in phenology in response to climate change. *Glob. Ecol. Biogeogr.* 15, 498–504. doi: 10.1111/j.1469-8137.2004.01003.x

Morellato, L. P. C., Alberti, L., and Hudson, I. L. (2010). "Applications of circular statistics in plant phenology: a case studies approach," in *Phenological Research*, eds I. Hudson and M. Keatley (Dordrecht: Springer), 339–359. doi: 10.1007/978-90-481-3335-2_16

Morellato, L. P. C., Alberton, B., Alvarado, S. T., Borges, B., Buisson, E., Camargo, M. G. G., et al. (2016). Linking plant phenology to conservation biology. *Biol. Conserv.* 195, 60–72. doi: 10.1016/j.biocon.2015.12.033

Nakonechnaya, O., Koren, O., Sidorenko, V., Shabalin, S., Markova, T., and Kalachev, A. (2021). Poor fruit set due to lack of pollinators in *Aristolochia manshuriensis* (Aristolochiaceae). *Plant Ecol. Evol.* 154, 39–48. doi: 10.5091/plecevo.2021.1747

Odell, E. H., Stork, N. E., and Kitching, R. L. (2019). Lianas as a food resource for herbivorous insects: a comparison with trees. *Biol. Rev.* 94, 1416–1429. doi: 10.1111/brv.12508

Oliveira, A. T., deMello, J. M., and Scolforo, J. R. S. (1997). Effects of past disturbance and edges on tree community structure and dynamics within a fragment of tropical semideciduous forest in south-eastern Brazil over a five-year period (1987-1992). *Plant Ecol.* 131, 45–66. doi: 10.1023/a:1009744207641

Pau, S., Okamoto, D. K., Calderón, O., and Wright, S. J. (2018). Long-term increases in tropical flowering activity across growth forms in response to rising CO_2 and climate change. *Glob. Change Biol.* 24, 2105–2116. doi: 10.1111/gcb.14004

Paul, G. S., and Yavitt, J. B. (2011). Tropical vine growth and the effects on forest succession: a review of the ecology and management of tropical climbing plants. *Bot. Rev.* 77, 11–30. doi: 10.1007/s12229-010-9059-3

Phillips, O., Vásquez Martínez, R., Arroyo, L., Baker, T., Killeen, T., Lewis, S., et al. (2002). Increasing dominance of large lianas in Amazonian forests. *Nature* 418, 770–774. doi: 10.1038/nature00926

Putz, F. E. (1984). The natural history of lianas on Barro-Colorado island, Panama. *Ecology* 65, 1713–1724. doi: 10.1890/12-1012.1

R Core Team (2019). *R: A Language and Environment for Statistical Computing*. Vienna: R Foundation for Statistical Computing.

Rathcke, B. J. (2000). Hurricane causes resource and pollination limitation of fruit set in a bird-pollinated shrub. *Ecology* 81, 1951–1958. doi: 10.1890/0012-9658(2000)081[1951:hcrapl]2.0.co;2

Rice, A. H., Pyle, E. H., Saleska, S. R., Hutyra, L., Palace, M., Keller, M., et al. (2004). Carbon balance and vegetation dynamics in an old-growth Amazonian forest. *Ecol. Appl.* 14, 55–71. doi: 10.1890/02-6006

Richardson, A. D., Keenan, T. F., Migliavacca, M., Ryu, Y., Sonnentag, O., and Toomey, M. (2013). Climate change, phenology, and phenological control of vegetation feedbacks to the climate system. *Agric. For. Meteorol.* 169, 156–173.

Schnitzer, S. A. (2005). A mechanistic explanation for global patterns of liana abundance and distribution. *Am. Nat.* 166, 262–276. doi: 10.1086/431250

Schnitzer, S. A., and Bongers, F. (2002). The ecology of lianas and their role in forests. *Trends Ecol. Evol.* 17, 223–230. doi: 10.1016/s0169-5347(02)02491-6

Schnitzer, S. A., and Bongers, F. (2011). Increasing liana abundance and biomass in tropical forests: emerging patterns and putative mechanisms. *Ecol. Lett.* 14, 397–406. doi: 10.1111/j.1461-0248.2011.01590.x

Schnitzer, S. A., and Carson, W. P. (2010). Lianas suppress tree regeneration and diversity in treefall gaps. *Ecol. Lett.* 13, 849–857. doi: 10.1111/j.1461-0248.2010.01480.x

Schnitzer, S. A., DeFilippis, D. M., Visser, M., Estrada-Villegas, S., Rivera-Camaña, R., Bernal, B., et al. (2021). Local canopy disturbance as an explanation for long-term increases in liana abundance. *Ecol. Lett.* 24, 2635–2647. doi: 10.1111/ele.13881

Schnitzer, S. A., and van der Heijden, G. M. F. (2019). Lianas have a seasonal growth advantage over co-occurring trees. *Ecology* 100:e02655. doi: 10.1002/ecy.2655

Schnitzer, S. A., van der Heijden, G., Mascaro, J., and Carson, W. P. (2014). Lianas in gaps reduce carbon accumulation in a tropical forest. *Ecology* 95, 3008–3017.

Swaine, M. D., and Grace, J. (2007). Lianas may be favoured by low rainfall: evidence from Ghana. *Plant Ecol.* 192, 271–276. doi: 10.1007/s11258-007-9319-4

Syktus, J., Trancoso, R., Ahrens, D., Toombs, N., and Wong, K. (2020). *Queensland Future Climate Dashboard: Downscaled CMIP5 climate projections for Queensland*. Available online at: https://www.longpaddock.qld.gov.au/qld-future-climate/ (accessed November 09, 2021).

Tang, J., Körner, C., Muraoka, H., Piao, S., Shen, M., Thackeray, S. J., et al. (2016). Emerging opportunities and challenges in phenology: a review. *Ecosphere* 7:e01436.

Ting, S., Hartley, S., and Burns, K. C. (2008). Global patterns in fruiting seasons. *Glob. Ecol. Biogeogr.* 17, 648–657. doi: 10.1111/j.1466-8238.2008.00408.x

Tracey, J. G. (1982). *The Vegetation of the Humid Tropical Region of North Queensland*. Melbourne, VIC: CSIRO.

Turton, S. M., and Stork, N. E. (2009). "Impacts of tropical cyclones on forests in the wet tropics of Australia," in *Living in a Dynamic Tropical Forest Landscape*, eds N. E. Stork and S. M. Turton (Carlton, VIC: Blackwell Publishing, Ltd), 47–58. doi: 10.1016/j.scitotenv.2016.05.107

Turton, S. M. (2012). Securing landscape resilience to tropical cyclones in Australia's Wet Tropics under a changing climate: lessons from Cyclones Larry (and Yasi). *Geogr. Res.* 50, 15–30.

Umaña, M. N., Forero-Montaña, J., Nytch, C. J., Thompson, J., Uriarte, M., Zimmerman, J. K., et al. (2019). Dry conditions and disturbance promote liana seedling survival and abundance. *Ecology* 100, 1–9. doi: 10.1002/ecy.2556

Wright, S., and Calderón, O. (2006). Seasonal, El Niño and longer term changes in flower and seed production in a moist tropical forest. *Ecol. Lett.* 9, 35–44.

Wright, S. J. (2005). Tropical forests in a changing environment. *Trends Ecol. Evol.* 20, 553–560. doi: 10.1016/j.tree.2005.07.009

Wright, S. J., and Calderón, O. (2018). Solar irradiance as the proximate cue for flowering in a tropical moist forest. *Biotropica* 50, 374–383. doi: 10.1111/btp.12522

Wright, S. J., Sun, I. F., Pickering, M., Fletcher, C. D., and Chen, Y. Y. (2015). Long-term changes in liana loads and tree dynamics in a Malaysian forest. *Ecology* 96, 2748–2757. doi: 10.1890/14-1985.1

Wuertz, D. (2020). *timeSeries: Financial Time Series Objects (Rmetrics). R package version 3062.100*.

Zar, J. H. (1999). *Biostatistical Analysis*, 4th Edn. Upper Saddle River, NJ: Prentice Hall.

Zar, J. H. (1996). "Circular distributions: descriptive statistics," in *Biostatistical Analysis*, 519–611.

Zhu, S. D., and Cao, K. F. (2010). Contrasting cost-benefit strategy between lianas and trees in a tropical seasonal rain forest in southwestern China. *Oecologia* 163, 591–599. doi: 10.1007/s00442-010-1579-3

Zich, F. A., Hyland, B. P. M., Whiffin, T., and Kerrigan, R. A. (2018). *Australian Tropical Rainforest Plants*, 7th Edn. Available online at: https://apps.lucidcentral.org/rainforest/text/intro/index.html (accessed November 09, 2021).

Zich, F. A., Hyland, B. P. M., Whiffin, T., and Kerrigan, R. A. (2020). *'Taxon Name'. Australian Tropical Rainforest Plants*, 8th Edn. Available online at: https://apps.lucidcentral.org/rainforest/ (accessed November 09, 2021).

Zimmerman, J. K., Wright, S. J., Calderón, O., Pagan, M. A., and Paton, S. (2007). Flowering and fruiting phenologies of seasonal and aseasonal neotropical forests: the role of annual changes in irradiance. *J. Trop. Ecol.* 23, 231. doi: 10.1017/s0266467406003890

Conflict of Interest: The authors declare that the research was conducted in the absence of any commercial or financial relationships that could be construed as a potential conflict of interest.

Frontiers in
Forests and Global Change

Informs and promotes sustainable management of the world's forests

An innovative journal that places forests at the forefront of attention for scientists, policy makers and the public. It advances our understanding of how forests 'work', spanning from molecules to ecosystems to the biosphere.

Discover the latest Research Topics

See more →

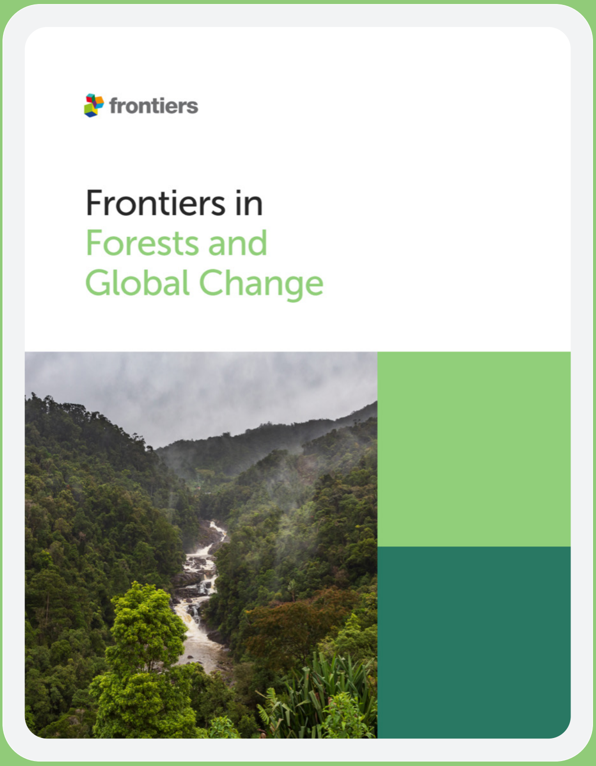

Frontiers

Avenue du Tribunal-Fédéral 34
1005 Lausanne, Switzerland
frontiersin.org

Contact us

+41 (0)21 510 17 00
frontiersin.org/about/contact